UNIVERSITY OF AGDER

FACULTY OF ENGINEERING AND SCIENCE

DUAL-SPEED PLANETARY GEARBOX FOR INTERNAL MOUNTING IN WINCH DRUM:

DESIGN, ACTUATION, AND CONTROL

By

Jørgen Bruun Tørnby

Jan Christian Bjerke Strandene

May 24, 2018

Supervisor:

Martin Marie Hubert Choux

This master's thesis is carried out as a part of the education at the University of Agder and is therefore approved as a part of this education.
However, this does not imply that the University answers for the methods that are used or the conclusions that are drawn.

Department of Engineering

Faculty of Engineering and Science

Any figure not referenced to a source in its caption is an original work created by the authors of the thesis. All original works may be freely used in non-commercial publications, as long as they are appropriately cited to this thesis and its authors.

Abstract

This thesis presents the work done to design a planetary gearbox which shall be mounted within a winch drum along with an electric motor, to actuate the drum. The aim of this design is for the gearbox to change between two gear ratios seamlessly while the input and output are in motion, and preferably with a load. The gearbox is designed with two steps, where the first is a modified Simpson gear-train with two gear-sets, and the second is a gear-set with a fixed gear ratio. The thesis describes the concept design, partly the mechanical design of the gearbox, and lastly the design and tuning of the control system for changing gears. To change between the gear ratios of the gearbox, there is designed an actuation system using brake discs and solenoids, which is supplemented by dogs for steady-state operation. The result of the thesis is a theoretical gearbox which can change gear near-seamlessly while in motion, and with an applied load up to ±1000Nm. It may also change gear at higher loads, but with more shock to the system.

A video of the assembly of the gearbox may be seen through the following link: https://youtu.be/PlHKU4L3ZyQ

Foreword & Acknowledgments

Projects we have completed
demonstrate what we know - Future
projects decide what we will learn
- Dr. Mohsin Tiwana

This master's thesis is the culmination of years of study for the authors. Through this thesis, we, the authors, would like to show the reader what we have learned through our studies, so that we may have the opportunity to learn more.

We have both started our path to this point through vocational schools. Though our paths differed after, the result is nonetheless two masters of engineering in mechatronics. Multiple teachers and co-students that have aided us to reach this milestone, there have been To mention all our contributors would be a lengthy and futile endeavor. We would, therefore, thank all our unmentioned guides, and give an honorary mention to some;

Martin Marie Hubert Choux, PhD. is the man that has guided us through this thesis through the last semester. His invaluable guidance has made this thesis what it would otherwise not be.

The thesis is mainly concerned with gearboxes, which would make us remiss in not mentioning professor Kjell Gunnar Robbersmyr, who laid the foundation for our knowledge of gearboxes.

The reason for us being able to work on this thesis is Alf Magne Midtbø Versland and his team at Flekkefjord Elektro, who have given us the assignment. The opportunity they have given us, the experience, and their humor shall not be forgotten.


Jørgen Bruun Tørnby


Jan Christian Bjerke Strandene

May 24, 2018

Contents

Glossary

Actuated step	The modified Simpon gear-train step of the gearbox.
AWE	Airborne Wind Energy.
CVT	Continuous Variable Transmission.
Fixed step	The fixed gear-ratio step of the gearbox.
Gear	A rotating disk with teeth about its perifery. Also used for a defined gear-ratio, for example: "high gear" or "low gear".
Intermediate shaft	Here: The shaft connecting the fixed step sun and carrier 2.
Module	The relation between the number of teeth and the diameter of a gear.
Overdrive	Gear-ratio which increases the speed of the output in relation to the input.
Pinion	The smaller gear in a meshing pair of gears.
Transmission	Unit for transmitting rotational power, with the possibility of conversion.
Underdrive	Gear-ratio which reduces the speed of the output in relation to the input.

Nomenclature

Variables

Some of the most used variables in this thesis are shown below.

$\boldsymbol{\omega}$	Angular velocity	$[^{rad}/_{s}]$
$\boldsymbol{d}$	Diameter	$[m]$, $[mm]$
$\boldsymbol{i}$	Gear ratio	$[-]$
$\boldsymbol{P}$	Number of teeth on planet	$[-]$
$\boldsymbol{R}$	Number of teeth on ring	$[-]$
$\boldsymbol{r}$	Radius	$[m]$, $[mm]$
$\boldsymbol{S}$	Number of teeth on sun	$[-]$
$\boldsymbol{v}$	Linear velocity	$[^{m}/_{s}]$

The variables should also be declared for most of the equations in the thesis, even though they are listed here. If variable names are used for different variables than described in the table above, they will always be declared close to their use.

Where there are multiple equations gathered near each other, the nomenclature will usually be located below the last equation in the group.

Subscripts

Throughout the thesis there are used subscripts on variables to specify the part that is concerned. The most used subscripts are the ones shown below. When other subscripts are used, they will always be declared close to their use.

$\boldsymbol{1}$	Stage 1 of actuated step of gearbox
$\boldsymbol{2}$	Stage 2 of actuated step of gearbox
$\boldsymbol{A}$	Actuated step of gearbox
$\boldsymbol{C}$	Carrier of planetary gear set
$\boldsymbol{F}$	Fixed step of gearbox
$\boldsymbol{i}$	Inner (usually diameter or radius)
$\boldsymbol{M}$	Motor
$\boldsymbol{o}$	Outer (usually diameter or radius)
$\boldsymbol{P}$	Planet of planetary gear-set
$\boldsymbol{R}$	Ring of planetary gear-set
$\boldsymbol{S}$	Sun of planetary gear-set

1 | Introduction

A multitude of applications uses winches, both on and off-shore, on vehicles, vessels, or ground-mounted. High-power winches have traditionally been hydraulic-powered, but are trending towards electrification.

The issues of using hydraulics for power are that there must be a source to provide the power, for the hydraulics to then transmit the power to a motor which turns the winch drum. The system involves a rather significant amount of components which require maintenance. A hydraulic system leaks oil, which requires waste-management. Petroleum-based oil is also an environmental issue, which is mostly avoided with an electric system.

An electric winch cannot, unlike the hydraulic system, leak oil except for the cooling and lubrication systems (if there are any). An electric winch is more straightforward to maintain, using mechanical connections. Traditional electric winches do though have some issues related to size. A conventional high-power electric winch has a motor offset from the winch drum, which must be placed relatively close to the drum to allow for the mechanical connection. A hydraulic power-supply could, however, be set further away from the drum, because pipes or hoses connect it to the winch.

Flekkefjord Elektro (FE) is creating an electric winch to solve the space issue, which shall be made to be compact and for relatively high load demands. There has been designed a motor by *FE Create* (FE R&D) which shall be placed inside the winch drum. Because of the high speed of the electric motor, and the high torque required of the drum, a transmission shall be designed, which shall also be placed within the drum. The currently developed transmission is not able to change gears while in motion.

Some applications are usable with a transmission which must be stopped to change gears, because the system need not continuous motion. If the transmission is able to change gears while in motion, its applicability will though increase. Changing gears while in motion may increase the effectiveness of the system, because it does not need to accelerate to and from standstill for the gear change. A gear-shift while in motion also allows it to handle possible emergency cases, where another gear is required, but stopping the system is detrimental.

FE has engaged two graduate students from the *University of Agder* (UiA) to research the possibilities and concepts to design an alternative transmission which can change gears while under load. This thesis describe their attempt to do so.

1.1 Problem Definition

The problem this thesis attempts to solve is the design of a planetary gearbox that shall fit within a winch drum. The gearbox must be able to connect to the drum and transmit the full power from a given motor. The gearbox shall be able to change between two gears while the system is in motion, and preferably while the winch is subject to a load.

The requirements of the gearbox are shown in the table below. The gearbox shall approach the median gear ratios for high and low gear, with an absolute requirement to be within the required range. For the dimensioning, for both the torque and speed, a safety factor of 1.15 is used.

Table 1.1: Requirements of gearbox.

Parameter	**Data**	**Data w/SF (15%)**
T_{in}	625	718.75
n_{in}	2000	2300
$i_{1,min}$	20.24	
$i_{1,max}$	21.18	
$i_{1,median}$	20.79	
$i_{2,min}$	3.00	
$i_{2,max}$	4.50	
$i_{2,median}$	3.75	
$d_{o,max}$	450	
Service interval	> 2500	

The parameters in the table are:

$\boldsymbol{d_o}$	Outer diameter	$[mm]$
$\boldsymbol{i}$	Gear ratio	$[-]$
$\boldsymbol{n}$	Rotational speed	$[rpm]$
$\boldsymbol{T}$	Torque	$[Nm]$
Service interval	Minimum life expectancy of parts	$[hours]$

1.2 Application and Motivation

The winch which the transmission is connected to is currently intended to use for trawling and airborne wind energy. The two gears will benefit both of the systems by increasing their productivity and safety.

Airborne Wind Energy (AWE) is the use of an aircraft to convert wind-power to electricity. The type of AWE that the related winch shall be used with is a ground-based system, which is illustrated in figure 1.1.

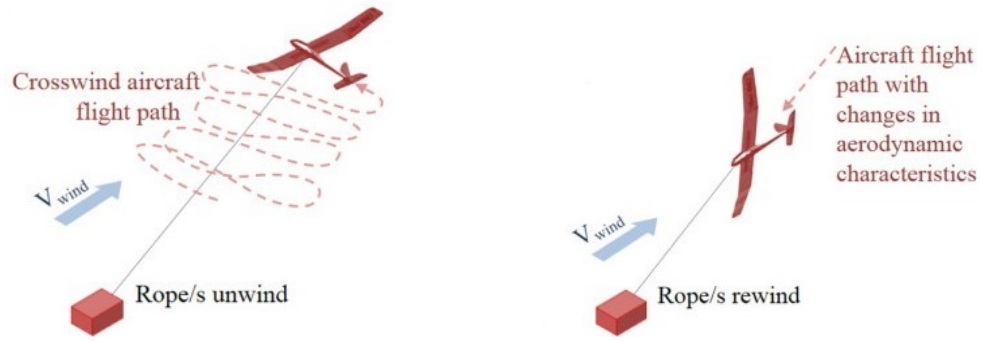

(a) Ascension, converting wind-power to electric power.

(b) Descent, recovery of aircraft.

Figure 1.1: Process of fixed ground based AWE system.
Cropped version of original, adapted from Cherubini [1] with permission [2].

A ground-based AWE uses an aircraft, attached to a tether to transmit mechanical power to a generator on the ground. The aircraft is used to drag out the tether, rotating the generator to create electric power. The aircraft is alternating between ascent and descent, to allow the wire to be spooled in for then to be dragged out to generate the electricity. [1]

When the aircraft is descending, the system does not generate power. There is, therefore, little to no load on the winch. The motor must be able to hold the aircraft to generate power when ascending, which requires a fairly high torque capability. When the aircraft descends, the motor for the winch is however limited to a certain speed. By using a gearbox with the ability to change between two gear ratios, the winch could be allowed to spool in the aircraft tether quite fast, without requiring the motor to achieve excessive speeds. By using a high gear ratio for generator mode, the high torque on the tether is exchanged for high speed to the generator. A low gear ratio for a light-load descent allows for greater speed on the drum, for the same speed on the motor. Two gear ratios will, therefore, make the system more effective than a single gear ratio, where the motor must instead produce both high torque and high speed. In addition to the spooling the tether of the aircraft in fast, the system should be able to shoot out the tether quickly, in case the wind catches wrong on the aircraft, and the tether is in danger of snapping. It is beneficial to have great step between the gear ratios to quickly shoot the tether. [3]

Trawling is the use of a net dragged behind a boat at sea to catch fish. The trawl is a net, usually cone-shaped with a collector at its back. The front of the trawl net is expansive to cover a large area for collection. Between the net and the wires to the winch are otter boards, which purpose is to spread the opening of the net by using hydrodynamics. An illustration of a trawling system is shown in figure 1.2. [4]

When trawling, the operation is reverse to AWE. The trawl is first shot out, where the winch-wire is spooled out quickly, with no load. The trawl is then dragged after the boat to gather fish, before being pulled in with a high torque load on the winch. The benefits for the normal of operation of the trawl is the same as for AWE. The trawl does though have an especially critical scenario, where the trawl snags on something. If the trawl catches, the wire must spool out quickly to avoid breaking the trawl or wire, until the boat can stop and turn about. [3]

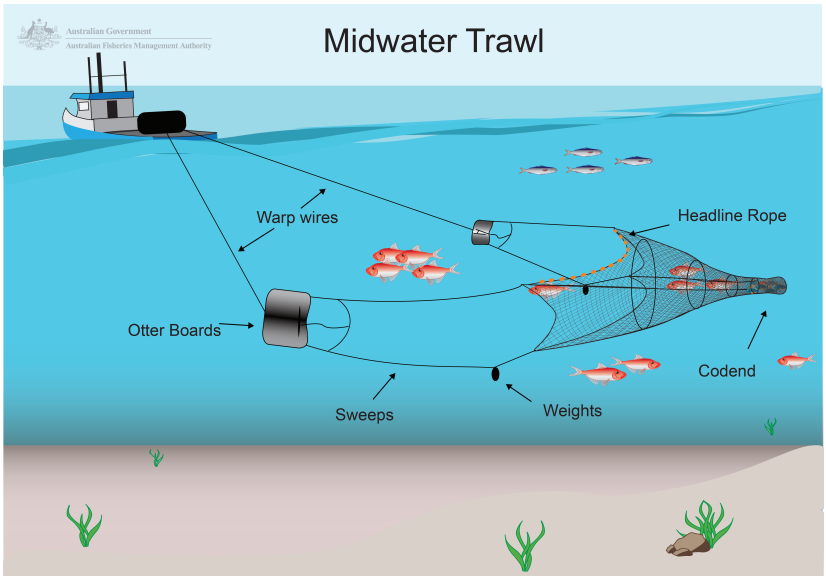

Figure 1.2: A midwater trawl system.
Copyright Australian Fisheries Management Authority [4].

1.3 Scope & Limitations

The thesis describes the theoretical design of a gearbox. Some required considerations for a realizable creation are therefore omitted.

Tribology is mostly ignored in the thesis, including the oil for cooling and lubrication, any form of grease required, and the friction of intersecting parts. Besides the lubrication, the cooling properties of the gearbox and the oil are not considered. The cooling may likely be an issue. These issues must, however, be investigated further along with the lubrication before an eventual construction of the gearbox. The oil seals required to keep the gearbox from leaking oil are also not designed or selected in this thesis.

The concept design of the gearbox is the primary focus. The mechanical properties of the shafts and gears are investigated and documented. The properties of the housing and some other parts of the gearbox are though not investigated or discussed, including the fits and tolerances. The 3D CAD model of the gearbox contains all the components required to hold the gearbox assembled in working condition, but the dimensions may not be sufficient for those parts not documented in this thesis.

The system model and control system assumes that the gearbox and other system components are ideal. There is considered to be no friction in the system, although the effects of viscous friction on the load were tested. All the parts are assumed to be ideally stiff and have no dampening. The temperature, or any other factors that may influence the behavior of the system, are neglected as well. A frequency response test should, either way, be used to verify the system model.

The control system for the motor is not a concern of the thesis. A control system was nonetheless created for an ideal torque sensor in the system simulation because it was required to simulate the system. This regulator does through not take into account the behavior of a real motor. The criteria for when the gearbox should shift gears, for the different possible applications are also not considered. The control system designed here is concerned merely with the gear change when given a signal, which is here produced by general criteria.

1.4 Disposition of Thesis

Chapter 1: The introduction to the thesis describes the problem, the motivation for the problem, and the scope of the thesis.

Chapter 2: The gearbox is conceptually designed. The gear ratios of the gearbox are found and optimized, and the gears are dimensioned to create the gear ratios while being able to withstand the required load.

Chapter 3: The brake and actuator systems are selected, based on some possible concepts. The systems are then dimensioned to be able to achieve their desired effects.

Chapter 4: All the mechanical parts of the gearbox except for the gears, the brakes, and the actuators are described. The shafts are dimensioned, and the bearings selected. The other supporting parts of the gearbox are conceptually described.

Chapter 5: The mathematical model and the simulation model are described. The method of control, and the process and the result of the brake actuator tuning are detailed.

Chapter 6: The findings and results of the of the thesis are summarized. Some aspects of the thesis are discussed and pointed out. Some alternative solutions to the design are presented, and the required further work of the design is presented.

2 | Design of Gear Ratio & Gears

The primary objective of this chapter is to summarize the conceptual design of the gearbox and how the gear ratio is designed. The mechanical design of the gears and some theory of transmissions is also covered.

2.1 Introduction to Transmissions

Several concepts for transmitting mechanical rotational power exist, and multi-speed transmissions may also be actuated to change gear by different methods, both manually and automatically. Following are three selected transmission types.

2.1.1 Traditional Gearbox

In a traditional gearbox, the gears are placed beside each other, as shown in figure 2.1. In this configuration, the rotational power is transferred from one shaft to another by the gears connected to each of the shafts. The axes of rotation for the gears are constant and located at the center of the shafts.

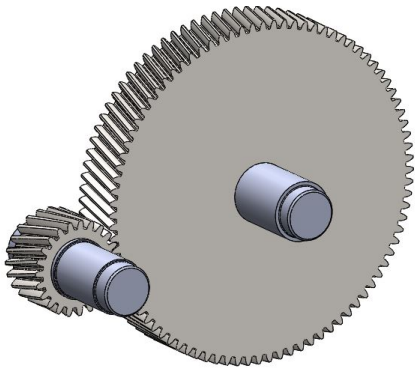

Figure 2.1: Traditional gear-set.

To change the gear ratio of a traditional gearbox, one must change one or both meshing gears, to get a combination with a different relation of radii. For a multi-speed gearbox, there must, therefore, be multiple gears, with the ability to engage or disengage different meshing pairs of gears.

The advantage of the traditional gearbox is its simplicity which also makes it relatively cheap. The disadvantage of the design is that it requires more space than other concepts. Depending on the configuration, another drawback is that the input and output are not in-line.

2.1.2 Continuously Variable Transmission

The theory presented in this section is based on Lechner & Naunheimer [5].

Continuously variable transmissions (CVT), are transmissions that have a continuously variable gear ratio instead of indexed gear ratios like the conventional gear-trains. CVTs are made by using belts or chains with sheaves which have a variable diameter.

A CVT uses two pulleys configured like the traditional gearbox, but with belts or pulleys connecting them instead of meshing gears. The pulleys have variable radii to achieve different gear ratios. This is illustrated in figure 2.2.

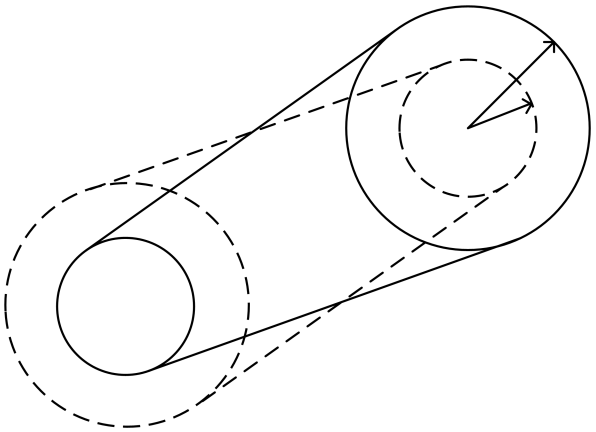

Figure 2.2: Concept of a CVT.

The advantage of a CVT is its ability to have a seamless transition of gear ratio, therefore not requiring the motor to change its power output in a stepwise manner. The motor will benefit from a CVT by gaining better efficiency, and reduced wear, as well as having an improved energy consumption. The main disadvantage of a CVT is that it will have a limited ability to transmit torque because the interaction between the parts is friction-based traction. If the torque is higher than what the friction is capable of holding, the parts will slip rather than transmit the power. A CVT also requires relatively much space, and has an offset configuration like the traditional gearbox. [6]

2.1.3 Planetary Gearbox

A planetary/epicyclical gear-train is an in-line configuration of gears used to transfer mechanical rotational power. The in-line configuration is achieved by meshing gears that are placed in a plane perpendicular to the input and output shafts which are concentric and constitute the centroid of the gear-train configuration. The configuration of a simple planetary gear-set is shown in figure 2.3.

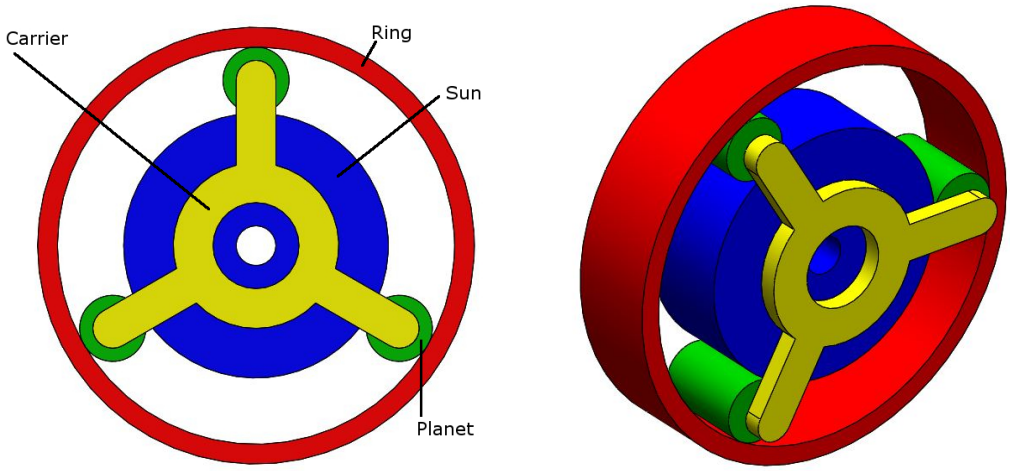

(a) 2D (b) 3D

Figure 2.3: Concept of a planetary gear-set with 3 planets.

As seen in the figure, the gear-train consists of 4 parts, which are described below:

Ring (Red)	Gear with internal gear teeth meshing with the planets.
Planets (Green)	Gears meshing with both the sun and the ring.
Carrier (Yellow)	Connection between the planets, keeping them evenly spaced throughout their available space, while not locking the rotation of the planets about their own axis.
Sun (Blue)	Inner gear, meshing with all the planets.

The sun, carrier, and ring may be assigned as the input or output of the gear train. By locking different components in place, and using various input/output configurations, the gear ratio between the input and output will change. It is also possible to use multiple sets of gear trains to achieve a greater selection of gear ratios.

The main advantage of a planetary gearbox is its compactness. It is also able to handle high torques while remaining compact due to multiple meshing gears distributing the torque load, thus also being able to have a greater per-step gear ratio than the traditional gearbox for the same overall torque. A planetary gearbox may be able to achieve a gear ratio of 10:1 per stage. [7]
The disadvantages of a planetary gearbox are its increased complexity in comparison to a traditional gearbox, and that the compact size with large power transmission may lead to heat dissipation issues. [8]

2.1.4 Gear Types

There are two common types of gears; Spur and helical. The standard kind of gear is the spur gear (figure 2.4a). A spur gear is a disk with teeth about its periphery, which are oriented perpendicular to the face of the side of the gear. The other type of gear is the helical gear (figure 2.4b). The helical gear is near equal to the spur gear, except that the gear teeth are skewed to an angle to the spur gear's teeth.

Spur gears cause only radial and tangential loads to occur. [9]
They will though cause some noise and vibration, due to the teeth of the gears colliding straight on each other when meshing. [10]
Helical gears, however, will make the meshing of the gears smoother, with less impact. [11]
In addition to radial and tangential forces, the helical gears will also produce axial forces through the meshing, because of the angle of the teeth. [9]

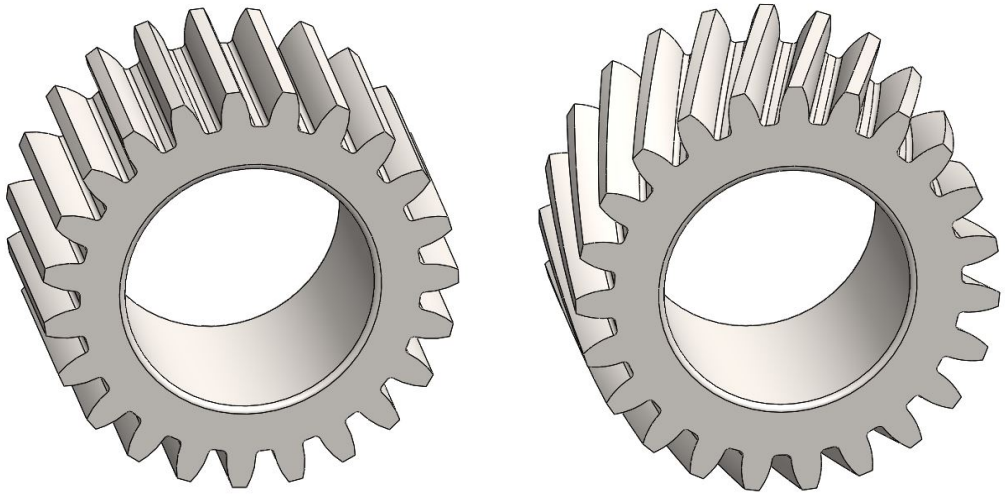

(a) Spur gear. (b) Helical gear.

Figure 2.4: Gears types.

2.2 Why Planetary Gearbox?

The requirements of the gearbox are shown in chapter 1.1. Of the requirements, there are three primary concerns for choosing the type of transmission; Firstly, the highest gear ratio is relatively large, and the difference between the gear ratios is also rather significant. Secondly, the torque input is relatively high. The last concern is the size of the transmission since it must fit within the winch-drum.

Because of the high torque, a CVT is not suitable. It could be made able to transmit the torque, but would then be far larger than what is allowable within the drum. Gears can transmit the torque without requiring as much space as a CVT. A traditional gearbox will, however, still struggle to fit within the drum.

A planetary gear-train has the advantage over the traditional gearbox that the input and output are in-line, and that the form of the gear-set is cylindrical with the input at its center. The cylindrical shape of the planetary gear-set allows it to utilize more of the space inside the drum than the traditional gear-train, where each gear-set is not in-line. Since the transmission shall be installed within the drum, the planetary gear-train is the best, and perhaps, due to size, the only reasonable transmission type to use.

2.3 Mathematical Model of a Planetary Gear-Set

The basis for any system of meshing gears is that the peripheral velocity of intersecting gears must be equal since there is no slip between the gears. The radii of the gears may, however, be different, which makes their angular velocity differ, thus creating a gear ratio between the gears.

In the planetary gearbox, the planets are meshing with both the ring and the sun, thus requiring them all to have the same peripheral velocity. Figure 2.5 show the interaction between a planet, ring, and sun.

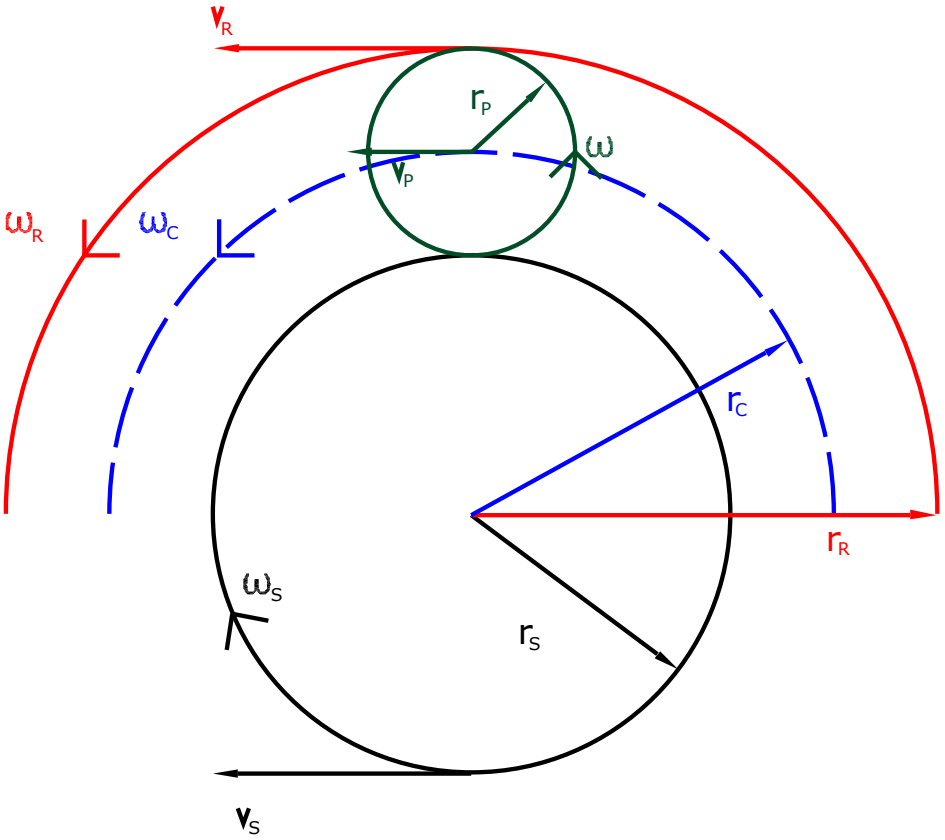

Figure 2.5: Illustration of velocities of the carrier (blue), sun (black), planet (green), and ring (ring) within a planetary gearbox. All rotations are shown in relation to mathematical positive rotation of planet.

2.3.1 Velocity of a Rolling Circle

Equation (2.1) describes the peripheral velocity on top of a circle rolling on a surface. The rolling circle is illustrated in figure 2.6. Due to no slip between the circle and the surface, the velocity of the circle at the point V_S (surface contact) is zero. The peripheral velocity of the circle is initially equal to the center-point velocity. However, since the surface contact does not move, the circle rotates, and the induced rotation leads to an increase in the peripheral velocity of the topmost point of the circle, opposite the surface contact. When the surface contact point has no velocity like this, the peripheral velocity at the top due to rotation of the circle is equal to the center-point velocity, because the radius from the center point to both the surface and the top is equal and parallel.

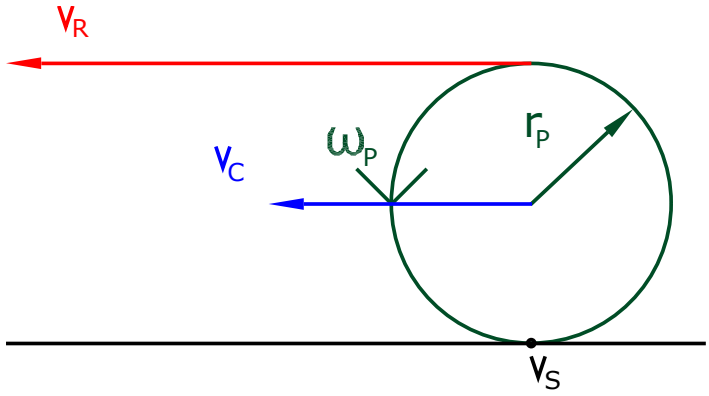

Figure 2.6: Illustration of circle rolling on a surface with no slip. Rotation in accordance with positive mathematical rotation.

$$v_R = v_C + \omega_P r_P = 2v_C \tag{2.1}$$

The parameters in the equation are:

$\boldsymbol{\omega}$	Angular velocity	$[^{rad}/_{s}]$
$\boldsymbol{r}$	Radius	$[m]$
$\boldsymbol{v}$	Linear velocity	$[^{m}/_{s}]$

The subscripts correspond to figure 2.6.

2.3.2 Governing Equations of a Planetary Gear-Set

The intermediate calculations for this section are shown in calculation 2.2.

The center-point translational velocity of the planet is the peripheral velocity of the carrier. The ring's peripheral velocity at the intersection with the planet must be equal to the peripheral velocity of the planet at the intersection, which leads to equation (2.2), which is the expanded form of the initial part of equation (2.1).

$$\omega_R r_R = \omega_C r_C + \omega_P r_P \tag{2.2}$$

If the ring is ignored, and the sun is instead rotating, the relations of the system are near equal. Equation (2.3) shows the velocity relations of the carrier-planet-sun system. The behavior of the sun is equal to that of the ring, except that the sun will rotate opposite of the planet, while the direction of rotation of the ring is equal to the planet, as illustrated in figure 2.5.

$$\omega_S r_S = \omega_C r_C - \omega_P r_P \tag{2.3}$$

If equations (2.2) and (2.3) are solved for $\omega_p r_P$ and set equal to each other, the result is equation (2.4).

$$2\omega_C r_C = \omega_R r_R + \omega_S r_S \tag{2.4}$$

r_C is the radius of the carrier as defined to be the radius to the center of the planets. r_C may be exchanged for:

$$2r_C = r_R + r_S \tag{2.5}$$

Equation (2.5) is proven in calculation 2.1, supported by the geometry in figure 2.5.

Equation (2.6) is a combination equations (2.4) and (2.5). This is the governing equation for a planetary gear-set used in this thesis.

$$\omega_C(r_R + r_S) = \omega_R r_R + \omega_S r_S \tag{2.6}$$

The parameters in the equations are:

$\boldsymbol{\omega}$	Angular velocity	$[^{rad}/_{s}]$
$\boldsymbol{r}$	Radius	$[m]$

The subscripts indicate the part of the planetary set the parameter refers to.

Calculation 2.1: **Proof of relation between carrier, sun, and ring radii.**

$$\begin{cases} r_C &= r_S + r_P \\ r_P &= \dfrac{r_R - r_S}{2} \end{cases}$$

$$r_C = r_S + \frac{r_R - r_S}{2}$$

$$r_C = \frac{r_S}{2} + \frac{r_R}{2}$$

$$2r_C = r_S + r_R \qquad \square$$

The parameters in the calculation are:

$\boldsymbol{r}$	Radius	$[m]$

The subscripts indicate the part of the planetary set the parameter refers to.

Calculation 2.2: **Intermediate calculations for governing equation of planetary gear-set.**

$$\begin{cases} \omega_R r_R = \omega_C r_C + \omega_P r_P \\ \omega_S r_S = \omega_C r_C - \omega_P r_P \end{cases}$$

$$\begin{cases} \omega_P r_P = \omega_R r_R - \omega_C r_C \\ \omega_P r_P = \omega_C r_C - \omega_S r_S \end{cases}$$

$$\omega_R r_R - \omega_C r_C = \omega_C r_C - \omega_S r_S$$

$$\omega_R r_R + \omega_S r_S = \omega_C r_C + \omega_C r_C$$

$$2\omega_C r_C = \omega_R r_R + \omega_S r_S \qquad ; 2r_C = r_S + r_R$$

$$\omega_C(r_R + r_S) = \omega_R r_R + \omega_S r_S \qquad \square$$

The parameters in the calculation are:

$\boldsymbol{\omega}$	Angular velocity	$[^{rad}/_{s}]$
$\boldsymbol{r}$	Radius	$[m]$

The subscripts indicate the part of the planetary set the parameter refers to.

2.4 Concept Design of Gearbox

It is necessary to use at least two gear-sets to achieve the gear ratio of the low gear because a single planetary gear-set should not reduce for a ratio greater than 10. [7]

The gearbox in this thesis is designed based on a Simpson gear-train. A Simpson gear-train uses two planetary gear stages in a compound gear-train, where the sun gear is common for both the stages. There is one ring for each of the stages, which are used as the input of the first step, and the output of the second. A Simpson gear-train allows for three forward gears, neutral, and a reverse gear. [12]

Because the gearbox for thesis needs only to achieve two gears, there is designed a modified version of it. The modified design in this thesis is based on the gear-train design used in Dr. Mousavi's PhD-thesis [13].

The gear-train used in this thesis is equal in form to the Simpson gear-train, except that the rings of the gear-sets are instead one common gear. Also, to allow for a more significant difference in gear ratios, the sun gear is split, to have individual sun gears for the two stages. The sun gears are though attached to the same shaft to have the same rotational velocity. The carrier of the first stage is used as the input, and the carrier of the second stage is used as the output.

The planetary gearbox's gear ratio is changed by braking/locking up different parts, either the sun, ring, or carrier. The input/output configuration may also vary, and create different gear ratios and change input/output rotational direction. If the ring and sun are in motion, their direction of rotation will be opposite (figure 2.7). The carrier is used as either the input or output because this gearbox shall change gear while in motion. Any combination using the carrier as input/output will make the rotation direct to both the sun and ring. It is assumed that not changing the rotation of rotation between the gears will be beneficial, because it does make it possible for the two gear-sets to have inverse rotations which could cause breakage.

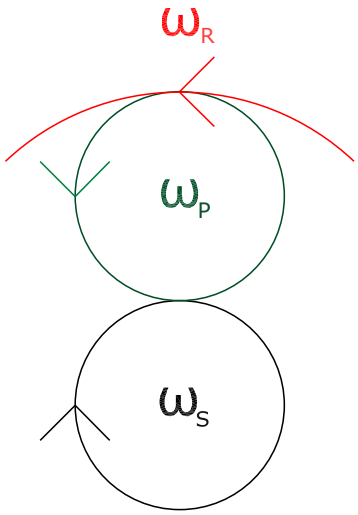

Figure 2.7: Illustration of rotations in gear-set.

An advantage of the described planetary gear set to the basic Simpson gear-train is that there is only needed two brakes, since there are only two parts that need to be stopped. Also, the modification of the sun-gear to be a common shaft allows for a greater difference between the gear ratios. The disadvantage is that the number of gears is limited, which is however not a problem for this thesis.

The power flow of the modified Simpson gear-train is through either the common ring or the sun shaft, when the opposing part is locked. If both brakes are disengaged, the gearbox does not go to a neutral disconnected gear, and the power flow is undefined but assumed to be through both the ring and the sun. The power flow, and concept of the modified Simpson gear-train is shown in figure 2.8.

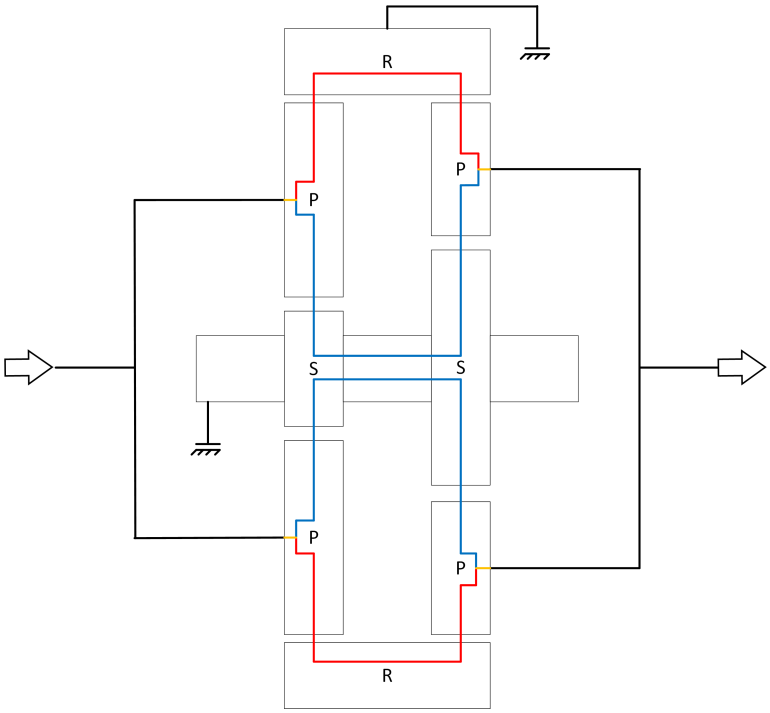

Figure 2.8: Power flow in modified Simpson gear-train with common ring and sun shaft.
Blue = Locked ring.
Red = Locked sun.

Spur gears are used for the initial design of the gearbox to simplify the calculations. Helical gears may be evaluated for use in an eventual re-design. The gears have a pressure angle of 20°, standard involute gear profiles, and integer module.

2.4.1 Gear Ratio of Modified Simpson Gear-Train

To calculate the gear ratio of the initial concept, the governing equation (2.6) is used. The equation is replicated below.

$$(r_R + r_S)\omega_C = r_S\omega_S + r_R\omega_R \tag{2.7}$$

The parameters in the equation are:

$\boldsymbol{\omega}$	Angular velocity	$[^{rad}/_s]$
$\boldsymbol{r}$	Radius	$[m]$

The subscripts indicate the part of the planetary set the parameter refers to.

When calculating the gear ratios, i.e., the relation between velocities. The radii of the gears are interchangeable with the number of teeth or the diameter of the gear. The number of teeth was used to design the gear ratios, because the number of teeth on the gears is constant, while the radius and diameter scale with the module.

The carrier is used as the input for the first step, and the output in the second step of the concept gear train. The intermittent transfer of power uses either the sun shaft or the ring, depending on which is locked. The two gears are defined by either the ring or sun being completely at a standstill, while the other rotates freely. If one or both of the brakes are partly engaged and slipping, the velocity relations are defined by equation (2.7), where there are three variables of angular velocity. It is not possible to find the gear ratio for such a case without additional equations for motion in the system. There are two definable gear ratios of the gear train, which are defined below.

When the ring is locked ($\omega_R = 0$), the gearing is an underdrive, and the gear ratio is found by

$$\frac{\omega_C}{\omega_S} = \frac{S}{R+S} \tag{2.8}$$

When the sun shaft is locked ($\omega_S = 0$), the gearing is an overdrive, and the ratio is found by

$$\frac{\omega_C}{\omega_R} = \frac{R}{R+S} \tag{2.9}$$

When connecting two different steps in series with carrier 1 as input, and carrier 2 as output - For the low gear, with the ring locked (underdrive), the gear ratio i_L is:

$$i_L = \frac{\omega_{C_1}}{\omega_{C_2}} = \frac{S_1(S_2+R)}{S_2(S_1+R)} \tag{2.10}$$

For the high gear, with locked sun shaft (overdrive), the gear ratio i_H is:

$$i_H = \frac{\omega_{C_1}}{\omega_{C_2}} = \frac{(R + S_2)}{(R + S_1)} \tag{2.11}$$

The parameters in the equations are:

$\boldsymbol{i}$	Gear ratio	$[-]$
$\boldsymbol{\omega}$	Angular velocity	$[^{rad}/_{s}]$
$\boldsymbol{R}$	Number of teeth on ring	$[-]$
$\boldsymbol{S}$	Number of teeth on sun	$[-]$

The subscripts indicate if the value is for the first or second gear set, starting from the input. The ring needs no subscript because it is common for both stages.

2.4.2 Applicability of Modified Simpson Gear-Train

Figure 2.9 shows the combination of suns that for a common ring provides the median gear ratios given in table 1.1.

The graph in figure 2.9 is produced by using equations (2.10) and (2.11). The graph is made by setting the number of teeth on the ring to be 100, iterating the number of teeth on the sun of the first step between 1 and the ring's number of teeth, and after that finding the number of teeth on the second sun to achieve the total gear ratio. The number of teeth on the ring and the first sun gear are the two degrees of freedom for the calculation, while the number of teeth of the second sun is dependent on the other two.

It is shown in figure 2.9 that the two gear ratios do not intersect, even when S_2 is scaled by a factor of $^1/_{100}$. It is through this proven that it is not possible to achieve both of the median gear ratios in table 1.1 with a constant but different number of teeth on the sun gears and a common ring. It is not possible to achieve both of the gear ratios, regardless of the number of teeth on the ring, which only scales the number of teeth required of the suns, while not changing the relations in the graph.

In addition to there being no single combination of gears able to provide the two gear ratios, sun 2 will have to be larger than the ring to achieve high gear, which is not possible for a traditional configuration of a planetary gear-set. The first form of the dual-stage system is therefore not possible to use for the required system of two underdrives. The gear-train will not work for any overdrive- or underdrive-only system, because one gear will always be underdrive, and the high gear always overdrive.

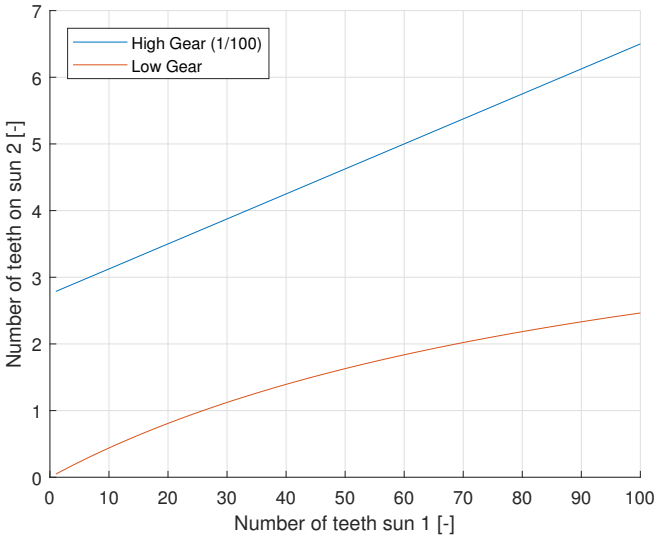

Figure 2.9: Required sun combinations for high and low gear for a ring with 100 teeth in the two-step planetary gearbox. Number of teeth on sun 2 is factored to $^1/_{100}$ for the high gear, sun 1 is unchanged for all cases.

2.4.3 Fixed Gear Ratio Step

The problem of the initial concept using only the modified Simpson gear train is that one gear produces an overdrive, while the other creates an underdrive gear ratio, while the designed gearbox shall have two underdrive gears. The solution to this problem is to add on a fixed gear ratio step (hereafter called "the fixed step") which changes both of the gear ratios to be underdrive.

The fixed step is in this design combined with the connection to the encompassing drum, as the last step of the gearbox. Because the last step must in some way connect to the drum, the ring is suitable to be used as the output to the encompassing drum. The carrier of the fixed step is locked, and is combined with the housing of the fixed step. The input of the fixed step is, therefore, the sun, which is connected to the carrier of the second stage of the modified Simpson's gear-train (hereafter called "the actuated step"). The shaft connecting the fixed step sun and carrier 2 is called the intermediate shaft. The fixed step gear ratio i_F is found by equation (2.12), which is reworked for a locked carrier from equation (2.7).

$$i = \frac{\omega_R}{\omega_S} = -\frac{R}{S} \tag{2.12}$$

The parameters in the equation are:

$\boldsymbol{i}$	Gear ratio	$[-]$
$\boldsymbol{\omega}$	Angular velocity	$[^{rad}/_s]$
$\boldsymbol{R}$	Number of teeth on fixed step ring gear	$[-]$
$\boldsymbol{S}$	Number of teeth on fixed step sun gear	$[-]$

The subscripts indicate the part of the planetary set the parameter refers to.

Equation (2.12) shows that the fixed step reverses the input and output. The reversing never changes, which means that the motor has to turn with opposing direction to the rotation of the drum.

The reason for locking the carrier is to allow it to be part of the housing, which allows access to the other end of the fixed step because there are no moving parts on the housing or around it. A rotating carrier would not allow external bypass, or passable areas in the housing.

2.4.4 Gear Ratio of Final Concept

The gear ratios of the concept of the modified Simpson gear train and the fixed step are shown below. The subscript A is used to indicates the actuated step (Simpson gear train), and F is used for the fixed gear ratio step. L indicates low gear (high gear ratio), and H indicates high gear (low gear ratio). The other subscripts are else like used before, where 1 and 2 indicate which set of the actuated step is referred to, starting from the input.

$$i_L = i_{AL} i_F = \frac{S_1(S_2 + R_A)}{S_2(S_1 + R_A)} \frac{R_F}{S_F} \tag{2.13}$$

$$i_H = i_{AL} i_F = \frac{(R_A + S_2)}{(R_A + S_1)} \frac{R_F}{S_F} \tag{2.14}$$

$\boldsymbol{i}$	Gear ratio	[−]
$\boldsymbol{R}$	Number of teeth on fixed step ring gear	[−]
$\boldsymbol{S}$	Number of teeth on fixed step sun gear	[−]

2.5 Optimization and Selection of Gear Ratios

A Matlab-script (appendix A) was created to find and optimize the gears for the gearbox, aiming to achieve the two gear ratios described in chapter 1.1.

The minimization in the script is done to the sum of the absolute error of the gear ratios E:

$$E = |\Delta i_H| + |\Delta i_L| \tag{2.15}$$

The parameters in the equation are:

$\boldsymbol{\Delta i}$	Difference between achieved and desired gear ratio	$[-]$

The conditions for the minimization are listed below. The parameters in the conditions are:

$\boldsymbol{i}$	Gear ratio	$[-]$
$\boldsymbol{n_P}$	Number of planets	$[-]$
$\boldsymbol{R}$	Number of teeth on ring	$[-]$
$\mathbb{R}$	Real number	$[-]$
$\boldsymbol{S}$	Number of teeth on sun	$[-]$
$\boldsymbol{Z}$	Number of teeth (general)	$[-]$
$\mathbb{Z}$	Integer number	$[-]$
$\boldsymbol{S}$	Number of teeth on sun	$[-]$

C1: All number of teeth Z must be integer and real:

$$C_1 : \qquad Z \in \mathbb{Z} \cup \mathbb{R} \tag{2.16}$$

C2: All number of teeth must be greater than 15, to ensure proper contact ratio:

$$C_2 : \qquad Z \geq 15 \tag{2.17}$$

C3: Meshing gears must be able to mesh, which requires the following condition, which is applied to every gear-set [14]:

$$C_3 : \qquad \frac{S + R}{n_p} \in \mathbb{Z} \tag{2.18}$$

C4: Meshing gears must have coprime number of teeth Z, meaning that the greatest common denominator (gcd) is 1:

$$C_4 : \qquad gcd\{Z_1, Z_2\} = 1 \tag{2.19}$$

The subscript refers to the two meshing gears.

The coprime condition is applied to lessen the impact of any possible faults of a gear. If the number of teeth on meshing gears are coprime, each tooth of each gear will intersect before the pair comes into contact again. If the number of teeth is not coprime, the teeth will intersect with a certain select number of other teeth in a pattern. If there is any fault on one of the teeth of either gear, the fault will for non-coprime numbers continually damage the same teeth.

C5: The ring must be larger than the sun:

$$C_5 : \qquad R > S \tag{2.20}$$

C6: Maximum gear ratio per gear-set i_{set} is 10:

$$C_6 : \qquad i_{set} \leq 10 \tag{2.21}$$

C7: Planets must not interfere with each other, which is ensured by applying the following condition to ever gear-set (proof in calculation 2.3):

$$C_7 : \qquad P \leq SF \sin\left(\frac{360}{2n_P}\right)\left(\frac{R+S}{2}\right) \tag{2.22}$$

A safety factor SF of *0.9* is used against the interference of the planets. The reason for using a safety factor is that the number of teeth is related to the pitch radius of the gears while the addendum radius (radius to top of teeth) is larger.

There is given a defined number of results, sorted from best to worse. The user will need to select how many planets the planetary steps shall utilize based on a scoring system, which indicates if the combination fulfills the two requirements for the planets.

Calculation 2.3: Proof of constraint for planet interference.

This calculation proves the maximum number of teeth the planets can have before they interfere with each other. The figure below illustrates the geometric relations.

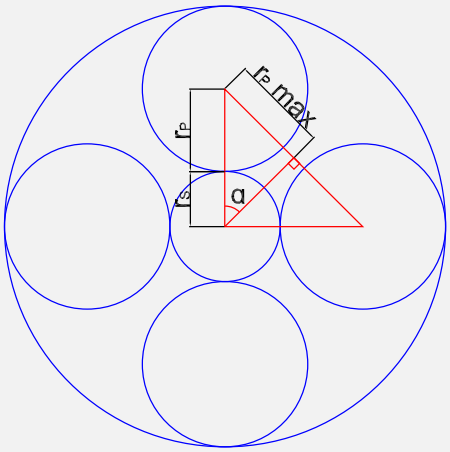

Figure 2.10: Illustration of geometry for control of planet interference.

$$r_{p,max} = \sin(\alpha)(r_S + r_P) \qquad ; r_P = \frac{r_R - r_S}{2}$$

$$r_{p,max} = \sin(\alpha)\left(r_S + \frac{r_R - r_S}{2}\right) \qquad ; \alpha = \frac{360}{2n_P}$$

$$r_{p,max} = \sin\left(\frac{360}{n_P}\right)\left(\frac{r_S}{2} + \frac{r_R}{2}\right) \qquad ; r = \frac{d}{2} = \frac{Zm}{2}$$

$$P_{max}\frac{m}{2} = \sin\left(\frac{360}{n_P}\right)\left(\frac{S}{2}\frac{m}{2} + \frac{R}{2}\frac{m}{2}\right)$$

$$P_{max} = \sin\left(\frac{360}{n_P}\right)\left(\frac{S}{2} + \frac{R}{2}\right)$$

The parameters in the calculation are:

$\boldsymbol{\alpha}$	Half of angle between planet centers	$[deg]$
$\boldsymbol{d}$	Diameter	$[mm]$
$\boldsymbol{m}$	Module	$[mm]$
$\boldsymbol{n_P}$	Number of planets	$[-]$
$\boldsymbol{P}$	Number of teeth on planet	$[-]$
$\boldsymbol{r}$	Radius	$[mm]$
$\boldsymbol{R}$	Number of teeth on ring	$[-]$
$\boldsymbol{S}$	Number of teeth on sun	$[-]$
$\boldsymbol{Z}$	General number of teeth	$[-]$

The subscripts indicate the part of the planetary set the parameter refers to.

2.6 Defining Features of Gears

The module of a gear decides its dimensions. The module must be equal for all gear in contact with each other. If the module of the gears is different, the gears may not be able to interact correctly.

2.6.1 Diameter of Gears

The diameter of a gear is based on the number of teeth and the module.

$$d = Zm \tag{2.23}$$

The parameters in the equation are:

$\boldsymbol{d}$	Diameter	$[mm]$
$\boldsymbol{m}$	Module	$[mm]$
$\boldsymbol{Z}$	Number of teeth	$[-]$

2.6.2 Width of Gears

The face width of a gear (width of the spur gear) is decided based on the module and a factor, and is found through equation (2.24).

$$b = \lambda m \tag{2.24}$$

The parameters in the equation are:

$\boldsymbol{b}$	Face width	$[mm]$
$\boldsymbol{\lambda}$	Tooth width factor	$[-]$
$\boldsymbol{m}$	Module	$[mm]$

The tooth width factor λ is decided according to table 2.1.

Table 2.1: Tooth width factor.
Reproduced from table 4.9 in 'Maskinkonstruksjon 2' [15].

Type of gear	λ
Embedded gears	30
Gears mounted closely to supports	15
Gears for simple applications	8

For the gearbox in this thesis, $\lambda = 15$.

2.7 Gear Tooth Stress Analysis

The calculations for this chapter were performed by the Matlab script in appendix B.

The bending and contact stresses in the gear-teeth were used to find the modules of the gears so that the gear teeth will not bend to breaking, or otherwise be subject to surface pitting due to the contact stress. The stresses for all integer modules from 1 to 10 were tested. The resulting modules of the gears were chosen to be the lowest allowable so that both the bending and contact stresses are within limits.

The teeth stresses were tested for nominal torque and speed from the motor, 625Nm at 2000rpm, with a safety factor of 1.15. The tables and values described in this section are for spur gears with a pressure angle of 20°, and full-depth teeth, corresponding to what is used in the gearbox.

2.7.1 Gear Tooth Velocity

The peripheral velocity of the contacting teeth is found through equation (2.1), which is reproduced in a specific form below.

$$v_P = 2v_C \tag{2.25}$$

The parameters in the equation are:

$\boldsymbol{v_P}$	Peripheral velocity of planet at gear contact	$[m/s]$
$\boldsymbol{v_C}$	Peripheral velocity of carrier (center-point of planet)	$[m/s]$

The relevant gear contact of the planet is towards the non-locked part (ring or sun), where the velocity is equal for both of the meshing gears. The velocities are only definable when either the sun or ring is locked, and the gears are therefore only analyzed for the defined gear ratios.

2.7.2 Lewis Bending Stress

The bending stress in the teeth may be found using Lewis' equation, shown in equation (2.26), which is gotten, with its sub-parts, from Budynas & Nisbett [16].

$$\sigma_L = \frac{K_v F_t}{bmY} \tag{2.26}$$

$K_v\,[-]$ is the velocity factor

$$K_v = \sqrt{\frac{5.56 + \sqrt{v}}{5.56}} \tag{2.27}$$

The parameters in the equations are:

b	Face width of teeth	$[mm]$
F_t	Tangential force on the teeth	$[N]$
m	Module	$[mm]$
σ_L	Lewis' bending stress	$[MPa]$
v	Peripheral velocity of gears at pitch diameter	$[^m/_s]$
Y	Lewis form factor, from tables, (table 2.2)	$[-]$

Table 2.2: Lewis form factor Y for pressure angle of 20°.
Reproduced from table 14-2 in 'Shigley's Mechanical Engineering Design' [16].

Number of teeth	**Y**	**Number of teeth**	**Y**
12	0.245	28	0.353
13	0.261	30	0.359
14	0.277	34	0.371
15	0.29	38	0.384
16	0.296	43	0.397
17	0.303	50	0.409
18	0.309	60	0.422
19	0.314	75	0.435
20	0.322	100	0.447
21	0.328	150	0.46
22	0.331	300	0.472
24	0.337	400	0.48
26	0.346	Rack	0.485

When finding the Lewis form factor from table 2.2, any number of teeth not in the table must be interpolated for. The proper equation for finding the factor may also be used, though is not considered necessary for this thesis, and is therefore not included.

Through equation (2.26) and table 2.2 it is deduced that the Lewis bending stress will be worse the smaller the gear is. The equation was therefore applied only to the pinion in each planetary stage of the gearbox (lowest Lewis form factor), which is the critical part.

Allowable Bending Stress

The allowable bending stress is found through the manufacturer or standard tables. For example ISO 6336-5 [17], which is used for this thesis.

If the allowable bending stress must be estimated, it may generally be set to $^1/_3\sigma_{ut}$. Which is a third of the ultimate tensile strength of the material. [18]

2.7.3 Hertz Contact Stress

Hertz' equation gives the surface contact stress in the teeth. Hertz' equation is shown in equation (2.28), which is gotten, with its sub-parts, from Juvinall & Marshek [19].

$$\sigma_C = C_p \sqrt{\frac{F_t}{b d_p G} K_v K_o K_m} \tag{2.28}$$

$C_p\,[\sqrt{MPa}]$ is the elastic coefficient

$$C_p = 0.564 \sqrt{\frac{1}{\frac{1-\nu_p^2}{E_p} + \frac{1-\nu_g^2}{E_g}}} \tag{2.29}$$

$G\,[-]$ is the geometry factor

$$I = \frac{\sin\phi \cos\phi}{2} \frac{k_d}{k_d + 1} \tag{2.30}$$

k_d is a relation between the gear and pinion

$$k_d = \frac{d_g}{d_p}$$

The parameters in the equations are:

$\boldsymbol{b}$	Face width of teeth	$[mm]$
$\boldsymbol{d}$	Pitch diameter of gear	$[mm]$
$\boldsymbol{E}$	E-modulus, subscript indicates pinion or gear	$[MPa]$
$\boldsymbol{F_t}$	Tangential force on the teeth	$[N]$
$\boldsymbol{K_v}$	Velocity factor, found through equation (2.27)	$[-]$
$\boldsymbol{K_o}$	Overload factor, from tables, (table 2.3)	$[-]$
$\boldsymbol{K_m}$	Mounting factor, from tables, (table 2.4)	$[-]$
$\boldsymbol{\nu}$	Poisson's ratio	$[-]$
$\boldsymbol{\sigma_H}$	Hertz' contact stress	$[MPa]$

Subscript *'g'* indicates gear and *'p'* indicates pinion.

As for the bending stress, the contact stress is apparently most significant in the teeth of the pinion of a meshing pair of gears. The smallest gear is, therefore, the tested one in each stage of the planetary gearbox, whether that is the sun or planets.

Allowable Contact Stress

As for the bending stress, the allowable surface stress is found through the manufacturer or standard tables. For example ISO 6336-5 [17], which is used for this thesis.

If tables are not available, the allowable surface pressure may be estimated by relating it to the hardness of the material. For steel, the allowable surface stress is given by equation (2.31), which is gotten from [20].

$$\sigma_{es} = 2.75 \cdot BHN - 70 \tag{2.31}$$

The parameters in the equation are:

$\boldsymbol{BHN}$	Brinell hardness	$[^{kgf}/_{mm^2}]$, $[^{kgf}/_{mm^2}]$
$\boldsymbol{\sigma_{es}}$	Allowable surface stress	$[MPa]$

The above equation is only applicable for BHN <350. After which experimental data must be used. [20]

Mounting and Overload Factor for Contact Stress

The tables below show the mounting and overload factors used for the contact stress.

Table 2.3: Overload factor K_o.
Reproduced from table 15.1 in 'Fundamentals of Machine Component Design' [19].

	Load behavior		
Source behavior	**Uniform**	**Moderate shock**	**Heavy shock**
Uniform	1.00	1.25	1.75
Light shock	1.25	1.50	2.00
Heavy shock	1.50	1.75	2.25

Table 2.4: Mounting factor K_m.
Reproduced from table 15.2 in 'Fundamentals of Machine Component Design' [19].
Converted from inches to mm by factor 25.4 $[^{mm}/_{inch}]$.

	Face width $[mm]$			
Mounting characteristics	**0 - 50.8**	**152.4**	**228.6**	**406.4 ->**
Accurate	1.3	1.4	1.5	1.8
Less accurate, full contact on face width	1.6	1.7	1.8	2.2
Lesser accuracy, not full contact on face width	> 2.2			

The gears are required to be mounted accurately, thus using the first row of factors from table 2.4 for determining the mounting factor. The factor still changes with the number of teeth.

The torque source (motor) is deemed to deliver uniform torque. The load (AWE) is expected to, at times, produce moderate shocks. The overload therefore being 1.25.

2.8 Contact Ratio and Interference of Gears

The calculations for this chapter were performed by the Matlab script in appendix B.

When the gears mesh together while rotating, at least one tooth from each cog must be in contact at any time, so that the mechanical connection is maintained. The contact ratio gives a measure of how many teeth are in contact at any time. The contact ratio should be greater than 1.5, because this will make the force transmitted between the teeth distribute over more than one set of teeth. [19]
In addition to the contact ratio being high enough, the meshing gears must also not interfere with each other beyond the intended contact about the pitch circle. Interference will mean that the tip of the gear teeth are longer than what there is room for. [19]

2.8.1 Contact Ratio

Equation (2.32) finds the contact ratio Cr between two meshing gears. [19]

$$Cr = \frac{\sqrt{r_{ap}^2 - r_{bp}^2} + \sqrt{r_{ag}^2 - r_{bg}^2} - c\sin\phi}{p_b} \tag{2.32}$$

p_b $[mm]$ is the base pitch

$$p_b = \frac{\pi d_b}{Z} = \frac{\pi d\cos\phi}{Z} \tag{2.33}$$

r_a $[mm]$ is the addendum radius

$$r_a = r + m \tag{2.34}$$

r_b $[mm]$ is the base circle radius

$$r_b = r\cos\phi \tag{2.35}$$

c $[mm]$ is the center distance between the gears

$$c = r_p + r_g \tag{2.36}$$

The parameters in the equations are:

$\boldsymbol{Cr}$	Contact ratio	$[-]$
$\boldsymbol{d}$	Diameter	$[mm]$
$\boldsymbol{\phi}$	Pressure angle	$[deg]$
$\boldsymbol{r}$	Radius, where subscript indicated pinion or gear	$[mm]$
$\boldsymbol{m}$	Module	$[mm]$

Subscript *'g'* indicates gear and *'p'* indicates pinion.

Internal Gears

For internal gears (the ring), the contact ratio is found by the equation below [21]:

$$Cr = \frac{\sqrt{r_{ap}^2 - r_{bp}^2} - \sqrt{r_{ag}^2 - r_{bg}^2} + c\sin\phi}{p_b} \tag{2.37}$$

c $[-]$ is

$$c = r_p - r_g \tag{2.38}$$

2.8.2 Interference

The safety against interference is found by finding the largest allowable addendum-radius of the gears, and testing that it is larger than the actual addendum-radius. Equation (2.39) finds the maximal addendum-radius. [19]

$$r_{a,max} = \sqrt{r_b^2 + c^2\sin(\phi)^2} \tag{2.39}$$

The parameters of the equation are:

$\boldsymbol{r_{a,max}}$	Maximum addendum radius of gear	$[mm]$
$\boldsymbol{r_b}$	Base radius of gear	$[mm]$
$\boldsymbol{\phi}$	Pressure angle	$[deg]$
$\boldsymbol{c}$	Center-distance between gears	$[mm]$

For the internal gears, the interference should be of no concern. According to Maitra [22], there is usually no interference for internal gears when the internal gear (ring) has a difference of teeth greater than 10 to the pinion (planet). The difference is always greater in this gearbox, and will usually be so for planetary gearboxes.

2.9 Result of Gear Design

All the calculations for the gear teeth were performed by the Matlab script presented in appendix B.

2.9.1 Gear Materials

For the gears, case hardened wrought steel is used with MQ manufacturing and core hardness $>$ 30 HRC (Rockwell hardness) according to ISO 6336-5 [17].
"MQ stands for requirements that can be met by experienced manufacturers at moderate cost." [17]

The properties of the gear-steel are shown below; the steel is selected to have generic values for elasticity. The density is used in accordance with the density of standard alloy steel in *Autodesk Inventor* where the parts were designed.

Table 2.5: Steel properties for gears.

Parameter	**Value**	**Unit**
Allowable bending stress σ_L:	500	$[Mpa]$
Allowable contact stress σ_H:	1500	$[Mpa]$
E-modulus:	210 000	$[MPa]$
Poisson's ratio	0.3	$[-]$
Density:	7730	$[kg/m^3]$

2.9.2 Gear Dimensions

The properties of the designed gears are shown in table 2.6.

Table 2.6: Result-parameters for gears.

	Actuated Step						**Fixed Step**			**Total**
	Stage 1			**Stage 2**						
Gear	R_1	S_1	P_1	R_2	S_2	P_2	R_F	S_F	P_F	
Z	121	87	17	121	15	53	86	16	35	
n_P			4			3			3	
i_L	3.7923						-5.3750			-20.3837
i_H	0.6538						-5.3750			-3.5144
m	3			3			5			
d	363	261	51	363	45	159	430	80	175	
b	45			45			75			
Cr	1.67			1.62			1.59			
		12.22			7.93			5.98		
Δr_a	0.22	29.98		15.29	-0.05		12.57	0.57		
$\sigma_{L_{Low}}$	23.53			146.01			118.46			
$\sigma_{L_{High}}$	23.53			31.3773			23.41			
$\sigma_{H_{Low}}$	232.16			1126.20			1008.90			
$\sigma_{H_{High}}$	232.16			522.04			448.50			

The parameters in the table are:

b	Face width	$[mm]$
Cr	Contact ratio	$[-]$
d	Pitch diameter	$[mm]$
Δr_a	Safety between maximum and actual addendum	$[mm]$
i_L	Gear ratio for low gear	$[-]$
i_H	Gear ratio for high gear	$[-]$
m	Module	$[-]$
n_P	Number of planets	$[-]$
P	Planet	$[-]$
R	Ring	$[-]$
S	Sun	$[-]$
σ_L	Lewis bending stress in gear teeth for critical gear	$[MPa]$
σ_H	Hertz contact stress in gear teeth for critical gear	$[MPa]$

The subscripts of the number of teeth indicate the part of the gear train the parameter refers to.

The width of the gears is given per set because they should be equally wide. The ring is common for both actuated steps, and must necessarily minimum cover both the sets.

As seen in table 2.6, the addendum radius of S_2 is larger than allowable. The teeth on S_2 must, therefore, be stubbed, to make them shorter. The stubbing should have no discernible impact on the stresses in the teeth, because of the safety factor and how little reworking is required to meet the requirement of the addendum.

3 | Design of Brakes & Actuators

The calculations for this chapter were performed by the Matlab script in appendix B.

The gearbox shall be actuated to be able to change gears. The actuator system shall do this by locking either the ring or the sun shaft. The system is, therefore, a brake system, which is a system that absorbs the kinetic energy of a moving body, and connects the body to another fixed body [23].

The system requires that the brakes must be able to stop the rotating ring or sun-shaft and hold it in place. The brakes must be able to hold at full torque input which is the same as used for the gearbox dimensioning, given in table 1.1.

3.1 Brake Design

3.1.1 Overview of Brake Systems

There were considered 3 different brake types for the application:

- Band or drum brake
- Disc or cone brake
- Dog clutch

Band or drum brakes work by a band or shoe pressing radially on the peripheral surface of a rotating disc and braking the rotation through friction. A band brake uses a band with friction material on it that encompasses a portion of the disc surface, and a tightening mechanism that increases the friction force to the disk when activated. A drum brake uses the same principle as the band brake, except that the drum disc is braked by forcing a shoe, which is a rigid friction element onto the drum from the outside or the inside. [23]
The braking power of a frictional penalty will increase with the surface area of the contact, and the moment arm of the brake. [19]

Disc and cone brakes work in the same way, by pressing together two circular surfaces axially, where one of them has friction material on it. A disk brake uses two disks, whose intersecting surfaces are parallel to each other and perpendicular to the shafts they are mounted on. A cone brake uses the periphery of the disc rather than the side of it. The periphery surface is though made to be a cone shape, so that the surfaces of the two discs intersect when they are axially moved towards each other. [19]

A cone clutch is illustrated in figure 3.1, where the working principle is equal for a brake. To increase the braking power of disc or cone brakes the surface area of the contact must be increased, like the band or drum brakes. The surface area may also be increased by placing multiple stages of braking in series. A multi-plate disc brake will use multiple plates, both for the fixed and the moving component, and actuates the brake by pushing all of the discs together. An advantage of a disc brake is that parallel discs utilize most of their surface area for braking, while each disc is relatively thin (approximately 1.5mm [19]), which makes it possible to increase the braking ability formidably without increasing the size of the system significantly. A cone brake does not use as significant a portion of the available surface on the disc, and therefore increases its space requirement faster than the disc brake.

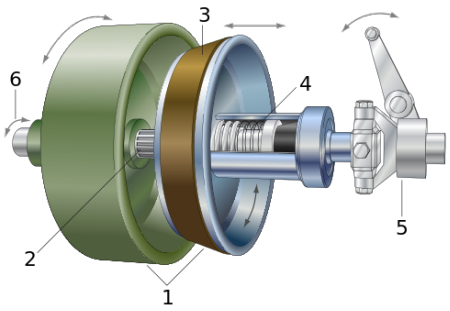

Figure 3.1: Illustration of cone clutch. (3) is the friction surface. Adapted from Sweber [24] with permission [25].

Dog clutches are discs that mesh mechanically to connect the parts, rather than using friction like the band, drum, disc, or cone brakes. As seen in figure 3.2, the two discs have dogs, or teeth, that are meshed when the discs are connected, i.e., that the brake is engaged. A dog clutch is a binary system, meaning that it is either engaged or disengaged. If the dogs are able to mesh, there is required little to no force to hold the connection; the necessary force does not increase with the braking power required either. There is also no chance of slip when the connection is made, unless there is a mechanical failure [16]. Engaging the discs while their velocities differ may significantly damage the dogs.

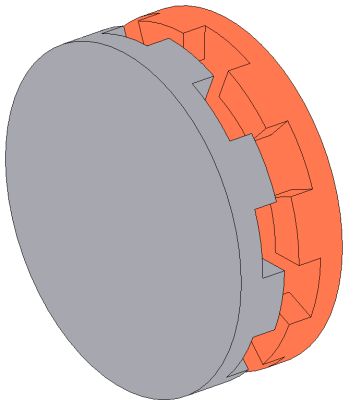

Figure 3.2: Illustration of dog clutch.

A dog brake may, however, be added upon to be a synchromesh system, where the dogs are engaged to each other only after the two discs maintain the same velocity. The engagement is done by first engaging friction surfaces, to synchronize the velocities, for then to slide the dogs to mesh. [26]
The friction surfaces for synchronizing may either be an independent or dependent system. A dependent system is when a cone brake that engages just before the dogs by the same motion. An independent system actuates the dogs and friction brakes independently.

The environment for the brakes is a factor that must be considered, especially for friction brakes. The friction coefficient of a material will change depending on the fluid that its surface is in contact with. The environment of the brakes may be dry or wet. A dry environment is when there is no liquid on it, i.e., it is located in an environment of air. A wet environment means that the friction contact has a liquid, typically oil, applied to it. A dry environment will make the brake capacity greater, because the friction coefficient is higher, while a wet brake will have reduced wear, and should be easier to keep cool through the oil. [23]

3.1.2 Selection of Brake System

A goal of the thesis is for the gearbox to be able to change between gears while the input and output are rotating and subject to a load. A dog clutch is therefore not usable by itself, because frictional penalties are required to slow down the parts before locking them.

Multi-disc brakes are used for both the ring and sun shaft, because the brake system itself may be fully in-line and encompassing the shafts they shall be mounted to. A cone brake would also accomplish this, but is considered to require to much space. The loads from a disc brake are pure torque (except for the weight), requiring no more from the bearings and fixings than for the gearbox itself. Drum and band brakes are considered to require too much space relative to the disk brakes. A band brake or single-side shoe drum brake would also apply a radial force on the shaft when the brakes are applied.

The ring brake is wet, the main reason being that the simplest location for it is within the housing of the actuated step of the gearbox, which shall be filled with oil for cooling. The sun shaft of the actuated step, however, was not found to be readily accessible from the actuated step housing, but is accessible by letting the shaft go through the interior of the intermediate shaft going to the fixed step, to then be located in its own compartment. This compartment, and therefore also the sun brake, is designed to be dry, to avoid sealing and bringing oil to it.

3.1.3 Brake Dimensioning

There are two methods for finding the brake disc parameters. The first is assuming that there is a uniform wear rate on the friction surface of the discs, while the other is assuming a uniform distribution of pressure across the friction surface.

The critical assumption is the one that gives the lowest torque capability on each friction surface, thus requiring more surfaces to handle the load. [23]

The surfaces were dimensioned for both assumptions, and the critical result was chosen from the two, to make the calculations conservative

Required Brake Torque

Equal for both of the methods is the torque that the brakes are required to hold. The torque required to hold the sun is found through equation (3.1), and for the ring through equation (3.2).

$$T_{S(required)} = SF \cdot T_M i_{SA} = SF \cdot T_M \frac{S_1}{R_A + S_1} \tag{3.1}$$

$$T_{R(required)} = SF \cdot T_M i_{RA} = SF \cdot T_M \frac{R_A}{R_A + S_1} \tag{3.2}$$

The parameters in the equations are:

$\boldsymbol{i}$	Gear ratio	$[-]$
$\boldsymbol{R}$	Number of teeth on ring	$[-]$
$\boldsymbol{S}$	Number of teeth on sun	$[-]$
$\boldsymbol{SF}$	Safety factor	$[-]$
$\boldsymbol{T_M}$	Input torque	$[Nm]$
$\boldsymbol{T_R}$	Stopping torque for ring gear (low gear)	$[Nm]$
$\boldsymbol{T_S}$	Stopping torque for sun shaft (high gear)	$[Nm]$

The subscripts of the number of teeth indicate the part of the actuated step the parameter refers to.

The gear ratios are the gear ratios for the first gear-set, which are gotten from equation (2.8) and (2.9).

The safety factor is set to 1.5, which is used in addition to the safety given for the gearbox requirements in chapter 1.1.

Brake Disk Dimensioning

The number of friction surfaces required to stop and hold the torques is decided by what each friction surface can stop by itself. What each surface is capable of stopping is decided by equation (3.3) for uniform wear, and equation (3.4) for uniform pressure. [23]

$$T_{max/surface} = \frac{\pi}{8}\mu p_{max} d_i (d_o^2 - d_i^2) \tag{3.3}$$

$$T_{max/surface} = \frac{\pi}{12}\mu p_{max} (d_o^3 - d_i^3) \tag{3.4}$$

The force required to actuate the brake discs to maximum, which is also the maximum allowable force, should also be known for dimensioning the actuator. Equation (3.5) shows the force for uniform wear, and equation (3.6) shows the force for uniform pressure. [23]

$$F_{max} = \frac{1}{2}\pi p_{max} d_i (d_o - d_i) \tag{3.5}$$

$$F_{max} = \frac{1}{4}\pi p_{max} d_i (d_o^2 - d_i^2) \tag{3.6}$$

The minimum number of discs are found through equation (3.7).

$$n_{plates,min} = \frac{1}{2}\,\frac{T_{required}}{T_{max/disc}} \tag{3.7}$$

The number of discs is halved, because there are two surfaces on each plate.

The maximum braking torque of each brake is found by multiplying the maximum braking torque of each surface with the number of surfaces, as shown in equation (3.8). The applied force required to achieve the required braking torque will be less than the maximum force, due to the maximum braking torque being larger than the required braking torque. The minimum required force to stop the system is found through equation (3.9).

$$T_{max} = T_{max/plate} \cdot n_{plates} \tag{3.8}$$

$$F_{min} = \frac{T_{required}}{T_{max}} F_{max} \tag{3.9}$$

For both the torque and force equations, the parameters are:

$\boldsymbol{d_i}$	Inner diameter of friction material	$[mm]$
$\boldsymbol{d_o}$	Outer diameter of friction material	$[mm]$
$\boldsymbol{F}$	Force	$[N]$
$\boldsymbol{\mu}$	Dynamic friction coefficient	$[-]$
$\boldsymbol{p_{max}}$	Maximum allowable pressure applied to discs	$[MPa]$
$\boldsymbol{T}$	Torque	$[Nm]$

Factors for Disc Brakes

The friction coefficients and maximum pressure were retrieved from tables 13.11 and 13.12 in [23]. The ring brake parameters were selected for wet brakes, and the sun shaft brake parameters for dry brakes, as they were selected to be in chapter 3.1.2. The material was selected to be molded for both brakes, for which the relevant properties are shown in table 3.1. From the source table, the lowest friction coefficients were chosen, to be conservative in the calculations.

Table 3.1: Factors for brake dimensioning.

Parameter	Ring [wet]	Sun [dry]
μ	0.06	0.25
p_{max}	1.03	1.03

The parameters in the table are:

$\boldsymbol{\mu}$	Dynamic friction coefficient	$[-]$
$\boldsymbol{p_{max}}$	Maximum allowable pressure on discs	$[MPa]$

3.2 Result of Brake Design

The properties of the brakes that are shown in table 3.2.

Table 3.2: Result parameters for brakes.

Parameter	**Brake**	
	Ring	**Sun**
$\boldsymbol{n_{plates}}$	1	1
$\boldsymbol{d_o}$	370.00	250.00
$\boldsymbol{d_i}$	260.00	150.00
$\boldsymbol{T_{required}}$	627.18	450.95
$\boldsymbol{T_{delivered,max}}$	874.55	1213.44
$\boldsymbol{F_{max}}$	46272.52	24268.80
$\boldsymbol{F_{min}}$	33184.05	9018.93
$\boldsymbol{\mu}$	0.06	0.25
$\boldsymbol{p_{max}}$	1.03	1.03
Critical assumption	Uniform wear	Uniform wear
Type	Wet	Dry
Material	Molded	Molded
SF	1.5	1.5

The parameters in the table are:

$\boldsymbol{d_i}$	Inner diameter of disks	$[mm]$
$\boldsymbol{d_o}$	Outer diameter of disks	$[mm]$
$\boldsymbol{F_a}$	Actuation force	$[N]$
$\boldsymbol{\mu}$	Dynamic friction coefficient	$[-]$
$\boldsymbol{n_{plates}}$	Number of disks (two-sided)	$[-]$
$\boldsymbol{p_{max}}$	Maximum surface pressure on disks	$[MPa]$
$\boldsymbol{T_{delivered}}$	Torque capability of brakes	$[Nm]$
$\boldsymbol{T_{required}}$	Torque required of brakes	$[Nm]$

3.3 Actuator Design

3.3.1 Overview of Actuator Systems

The brakes require an actuating force to be applied. There were considered three methods of delivering this force:

- Electro-mechanical
- Hydraulic
- Self-contained electro-hydraulic

Electro-mechanical actuation could be done through some different methods. The result is either way that the actuator must deliver the required force and linear stroke through a mechanical connection. Two methods of electric actuation were considered; Rotational and electromagnetic force (solenoid). A rotational actuator is a conventional motor, which would be combined with a rack and pinion, or screw to create linear movement. A solenoid is an electro-magnet pushing on a plunger, which produces linear movement directly.

The advantage of electromechanical actuation is that there is no chance of oil leaks. It is also little to no maintenance on an electric actuator. An electro-mechanical system is also assumed to be easier to model and control than a hydraulic system, because a hydraulic system will likely be non-linear, while an electric system is linear.

Hydraulic actuation works by a pressure/flow source delivering hydraulic power to a cylinder, where the piston is connected to the actuated component (for this case, the brake). The advantage of a hydraulic system is that it can deliver more power than any other system [27], and can be fairly compact while doing so. The hydraulic power unit (HPU) may also be placed away from the cylinder, connected only by pipes or hoses.

Self-contained electro-hydraulic actuators use an electric actuator to create fluid-pressure in a system, which then converts and transmits the power to the external connection. A self-contained hydraulic system shares many of the advantages of other fluid systems. The self-contained system should though not be susceptible to leaks, and does not require an external pressure/flow source.

3.3.2 Selection of Actuator System

A solenoid was chosen to be used as the actuation for the brakes. The design of the solenoid shall be described in this thesis. The reasons for choosing the solenoid is the ease of control and modeling, ease of design, and low maintenance. The background for this thesis is also the use of electric winches instead of hydraulic, which is brought into the consideration of the actuator.

Through some market research, there was found no readily available electro-mechanical actuator with rotation as a source that could produce the force required while being reasonably small to mount inside or on the gearbox. A self-contained hydraulic system was also discarded for the same reasons.

A hydraulic system with a stand-alone HPU could be made to deliver enough force and be small enough to fit the gearbox. The use of hydraulics would make the system harder to model and control. The advantage of using hydraulics is that the would be less produced heat, at least depending on the system configuration.

3.3.3 Design of Solenoid

The concept design of the electromagnetic actuator is that a core is equipped with permanent magnets, to produce a constant uniform magnetic field. Encompassing the core is a hollow ring on the periphery of which there is wound coils of wire. The wire is lain on the ring perpendicular to the axial direction of the brakes, due to the electromagnetic force acting perpendicularly to the current traveling in the wire. A cross-section view of the concept is shown in figure 3.3, where the core is also hollow to allow for the shaft of the rotating part to go through it.

The direction of the force is related to the direction of the current. The direction of the force is shown in figure 3.3. [28]

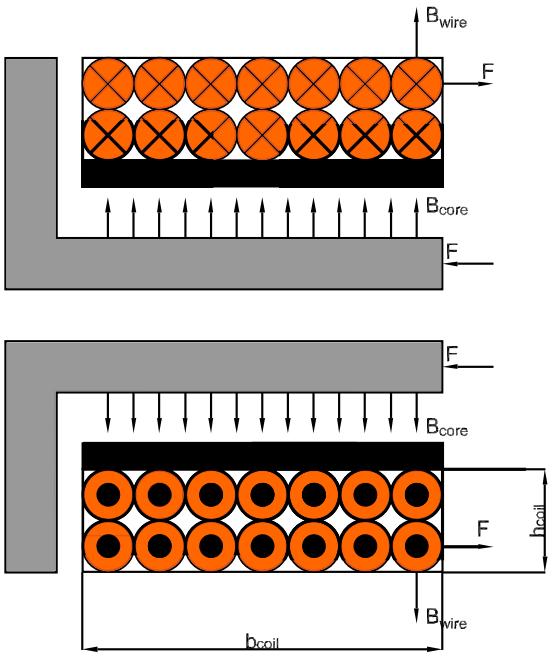

Figure 3.3: Cross section of concept for electromagnetic actuator. Crosses indicate inwards, and dots outwards.
Orange = Wire
Gray = Core
Black = Casing

The amplitude of the electromagnetic force acting on the core is found through equation (3.10), which is gotten from Mohan [28]. Because the direction and amplitude of the current are the controllable parameters, the current must be DC for directional control.

$$F_{em} = B\ I\ l \tag{3.10}$$

The parameters in the equation are:

$\boldsymbol{F_{em}}$	Force acting on core	$[N]$
$\boldsymbol{B}$	Flux density of core	$[T]$
$\boldsymbol{I}$	Current in wire	$[A]$
$\boldsymbol{l}$	Length of wire	$[m]$

There is one wire going about the casing, with multiple turns. The area of the cross-section was defined to decide how many turns there is space for, and the length of the wire was thus found through the number of turns and the circumference of the average diameter. The length of the wire for both actuators was found using equation (3.11).

$$l_{wire} = n_{wires} \cdot d_{mid}\pi \tag{3.11}$$

d_{mid} $[m]$ is the average diameter of the wire coils.

$$d_{mid} = \frac{d_o + d_i}{2} \tag{3.12}$$

n_{wires} $[-]$ is the number of wires in the cross-section area.

$$n_{wires} = \frac{A_{crosssection}}{A_{wire,square}} \tag{3.13}$$

$A_{crosssection}$ $[m]$ is the cross-sectional area of the coil.

$$A_{crosssection} = \frac{d_o - d_i}{2} \cdot b_{coil} \tag{3.14}$$

The parameters in the equations are:

$\boldsymbol{A_{wire,square}}$	Square cross-sectional area of wire	$[m^2]$
$\boldsymbol{b_{coil}}$	Width of cross section of coil	$[m]$
$\boldsymbol{d_i}$	Inner diameter of coil	$[m]$
$\boldsymbol{d_o}$	Outer diameter of coil	$[m]$
$\boldsymbol{l_{wire}}$	Length of wire	$[m]$

$A_{wire,square}$ is the equivalent area that each wire-pass requires of the cross-section area of the coil when the wires are stacked like shown in figure 3.3. The equivalent area is the area of a square where each side is the length of the diameter of the wire.

The dimensions for each actuator was made as large as reasonable within the space of the existing geometry of the gearbox. Equation (3.10) was solved for the current, because B is constant for permanent magnets, and is given by the producer or standards, and the dimensions of the brake give the necessary force (table 3.2).

The calculations for the wire assumes that the enameled wire has an outer diameter equal to the diameter of the copper. The real outer diameter will be slightly larger, but does not change the force-properties of the actuator, only the physical dimensions of the actuator. Due to the theoretical nature of the thesis, the real diameter is neglected.

When the magnetic fields move relative to each other, i.e., that the core of the actuator is put into motion, there will be an induced electromotive force that the electricity must combat. [28]
The is however expected little to no movement in this system when the force is applied. The stroke of the brakes is small ($\leq 10mm$) and the actuator does not need to exceed any large force until the brakes are at near standstill. The electromotive force is therefore neglected, because of negligible movement speed.

3.3.4 Maximum Force & Electrical Current in Solenoid Coil

The maximum force allowed for the brakes may not be exceeded, because the brake discs may fail. The relation between force and current for the electromagnetic actuator described here is linear. The allowable current is therefore found by the equation below.

$$I_{max} = I_{min}\frac{F_{max}}{F_{min}} \tag{3.15}$$

The parameters in the equation are:

$\boldsymbol{F}$	Force	$[N]$
$\boldsymbol{I}$	Current	$[A]$

3.3.5 Temperature Considerations for Solenoid Coil

The current flowing through the wire of the actuators will create heat, which may cause the copper wiring, or the parts around it, to take damage. For this thesis, only the melting temperature of the coating on the copper is considered, which is assumed to be the critical component for temperature.

By knowing the losses in the wire due to the resistance, and the maximum allowable temperature increase, it is possible to calculate the time it takes for the temperature to become critical.

The heat produced from a material is given by equation (3.16) [29]. Equation (3.17) shows Joule's law, which was combined with equation (3.16) to create the expression for the time required for the material to increase its temperature in equation (3.18).

$$Q = c \cdot m \cdot \Delta T \tag{3.16}$$

$$Q = Pt \tag{3.17}$$

$$t = \frac{c \cdot m \cdot \Delta T}{P} \tag{3.18}$$

The parameters in the equation are:

$\boldsymbol{c}$	Specific heat capacity of material	$[^{J}/_{kgK}]$
$\boldsymbol{\Delta T}$	Change in temperature	$[K]$, $[C]$
$\boldsymbol{m}$	Mass of material	$[kg]$
$\boldsymbol{P}$	Power lost to material	$[W]$
$\boldsymbol{Q}$	Heat in material	$[J]$
$\boldsymbol{t}$	Time	$[s]$

The mass of the material (the wire) is calculated using equation (3.19).

$$m = lAD \tag{3.19}$$

The parameters in the equation are:

$\boldsymbol{A}$	Area of wire	$[m^2]$
$\boldsymbol{D}$	Mass density of wire	$[^{kg}/_{m^3}]$
$\boldsymbol{l}$	Length of wire	$[m]$
$\boldsymbol{m}$	Mass of wire	$[kg]$

The power lost to the wire is calculated using equation 3.20.

$$P = RI^2 \tag{3.20}$$

R is the resistance of the wire

$$R = \rho\frac{l}{A} \tag{3.21}$$

The parameters in the equations are:

$\boldsymbol{A}$	Area of wire	$[m^2]$
$\boldsymbol{I}$	Current through wire	$[A]$
$\boldsymbol{l}$	Length of wire	$[m]$
$\boldsymbol{P}$	Power loss in wire	$[W]$
$\boldsymbol{R}$	Resistance in wire	$[\Omega]$
$\boldsymbol{\rho}$	Resistivity of wire material	$[\Omega m]$

The resistivity of the material will increase with the temperature. The base resistivity is given for $20°C$, which is used for any event for this case because the cooling properties are unknown and it is not within the scope of the thesis to design it.

3.4 Result and Realization of Actuator Design

The design of the actuator is shown in figure 3.4.

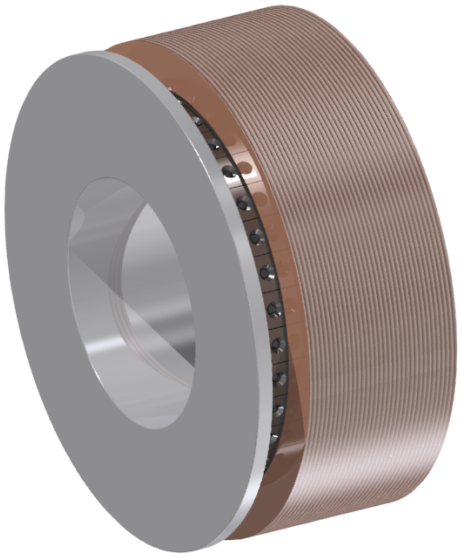

Figure 3.4: Design of solenoid actuator.
Brown = Coil.
Gray (light) = Plunger.
Gray(dark) = Neodymium magnets.

The wiring for the coils is a copper wire supplied by the LWW group, named DAMID-BOND 200 [30], which datasheet is shown in appendix I. The allowable temperature of which is $200°C$. The temperature increase is limited to $100°C$, to ensure that the brakes do not overheat. The resistivity for equation (3.21) is gotten from the product datasheet [30].

All the non-electric properties of copper are gotten from [29].

The core of the actuator is assumed to be an ideal neodymium magnet of the grade IEC 60404-8-1 - 360/90, which has a flux density of 1.35 T.

The cross-sectional area that the coil covers assume that the wires are stacked perfectly orthogonally, as shown in figure 3.3. The wire will likely not be wound like the case presented here, but rather tighter so that the gaps are filled. The area covered by the coil should, therefore, be less in reality, which however compensates for the slight increase in the area that the enamel on the wires will add to the copper's cross-section. Only the copper's cross-section area is used for the calculations here.

Table 3.3: Result of electromagnetic actuator design.

Parameter	**Actuator**	
	Ring	**Sun**
$\boldsymbol{d_o}$	400.00	270.00
$\boldsymbol{d_i}$	260.00	150.00
$\boldsymbol{b_{coil}}$	30.00	25.00
$\boldsymbol{d_{wire}}$	1.00	1.00
$\boldsymbol{l_{wire}}$	2177.12	989.60
$\boldsymbol{B_{core}}$	1.35	1.35
$\boldsymbol{F_N}$	33184.05	9018.93
$\boldsymbol{I_N}$	11.29	6.75
$\boldsymbol{U_N}$	539.56	146.65
$\boldsymbol{\rho}$	$1.724 \cdot 10^{-8}$	$1.724 \cdot 10^{-8}$
$\boldsymbol{R}$	47.79	21.72
$\boldsymbol{P}$	6589.04	1070.77
$\boldsymbol{\Delta T}$	100.00	100.00
$\boldsymbol{c}$	385.00	385.00
$\boldsymbol{D}$	8930.00	8930.00
$\boldsymbol{t_N}$	96.50	269.92
$\boldsymbol{F_{max}}$	46272.52	24268.80
$\boldsymbol{I_{max}}$	15.74	18.17
$\boldsymbol{U_{max}}$	752.38	394.60
$\boldsymbol{t_{@max}}$	49.63	37.28

The parameters in the table are:

$\boldsymbol{b}$	Width of coil	$[mm]$
$\boldsymbol{B_{core}}$	Flux density of core	$[T]$
$\boldsymbol{c}$	Specific heat capacity	$[^{J}/_{kgK}]$
$\boldsymbol{D}$	Volumetric mass density	$[^{kg}/_{m^3}]$
$\boldsymbol{d_o}$	Outer diameter of coil	$[mm]$
$\boldsymbol{d_i}$	Inner diameter of coil	$[mm]$
$\boldsymbol{d_{wire}}$	Diameter of wire	$[mm]$
$\boldsymbol{\Delta T}$	Allowable increase in temperature	$[K]$, $[C]$
$\boldsymbol{l_{wire}}$	length of wire	$[m]$
$\boldsymbol{F}$	Produced force	$[N]$
$\boldsymbol{I}$	Current	$[A]$
$\boldsymbol{\rho}$	Resistivity	$[\Omega m]$
$\boldsymbol{R}$	Resistance	$[\Omega]$
$\boldsymbol{t}$	Time to increase temperature to allowable	$[s]$
$\boldsymbol{U}$	Voltage required to achieve current in wire	$[V]$

Subscript 'N' indicates nominal values, and 'max' indicates maximum allowable values. The nominal values are the ones required for the brakes to meet their required values.

From the results of the electromagnetic actuator in table 3.3, it is seen that the actuation system using brake discs is only able to hold for a limited time before the temperature gets too high. The brake disc system does work, but must be supplemented by another system for steady-state operations.

3.5 Final Design of Actuation System

Since the solenoids cannot hold the brakes infinitely, they must be supplemented by another system. As described in chapter 3.1.2, a dog clutch may be used to lock the parts when firstly the friction brakes have caught the rotating parts. There is required little to no force to actuate dog clutches for steady-state operation. It is assumed that electromagnetic actuators of the kind used for friction brakes could be used for the dogs as well, although they will not be designed in this thesis In the design for this thesis, the system shall be actuated only by the disc brakes and the electromagnetic actuators. The dog clutch system must, however, be implemented unless the cooling issue is otherwise solved. The sequence of the gear-change that should be implemented with the dog clutch is shown in figure 3.5.

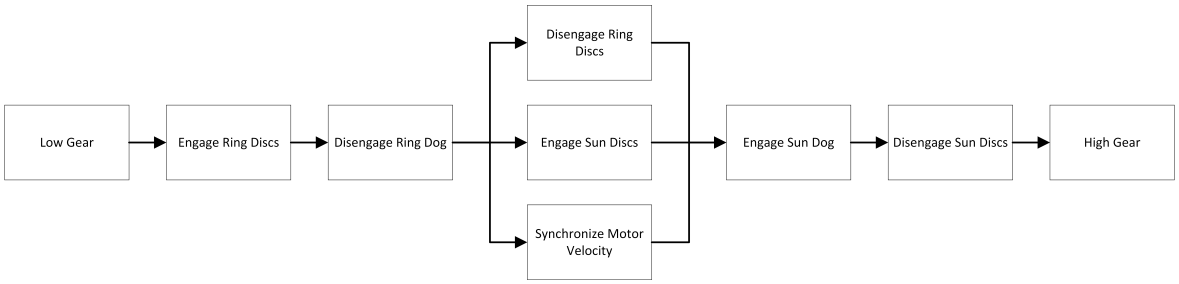

Figure 3.5: Sequence for changing from low to high gear with friction and dog clutches. Opposite gear change uses reverse direction.

The actuators are designed to apply the minimum force required for the brakes to stop their respective parts. This minimum is however for a full load with a safety factor of 15%, and should, therefore, be over-dimensioned to be able to overcome any uncertainties in the design. The power supply for the actuators should, however, be designed to be able to deliver more power than the minimum, in case more should be desired.

Because of the 15% safety factor, 100% of the nominal force from the actuators is higher than what should be required. The two different brakes should, however, reach the real required braking torque at the same time, because of the equally applied percentage increase.

The applied force must never exceed what is allowable for the pressure on the brake discs, else the discs may break. A failsafe should, therefore, be implemented in the control system or power supply of the actuators. A failsafe could be made to limit the current to the actuator (by limiting the voltage). Since the force is proportional to the current, a limit on it would directly limit the force.

The brake disc frictions were chosen conservatively to be the lowest given for their materials. The braking ability for a real system should, therefore, be higher than the theoretically calculated braking ability.

4 | Mechanical Design

This chapter shows the method of mechanical dimensioning for the general parts of the gearbox (all mechanical parts except for the gears). The shafts were dimensioned based on the allowable stresses of the material, while the other mechanical parts were reasonably designed in concept. The selection of the bearings is also described in this chapter.

The calculations for this chapter were performed by the Matlab script in appendix B.

All the mechanical drawings may be seen in appendix G.

4.1 Material of General Parts

The general parts were decided to be the steel: ISO 42CrMo4. Which parameters are given below as conservative properties [31]. The elasticity and density are the same as for the gear steel, with general properties for elasticity, and the density that is given for standard alloy steel in *Autodesk Inventor* where the parts were designed.

Table 4.1: Steel properties: ISO 42CrMo4.

Parameter	**Value**	**Unit**
Yield strength	390	$[MPa]$
Tensile strength	600	$[MPa]$
E-modulus	210 000	$[MPa]$
Poisson's ratio	0.3	$[-]$
Density	7730	$[^{kg}/_{m^3}]$

4.2 Mechanical Design of Supporting Parts

All the general parts except the shafts were designed without testing their stresses. Their design is therefore conceptual, but in concept assumed to be correct, although the dimensions may be required to change depending on their stresses.

The leading dimensions of the gearbox are the gears. All of the supporting parts were designed to fit relatively snugly around the gears and each other (including room for the brakes).

Carrier 1, sun 1, and the actuated ring were skeletonized, meaning that material assumed to be unnecessary was removed. By doing so, the mass of the parts was lowered, therefore also lowering their moment of inertia. The moment of inertia of the parts before and after the skeletonizing is shown in table 4.2. All other parts were created using simpler designs. Carrier 2 was also considered for skeletonizing, because its inertia will be relatively important for the total inertia. Because of the size of the planets on carrier 2, the possible reduction of inertia was considered too small to warrant the design change.

Table 4.2: Moment of inertia of parts before and after skeletonizing.

Part	***I***	
	Basic	**Skeletonized**
$\boldsymbol{C_1}$	0.3297	0.3051
$\boldsymbol{R_A}$	1.8405	1.5226
$\boldsymbol{S_1}$	0.1576	0.0833

The parameters in the table are:

$\boldsymbol{I}$	Moment of inertia of part	$[kgm^2]$
$\boldsymbol{P}$	Planet	$[-]$
$\boldsymbol{R}$	Ring	$[-]$
$\boldsymbol{S}$	Sun	$[-]$

The subscripts indicate the part of the gear-train the parameter refers to.

Figures 4.1, 4.2, and 4.3 show the parts before and after the skeletonizing.

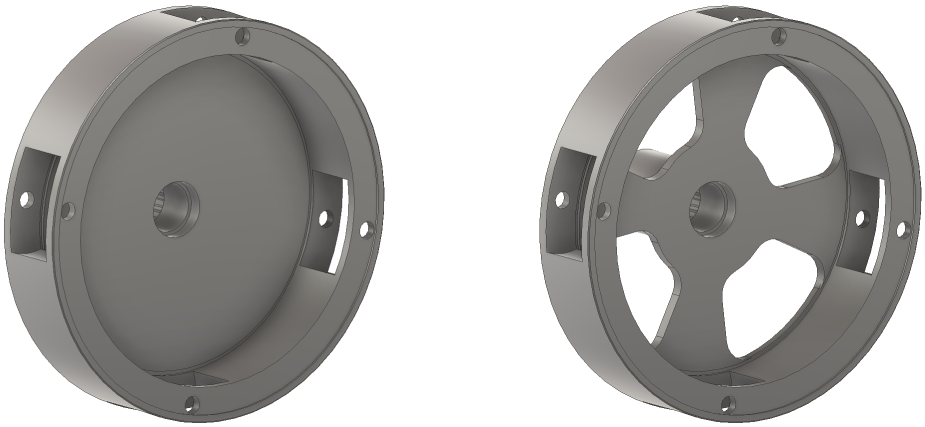

(a) Basic carrier 1. (b) Skeletonized carrier 1.

Figure 4.1: Basic vs skeletonized design of carrier 1.

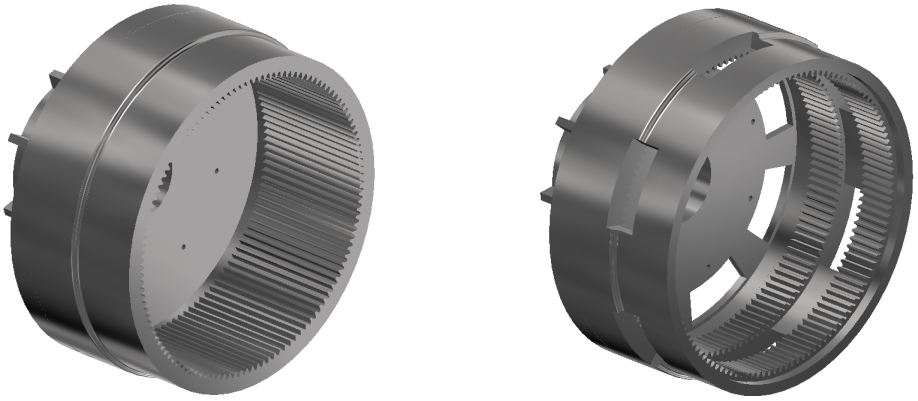

(a) Basic actuated ring. (b) Skeletonized actuated ring.

Figure 4.2: Basic vs skeletonized design of actuated ring.

(a) Basic sun 1. (b) Skeletonized sun 1.

Figure 4.3: Basic vs skeletonized design of sun 1.

4.3 Shaft Design

4.3.1 Stresses & Deflection

Shaft stresses and deflections were used to dimension the shafts.

Most of the shafts in the gearbox are subject only to torsion, because of the design of the planetary gearbox. The only exception is the planet shafts, which are subject to bending and shear stresses, but no torsion, because the planets will spin freely on bearings.

The minimum shaft dimensions were found by using the von Mises stress equation, which was used in a simplified form fitting for shafts, which is gotten from Budynas & Nisbett [16]. The simplified von Mises equation is shown in equation (4.1).

$$\sigma_{max} = \sqrt{(\sigma_b)^2 + 3\left(\tau_T + \tau_S\right)^2} \tag{4.1}$$

σ_b $[MPa]$ is the bending stress [19]:

$$\sigma_b = K_f \frac{M_b}{I} y = K_f \frac{M_b}{2I} d \tag{4.2}$$

M_b $[Nmm]$ is the bending moment. Which is, for a simply supported beam with a centered load [19]:

$$Mb = \frac{FL}{4} \tag{4.3}$$

I $[mm^4]$ is the moment of inertia. Which is, for a round shaft [19]:

$$I = \frac{\pi}{64}(d_o^4 - d_i^4) \tag{4.4}$$

τ_T $[MPa]$ is the torsion stress [19]:

$$\tau_T = K_{fs} \frac{T}{J} r = K_{fs} \frac{T}{2J} d \tag{4.5}$$

J $[mm^4]$ is the polar moment of inertia. Which is, for a round shaft [19]:

$$J = \frac{\pi}{32}(d_o^4 - d_i^4) \tag{4.6}$$

τ_S $[MPa]$ is the shear stress. Which is, for a round shaft [19]:

$$\tau_S = K_{fs} \frac{4}{3} \frac{F}{A} = K_{fs} \frac{4}{3} \frac{4F}{\pi(d_o^2 - d_i^2)} \tag{4.7}$$

K_f $[-]$ is the notch sensitivity factor for normal stress :

$$K_f = 1 + q(K_t - 1) \tag{4.8}$$

K_{fs} $[-]$ is the notch sensitivity factor for shear stress :

$$K_{fs} = 1 + q_{shear}(K_{ts} - 1) \tag{4.9}$$

The parameters in the equations are:

$\boldsymbol{A}$	Area of cross-section	$[mm^2]$
$\boldsymbol{d_i}$	Inner diameter of shaft (when hollow)	$[mm]$
$\boldsymbol{d_o}$	Outer diameter of shaft	$[mm]$
$\boldsymbol{F}$	Force	$[N]$
$\boldsymbol{K_t}$	Stress concentration factor for normal stress	$[-]$
$\boldsymbol{K_{ts}}$	Stress concentration factor for shear stress	$[-]$
$\boldsymbol{L}$	Total length of shaft	$[mm]$
$\boldsymbol{M_b}$	Bending moment	$[Nmm]$
$\boldsymbol{q}$	Notch sensitivity factor	$[-]$
$\boldsymbol{r}$	Outer radius of shaft	$[mm]$
$\boldsymbol{\sigma_{max}}$	Maximum von Mises stress	$[MPa]$
$\boldsymbol{T}$	Torsion moment	$[Nmm]$
$\boldsymbol{y}$	Distance from neutral axis to periphery	$[mm]$

The planet shafts are subject to bending moment and are therefore also deflected (bent). Equation (4.10) shows how the shaft is assumed to deflect with the radial load from the planet as a point-load at the exact center of the shaft, and the shaft being simply supported, which is the worst case scenario [19].

$$\delta_{max} = \frac{FL^3}{48EI} \tag{4.10}$$

The parameters in the equation are:

$\boldsymbol{\delta_{max}}$	Maximum deflection	$[mm]$
$\boldsymbol{E}$	E-Modulus	$[MPa]$
$\boldsymbol{F}$	Point force	$[N]$
$\boldsymbol{I}$	Moment of inertia of cross-section	$[mm^4]$
$\boldsymbol{L}$	total length of shaft	$[mm]$

4.3.2 Factors & Relevant Stresses

According to Budynas & Nisbett [16], it is always safe to set $K_f = K_t$ if there are uncertainties for the notch sensitivity factor, which is also assumed to apply for $K_{fs} = K_{ts}$. Table 7-1 in [16] indicates that the worst-case factor for any load on a sharp fillet would be *3.0* which is the case for axial loading, but is here used as a common safety factor for any of the loads. The common factor of *3.0* is called K_t for both normal and shear stresses.

The shafts supporting the planets were dimensioned for three conditions: Shear stress, bending stress, and deflection. The stresses were tested independently, because the maximum of the stresses occurs in different locations. The deflection is not a stress, and is therefore necessarily independent. The worst case of the three was then used as the governing requirement of diameter.

All other shafts than the planets' are subject to symmetric loads, which means that there should be no bending moments acting on them, and the shear forces shall be supported by opposite and equal forces about the shafts. The only dimensioning stress is, therefore, torsional stress.

By combining the parts of the von Mises equation, the von Mises stress for bending and torsion is expressed in equation (4.11).

$$\sigma_{max} = \sqrt{\left(K_t \frac{32 M_b d_o}{\pi (d_o^4 - d_i^4)}\right)^2 + 3\left(K_t \frac{16 T d_o}{\pi (d_o^4 - d_i^4)}\right)^2} \tag{4.11}$$

By solving the equation above for the outer diameter, and using the result for solid shafts, the minimum diameter is found by:

$$d_{min} = \sqrt[3]{\frac{32 K_t}{\pi \sigma_{max}} \sqrt{M_b^2 + 0.75 T^2}} \tag{4.12}$$

where $K_t = 3.0$.

Equation (4.12) was used to dimension all of the shafts except for the hollow intermediate shaft. In addition, equation (4.13) and (4.14) were used for the planet shafts.

Equation (4.13) is the expanded form of equation (4.10) solved for the diameter in the moment of inertia, assuming a solid shaft. Equation (4.14) is equation (4.7) solved for the diameter, assuming a solid shaft.

$$d_{min} = \sqrt[4]{\frac{3072 \pi E \delta_{max}}{F L^3}} \tag{4.13}$$

$$d_{min} = \sqrt{K_{fs} \frac{4}{3} \frac{4F}{\pi \tau_S}} \tag{4.14}$$

The deflection of the planet shafts δ is set to be maximum $1\mu m$, which is assumed to be sufficiently small to be negligible.

The intermediate shaft (carrier 2 $\rightarrow$ fixed sun) is the only hollow shaft in the gearbox. Equation (4.11) may not be solved directly for both the inner and outer diameter of the shaft, without applying an additional equation of restraint for the relation of the diameters or otherwise specifying one of them. This shaft is therefore tested for a manually selected diameter size, for if the stress is within the yield strength of the material.

The actuated sun shaft is subject to two load cases. The first is the normal operation of the gearbox, where the sun rotates and transmits torque. The second case is when the brake on the sun is applied, where the torque in the shaft is assumed to be the required braking torque. The first load case is equal to that of the other shafts, where the motor torque is transmitted to the shaft through the meshing gears. The sun shaft was tested for both the cases, and the conservative minimum diameter was used.

4.3.3 Occurring Forces & Stresses

The table below shows the forces and moments acting on the shafts of the gearbox.

Table 4.3: Forces and moments acting on the shafts in the gearbox.

Shaft	$\boldsymbol{T}$	$\boldsymbol{F}$	$\boldsymbol{M_b}$
$\boldsymbol{C_1}$	718.75	NA	NA
$\boldsymbol{C_2 \rightarrow S_F}$	2725.70	NA	NA
$\boldsymbol{P_1}$	NA	575.92	6479.70
$\boldsymbol{P_2}$	NA	4453.80	50110.00
$\boldsymbol{P_F}$	NA	11357.00	212960.00
$\boldsymbol{S_A}$ **(Normal)**	75.16	NA	NA
$\boldsymbol{S_A}$ **(Brake)**	300.63	NA	NA

The parameters in the table are:

$\boldsymbol{C}$	Carrier	$[-]$
$\boldsymbol{F}$	Force (radial)	$[N]$
$\boldsymbol{M_b}$	Bending moment	$[Nmm]$
$\boldsymbol{P}$	Planet	$[-]$
$\boldsymbol{S}$	Sun	$[-]$
$\boldsymbol{T}$	Torsional moment	$[Nmm]$

The subscripts of the number of teeth indicate the part of the gear train the parameter refers to.

4.3.4 Shaft Dimensions

Table 4.4 shows the minimum shaft diameters based on the von Mises stress compared to the allowable yield stress.

Table 4.4: Minimum shaft diameters.

Parameter	**Shaft**					
	C_1	P_1	P_2	P_F	S_A	
					Normal	**Brake**
d_{min}	36.54	7.98	15.78	25.55	17.21	27.32

The parameters in the table are:

C	Carrier	$[-]$
d_{min}	Minimum diameter	$[mm]$
F	Force (radial)	$[N]$
M_b	Bending moment	$[Nmm]$
P	Planet	$[-]$
S	Sun	$[-]$
T	Torsional moment	$[Nmm]$

The subscripts of the number of teeth indicate the part of the gear train the parameter refers to.

The brake torque for the sun shaft takes into account the overall safety factor of 1.15, described in chapter 1.1, but does not use the safety factor for the brakes (1.5).

The hollow carrier 2 to fixed sun shaft was post-design tested for its stress. The dimensions and the stress in the hollow sun are shown in the table below, where it is shown that the stress is lower than the yield strength.

Table 4.5: Dimensions and stress of the hollow shaft between carrier 2 and the fixed sun (intermediate shaft).

Parameter	**Shaft**
	$C_2 \rightarrow S_F$
d_o	55
d_i	42
σ	10.94

The parameters in the table are:

d	Diameter	$[mm]$
σ	von Mises stress	$[MPa]$

The shafts were designed to be at least the minimum diameters, and rounded up to fitting "normal" dimensions for ease of acquisition and fitting of bearings and gears. The exact dimensions of the shafts are given in the mechanical drawings of the gearbox in appendix G.

4.4 Selection of Bearings

There is required to have bearings for the following parts of the gearbox:

- Actuated step (Input shaft & Carrier 2)
- Actuated ring.
- Actuated sun shaft.
- Carrier 1 & 2.
- Planets 1, 2, & F

4.4.1 Life Expectancy

The bearings were tested for the criteria listed below. These criteria are described by SKF [32], which is also the producer that is used.

- Basic life expectancy
- Maximum speed
- Minimum load

Because the oil in the gearbox is unknown, and is not in the scope of the project, only the basic life expectancy was found. When the oil is known, the calculations should be made anew for a modified life expectancy, that takes all factors into account.

The life expectancy of the bearings was used as the dimensioning factor. The requirement of the bearings is given in running hours, which first requires the calculation of the number of cycles, for then to find the equivalent hours through the rotational speed. Equation (4.15) is used for the number of cycles, and (4.16) is used for the hours. Both of these equations are for 90% reliability. [32]

The maximum speed and minimum load were controlled for after the life expectancy dimensioning, as absolute requirements for elimination.

$$L_{10} = \left(\frac{C}{P}\right)^p \tag{4.15}$$

$$L_{10h} = \frac{10^6}{60n} L_{10} \tag{4.16}$$

The parameters in the equations are:

$\boldsymbol{L_{10}}$	Expected lifetime	$[Million\, revolutions]$
$\boldsymbol{L_{10h}}$	Expected lifetime	$[hours]$
$\boldsymbol{C}$	Basic dynamic load rating	$[kN]$
$\boldsymbol{P}$	Equivalent dynamic bearing load	$[kN]$
$\boldsymbol{n}$	Rotational speed	$[rpm]$
$\boldsymbol{p}$	Factor for bearing type	$[-]$

For ball bearings, $p = 3$, and for roller bearings $p = 10/3$.

The basic dynamic load rating C is read from the product tables.

The equivalent dynamic bearing load P is found through the equation below [32]:

$$P = XF_r + YF_a \tag{4.17}$$

The parameters in the equation are:

$\boldsymbol{F_r}$	Radial bearing load	$[kN]$
$\boldsymbol{F_a}$	Axial bearing load	$[kN]$
$\boldsymbol{X}$	Radial load factor	$[-]$
$\boldsymbol{Y}$	Axial load factor	$[-]$

If there are only radial loads applied to radial bearings, or only axial loads on thrust bearings, $P = F$. [32]

The bearings for each application was found by using the equations above, and selecting the bearings from SKF's catalog [32]. The bearings were tested for their life expectancy in relation to the required 2500 hours.

4.4.2 Applied Loads

The direction of the loads on the bearings is equivalent to the loads on the shafts, except that the weight of the components is considered for the axial loads for the bearings. There are no axial loads on any of the bearings, therefore; $P = F_r$ (radial force) for the life expectancy calculations. The weight of the parts are the only forces on all but the planets, where the bending forces for the shaft are also the radial force on the bearings. The weight applied radially to the planet bearings are insignificant, and were therefore ignored in favor of the radial forces from the transmission of power.

All the loads for all the parts were for the calculations assumed to be point loads at the center of the distributed load, or at the center of mass for the weights. The center of mass for the relevant parts was placed using Autodesk Inventor's toolbox to find it automatically. The lengths to the point loads were also measured directly from the 3D CAD model.

The free body diagrams for the calculations of the forces are shown in appendix C. There is also shown the forces, masses and the lengths.

4.4.3 Selected Bearings

Table 4.6 show the selected bearings and their location. The datasheet for the bearings are attached in appendix H. All the bearings were selected from SKF's catalogs.

Table 4.6: Selected Bearings.

Bearing	**SKF #**	**C**	**Life expectancy**	
			Low	**High**
***Carrier* 1 (a)**	**NKX 70**	4.46E+04	1.55E+09	1.55E+09
***Carrier* 1 (b)**	**NKX 30**	2.29E+04	9.99E+06	9.99E+06
***Carrier* 2 (a)**	**NKX 30**	2.29E+04	1.90E+06	3.27E+05
***Carrier* 2 (b)**	**30216**	1.84E+05	1.49E+10	2.56E+09
Fixed Planet	**K 35x45x30**	4.68E+04	1.49E+04	8.98E+05
Fixed Sun	**30211**	1.11E+05	$\rightarrow \infty$	$\rightarrow \infty$
***Main* (a)**	**33012**	1.13E+05	1.13E+09	1.13E+09
***Main* (b)**	**30216**	1.84E+05	7.35E+08	7.35E+08
***Planet* 1**	**K 15x21x21**	1.87E+04	1.14E+05	1.14E+05
***Planet* 2**	**K 30x40x18**	3.03E+04	1.12E+04	6.78E+05
***Ring A* (a)**	**33012**	1.13E+05	$\rightarrow \infty$	9.74E+08
***Ring A* (b)**	**NKX 70**	4.46E+04	$\rightarrow \infty$	2.07E+06
***Sun A* (a)**	**NKX 30**	2.29E+04	1.91E+09	$\rightarrow \infty$
***Sun A* (b)**	**NKX 30**	2.29E+04	1.91E+09	$\rightarrow \infty$

The parameters in the table are:

C	Basic dynamic load rating	$[kN]$
Life expectancy	Life expectancy in high or low gear	$[hours]$
SKF #	Model number in SKF catalog	$[-]$

Note that the bearing on the input shaft and carrier 2 (b) supports the whole actuated step. The bearing used on carrier 2 (b) was tested for both the forces from the assembly of the actuated step, and the carrier individually. The bearings between the sun shaft and the carriers were tested for the sun shaft, and the carriers individually. The results show the individual results, with no regard for the combined forces. The life expectancy for all of them is though so high that the combination of the forces would not make the life expectancy lower than the required lifetime of 2500 hours.

The bearing on the fixed sun is estimated to not hold any radial force, since the spline is assumed to hold the full weight of the sun. The sun is also assumed to be sufficiently stiff to not cause any deflection of note for the applied mass. There must though be a bearing to hold the assembly in place in the axial direction. The bearing was instead of the forces, selected based on its inner diameter, to fit the shaft.

4.5 Gear Mounting

All the planets shall be slip-fitted onto their bearings, in accordance to bearing-manufacturer specifications. The bearings shall be slip-fitted to the planet shafts.

The ring shall be mounted on bearings held up by the sun shaft.

The sun gears are designed to be machined as one part, along with the sun shaft. Sun 2 must be machined together with the shaft as one part to avoid breaking the gear, because it has a small diameter relative to the shaft diameter. Sun 1 is also machined with the shaft for ease of design, although this would require a pre-formed piece of material for the machining to reduce the machining job and loss of material.

4.6 Summary & Result of Mechanical Design

The mechanical design of the gearbox is shown in figure 4.4, 4.5, and F.5. Schematics are found in appendix G.

The gearbox design consists of two sets of planetary gear-trains, one actuated and one with a fixed gear ratio. The actuated stage is a modified Simpson gearbox providing two gear ratios. The actuated stage is controlled with four brakes, two friction and two "dog" (3.5 for details). The fixed step is the connection to the drum, and reverses the rotation of the input. The gearbox ends at the planets of the fixed step, the connection to the drum is through the ring of the fixed step being part of the drum. The gearbox is the load-carrying unit; The motor is flange-mounted to it, and the gearbox itself is mounted to the stationary part of the drum by a bell which also covers the motor. The drum, bell, and the electric motor are not designed or calculated for in this thesis; hence no data for these parts are available. The gearbox mounted inside a concept drum is shown in figure 4.7.

The gearbox has no true neutral or reverse. The reverse is not needed given that the system is powered by an electric motor, which can rotate in both directions. The lack of a neutral gear means that free-spooling of the winch makes the motor rotate proportionally fast, unless a clutch is put between the motor and gearbox. It is therefore in a free-spool situation essential to monitor the motor speed.

Figure 4.4: Isometric view of gearbox.

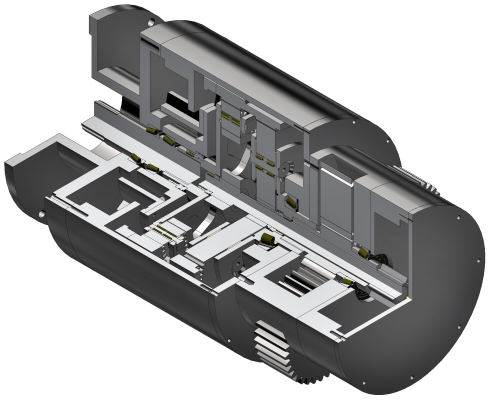

Figure 4.5: Isometric, three quarter, view of gearbox.

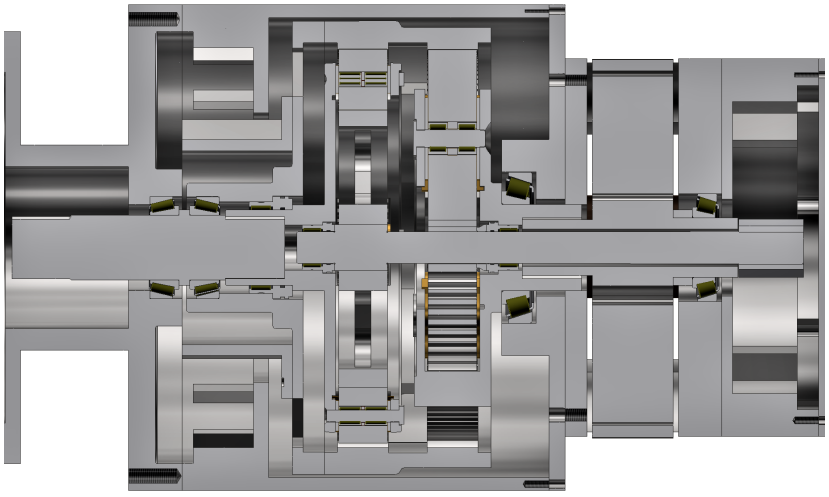

Figure 4.6: Half-section view of gearbox.

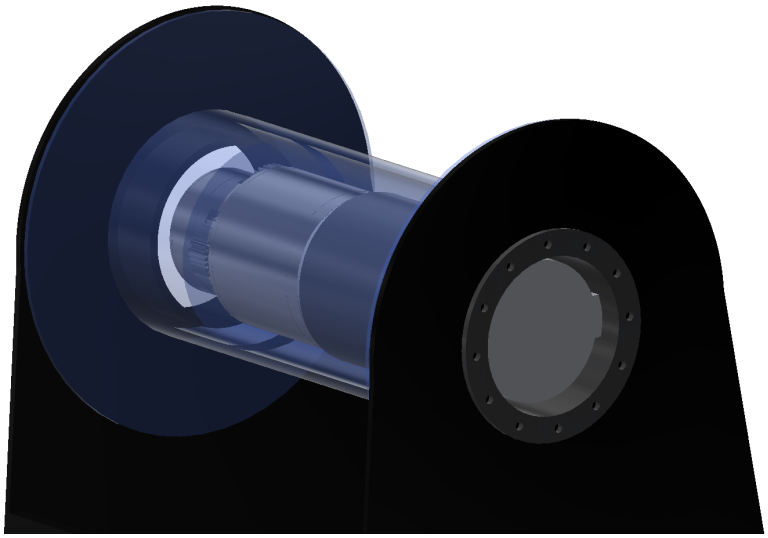

Figure 4.7: Example of the gearbox connected to a motor and mounted in a drum.

All the mechanical parts are of the same steel, *ISO 42CrMo4* (4.2 for details), and designed to be machined to a high standard. Some parts are skeletonized to reduce their moment of inertia so that the gearbox has as little resistance to accelerations as possible. All drive-line parts of the gearbox are designed to be able to handle all the load criteria defined in table 1.1. The internal parts of the gearbox are supported on bearings have to be preloaded to achieve the minimum load required to ensure correct operation. The gearbox is designed so that it can be assembled from one side, but at the same time be able to access the brakes for inspection without the need for a full disassembly.

5 | Control System Design

This chapter describes the design of the control system based on the dynamic model of the system. First, an ideal system model based on the gear ratios and inertias of the system is created. Then, a system model created in Matlab-Simulink is described. Lastly, the control system and tuning of it is described.

5.1 Placement of Encoders

The rotational velocity of the drum shall be controlled, which means that there must be an encoder to read it for the controller. Because the drum design is not part of this thesis, the encoder is placed in the gearbox itself. The encoder should ideally read directly from the drum, to avoid faulty reading if there are any mechanical issues before the drum. In the gearbox itself, the encoder should be placed as close to the output (fixed step ring) as possible.

The encoder is placed on the hollow shaft between the fixed-step sun and carrier 2. This is the closest to the drum it could be placed, except for the planets of the fixed-step. Placing the encoder on the planets would, however, require more space in the lengthwise direction of the gearbox, leading to a more-than-necessary length. The encoder value must be divided by the gear ratio of the fixed step of the gearbox to obtain the velocity of the drum. This factor is always constant, and should therefore not cause any issues.

In addition to the encoder used in the control loop for the velocity, there is also created a space for another encoder on the input shaft of the gearbox. This encoder shall measure the motor velocity, which could be compared to the velocity measured by the encoder on the intermediate shaft of the gearbox. The comparison of the encoder measurements may be used to detects faults in the gearbox. The measurements could, for example, be used to check that the gear ratios are as intended, which indicates whether the brakes work correctly, and that there are no breaks in the mechanical system.

The encoders are not selected or designed. Their location is the sole concern for this thesis. The locations are however reflected in the Simulink system model, so that the control system emulates a realizable system.

5.2 Motor Model

Equation (5.1) gives the governing equation for the rotation of the rotor of the motor, which is Newton's second law (for rotation).

$$\sum T = I\dot{\omega} \tag{5.1}$$

The parameters in the equation are:

$\boldsymbol{I}$	Moment of inertia connected to rotor	$[kg \cdot m^2]$
$\dot{\boldsymbol{\omega}}$	Angular acceleration of rotor	$[^{rad}/_{s^2}]$
$\boldsymbol{T}$	Torsional moment (torque)	$[Nm]$

The sum of torque on the motor is found by:

$$\sum T = T_M - T_L \tag{5.2}$$

The parameters in the equation are:

$\boldsymbol{T_L}$	Load torque	$[Nm]$
$\boldsymbol{T_M}$	Motor torque	$[Nm]$

5.3 Model of Drivetrain

The model of the gearbox and drum assumes that there is no friction, and that there is ideal stiffness in all components of the system, including the input shaft of the gearbox.

The equivalent inertia, as seen by the motor, is the relevant inertia of the model, because it is this inertia that the motor must overcome with its torque. To find the equivalent inertia, the inertia of the parts, and their gear ratio to the motor must be known.

The parts that can move in the motor, gearbox, and drum, and thus contribute to the inertia are listed below:

- Motor rotor
- Carrier 1 & input-shaft
- Planets 1,2, & 3
- Actuated ring
- Actuated sun shaft
- Carrier 2, intermediate shaft, & fixed step sun
- Fixed step ring & drum

5.3.1 Internal Gear Ratios

Equation (5.3) shows the low gear ratio of the actuated step i_{AL}, and equation (5.4) shows the gear ratio of the high gear i_{AH}. Both the gear-specific ratios are duplicates of equations (2.10) and (2.10) respectively. Equation (2.12) shows the gear ratio of the fixed step, which is duplicated from equation (2.12).

$$i_{AL} = \frac{\omega_{C_1}}{\omega_{C_2}} = \frac{S_1(R_A + S_2)}{S_2(R_A + S_1)} \tag{5.3}$$

$$i_{AH} = \frac{\omega_{C_1}}{\omega_{C_2}} = \frac{R_A + S_2}{R_A + S_1} \tag{5.4}$$

$$i_F = -\frac{R_F}{S_F} \tag{5.5}$$

The parameters in the equations are:

$\boldsymbol{\omega_C}$	Angular velocity of carrier	$[^{rad}/_s]$
$\boldsymbol{\omega_R}$	Angular velocity of ring	$[^{rad}/_s]$
$\boldsymbol{\omega_S}$	Angular velocity of sun	$[^{rad}/_s]$
$\boldsymbol{r}$	Radius of gear	$[m]$
$\boldsymbol{R}$	Number of teeth on ring	$[-]$
$\boldsymbol{S}$	Number of teeth on sun	$[-]$

The subscripts of the number of teeth indicate the part of the gear train the parameter refers to.

The following equations show the gear ratio from the motor to relevant parts. All the equations are based on equations (2.2) - (2.6).

Planets on Carrier 1

$$i_{P1} = \frac{2P_1}{R_A + S_1} \tag{5.6}$$

Actuated Ring (High Gear)

$$i_{RA} = \frac{R_A}{R_A + S_1} \tag{5.7}$$

Actuated Sun Shaft (Low Gear)

$$i_{SA} = \frac{S_1}{R_A + S_1} \tag{5.8}$$

Planets on Carrier 2

$$i_{P2} = \frac{2P_2}{R_A + S_2} i_A \tag{5.9}$$

Fixed Step Planets

$$i_{PF} = \frac{2P_F}{R_F + S_F} i_A \tag{5.10}$$

The parameters in the equations are:

$\boldsymbol{i}$	Gear ratio	[−]
$\boldsymbol{P}$	Number of teeth on planet	[−]
$\boldsymbol{R}$	Number of teeth on ring	[−]
$\boldsymbol{S}$	Number of teeth on sun	[−]

5.3.2 Equivalent Inertia of Gearbox

The equivalent inertia, as seen by the motor from the gearbox is shown in equation (5.11).

$$\begin{aligned} I_{eq} =& I_{C1} + n_{P1}\frac{I_{P1}}{i_{P1}^2} + \frac{I_{RA}}{i_{RA}^2} + \frac{I_{SA}}{i_{S1}^2} + n_{P2}\frac{I_{P2}}{i_{P2}^2} + \frac{I_{C2} + I_{SF}}{i_A^2} \\ &+ n_{PF}\frac{I_{PF}}{i_{PF}^2} + \frac{I_{RF}}{i^2} \end{aligned} \tag{5.11}$$

The parameters of the equation are:

$\boldsymbol{I}$	Moment of inertia of part	$[kgm^2]$
$\boldsymbol{i}$	Gear ratio to part in relation to motor	$[-]$
$\boldsymbol{n_P}$	Number of planets	$[-]$

The subscripts indicate the part of the gear train the parameter refers to.

The gear ratios for each part are found in chapter 5.3.1.

The fixed step ring is seen by the motor through the entire gearbox, using the total gear ratio of the gearbox.

Carrier 2 and the fixed sun is one composite part. The gear ratio relevant to them is the actuated step gear ratio.

Most of the local gear ratios change depending on the state of the actuated step (high or low gear). Those gear ratios using i_A (actuated step gear ratio) or i (total gearbox gear ratio) must be found using both high and low gear.

The moment of inertia is found through the equation below [33].

$$I = \int_M r^2 dm \tag{5.12}$$

The parameters of the equation are:

$\boldsymbol{M}$	Section of mass	$[-]$
$\boldsymbol{m}$	Mass	$[kg]$
$\boldsymbol{r}$	Radius	$[m]$

5.3.3 Equivalent Inertia of Drum

The motor sees the winch drum through the entire gearbox. The drum and load's contribution to the equivalent inertia is therefore as shown below.

$$I_{eq,drum} = \frac{I_L}{i^2} \tag{5.13}$$

The parameters in the equation are:

$\boldsymbol{I_L}$	Moment of inertia of drum and load	$[kgm^2]$
$\boldsymbol{i}$	Gear ratio of gearbox	$[-]$

The gear ratio of the gearbox is different for high and low hear. The equivalent drum inertia must, therefore, be found for both defined gear ratios.

5.4 System Model

The calculations for this chapter were performed by the Matlab script in appendix D.

The governing equation of the system is Newton's second law in an expanded form, created by combining equations (5.1) and (5.2). The governing equation is shown below.

$$T_M - T_L = I_{eq}\dot{\omega} \tag{5.14}$$

I_{eq} $[kgm^2]$ is the total equivalent inertia

$$\begin{aligned} I_{eq} =& I_M + I_{C1} + n_{P1}\frac{I_{P1}}{i_{P1}^2} + \frac{I_{RA}}{i_{RA}^2} + \frac{I_{SA}}{i_{S1}^2} + n_{P2}\frac{I_{P2}}{i_{P2}^2} + \frac{I_{C2} + I_{SF}}{i_A^2} \\ &+ n_{PF}\frac{I_{PF}}{i_{PF}^2} + \frac{I_{RF} + I_L}{i^2} \end{aligned} \tag{5.15}$$

The parameters in the equations are:

$\boldsymbol{C}$	Carrier	$[-]$
$\boldsymbol{I}$	Moment of inertia of part	$[kgm^2]$
$\boldsymbol{i}$	Gear ratio to part in relation to motor	$[-]$
$\boldsymbol{n_P}$	Number of planets	$[-]$
$\boldsymbol{T_L}$	Load moment	$[Nm]$
$\boldsymbol{T_M}$	Torque of motor	$[Nm]$

The subscripts indicate the part of the system the parameter refers to.

The gear ratios of the system are shown in table 5.1, while table 5.2 shows the inertias.

Flekkefjord Elektro [3] supplied the inertias of the drum and motor. The inertia of the drum/load should also include the winch wire stored on the drum, but this is at the time of writing unknown, and therefore omitted.

The inertias of the gearbox were read out from Autodesk Inventor where the 3D CAD model was created.

The brake discs on the sun shaft and the ring were ignored, because the mass of the discs mounted to the ring and sun shaft is insignificant compared to the parts themselves.

The fixed ring was omitted for the model, because of its insignificance compared to the drum to which it shall be attached.

All the planets contribute to the moment of inertia by rotating about their center axes. In addition to their individual moment of inertia, the planets on carrier 1 and 2 contribute to the moment of inertia on the carriers themselves, by rotating with the carriers about the input-output center axis, the carrier inertias are therefore for the entire carrier assemblies.

Table 5.1: Gear ratios of gearbox.

Part	i_L	i_H
C_1	1.000	1.000
C_2	3.792	0.654
L	20.384	3.514
M	1.000	1.000
P_1	0.163	0.163
P_2	23.200	0.510
P_F	8.296	1.430
R_A	NA	0.582
S_A	0.418	NA
S_F	3.792	0.654

Table 5.2: System inertias.

Part	I	n_P
C_1	0.38679	
C_2	0.45600	
L	25.14933	
M	0.28500	
P_1	0.00026	4
P_2	0.02221	3
P_F	0.05521	3
R_A	1.52261	
S_A	0.08378	
S_F	0.00436	

The parameters in the tables are:

$\boldsymbol{C}$	Carrier	$[-]$
$\boldsymbol{I}$	Moment of inertia	$[kgm^2]$
$\boldsymbol{i}$	Gear ratio in relation to motor	$[-]$
$\boldsymbol{n_P}$	Number of planets	$[-]$
$\boldsymbol{L}$	Load/drum	$[-]$
$\boldsymbol{M}$	Motor	$[-]$
$\boldsymbol{P}$	Planet	$[-]$
$\boldsymbol{R}$	Ring	$[-]$
$\boldsymbol{S}$	Sun	$[-]$

The subscripts indicate the set in the gear train the parameter refers to.

The presented inertias are per part, including the planets. The total inertia of the planet sets is therefore the inertia multiplied by the number of planets n_P.

5.5 Result of Equivalent Inertia Calculations

The calculations for this chapter were performed by the Matlab script in appendix D, using the method and values from chapter 5.4.

The equivalent inertias of the system, with the values from chapter 5.4, are shown in table 5.3.

Table 5.3: Resulting equivalent inertias of the system.

State	$\boldsymbol{I_{eq}}$
Low gear	1.292
High gear	8.661

The parameters in the table are:

$\boldsymbol{I_{eq}}$	Moment of inertia of entire system, as seen by the motor	$[kgm^2]$

5.6 Transfer Functions of System

The calculations for this chapter were performed by the Matlab script in appendix D.

The general transfer function of the system is shown in equation (5.16). The transfer function is based on equation (5.14), and proven through calculation 5.1.

$$TF = \frac{\omega_L}{T_M} = \frac{1}{iI_{eq}}\frac{1}{s} \tag{5.16}$$

The parameters in the equation are:

$\boldsymbol{i}$	Gear ratio in relation to motor	$[-]$
$\boldsymbol{I_{eq}}$	Moment of inertia as seen by motor	$[kgm^2]$
$\boldsymbol{\omega_L}$	Velocity of motor	$[^{rad}/_s]$
$\boldsymbol{s}$	Complex frequency	$[-\sigma \pm j\omega]$
$\boldsymbol{T_M}$	Torque from motor	$[Nm]$

The specific transfer function is shown for low gear in equation (5.17), and for high gear in equation (5.18). Figure 5.1 shows the bode plot of the transfer functions.

$$TF_L = -\frac{0.03797}{s} \tag{5.17}$$

$$TF_H = -\frac{0.03286}{s} \tag{5.18}$$

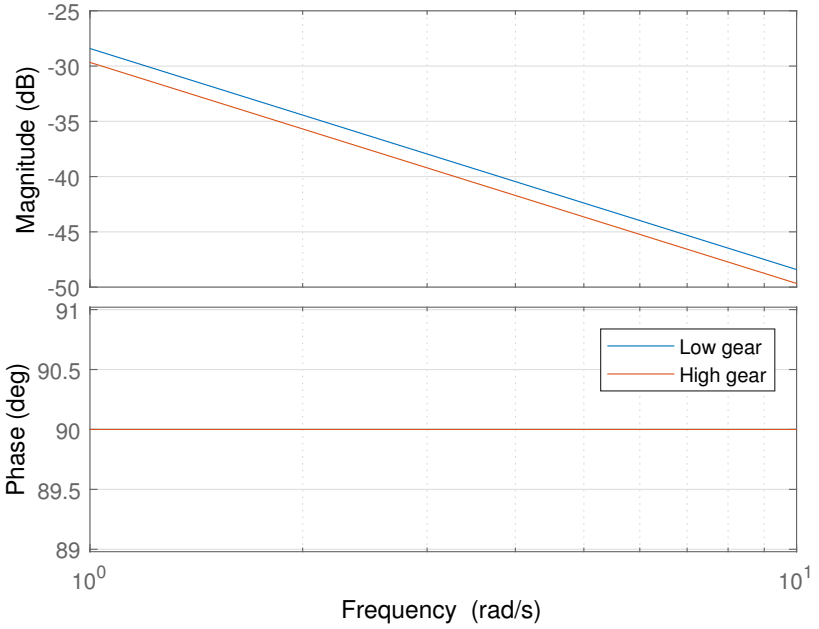

Figure 5.1: Bode plot of theoretical transfer functions. Phases are identical.

Calculation 5.1: Proof of transfer function between motor torque and load velocity.

$$
\begin{aligned}
T_M - T_L &= I_{eq}\dot{\omega}_M && ;T_L = 0, \text{because unknown} \\
T_M &= I_{eq}\dot{\omega}_M \\
\mathcal{L}\{T_M\} &= \mathcal{L}\{I_{eq}\dot{\omega}\} \\
T_M &= I_{eq}\omega_M s && ;\omega_M = \omega_L i \\
T_M &= I_{eq}\omega_L i s \\
\frac{\omega_L}{T_M} &= \frac{1}{iI_{eq}}\frac{1}{s} && \square
\end{aligned}
$$

The parameters in the calculation are:

$\boldsymbol{i}$	Gear ratio in relation to motor	$[-]$
$\boldsymbol{I_{eq}}$	Moment of inertia as seen by motor	$[kgm^2]$
$\boldsymbol{\omega}$	Angular velocity	$[^{rad}/_s]$
$\boldsymbol{s}$	Complex frequency	$[-\sigma \pm j\omega]$
$\boldsymbol{T}$	Torque	$[Nm]$

5.7 Simple System Simulation Model

A Matlab-Simulink model of the planetary gear train is created. The model has been analyzed using Simulink's analysis toolbox to find its transfer functions, to verify that the theoretical transfer functions are correct. The model is shown in figures 5.2 and 5.3, which show the model configuration for high and low gear respectively. The systems are identical, except for which part is locked (inside the red frame).

The gearbox is made by using Simulink/Simscape's planetary gear-set modules, where the number of teeth is input to achieve proper behavior. The source in the model is an ideal torque source, while an ideal rotational sensor measures the velocity of the drum.

The inertias in the model are input as those in table 5.2, which are gotten from the Autodesk Inventor 3D CAD-models of the parts. The inertias of the planets are put directly into the blocks.

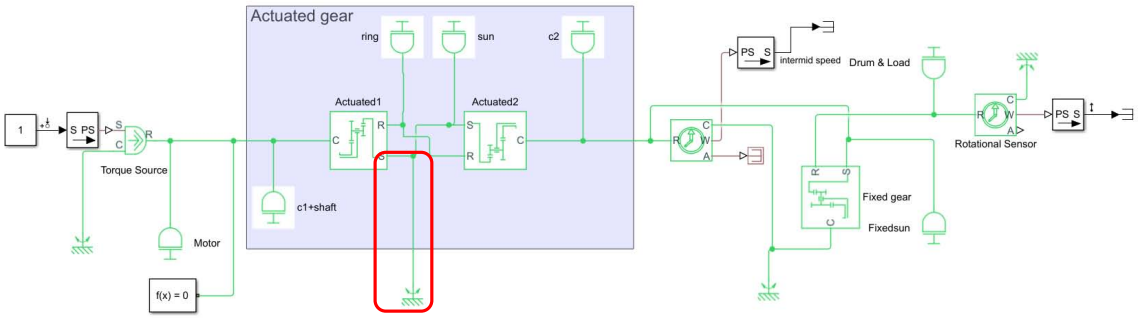

Figure 5.2: Simulink/Simspace model of system in high gear.

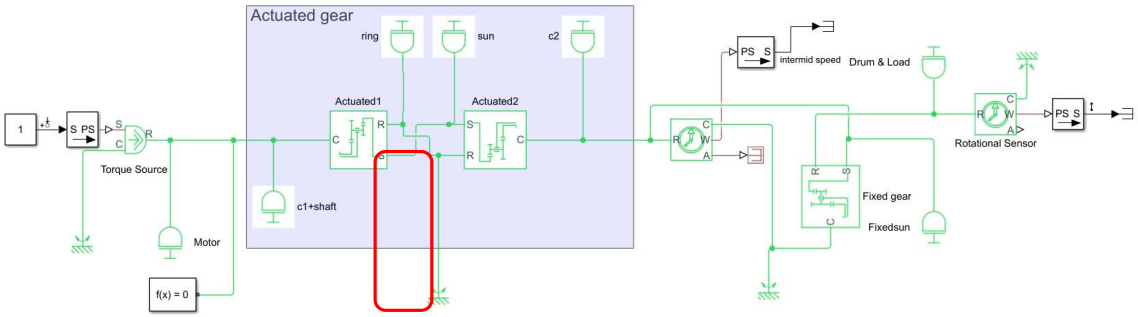

Figure 5.3: Simulink/Simscape model of system in low gear.

In the model, the ideal torque source and rotational sensor combination an additional transfer function. The transfer function of the source/sensor combination is shown in equation (5.19). It has a free integrator, which is the integration of torque/acceleration to velocity, which is also present in the theoretical transfer functions.

$$\frac{Sensor}{Source} = \frac{1000}{s + 1000}\left(\frac{1}{s}\right) \tag{5.19}$$

The source/sensor combination is shown in figure 5.4, which is the parts producing the transfer function above.

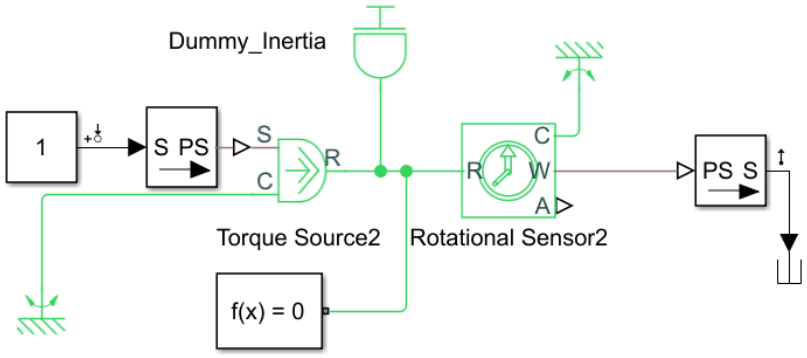

Figure 5.4: Simulink model used for finding the transfer function of the source/sensor combination.

The transfer functions of the models in figure 5.2 and 5.3 found through Simulink's toolbox are shown in equations (5.20) and (5.21). These functions are near-identical to the theoretical transfer functions in equations (5.17) and (5.18). The transfer function of the source/sensor combination, except for the free integrator, are suppressed from the transfer functions below.

$$TF_{L(Simulink)} = -\frac{-0.03795}{s} \tag{5.20}$$

$$TF_{H(Simulink)} = -\frac{-0.03285}{s} \tag{5.21}$$

5.8 Operational Range for Gear-Shift

5.8.1 Maximum Acceleration of Motor

The maximum acceleration of the motor was found through the equivalent inertia of the system, by using equation (5.22). The maximum acceleration is achievable when there is no load on the drum. The maximum acceleration and the time that the motor requires from *0* to *2000* $[rpm]$ is shown in table 5.4.

$$\dot{\omega} = \frac{T}{I_{eq}} \tag{5.22}$$

Table 5.4: Maximum acceleration of motor with no load.

State	$\dot{\boldsymbol{\omega}}_{\boldsymbol{max}}$	$\boldsymbol{\Delta t}$
Low gear	483.68	0.43
High gear	72.17	2.90

The parameters in the table and equation are:

$\boldsymbol{I_{eq}}$	Equivalent inertia, as seen by motor	$[kgm^2]$
$\dot{\boldsymbol{\omega}}_{\boldsymbol{max}}$	Maximum acceleration of motor	$[^{rad}/_{s^2}]$
$\boldsymbol{\Delta t}$	Time used to accelerate from 0 to $2000rpm$	$[s]$

5.8.2 Allowable Load Torque

When the gearbox changes gears, the motor should ideally change its speed by the change in gear ratio. The gearbox should be able to change gears while a load is applied. The load will hinder the motor's ability to accelerate by lessening the sum of torque at the motor. When there is an applied load, the possible acceleration is found by equation (5.23).

$$\dot{\omega}_M = \frac{T_M - T_{L(@M)}}{I_{Eq}} \tag{5.23}$$

$\boldsymbol{I_{eq}}$	Equivalent inertia, as seen by motor	$[kgm^2]$
$\boldsymbol{T_M}$	Motor torque	$[Nm]$
$\boldsymbol{T_{L(@M)}}$	Load torque, as seen by motor through gearbox	$[Nm]$
$\dot{\boldsymbol{\omega}}_{\boldsymbol{M}}$	Acceleration of motor	$[^{rad}/_{s^2}]$

The time required to accelerate between *0* to *2000* $[rpm]$ was found for high and low gear for when there is a load attached to the gearbox. This test was done by setting the motor torque to max (625Nm) and stepping the load on the gearbox. The load was set between *0* to *2108* $[Nm]$ ($i_H \cdot 600Nm = 2108Nm$). The maximum load was

decided to be nearly the maximum load that could be applied to the motor in high gear because the motor must have some reserve of torque to accelerate, and it cannot be higher even for low gear, because the motor/gearbox may break if shifting to or from high gear with any higher load. Figure 5.5 shows the time required for the speed change in relation to the load on the gearbox.

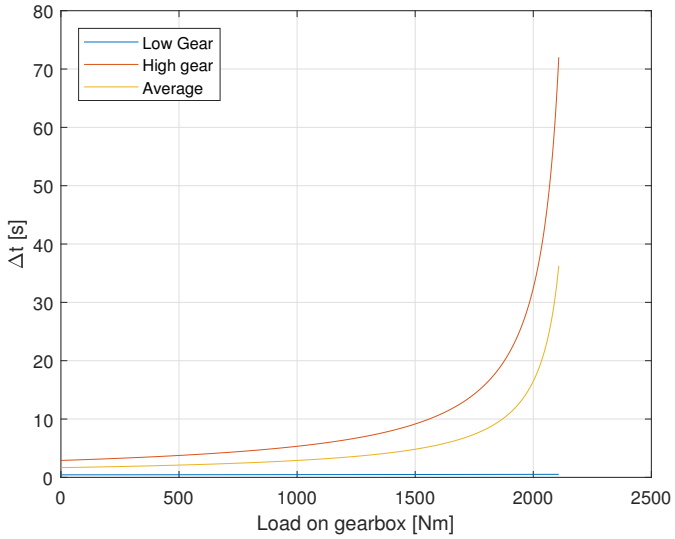

Figure 5.5: Time required for motor to accelerate from 0 to 2000rpm, in relation to load.

Figure 5.5 shows that the average acceleration time of the motor exceeds 5 seconds, which was initially assumed to be a reasonable shifting time at any load higher than approximately 1500Nm. The plot was therefore re-made with the gearbox load limited to 1500Nm. The result of the second test is shown in figure 5.6.

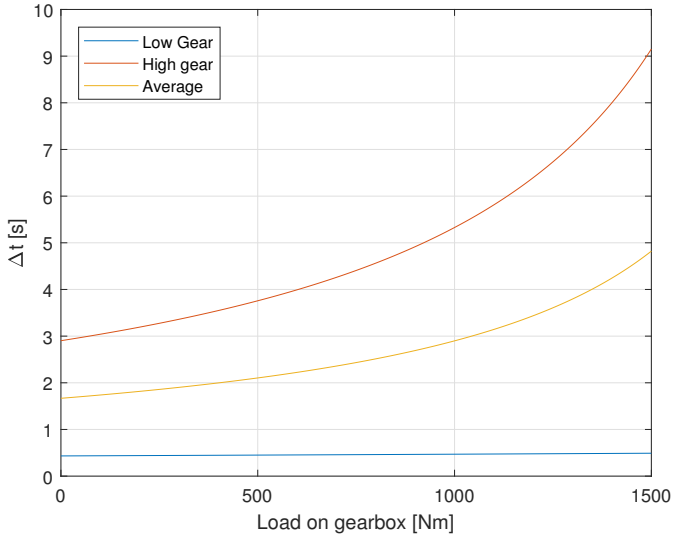

Figure 5.6: Time required for motor to accelerate from 0 to 2000rpm, in relation to a load up to 1500Nm.

The motor should never be required to go from standstill to maximum speed while shifting gear. The maximum change of speed was found by the difference of speed when changing gears. Calculation 5.2 shows the speed of the motor in high gear, when the drum has the speed corresponding to when the motor is in low gear and at maximum speed (2000 rpm).

Calculation 5.2: Proof of transfer function between motor torque and drum speed.

$$n_{D(@n_M=2000,\, low\ gear)} = \frac{n_M}{i_L} = \frac{2000}{20.38} = 98.1354$$

$$n_{M(@n_D=98.1354,\, high\ gear)} = n_D i_H = 98.1354 \cdot 3.51 = 344.45 \qquad \square$$

The parameters in the calculation are:

$\boldsymbol{i}$	Gear ratio	$[-]$
$\boldsymbol{n}$	Speed	$[rpm]$

The leap from 2000 to 344.45 rpm, or opposite, is the most significant change of speed that the motor should be required to perform while the gear shift is in progress. The change of speed is also relative, by the factor of the difference in gear ratios. A lower initial speed of the motor will therefore also make the absolute change in speed when changing gears smaller. The most significant change of speed is therefore from 344.45 to 2000 rpm.

The acceleration-times for the system in relation to the load on the gearbox, with nearly maximum required change of speed, is shown in figure 5.7. The acceleration was set to be from 340 to 2000 rpm to be slightly conservative.

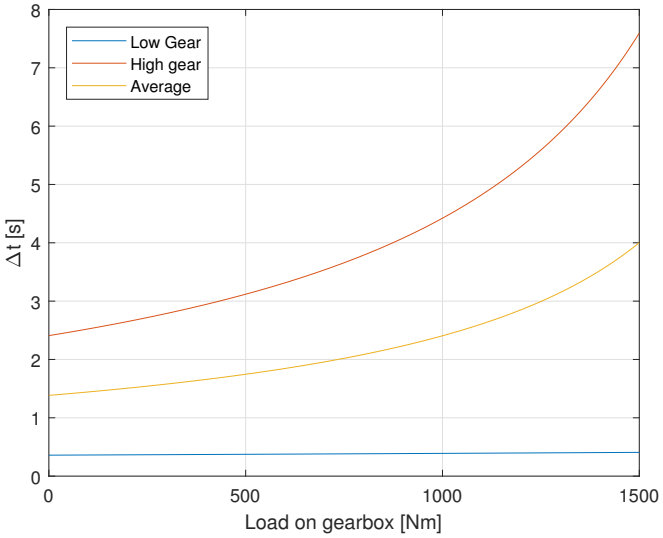

Figure 5.7: Time required for motor to accelerate from 340 to 2000rpm, in relation to a load up to 1500Nm.

5.9 Brake Force Profiles

The profiles of the ring and sun brake forces were made to be so that they transition from 0 to 1, or opposite, where 1 is a full braking force, and 0 is a full release of the brake. Equation (5.29) is the profile for the release of the brakes, and equation (5.30) is the profile for the engagement of the brakes.

$$y_{disengage} = \frac{e^{-at} - e^{-af}}{1 - e^{-af}} \tag{5.24}$$

$$y_{engage} = \frac{e^{-a(f-t)} - e^{-af}}{1 - e^{-af}} \tag{5.25}$$

The parameters in the equations are:

$\boldsymbol{a}$	Slope factor	$[1/s]$
$\boldsymbol{f}$	End-time of transition	$[s]$
$\boldsymbol{t}$	Time	$[s]$
$\boldsymbol{y}$	Brake actuation fraction	$[-]$

There are two degrees of freedom for the profile; the steepness of the slope and the end-time of the transition. The slope-factor and the end-time were set to be equal for the engaging and disengaging brakes. The end-time defines how long the gear change lasts; the slope, however, is used to define the force applied to the brakes at the half-way point of the transition (crossover point).

5.9.1 Crossover Point

The crossover point of the brakes' transition is the point where the two profiles intersect, which happens at half of the end-time f. At the crossover point, the output is the same for both of the profiles. The brake force at the crossover is shown in equation (5.26).

$$y_{\left(\frac{f}{2}\right)} = \frac{e^{-a\frac{f}{2}} - e^{-af}}{1 - e^{-af}} \tag{5.26}$$

Equation (5.27) shows equation (5.26) solved for the slope factor a. Through this form of the equation, the crossover point may be manipulated by selecting the crossover value y, and inputing the total transition-time f. The intermediate calculations between equations (5.26) and (5.27) are shown in calculation 5.3.

$$a = \frac{2}{f} \ln\left(\frac{1}{y_{\left(\frac{f}{2}\right)}} - 1\right) \tag{5.27}$$

The parameters in the equations are:

$\boldsymbol{a}$	Slope factor	$[1/s]$
$\boldsymbol{f}$	End-time of transition	$[s]$
$\boldsymbol{t}$	Time	$[s]$
$\boldsymbol{y}$	Brake actuation fraction	$[-]$

Calculation 5.3: **Intermediate calculation for finding the slope-factor to achieve desired crossover point.**

$$y_{\left(\frac{f}{2}\right)} = \frac{e^{-a\frac{f}{2}} - e^{-af}}{1 - e^{-af}}$$

$$y_{\left(\frac{f}{2}\right)} = \frac{e^{-a\frac{f}{2}}\left(1 - e^{-a\frac{f}{2}}\right)}{\left(1 - e^{-a\frac{f}{2}}\right)\left(1 + e^{-a\frac{f}{2}}\right)}$$

$$y_{\left(\frac{f}{2}\right)} = \frac{e^{-a\frac{f}{2}}}{1 + e^{-a\frac{f}{2}}}$$

$$y_{\left(\frac{f}{2}\right)} = \frac{1}{e^{a\frac{f}{2}} + 1}$$

$$e^{a\frac{f}{2}} = \frac{1}{y_{\left(\frac{f}{2}\right)}} - 1$$

$$a\frac{f}{2} = \ln\left(\frac{1}{y_{\left(\frac{f}{2}\right)}} - 1\right)$$

$$a = \frac{2}{f}\ln\left(\frac{1}{y_{\left(\frac{f}{2}\right)}} - 1\right) \qquad \square$$

The parameters in the calculation are:

$\boldsymbol{a}$	Slope factor	$[1/s]$
$\boldsymbol{f}$	End-time of transition	$[s]$
$\boldsymbol{y}$	Brake actuation fraction	$[-]$

5.10 Full System Simulation Model

Main Simulation Model

The gearbox is simulated using Simulink/Simscape. The model is shown in figure 5.8. It includes the gearbox itself, with the actuated and fixed steps, an ideal torque source limited to $625[Nm]$ to emulate the electric motor, and an ideal torque connected to the output as a load on the drum. A state machine is used to control the gear shift operation. Scopes and other readouts are used to monitor how the gearbox is behaving.

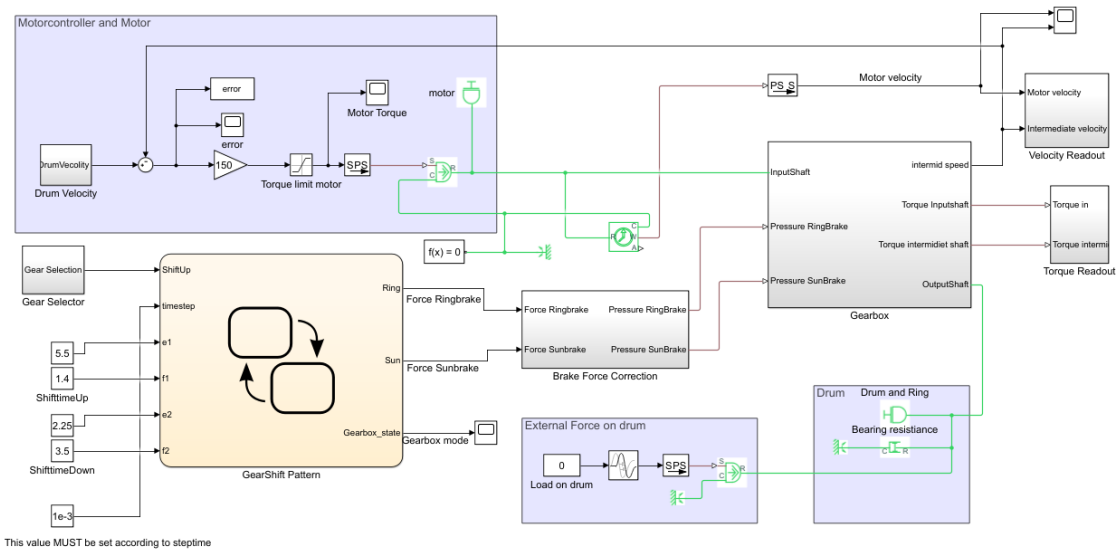

Figure 5.8: Full system simulation model.

The "Drum Velocity" block creates the velocity profile for the intermediate shaft (carrier 2 → fixed sun) shown in figure 5.9.

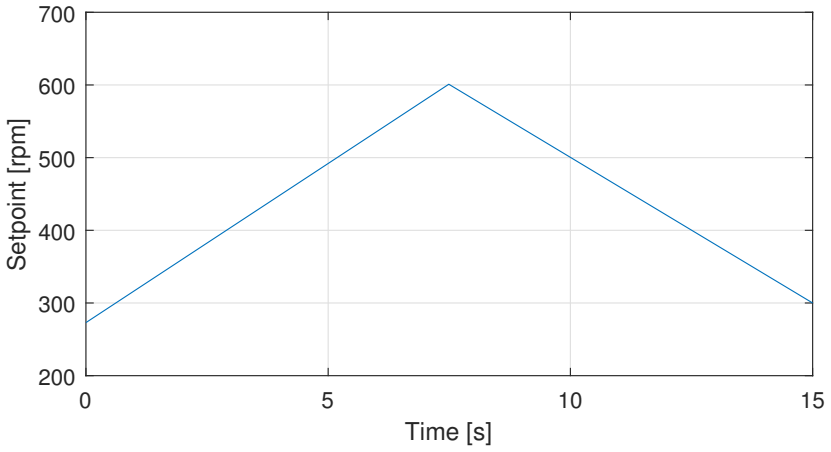

Figure 5.9: Velocity setpoint profile for model.

The "Gear Selector" block times the gear-shift operations. The system is initially in low gear, then made to go to high gear at $5[s]$, and back to low gear at $10[s]$. The gear-changes occur when the motor's velocity is $2000[rpm]$ in low gear.

The model is built using sub-models to increase readability. In the main model, filled frames are used to indicate subsystems.

The control system for the torque source (motor) is made with a single feedback with proportional gain. The control system is minimal, because the motor is unknown, and its control is not within the scope of the thesis. A relatively high gain is used to make the system fairly quickly. The steady state error is of little concern to the gear-change operation, and is therefore assumed not to affect the findings.

The thesis assumes that there is no friction in the system. A rotational viscous damper with a friction-coefficient of $0.4\,[^{Nm}/_{(rad/s)}]$ was through attached to the drum and tested for its effects. The friction coefficient was intentionally set quite high, to emulate multiple frictions, and make the results distinct. For bearings, the friction-coefficient will typically be between 0.0015 and 0.0050 $[^{Nm}/_{(rad/s)}]$ [34]. The friction on the drum was used for all of the tests after its effect was tested.

Gearbox sub-Model

Figure 5.10 shows the gearbox sub-model. The sub-model contains both the fixed and actuated step, and the multi-disc brakes. The gearbox part of the sub-model uses the simple model in chapter 5.7.

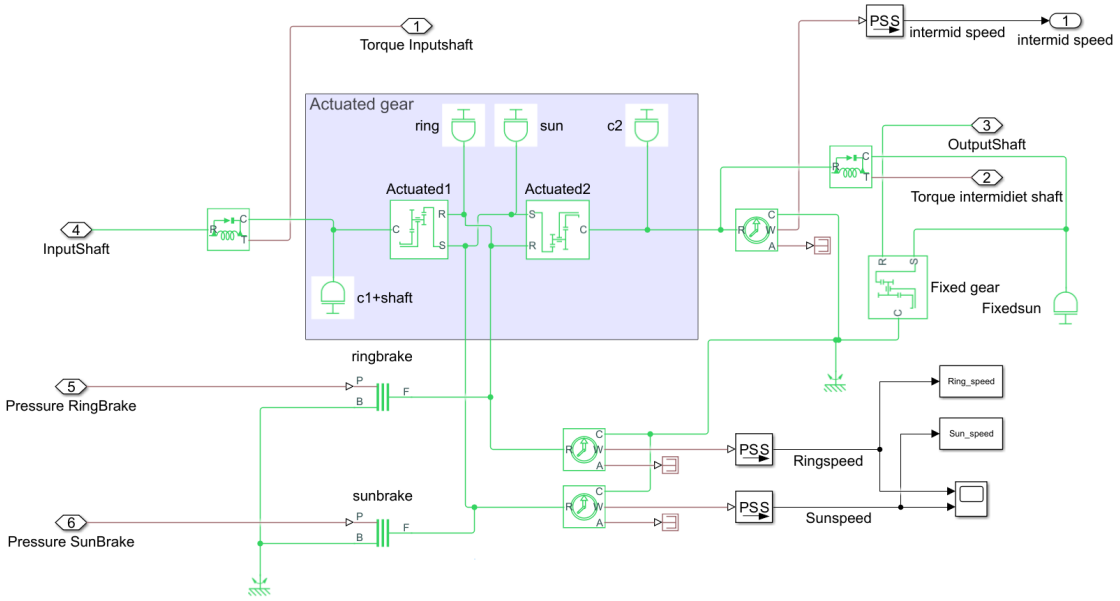

Figure 5.10: Gearbox sub-model.

The dynamic friction of the brake surfaces are the same as described in chapter 3.1.3 (0.25 & 0.06). The static frictions were set to be 0.30 & 0.065, because Simulink requires higher static friction.

GearShift Pattern State Machine

The state machine which controls the gearbox is shown in figure 5.11. The state machine has four holding states:

- State 1: LowGear
- State 2: ShiftUp
- State 3: HighGear
- State 4: ShiftDown

There are also two transition states, which initialize for the shift states.

The state model uses the time-step of the model to create the ramps of the brakes numerically, through the equations in the ShiftUp and ShiftDown states. The initialization states reset the timer before the shifts are performed. The shift pattern is altered by adjusting the time and ramp values, and it is possible to have a different pattern for up-shift and down-shift. The inputs and outputs for this block are shown in table 5.5.

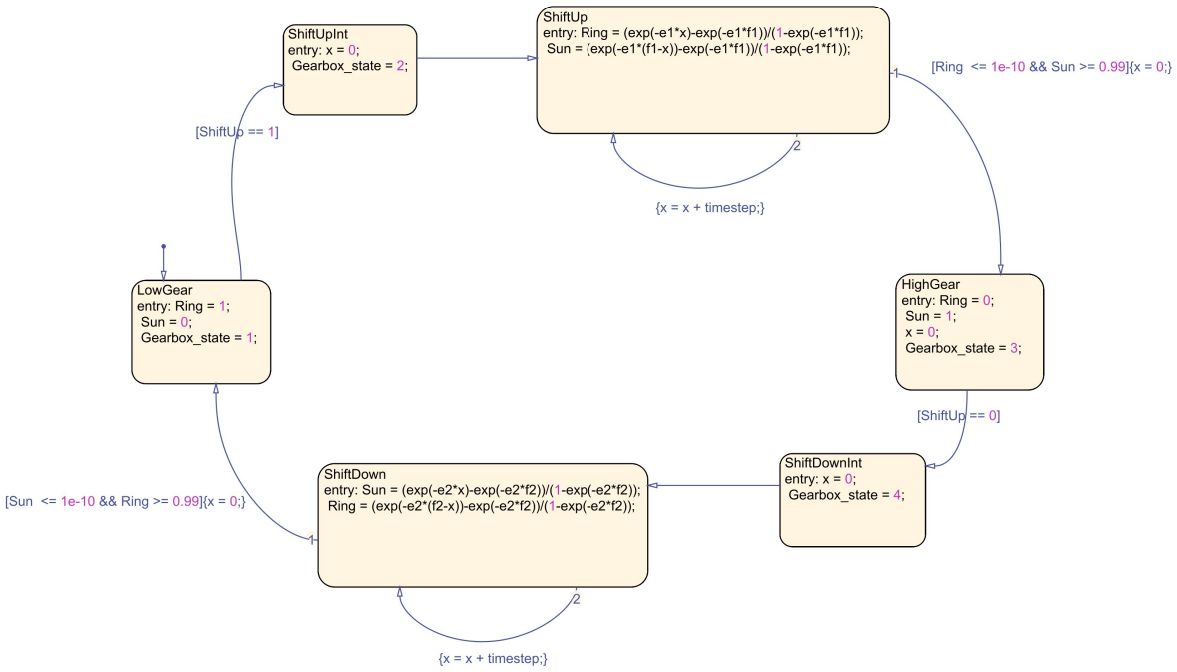

Figure 5.11: State machine for gearbox control.

Table 5.5: I/O for the state machine.

Variable	Signal type	Description	Value
ShiftUp	Input boolean	If high, the gearbox shifts in to high gear. If low, the gearbox shifts in to high gear.	$\in [0, 1]$
timestep	Input Real	The steptime for the simulation / controller.	
e1	Input Real	The slope-factor for upshift.	
e2	Input Real	The slope-factor for downshift.	
f1	Input Real	The transition-time of the slope for upshift.	
f2	Input Real	The transition-time of the slope for downshift.	
Ring	Output Real	Signal for how much the ring brake is to be applied.	$\in [0, 1]$
Sun	Output Real	Signal for how much the sun brake is to be applied.	$\in [0, 1]$
Gearbox_state	Output int	Signal for which state the gearbox is in.	$\in [0, 4]$

In the model, the slope-factor is e, while the thesis uses a.

Brake Force Correction sub-Model

This sub-model (figure 5.12) converts the 0-1 signal from the state machine to corresponding pressures to the brakes.

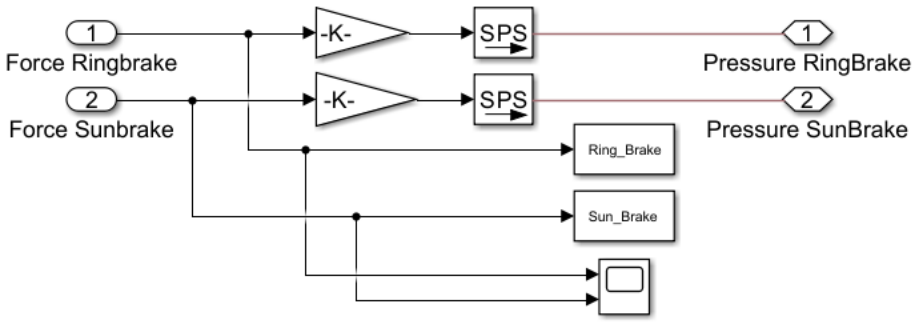

Figure 5.12: Brake Force Correction sub-Model.

The gains contain the equation:

$$p = \frac{F}{\pi(d_o - d_i)^2 \frac{1}{4}} k \tag{5.28}$$

The parameters in the equation are:

$\boldsymbol{d}$	Diameter of brake surface	$[m]$
$\boldsymbol{F}$	Maximum force	$[N]$
$\boldsymbol{k}$	Input fraction	$[-]$
$\boldsymbol{p}$	Output pressure	$[Pa]$

The maximum force in the equation is the necessary force of the brakes, described in table 3.2.

Velocity Readout sub-Model

This sub-model (figure 5.13) logs the velocities of the input and output of the actuated part of the gearbox, and the actual gear-ratio in the gearbox.

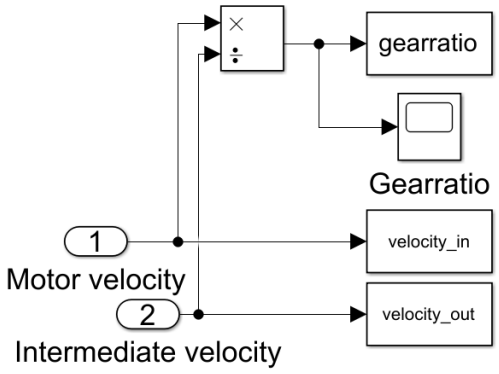

Figure 5.13: Velocity Readout sub-Model.

Torque Readout sub-Model

This sub-model (figure 5.14) logs the torque of the input and output of the actuated part of the gearbox.

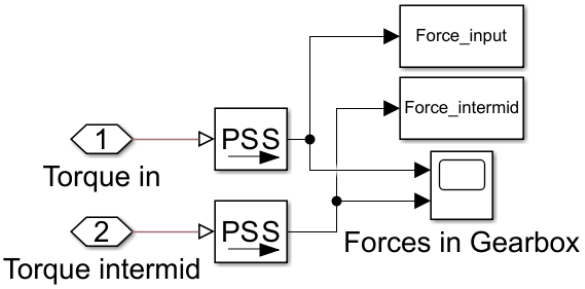

Figure 5.14: Torque Readout sub-Model.

5.11 Tuning of Brake Force Profiles

The brake force profiles described in chapter 5.9 were tuned for the model in chapter 5.10. The equations for the brake force profiles are reproduced below, where equation (5.29) is for the release of a brake, and (5.30) is for the engagement.

$$y_{disengage} = \frac{e^{-at} - e^{-af}}{1 - e^{-af}} \tag{5.29}$$

$$y_{engage} = \frac{e^{-a(f-t)} - e^{-af}}{1 - e^{-af}} \tag{5.30}$$

The parameters in the equations are:

$\boldsymbol{a}$	Slope-factor	$[1/s]$
$\boldsymbol{f}$	End-time of transition	$[s]$
$\boldsymbol{t}$	Time	$[s]$
$\boldsymbol{y}$	Brake actuation fraction	$[-]$

The tuning was done by altering the slope-factor and shift time of the brake profiles (on the input of the state machine in figure 5.8). The initial attempt at shifting gears used the simplest form of the brake profiles, with an arbitrarily set short shift-time ($f = 0.2[s]$) and a near-linear profile ($a = 1 \cdot 10^{-10}\,[1/s]$). After the initial test, the shift time was incremented by relatively small steps ($0.2[s]$ or $0.5[s]$) and some designer-selected slope-factors were tested for each of the times. The tested values may be seen in chapter E.1 of appendix E.

Both the engagement and disengagement profiles were initially iterated identically, until one of them was found to be sufficiently tuned, after which the other was further tuned by the same method. The tuning was initially performed with no load attached to the drum. After tuning the system for the no-load case, the tuned parameters were tested for load cases. The system was tested for both negative and positive loads up to $1500[Nm]$, which is the estimated maximum torque described in chapter 5.8. The loads were stepped from $0[Nm]$ with steps of $250[Nm]$.

The brake force profiles were tuned for the maximum load, $\pm 1500[Nm]$, by changing the slope-factors gradually by steps of $0.25[1/s]$ until a satisfactory result was achieved, without changing the shift time. The base for the load-tuning was the no-load tuned values. The slope-factors were initially shifted up and down; then the improving direction was pursued until satisfactory. The final brake force profiles were lastly tested for the range of loads between $\pm 1500[Nm]$ to find the actual operational range.

The tuning was performed on the Simulink model shown in chapter 5.10. The tuning was performed to the setpoint profile shown in figure 5.15. The measured output value for the feedback is from the intermediate shaft (carrier 2 $\rightarrow$ fixed sun), because of the placement of the encoder (chapter 5.1). The system is initially in low gear, then made to go to high gear at $5[s]$, and back to low gear at $10[s]$. The gear-changes occur when the motor's velocity is $2000[rpm]$ in low gear.

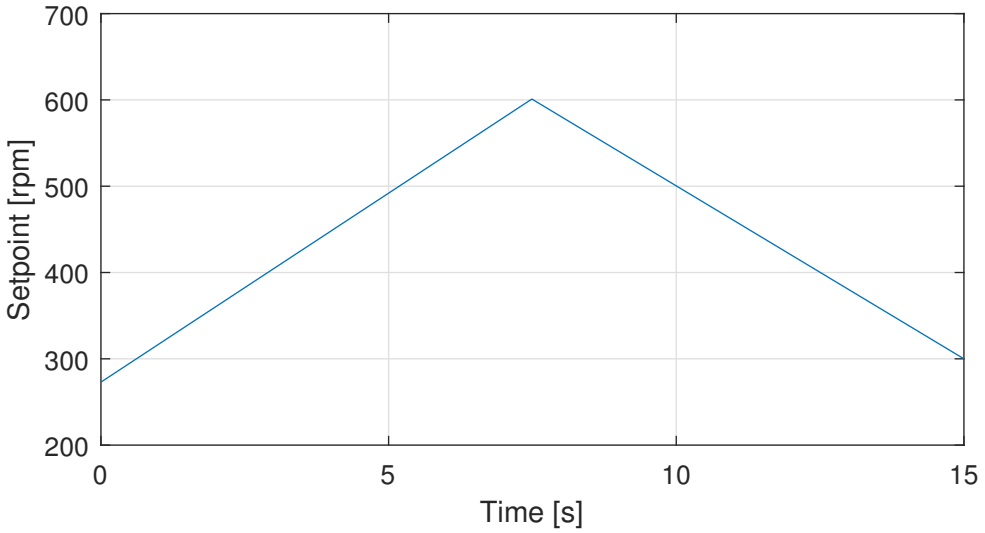

Figure 5.15: Velocity setpoint profile for intermediate shaft used for tuning.

5.12 Result and Discussion of Brake Tuning

The parameters and results of all the tests are shown in appendix E. The most relevant are presented here.

In the captions of the result-figures, f is the shift-time, and a is the slope-factor of the brake force profiles described in chapter 5.9.

5.12.1 Initial Test

The initial attempt at shifting gears used the simplest form of the brake profiles, with an arbitrarily set short shift-time ($f = 0.2[s]$) and a near-linear profile ($a = 1 \cdot 10^{-10}\,[1/s]$). Figure 5.16 shows the described profiles. The results for this test can be seen in figure 5.17.

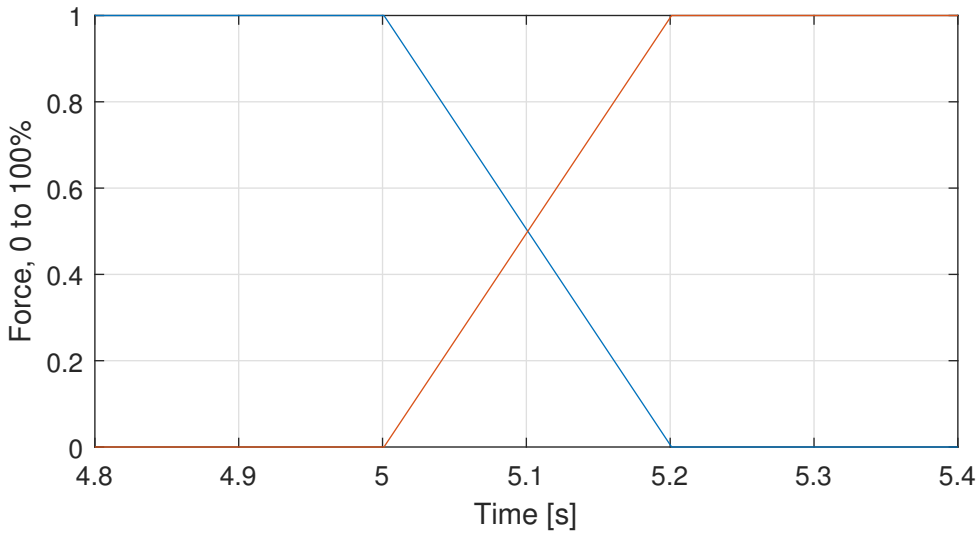

Figure 5.16: Brake force profile.
Up-shift:$f = 0.20[s]$, $a = 1 \cdot 10^{-10}\,[1/s]$.
Down-shift:$f = 0.20[s]$, $a = 1 \cdot 10^{-10}\,[1/s]$.
Only up-shift is shown, down-shift is identical.
Up-shift at $5[s]$.
Blue = Disengaging.
Orange = Engaging.

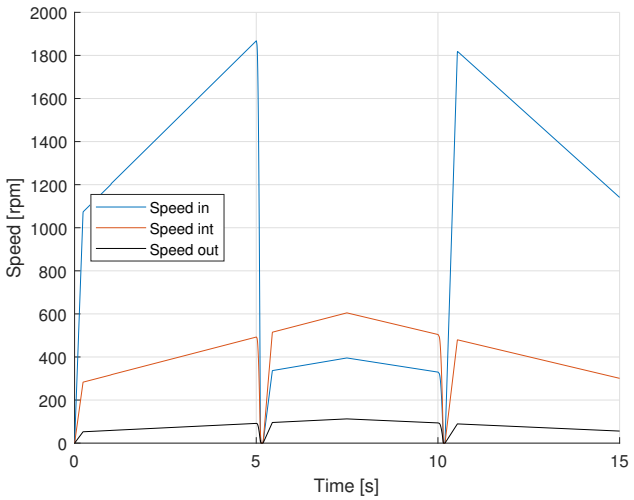

Figure 5.17:
Speeds of the gearbox and motor.
Load $= 0[Nm]$.
Up-shift:$f = 0.20[s]$, $a = 1 \cdot 10^{-10}$ $[1/s]$.
Down-shift:$f = 0.20[s]$, $a = 1 \cdot 10^{-10}$ $[1/s]$.
Up-shift at $5[s]$. Down-shift at $10[s]$.

The behavior of the system indicates that the gearbox as a whole is braked when the crossover point of the brake force profiles is too high. The lock-up is reasonable, because both the brakes are braking relatively much at the same time, which means they try to counteract each other.

5.12.2 Tuning for No-Load Case

Figures 5.18 and 5.20 shows the maximum error of the intermediate shaft velocity in relation to the setpoint, in relation to the crossover point and shift time, for up-shifts and down-shifts respectively. The graphs are illustrated from the values in appendix E, table E.1. Figures 5.19 and 5.21 show the same values as the other two figures, except that the shift time values have been limited to get a more detailed view of the final part of the tuning process.

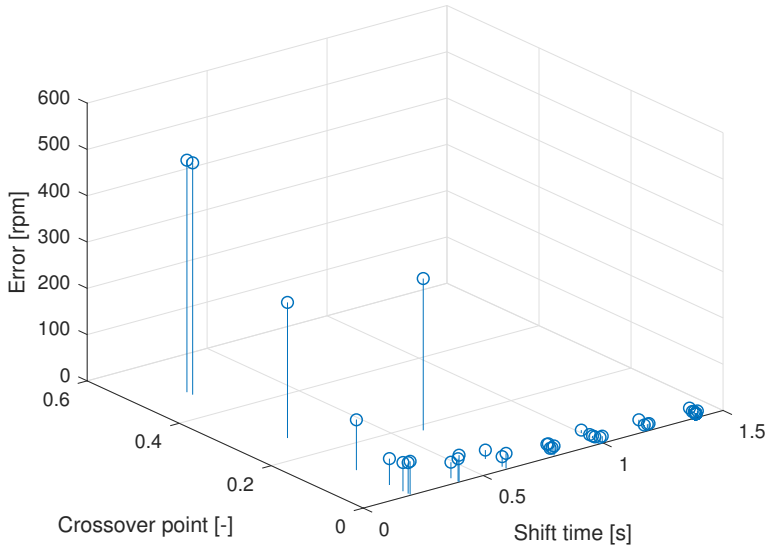

Figure 5.18: Maximum error of intermediate shaft velocity in relation to setpoint for up-shift in relation to crossover point and shift time.

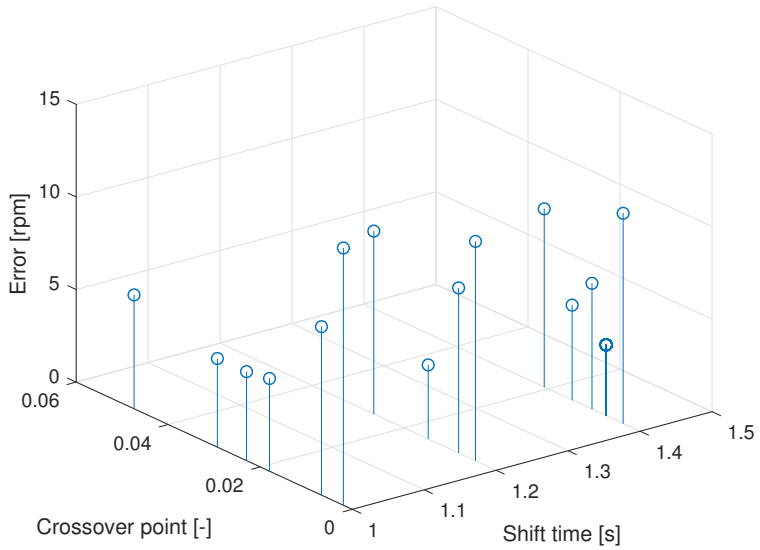

Figure 5.19: Maximum error of intermediate shaft velocity in relation to setpoint for up-shift in relation to crossover point and shift time > 1.

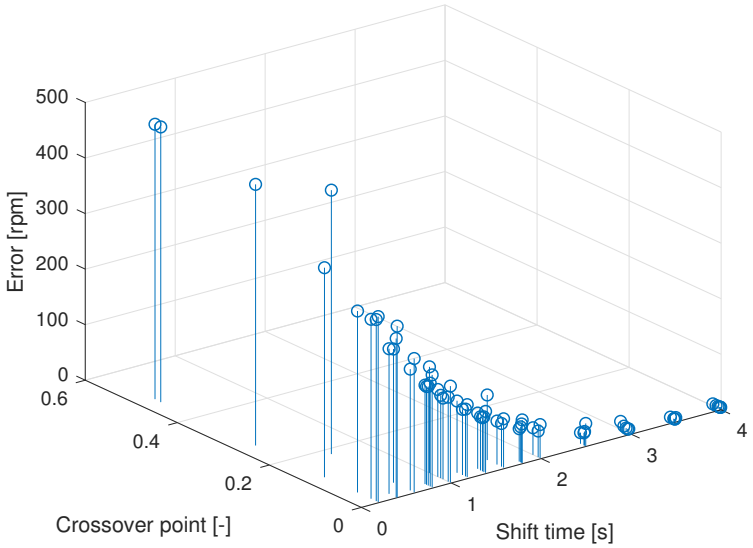

Figure 5.20: Maximum error of intermediate shaft velocity in relation to setpoint for down-shift in relation to crossover point and shift time.

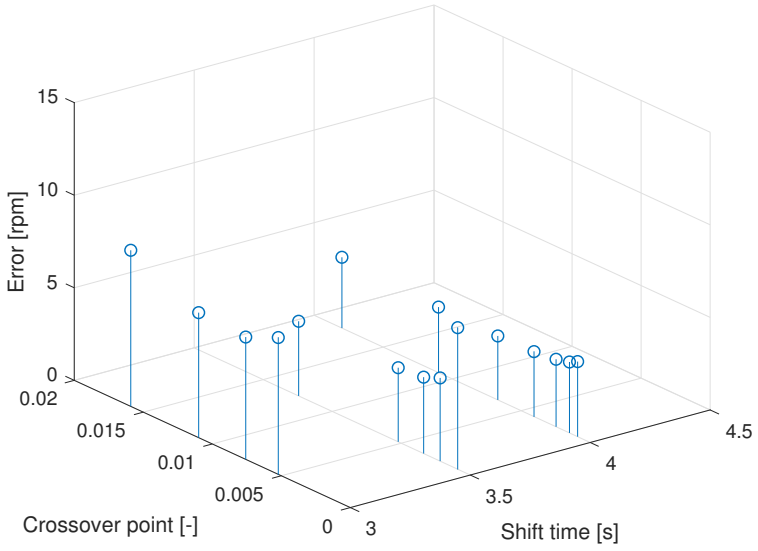

Figure 5.21: Maximum error of intermediate shaft velocity in relation to setpoint for down-shift in relation to crossover point and shift time > 3.

The errors for both the up- and shown-shifts are apparently reduced for higher shift-times and lover crossover points. For higher crossover points, the gearbox locks up, like for the initial test. It is therefore deduced that the gearbox benefits from the disengaging brake being nearly released before the other starts to engage.

Some error-values do not conform to the general behavior. These are considered anomalies due to the numerical solver of Simulink, which tends to create sharp spikes when there are quick changes in the system.

The no-load brake force profile parameters which granted the lowest errors are for up-shift a shift time of $1.40[s]$ and slope factor of $7.00[1/s]$. And the down-shift a shift time of $3.50[s]$ and slope factor of $2.50[1/s]$.

The figures below show the behavior of the gear shifts when using the profiles described above, with no attached load. In the captions, f is the shift-time, and a is the slope-factor of the brake force profiles described in chapter 5.9. The brake force profiles are illustrated graphically in figure 5.24.

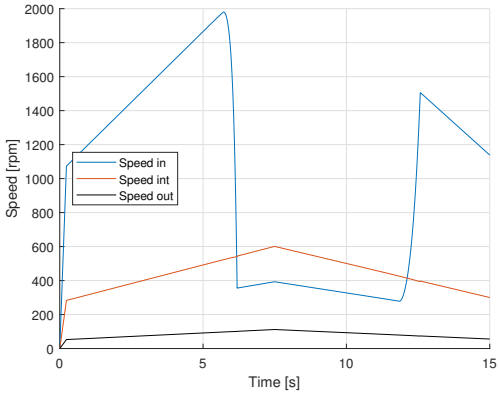

Figure 5.22: Speeds of gearbox.
Load $= 0[Nm]$.
Up-shift:$f = 1.40[s]$, $a = 7.00\,[1/s]$.
Down-shift:$f = 3.50[s]$, $a = 2.50\,[1/s]$.
Up-shift at $5[s]$. Down-shift at $10[s]$.

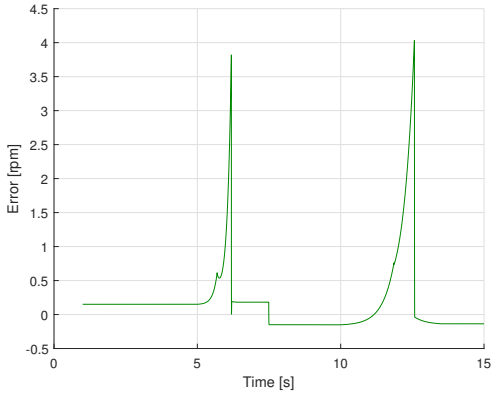

Figure 5.23: Error of intermediate shaft velocity in relation to setpoint.
Load $= 0[Nm]$.
Up-shift:$f = 1.40[s]$, $a = 7.00\,[1/s]$.
Down-shift:$f = 3.50[s]$, $a = 2.50\,[1/s]$.
Up-shift at $5[s]$. Down-shift at $10[s]$.

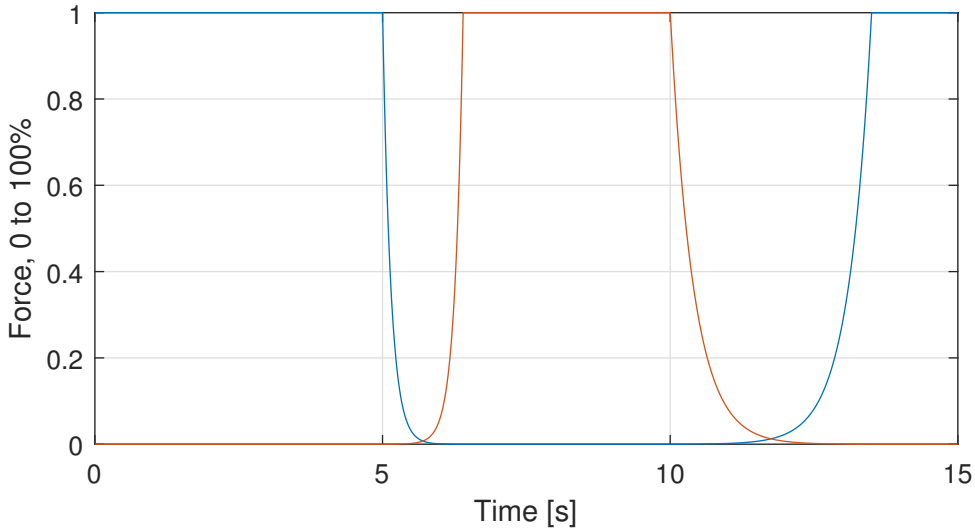

Figure 5.24: Brake force profiles.
Up-shift:$f = 1.40[s]$, $a = 5.50\,[1/s]$.
Down-shift:$f = 3.50[s]$, $a = 2.25\,[1/s]$.
Blue = Ring brake.
Orange = Sun brake.

5.12.3 Positive/Opposing Load Test

The figures below show the behavior of the no-load tuned system at two considered relevant positive loads. Additional results are located in appendix E, chapter E.2.

In the captions, f is the shift-time, and a is the slope-factor of the brake force profiles described in chapter 5.9.

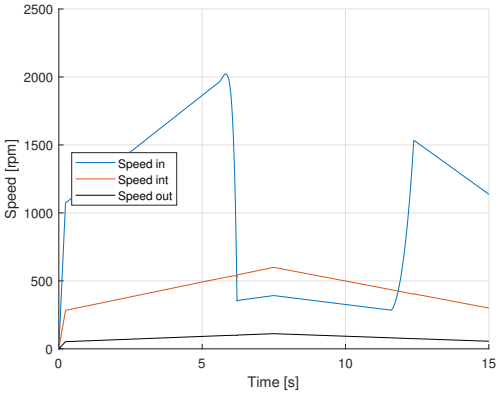

Figure 5.25: Speeds of gearbox.
Load = 750$[Nm]$.
Up-shift:$f = 1.40[s]$, $a = 7.00\,[1/s]$.
Down-shift:$f = 3.50[s]$, $a = 2.50\,[1/s]$.
Up-shift at $5[s]$. Down-shift at $10[s]$.

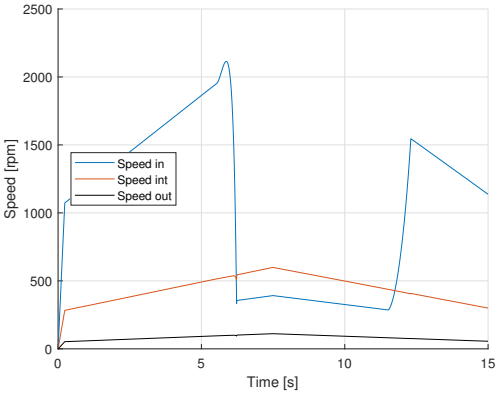

Figure 5.26: Speeds of gearbox.
Load = 1000$[Nm]$.
Up-shift:$f = 1.40[s]$, $a = 7.00\,[1/s]$.
Down-shift:$f = 3.50[s]$, $a = 2.50\,[1/s]$.
Up-shift at $5[s]$. Down-shift at $10[s]$.

750$[Nm]$ is apparently the greatest positive load that is reasonable for when the gearbox changes gear using the no-load tuned profiles. The reason that *1000*$[Nm]$ is considered to be too high is the behavior of the input velocity at the up-shift, where the motor works excessively, and over-revs, to maintain the drum-velocity.

5.12.4 Negative/Contributing Load Test

The figures below show the behavior of the no-load tuned system at two considered relevant negative loads. Additional results are located in appendix E, chapter E.2.

In the captions, f is the shift-time, and a is the slope-factor of the brake force profiles described in chapter 5.9.

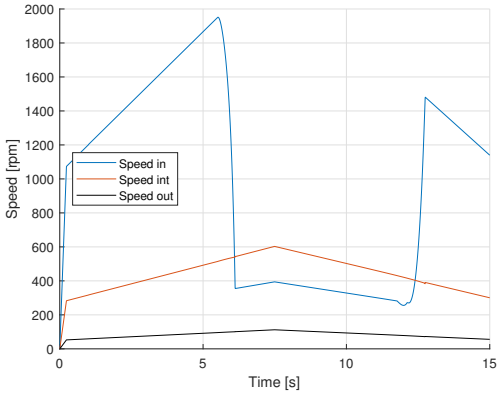

Figure 5.27: Speeds of gearbox.
Load $= -1000[Nm]$.
Up-shift:$f = 1.40[s]$, $a = 7.00\,[1/s]$.
Down-shift:$f = 3.50[s]$, $a = 2.50\,[1/s]$.
Up-shift at $5[s]$. Down-shift at $10[s]$.

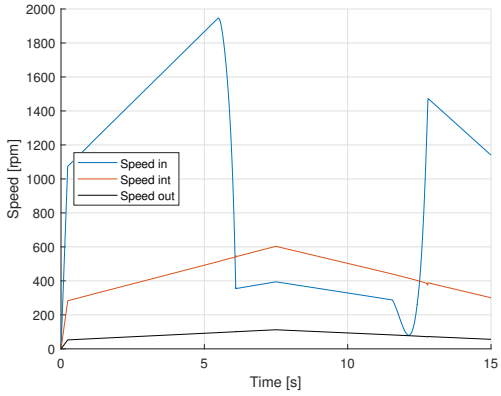

Figure 5.28: Speeds of gearbox.
Load $= -1250[Nm]$.
Up-shift:$f = 1.40[s]$, $a = 7.00\,[1/s]$.
Down-shift:$f = 3.50[s]$, $a = 2.50\,[1/s]$.
Up-shift at $5[s]$. Down-shift at $10[s]$.

For negative loads, *-1000*$[Nm]$ appears to be the limit with the no-load tuned profiles, because of the behavior of the input velocity at the down-shift, which behaves similarly to the positive load above *750*$[Nm]$.

5.12.5 Tuning of Down-Shift for Negative Loads

The tuning of the down-shift for negative loads led to a shift time of *3.50*$[s]$ and slope-factor of *2.25*$[1/s]$ for the down-shift. The up-shift did not need tuning for negative loads. The behavior for the tuned profile at *-1500*$[Nm]$ is shown in the figures below. The results for each iteration of manual tuning are located in appendix E, chapter E.4.

In the captions, f is the shift-time, and a is the slope-factor of the brake force profiles described in chapter 5.9.

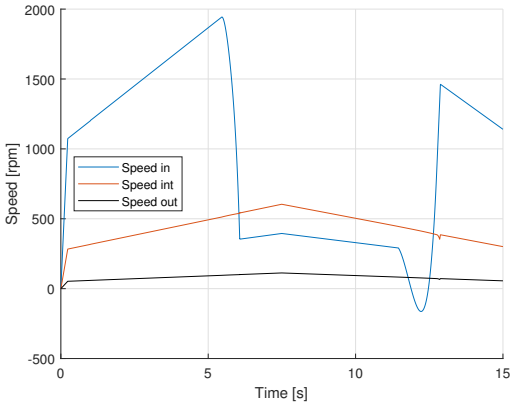

Figure 5.29: Speeds of gearbox.
Load $= -1500[Nm]$.
Up-shift:$f = 1.40[s]$, $a = 7.00\,[1/s]$.
Down-shift:$f = 3.50[s]$, $a = 2.50\,[1/s]$.
Up-shift at $5[s]$. Down-shift at $10[s]$.

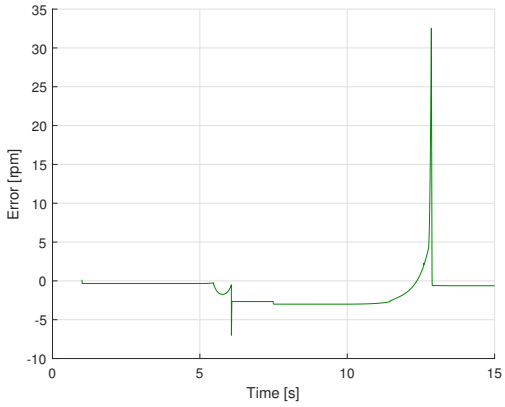

Figure 5.30: Error of intermediate shaft velocity in relation to setpoint.
Load $= -1500[Nm]$.
Up-shift:$f = 1.40[s]$, $a = 7.00\,[1/s]$.
Down-shift:$f = 3.50[s]$, $a = 2.50\,[1/s]$.
Up-shift at $5[s]$. Down-shift at $10[s]$.

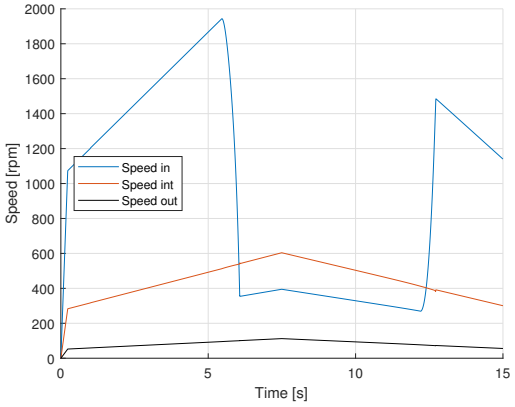

Figure 5.31: Speeds of gearbox.
Load $= -1500[Nm]$.
Up-shift:$f = 1.40[s]$, $a = 7.00\,[1/s]$.
Down-shift:$f = 3.50[s]$, $a = 2.25\,[1/s]$.
Up-shift at $5[s]$. Down-shift at $10[s]$.

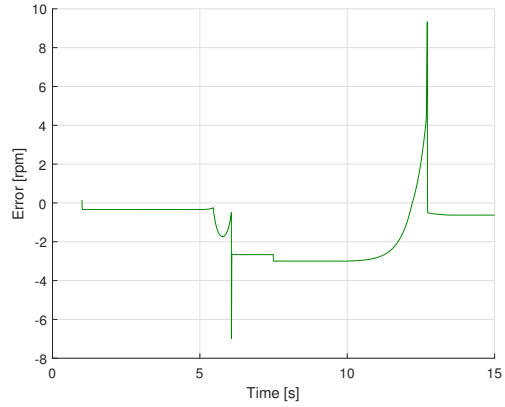

Figure 5.32: Error of intermediate shaft velocity in relation to setpoint.
Load $= -1500[Nm]$.
Up-shift:$f = 1.40[s]$, $a = 7.00\,[1/s]$.
Down-shift:$f = 3.50[s]$, $a = 2.25\,[1/s]$.
Up-shift at $5[s]$. Down-shift at $10[s]$.

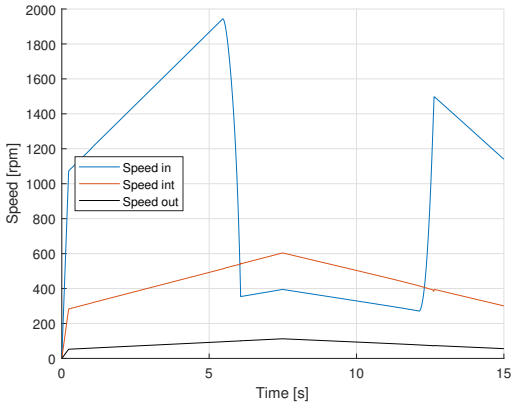

Figure 5.33: Speeds of gearbox.
Load $= -1500[Nm]$.
Up-shift:$f = 1.40[s]$, $a = 7.00\,[1/s]$.
Down-shift:$f = 3.50[s]$, $a = 2.00\,[1/s]$.
Up-shift at $5[s]$. Down-shift at $10[s]$.

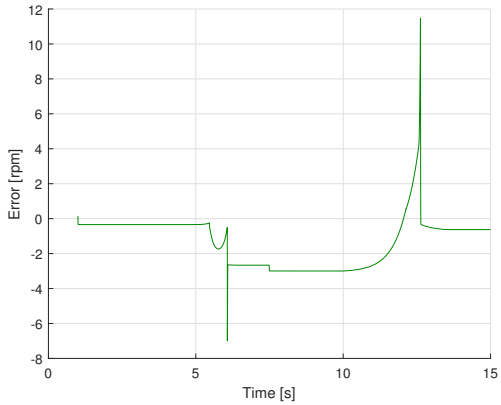

Figure 5.34: Error of intermediate shaft velocity in relation to setpoint.
Load $= -1500[Nm]$.
Up-shift:$f = 1.40[s]$, $a = 7.00\,[1/s]$.
Down-shift:$f = 3.50[s]$, $a = 2.00\,[1/s]$.
Up-shift at $5[s]$. Down-shift at $10[s]$.

5.12.6 Tuning of Up-Shift for Positive Loads

The tuning of the up-shift for negative loads led to a shift time of $1.40[s]$ and slope-factor of $5.5[1/s]$ for the up-shift. The down-shift did not need tuning for positive loads. The behavior for the tuned profile at $1500[Nm]$ is shown in the figures below. The results for each iteration of manual tuning are located in appendix E, chapter E.5.

In the captions, f is the shift-time, and a is the slope-factor of the brake force profiles described in chapter 5.9.

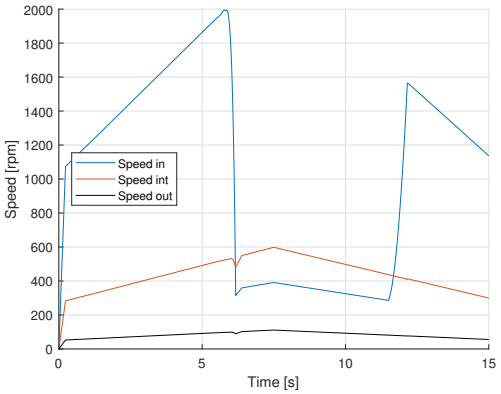

Figure 5.35: Speeds of gearbox.
Load = $1500[Nm]$.
Up-shift:$f = 1.40[s]$, $a = 5.75\,[1/s]$.
Down-shift:$f = 3.50[s]$, $a = 2.25\,[1/s]$.
Up-shift at $5[s]$. Down-shift at $10[s]$.

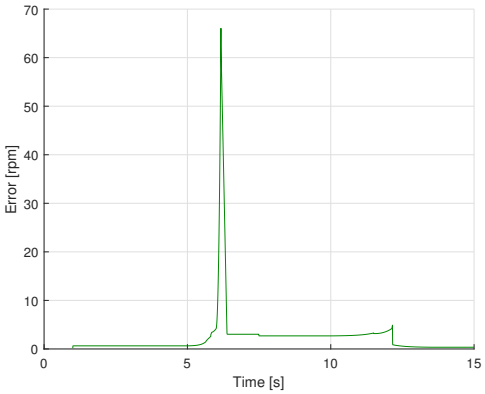

Figure 5.36: Error of intermediate shaft velocity in relation to setpoint.
Load = $1500[Nm]$.
Up-shift:$f = 1.40[s]$, $a = 5.75\,[1/s]$.
Down-shift:$f = 3.50[s]$, $a = 2.25\,[1/s]$.
Up-shift at $5[s]$. Down-shift at $10[s]$.

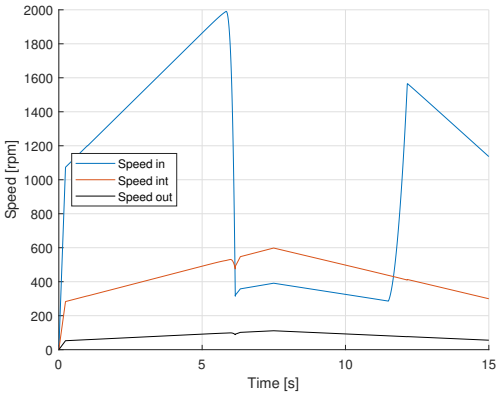

Figure 5.37: Speeds of gearbox.
Load = $1500[Nm]$.
Up-shift:$f = 1.40[s]$, $a = 5.50\,[1/s]$.
Down-shift:$f = 3.50[s]$, $a = 2.25\,[1/s]$.
Up-shift at $5[s]$. Down-shift at $10[s]$.

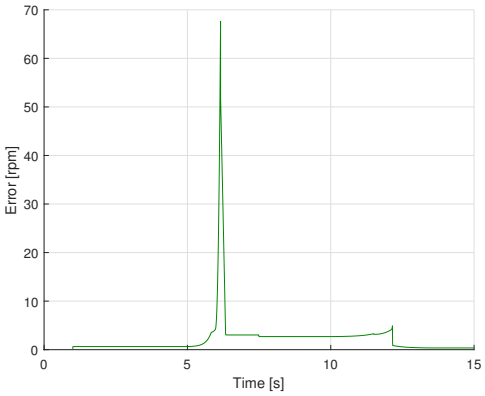

Figure 5.38: Error of intermediate shaft velocity in relation to setpoint.
Load = $1500[Nm]$.
Up-shift:$f = 1.40[s]$, $a = 5.50\,[1/s]$.
Down-shift:$f = 3.50[s]$, $a = 2.25\,[1/s]$.
Up-shift at $5[s]$. Down-shift at $10[s]$.

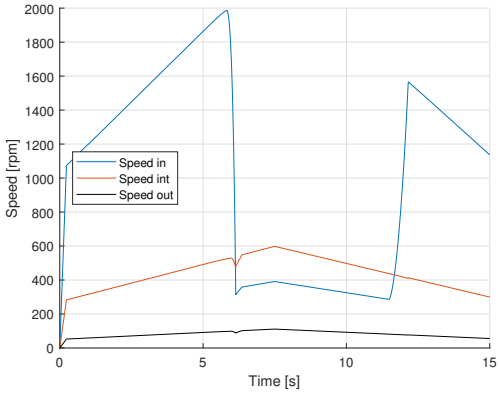

Figure 5.39: Speeds of gearbox.
Load $= 1500[Nm]$.
Up-shift:$f = 1.40[s]$, $a = 5.25\,[1/s]$.
Down-shift:$f = 3.50[s]$, $a = 2.25\,[1/s]$.
Up-shift at $5[s]$. Down-shift at $10[s]$.

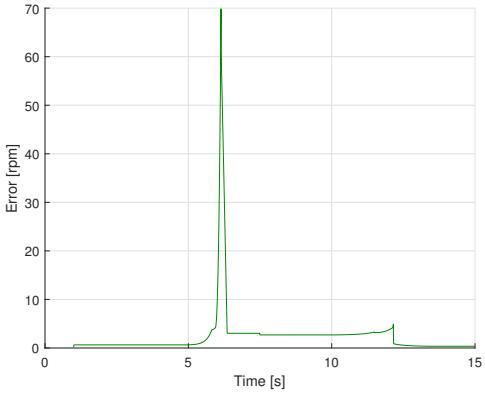

Figure 5.40: Error of intermediate shaft velocity in relation to setpoint.
Load $= 1500[Nm]$.
Up-shift:$f = 1.40[s]$, $a = 5.25\,[1/s]$.
Down-shift:$f = 3.50[s]$, $a = 2.25\,[1/s]$.
Up-shift at $5[s]$. Down-shift at $10[s]$.

5.12.7 Final Tuning Parameters & Allowable Torque

The final, assumed best, brake force profile parameters are for the up-shift a shift time of $1.40[s]$ and slope factor of $5.50[1/s]$. And the down-shift a shift time of $3.50[s]$ and slope factor of $2.25[1/s]$. The equations below describe the profiles that are the final result. The crossover points are, for the up-shift at $y = 0.0074$, and for the down-shift at $y = 0.0067$. Figure 5.41 shows how the profiles appear graphically.

$$y_{disengage(up-shift)} = \frac{e^{-5.5(1.4-t)} - e^{-5.5 \cdot 1.4}}{1 - e^{-5.5 \cdot 1.4}} \tag{5.31}$$

$$y_{engage(up-shift)} = \frac{e^{-5.5t} - e^{-5.5 \cdot 1.4}}{1 - e^{-5.5 \cdot 1.4}} \tag{5.32}$$

$$y_{disengage(down-shift)} = \frac{e^{-2.25(3.5-t)} - e^{-2.25 \cdot 3.5}}{1 - e^{-2.25 \cdot 3.5}} \tag{5.33}$$

$$y_{engage(down-shift)} = \frac{e^{-2.25t} - e^{-2.25 \cdot 3.5}}{1 - e^{-2.25 \cdot 3.5}} \tag{5.34}$$

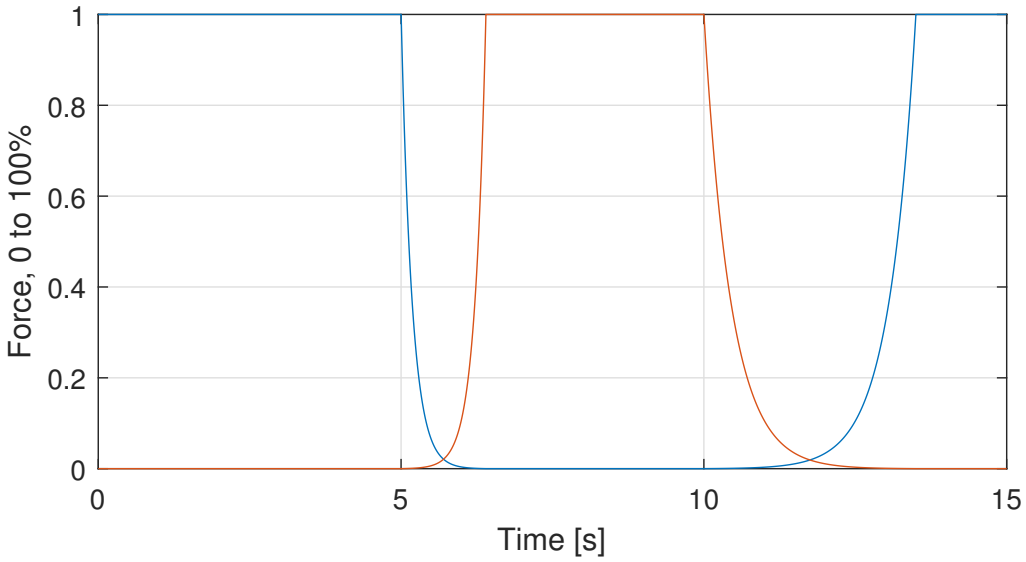

Figure 5.41: Brake force profiles.
Up-shift:$f = 1.40[s]$, $a = 5.50\,[1/s]$.
Down-shift:$f = 3.50[s]$, $a = 2.25\,[1/s]$.
Blue = Ring brake.
Orange = Sun brake.

The final brake force profiles produce the behavior shown in the figures below, for different loads.

In the captions, f is the shift-time, and a is the slope-factor of the brake force profiles described in chapter 5.9.

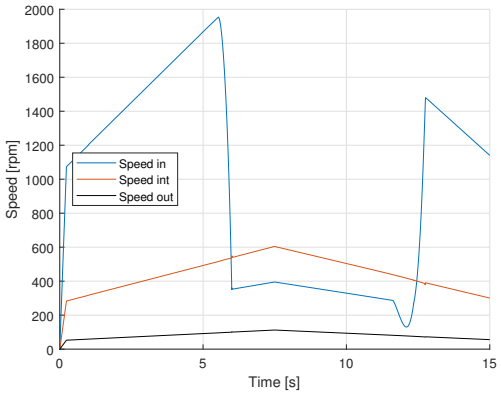

Figure 5.42: Speeds of gearbox.
Load $= -1750[Nm]$.
Up-shift:$f = 1.40[s]$, $a = 5.50\,[1/s]$.
Down-shift:$f = 3.50[s]$, $a = 2.25\,[1/s]$.
Up-shift at $5[s]$. Down-shift at $10[s]$.

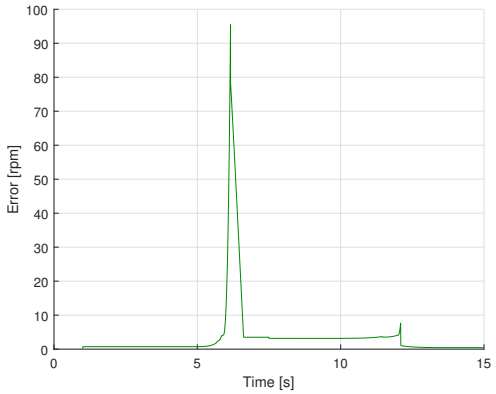

Figure 5.43: Error of intermediate shaft velocity in relation to setpoint.
Load $= -1750[Nm]$.
Up-shift:$f = 1.40[s]$, $a = 5.50\,[1/s]$.
Down-shift:$f = 3.50[s]$, $a = 2.25\,[1/s]$.
Up-shift at $5[s]$. Down-shift at $10[s]$.

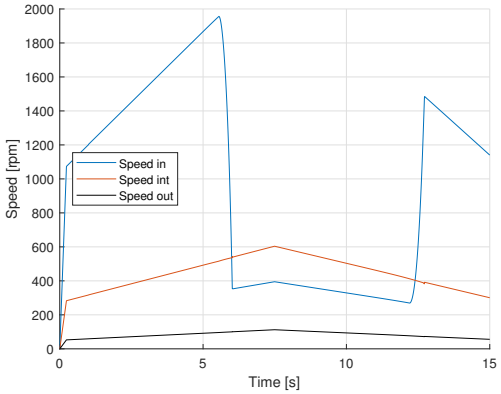

Figure 5.44: Speeds of gearbox.
Load $= -1500[Nm]$.
Up-shift:$f = 1.40[s]$, $a = 5.50\,[1/s]$.
Down-shift:$f = 3.50[s]$, $a = 2.25\,[1/s]$.
Up-shift at $5[s]$. Down-shift at $10[s]$.

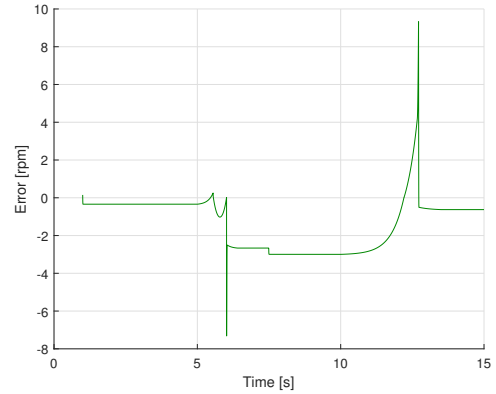

Figure 5.45: Error of intermediate shaft velocity in relation to setpoint.
Load $= -1500[Nm]$.
Up-shift:$f = 1.40[s]$, $a = 5.50\,[1/s]$.
Down-shift:$f = 3.50[s]$, $a = 2.25\,[1/s]$.
Up-shift at $5[s]$. Down-shift at $10[s]$.

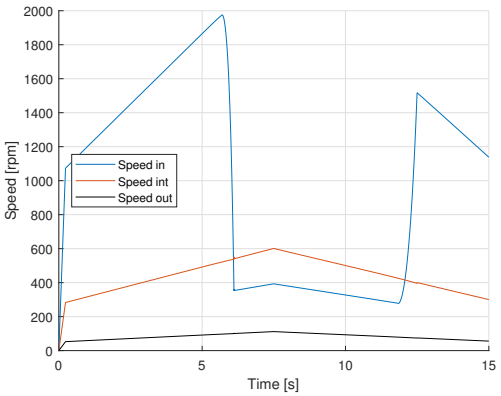

Figure 5.46: Speeds of gearbox.
Load = $0[Nm]$.
Up-shift:$f = 1.40[s]$, $a = 5.50\,[1/s]$.
Down-shift:$f = 3.50[s]$, $a = 2.25\,[1/s]$.
Up-shift at $5[s]$. Down-shift at $10[s]$.

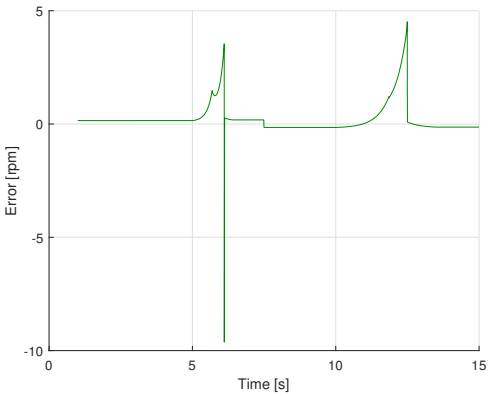

Figure 5.47: Error of intermediate shaft velocity in relation to setpoint.
Load = $0[Nm]$.
Up-shift:$f = 1.40[s]$, $a = 5.50\,[1/s]$.
Down-shift:$f = 3.50[s]$, $a = 2.25\,[1/s]$.
Up-shift at $5[s]$. Down-shift at $10[s]$.

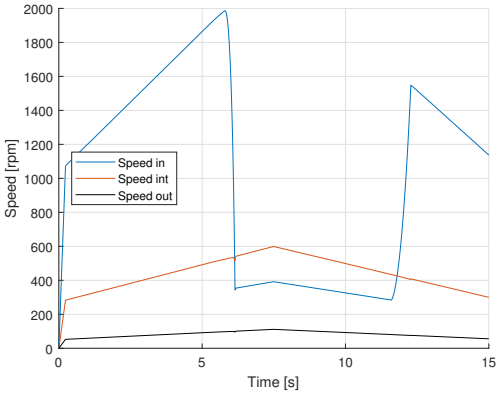

Figure 5.48: Speeds of gearbox.
Load = $1000[Nm]$.
Up-shift:$f = 1.40[s]$, $a = 5.50\,[1/s]$.
Down-shift:$f = 3.50[s]$, $a = 2.25\,[1/s]$.
Up-shift at $5[s]$. Down-shift at $10[s]$.

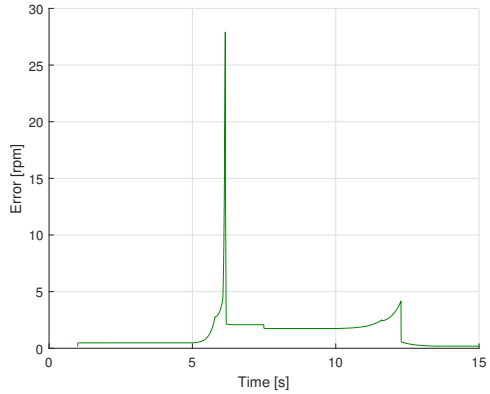

Figure 5.49: Error of intermediate shaft velocity in relation to setpoint.
Load = $1000[Nm]$.
Up-shift:$f = 1.40[s]$, $a = 5.50\,[1/s]$.
Down-shift:$f = 3.50[s]$, $a = 2.25\,[1/s]$.
Up-shift at $5[s]$. Down-shift at $10[s]$.

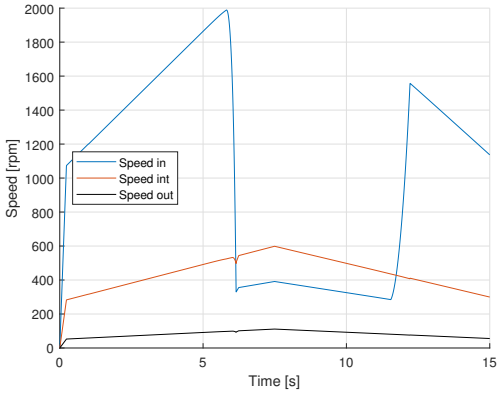

Figure 5.50: Speeds of gearbox.
Load = 1250$[Nm]$.
Up-shift:$f = 1.40[s]$, $a = 5.50\,[1/s]$.
Down-shift:$f = 3.50[s]$, $a = 2.25\,[1/s]$.
Up-shift at 5$[s]$. Down-shift at 10$[s]$.

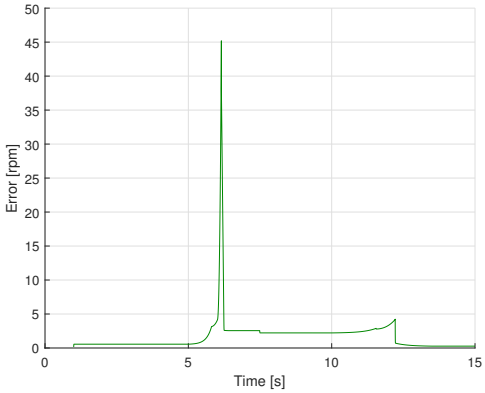

Figure 5.51: Error of intermediate shaft velocity in relation to setpoint.
Load = 1250$[Nm]$.
Up-shift:$f = 1.40[s]$, $a = 5.50\,[1/s]$.
Down-shift:$f = 3.50[s]$, $a = 2.25\,[1/s]$.
Up-shift at 5$[s]$. Down-shift at 10$[s]$.

The figures above describe the no-load case, and what are determined to be the maximum allowable loads. The maximum positive load is *1000*$[Nm]$. Above *1000*$[Nm]$, the system will jerk more than is deemed to be allowable. At *1000*$[Nm]$, there is also some spike in the speed. Most of the spike is however assumed to be numerical from the simulation, and is therefore considered negligible. The negative load is shown to produce reasonably stable behavior up to *-1500*$[Nm]$. At negative loads above *-1500*$[Nm]$, the motor works excessively on the down-shift, and the error for the up-shift is rather large. The down-shift is tuned for *-1500*$[Nm]$, and the up-shift is tuned for *1500*$[Nm]$ which may be the reason for why the system has a non-desirable behavior below this. Additional results from within and out of the operational range may be seen in appendix E, chapter E.6. The behavior at those other loads may be evaluated for if they are allowable for use by the customer for a real-life operational limit. The recommendation in this thesis is however for the gearshift to be performed between *-1500*$[Nm]$ and *1000*$[Nm]$. If one absolute torque-limit should be set, it is recommended that it is $\pm$*1000*$[Nm]$.

5.13 Sources of Errors and Inaccuracies

The thesis is purely theoretical, which excludes any real-life inaccuracies. The use of computers for calculations (Matlab) and simulation (Matlab-Simulink) does though bring some issues related to numeric solvers.

Matlab is assumed to be accurate enough for this thesis' use that the calculations performed and their results are assumed to be perfect. None of the results in the thesis from Matlab-calculations have used all the decimals that Matlab provide. According to Mathworks [35], Matlab provides 16 digits of precision, while this thesis never uses more than six digits after the decimal point.

The numeric solver in Simulink has been shown to be an issue. For the step-size used in the simulations for this thesis, the solver produces some spikes in the speed of the parts when there are rapid changes. The spikes are improved by lowering the step time. The decrease in step-time does, however, require more computational power. The behavior of the spikes was therefore partly ignored, based on assumed behavior.

6 | Conclusion

The designed gearbox fulfills all the requirements defined in table 1.1. The gear ratios are within the requirements, but not exactly the median values that were aimed for. The gear ratios are though optimized to all the conditions set to the gear train. All the mechanical parts that have been dimensioned can withstand the required load plus a safety factor. The gearbox is also small enough to be mounted inside the winch drum, assuming that the housing of the gearbox does not need to be wider than what is proposed. The gear-train is observed to be near the possible limits when it comes to the difference between the gear ratios. If the difference should be greater, it may be required to have at least one more gear-set, or even use a modified gear-set or a different form of the gear-train.

The designed gear-shift actuation system is proven to theoretically be able to change between the gears at any load between *-1500*$[Nm]$ and *1000*$[Nm]$, and should be able to change gears at any load, up to the mechanical limits of the gearbox. The system as a whole is however recommended to not change gears outside the range [*-1500*$[Nm]$, *1000*$[Nm]$] in consideration of the motor and the mechanical parts of the system. The true practical operational range of load for the gear-shift must be practically verified on a full-scale model.

6.1 Further Work

The shaft diameters must be re-checked for their final design. Especially the notches that have been made for fitting the parts must be taken into the calculations. The shafts are however assumed to be so over-dimensioned that they should not prove an issue. The bending effect of the weight of the parts should be taken into consideration for possible critical speeds, which are not tested for in this thesis.

The bearings should also be post-design controlled to include all factors, like the viscosity of the oil, and the temperature of operation. For the bearings, there must be selected tension-springs to provide the minimum axial load required. The CAD model of the gearbox includes spaces to mount the springs, and the assembly guide in appendix F describes the mounting.

Only the shafts and gears of the gearbox are dimensioned by calculations. Of the remaining parts, the housing is especially critical to dimension, because it is the load-bearing structure which supports most of the parts, including the flange mounted motor. The housing must also be able to cope with the torque applied to the drum. The carriers, and the skeletonized gears, must also be tested for the forces but are assumed not to be an issue with the current design.

The gearbox shall hold the motor, and the whole assembly shall be held up by a bell encapsuling the motor, which is mounted to some unknown contraption on the other end of the motor. The bell must be designed in its entirety, including the mounting holes on the gearbox, which are conceptually put into the model in this thesis.

The gearbox shall be cooled and lubricated by oil. The actuated step of the gearbox shall have its own compartment which shall be filled with oil, supplied by the same source cooling the motor. The oil for the actuated step must, therefore, be decided in unison with the motor's cooling-oil. The fixed step is open, and can therefore not contain oil. It must therefore be lubricated by grease, which properties must be selected.

All the orifices of the housing for the actuated step of the gearbox will need oil-seals. The area around input shaft and the intermediate shaft which connects to the fixed step are considered especially prone to leaks, because the shafts rotate. The intermediate shaft is hollow, with the sun shaft going through it, which requires seals both outside and inside this shaft.

Dog brakes to supplement the disc brakes must be designed, as described in chapter 3.5. Both the dogs, the actuators and the control system for them must be designed.

There should be performed a practical system identification to verify the theoretical system model. The verification would indicate if the system model is correct, or if it is assumed to be too ideal. A real system is likely to differ from the theoretical somewhat, because of at least frictions, and stiffness and damping of the mechanical parts.

To verify the design, it is proposed to first create a scale model of the gearbox to test that the system actually works. A full-scale creation is necessarily the one that must be finally tested, both for applicability and system identification, but is likely far more expensive to build than a scale concept model.

6.2 Alternative Solutions and Possibilities

Only the basic type of planetary gear-set is used in this thesis. Different types of planetary set configurations could be attempted to improve the system. There is, for instance, the possibility of using multiple planets in series, or using a stepped planet, which will make the gearbox behave differently. In addition to the planetary set itself, the gear train configuration could also be different from the modified Simpson's gear train described in this thesis. The design could, for instance, be a conventional Simpson's gear train, another traditional gear train or some new invention.

Instead of machining sun 1 directly onto the actuated sun shaft, it could be machined by itself and fitted to the shaft by a fit and key (or spline). Sun 2 should though be machined directly onto the shaft regardless, because of its relative size.

For a large electric motor, it could be possible to make the rotor and shaft hollow, according to FE [3]. If the rotor and shaft were made hollow, the actuated sun shaft could be put into the hollow, and lead through the motor. This configuration allows the brake of the actuated sun to be placed on the other end of the motor, instead of after the fixed step. By using this solution, the design of the motor and gearbox would, however, need to be more integrated, because they would then be a more complicated combined unit.

Bibliography

[1] A. Cherubini, A. Papini, R. Vertechy, and M. Fontana, "Airborne wind energy systems: A review of technologies," *Renewable & Sustainable Energy Reviews*, vol. 51, pp. 1461–1476, 2015.

[2] Creative Commons, "Attribution 4.0 international (cc by 4.0)." [Online]. Available: https://creativecommons.org/licenses/by/4.0/

[3] Flekkefjord Elektro, "Personal communication with Flekkefjord Elektro," 2018.

[4] A. F. M. Authority, "Homepage." [Online]. Available: http://www.afma.gov.au/

[5] G. Lechner and H. Naunheimer, *Automotive Transmissions: Fundamentals, Selection, Design and Application*. Springer, 1999.

[6] N. Srivastava and I. Haque, "Clearance and friction-induced dynamics of chain cvt drives," *Multibody System Dynamics*, vol. 19, pp. 255–280, 2008.

[7] C. S. Kaim, "The world of planetary gears," Mar. 2000. [Online]. Available: http://www.machinedesign.com/motion-control/world-planetary-gears

[8] Gordon Russel LTD, "The pros and cons to different gear motors," Nov. 2016. [Online]. Available: http://www.gordonrussell.com/articles-10-the-pros-and-cons-to-different-gear-motors

[9] Neugart USA, "Helical planetary gearboxes: Understanding the tradeoffs," Article, Aug. 2015. [Online]. Available: http://www.machinedesign.com/sites/machinedesign.com/files/uploads/2015/05/Neugart_GearPaper.pdf

[10] C. Gonzales, "What's the difference between spur, helical, bevel, and worm gears?" Article, Jul. 2015. [Online]. Available: http://www.machinedesign.com/whats-difference-between/what-s-difference-between-spur-helical-bevel-and-worm-gears

[11] K. G. Robbersmyr, "Lectures in MAS413 - mechanical systems 1 at the University of Agder," 2016.

[12] J. Erjavec and K. Pickerill, *Today's Technician: Automatic Transmissions and Transaxles Classroom Manual and Shop Manual*. Cengage Learning, 2015.

[13] M. S. R. Mousavi, "Seamless dual-brake transmission for electric vehicles: Design, modeling, estimation, and control," Ph.D. dissertation, McGill University, 2017.

[14] A. F. Faydor L. Litvin, *Gear Geometry and Applied Theory*. CAMBRIDGE UNIV PR, 2004.

[15] C. Zegveld and J. Meijer, *Maskinkonstruksjon 2*. NKI, 1993.

[16] R. G. Budynas and K. J. Nisbett, *Shigley's Mechanical Engineering Design (McGraw-Hill Series in Mechanical Engineering)*, 10th ed. McGraw-Hill Education, 2014.

[17] *ISO 6336-5:2016 – Calculation of load capacity of spur and helical gears – Part 5: Strength and quality of materials*, International Organization for Standardization ISO.

[18] W. H. Dornfeld, "Gear tooth strength analysis," Lecture in advanced machine design at Fairfield University.

[19] R. C. Juvinall and K. M. Marshek, *Fundamentals of Machine Component Design*, 5th ed. Wiley, 2012.

[20] P. C. Gope, *MACHINE DESIGN: Fundamentals and Applications*. PHI, 2011.

[21] SDP/SI, "Elements of metric gear technology." [Online]. Available: https://www.sdp-si.com/D805/D805_PDFS/Technical/8050T108.pdf

[22] G. M. Maitra, *Handbook of Gear Design*. McGraw-Hill Professional Publishing, 1994.

[23] A. C. Ugural, *Mechanical Design of Machine Components, Second Edition*. CRC Press, 2015.

[24] Sweber.de. [Online]. Available: https://commons.wikimedia.org/wiki/File%3ACone_clutch.svg

[25] Creative Commons, "Attribution-sharealike 3.0 unported (cc by-sa 3.0)." [Online]. Available: https://creativecommons.org/licenses/by-sa/3.0/deed.en

[26] MAT foundry group LTD, "How does synchromesh work." [Online]. Available: https://www.matfoundrygroup.com/News%20and%20Blog/How_Does_Synchromesh_Work

[27] Duff-Norton, "Hydraulic vs electric linear actuators: Which is best?" [Online]. Available: https://www.duffnorton.com/blog/hydraulic-vs-electric-linear-actuators

[28] N. Mohan, *Electric Drives: An Integrative Approach*. MNPERE, 2003.

[29] S. E. Pedersen, J. Gustavsen, S. Kaasa, and O. Olsen, *Teknisk formelsamling med tabeller*. Gyldendal undervisning, 2015.

[30] LWW Group, "Datasheet for damidbond 200 copper wire," round enamelled winding wire of copper, bondable, class 200.

[31] European steel and alloy grades/numbers, "42crmo4." [Online]. Available: http://www.steelnumber.com/en/steel_composition_eu.php?name_id=335

[32] SKF, "Rolling bearings: Product catalogue," Web.

[33] J. O. Smith, "Mass moment of inertia." [Online]. Available: https://ccrma.stanford.edu/~jos/pasp/Mass_Moment_Inertia.html

[34] American roller bearing company, "Friction & frequency factors," Web. [Online]. Available: https://www.amroll.com/friction-frequency-factors.html

[35] Mathworks, "Digits." [Online]. Available: https://se.mathworks.com/help/symbolic/digits.html

Appendices

Appendix A:
Gear Ratio Design

In this appendix is the Matlab script used to find and optimize the gear ratios for the planetary gearbox from the criteria described in chapter 2.5.

```
%% Optimalization

clc; clear all; close all; %Prepare the workspace by cleaning up ...
    everything
tic %Start recording of time when running script

%% Intro

% The script finds the best options for cogwheel dimensions for the ...
    dual-stage actuated transmission with an additional fixed step. ...
    All the dimensions are given in number of teeth of the gears.

% RF = number of teeth in fixed step ring
% SF = number of teeth in fixed step sun
% PF = number of teeth on fixed step planets
% RA = number of teeth in actuated step ring
% S1 = number of teeth in actuated step first stage sun
% S2 = number of teeth in actuated step second stage sun
% P1 = number of teeth in actuated step first stage planets
% P2 = number of teeth in actuated step second stage planets

nResults = 5; % Define how many results are desired

SfP = 0.9; % Safety factor for planet interference.

grL = 20.79;    % Define total low gear ratio.
grH = 3.75;     % Define total high gear ratio.

% Define max/min parameters
minRF = 80;
maxRF = 90;
minSF = 15;
maxSF = maxRF;

minRA = 50;
maxRA = 200;

minS1 = 15;
maxS1 = 90;

minS2 = 15;
maxS2 = maxRA * 0.8;
```

```
minNP = 3;
maxNP = 5;


%% %% Actuated Step %% %%

%% Actuated Step Combination Generation
a = 1;
% Run through fixed step gear-ratios
for tempGr = 1: 0.1: 10

    % Save fixed gear-ratio
    grF(a,1) = tempGr;

    b = 1;

    % Run through possible rings on actuated step
    for tempR = minRA: 1: maxRA

        % Find required low gear ratio of actuated step
        grAL(a,b) = grL / tempGr;
        % Find required high gear ratio of actuated step
        grAH(a,b) = grH / tempGr;
        % Retrieve all ring dimensions to use for actuated step
        RA(a,b) = tempR;

        c = 1;
        % Run through select range of suns for stage 1 of actuated step
        for tempS1 = minS1: 1: maxS1

            % Calculate S2 to match the low gear ratio
            tempS2L(c)  = ( tempS1 * RA(a,b) ) / ( grAL(a,b) * ...
                (RA(a,b) + tempS1) - tempS1);
            % Calculate S2 to match the high gear ratio
            tempS2H(c) = grAH(a,b) * ( RA(a,b) + tempS1) - RA(a,b);

            % Read out values for each combination
            tempS1_2(c) = tempS1;

            c = c + 1;

        end

        % Find the sun2 matching both high and low gear ratios
        diffS2 = tempS2H - tempS2L;
        [NA,index(a,b)] = min(abs(diffS2));

        % Retrieve sun1 and 2 creating correct high and low gear ratios
        matchS1(a,b) = tempS1_2(index(a,b));
        matchS2(a,b) = tempS2L(index(a,b));

        if (matchS2(a,b)<minS2) || (matchS2(a,b)>maxS2)
            matchS2(a,b) = 0;
        end

        % Round of sun1 and 2 down and up to get integers next to ...
```

```
            matching values.
        S1Integer(a,b,1) = floor(matchS1(a,b));
        S1Integer(a,b,2) = ceil(matchS1(a,b));
        S2Integer(a,b,1) = floor(matchS2(a,b));
        S2Integer(a,b,2) = ceil(matchS2(a,b));

        b = b + 1;

    end

    a = a + 1;

end


%% Actuated Step Combination Elimination

% Run through all possible sun combinations.
for a = 1: 1: length(S1Integer(:,1,1))
    for b = 1: 1: length(S1Integer(1,:,1))
        for c = 1: 1: length(S1Integer(1,1,:)) % Run through all ...
            floor-ceiling combinations of integers for matches.

            P1(a,b,c) = (RA(a,b) - S1Integer(a,b,c)) / 2; % Find ...
                planet matching sun-ring combination.
            P1(a,b,c) = floor(P1(a,b,c)); % Round of planet to below ...
                integer.
            S1Integer(a,b,c) = RA(a,b) - 2*P1(a,b,c); % Find new sun ...
                matching rounded planet.

            P2(a,b,c) = (RA(a,b) - S2Integer(a,b,c)) / 2; % Find ...
                planet matching sun-ring combination.
            P2(a,b,c) = floor(P2(a,b,c)); % Round of planet to below ...
                integer.
            S2Integer(a,b,c) = RA(a,b) - 2*P2(a,b,c); % Find new sun ...
                matching rounded planet.

            % Test for nonpositive planets
            if P1(a,b,c) > 0
                positiveControlP1(a,b,c) = 1;
            else
                positiveControlP1(a,b,c) = 0;
            end

            if P2(a,b,c) > 0
                positiveControlP2(a,b,c) = 1;
            else
                positiveControlP2(a,b,c) = 0;
            end

            % Test for coprime number of teeth
            if (gcd(P1(a,b,c), S1Integer(a,b,c)) == 1) && ...
                (gcd(P1(a,b,c), RA(a,b)) == 1)
                coprimeControlP1(a,b,c) = 1;
            else
                coprimeControlP1(a,b,c) = 0;
```

```
        end

        if (gcd(P2(a,b,c), S2Integer(a,b,c)) == 1) && ...
            (gcd(P2(a,b,c), RA(a,b)) == 1)
            comprimeControlP2(a,b,c) = 1;
        else
            comprimeControlP2(a,b,c) = 0;
        end

    end

    % Run through floor or ceiling roundings
    for c = 1: 1: length(S1Integer(1,1,:))
        % Run through desired evenly distributed number of planets
        for d = minNP: 1: maxNP

            % Test for interference of planets
            % Find angle between planets
            alpha(a,b,d-2) = 360 / (d * 2);

            % Find maximum allowable planet radii. 3D = floor (1) ...
               or ceil (2)
            maxP1(a,b,c,d-2) = SfP*(sind(alpha(a,b,d-2)) * ...
                (S1Integer(a,b,c)/2 + RA(a,b)/2));
            maxP2(a,b,c,d-2) = SfP*(sind(alpha(a,b,d-2)) * ...
                (S2Integer(a,b,c)/2 + RA(a,b)/2));

            % Test the size of the planets for their maximum
            if maxP1(a,b,c,d-2) > P1(a,b,c)
                nPControlP1(a,b,c,d-2) = 1;
            else
                nPControlP1(a,b,c,d-2) = 0;
            end

            if maxP2(a,b,c,d-2) > P2(a,b,c)
                nPControlP2(a,b,c,d-2) = 1;
            else
                nPControlP2(a,b,c,d-2) = 0;
            end

            % Test for meshing between planets and ring and sun
            meshControlP1(a,b,c,d-2) = (RA(a,b) + ...
               S1Integer(a,b,c)) / d;
            meshControlP2(a,b,c,d-2,2,1) = (RA(a,b) + ...
               S2Integer(a,b,c)) / d;

            % If meshing not possible, eliminate
            if meshControlP1(a,b,c,d-2) == ...
               floor(meshControlP1(a,b,c,d-2))
                meshControlP1(a,b,c,d-2) = 1;
            else
                meshControlP1(a,b,c,d-2) = 0;
            end

            if meshControlP2(a,b,c,d-2) == ...
               floor(meshControlP2(a,b,c,d-2))
```

```
                    meshControlP2(a,b,c,d-2) = 1;
                else
                    meshControlP2(a,b,c,d-2) = 0;
                end

            end

            % Elimination
            % If sun does not allow for any tested number of planets, ...
               make the dimension 0, to exclude from applicability
            if ((nPControlP1(a,b,c,1)==0) || ...
                (meshControlP1(a,b,c,1)==0)) && ...
                ((nPControlP1(a,b,c,2)==0) || ...
                (meshControlP1(a,b,c,2)==0)) && ...
                ((nPControlP1(a,b,c,3)==0) || ...
                (meshControlP1(a,b,c,3)==0)) || ...
                coprimeControlP1(a,b,c)==0 || positiveControlP1(a,b,c)==0
                 S1Integer(a,b,c) = 0;
            end

            if ((nPControlP2(a,b,c,1)==0) || ...
                (meshControlP2(a,b,c,1)==0)) && ...
                ((nPControlP2(a,b,c,2)==0) || (P2Control(a,b,c,2)==0)) ...
                && ((nPControlP2(a,b,c,3)==0) || ...
                (meshControlP2(a,b,c,3)==0)) || ...
                comprimeControlP2(a,b,c)==0 || positiveControlP2(a,b,c)==0
                 S2Integer(a,b,c) = 0;
            end

        end

    end
end


%% %% Fixed Step %% %%

%% Fixed Step Combination Generation

% Run through gear ratios for fixed step
for a = 1: 1: length(grF)

    b = 1;
    % Run through number of teeth on ring for fixed step
    for tempR = minRF: 1: maxRF

        % Find sun to match ring and gear ratio
        SF(a,b) = round(tempR / grF(a));
        % Save the corresponding ring
        RF(a,b) = round(tempR);

        %Test that the sun is within limits
        if (SF(a,b) < minSF) ||(SF(a,b) > maxSF)
            SF(a,b) = 0;
        end
```

```
        b = b + 1;

    end

end

PF = (RF - SF) / 2; % Find planet matching ring and sun
PF = floor(PF);     % Round down the number of teeth on planets to ...
   integer
SF = RF - 2*PF;     % Find sun matching new planets

for a = 1: 1: length(PF(:,1))
    for b = 1: 1: length(PF(1,:))

        grF(a,b) = (RF(a,b) / SF(a,b)); %Find gear ratios for the new sun

    end
end


%% Fixed Step Combination Elimination

for a = 1: 1: length(PF(:,1))
    for b = 1: 1: length(PF(1,:))

        % Test for nonpositive planets
        if PF(a,b) > 0
            positiveControlPF(a,b) = 1;
        else
            positiveControlPF(a,b) = 0;
        end

        % Test for coprime number of teeth
        if (gcd(PF(a,b),SF(a,b)) == 1) && (gcd(PF(a,b),RF(a,b)) == 1)
            coprimeControlPF(a,b) = 1;
        else
            coprimeControlPF(a,b) = 0;
        end

        % Run through desired evenly distributed number of planets
        for c = minNP: 1: maxNP

            % Test for interference of planets
            % Find angle between planets
            alpha(a,b,c-2) = 360 / (c * 2);

            % Find maximum allowable planet radii
            maxPF(a,b,c-2) = SfP*(sind(alpha(a,b,c-2)) * (SF(a,b) / 2 ...
                + RF(a,b) / 2));

            % If not space for number of planets, eliminate
            if maxPF(a,b,c-2) > PF(a,b)
                nPControlPF(a,b,c-2) = 1;
            else
                nPControlPF(a,b,c-2) = 0;
            end
```

```
            % Test for meshing between planets and ring and sun
            meshControlPF(a,b,c-2) = (RF(a,b) + SF(a,b)) / c;

            % If meshing not possible, eliminate
            if meshControlPF(a,b,c-2) == floor(meshControlPF(a,b,c-2))
                meshControlPF(a,b,c-2) = 1;
            else
                meshControlPF(a,b,c-2) = 0;
            end

        end

        % If sun-ring combo does not allow for any tested number of ...
           planets, make the gear ratio 0, to exclude from applicability
        if ((nPControlPF(a,b,1)==0) || (meshControlPF(a,b,1)==0)) && ...
           ((nPControlPF(a,b,2)==0) || (meshControlPF(a,b,2)==0)) && ...
           ((nPControlPF(a,b,3)==0) || (meshControlPF(a,b,3)==0)) || ...
           coprimeControlPF(a,b)==0 || positiveControlPF(a,b)==0
            grF(a,b) = 0;
        end

    end
end


%% Total Result Identification

for a = 1: 1: length(S1Integer(:,1,1))
    for b = 1: 1: length(S1Integer(1,:,1))
        for c = 1: 1: length(grF(:,1))
            for d = 1: 1: length(grF(1,:))

                % If sun1 has value 0, make gear ratio 0, else ...
                   calculate corresponding gear ratio for high and ...
                   low gear by sun and ring, for both floor and ceil ...
                   rounded sun
                if S1Integer(a,b,1)==0 || S2Integer(a,b,1)==0
                    PossibleGrH(a,b,c,d,1) = 0;
                    PossibleGrL(a,b,c,d,1) = 0;
                else
                    PossibleGrH(a,b,c,d,1) = grF(c,d) * ((RA(a,b) + ...
                       S2Integer(a,b,1)) / (RA(a,b) + S1Integer(a,b,1)));
                    PossibleGrL(a,b,c,d,1) = grF(c,d) * ((1+(RA(a,b) ...
                       / S2Integer(a,b,1))) / (1 + (RA(a,b) / ...
                       S1Integer(a,b,1))));
                end

                if S1Integer(a,b,1)==0 || S2Integer(a,b,2)==0
                    PossibleGrH(a,b,c,d,2) = 0;
                    PossibleGrL(a,b,c,d,2) = 0;
                else
                    PossibleGrH(a,b,c,d,2) = grF(c,d) * ((RA(a,b) + ...
                       S2Integer(a,b,2)) / (RA(a,b) + S1Integer(a,b,1)));
                    PossibleGrL(a,b,c,d,2) = grF(c,d) * ((1 + ...
                       (RA(a,b) / S2Integer(a,b,2))) / (1 + (RA(a,b) ...
```

```
        / S1Integer(a,b,1))));
end

if S1Integer(a,b,2)==0 || S2Integer(a,b,1)==0
    PossibleGrH(a,b,c,d,3) = 0;
    PossibleGrL(a,b,c,d,3) = 0;
else
    PossibleGrH(a,b,c,d,3) = grF(c,d) * ((RA(a,b) + ...
        S2Integer(a,b,1)) / (RA(a,b) + S1Integer(a,b,2)));
    PossibleGrL(a,b,c,d,3) = grF(c,d) * ((1 + ...
        (RA(a,b) / S2Integer(a,b,1))) / (1 + (RA(a,b) ...
        / S1Integer(a,b,2))));
end

if S1Integer(a,b,2)==0 || S2Integer(a,b,2)==0
    PossibleGrH(a,b,c,d,4) = 0;
    PossibleGrL(a,b,c,d,4) = 0;
else
    PossibleGrH(a,b,c,d,4) = grF(c,d) * ((RA(a,b) + ...
        S2Integer(a,b,2)) / (RA(a,b) + S1Integer(a,b,2)));
    PossibleGrL(a,b,c,d,4) = grF(c,d) * ((1 + ...
        (RA(a,b) / S2Integer(a,b,2)))/(1 + (RA(a,b) / ...
        S1Integer(a,b,2))));
end

% Run through all ceiling/floor combinations of both ...
   actuated stages to find best combined high/low ...
   ratio for each fixed gear ratio
for e = 1 :1: 4

    grDeviation(a,b,c,d,e) = ...
        abs(grH-PossibleGrH(a,b,c,d,e)) + ...
        abs(grL-PossibleGrL(a,b,c,d,e));
    [NA,bestGrRoundIndex(a,b,c,d)] = ...
        min(grDeviation(a,b,c,d,:));

end

% Locate the ceiling/floor configuration for actuated ...
   stage from the combined optimal
if bestGrRoundIndex(a,b,c,d) == (1||2)
    bestGrRoundIndexS1(a,b,c,d) = 1;
else
    bestGrRoundIndexS1(a,b,c,d) = 2;
end

if bestGrRoundIndex(a,b,c,d) == (1||3)
    bestGrRoundIndexS2(a,b,c,d) = 1;
else
    bestGrRoundIndexS2(a,b,c,d) = 2;
end

% Retrieve the best combined ratio deviation
bestGrDeviation(a,b,c,d) = ...
   grDeviation(a,b,c,d,bestGrRoundIndex(a,b,c,d));
```

```
            end
        end
    end
end

% Find select n best gear ratio configurations
[c, bestGrIndex] = mink(bestGrDeviation(:), nResults);
[best1D, best2D, best3D, best4D] = ind2sub(size(bestGrDeviation), ...
   bestGrIndex);

for a = 1: 1: nResults % Run through all results

    % Retrieve best gear ratios
    resultGrH(a) = PossibleGrH(best1D(a), best2D(a), best3D(a), ...
       best4D(a), bestGrRoundIndex(best1D(a), best2D(a), best3D(a), ...
       best4D(a)));
    resultGrHPerCent(a) = 100 * (grH - resultGrH(a)) / grH;
    resultGrL(a) = PossibleGrL(best1D(a), best2D(a), best3D(a), ...
       best4D(a), bestGrRoundIndex(best1D(a), best2D(a), best3D(a), ...
       best4D(a)));
    resultGrLPerCent(a) = 100 * (grL - resultGrL(a)) / grL;

    % Retrieve best cogwheel combinations for actuated step
    resultS1(a) = S1Integer(best1D(a), best2D(a), ...
       bestGrRoundIndexS1(best1D(a), best2D(a), best3D(a), best4D(a)));
    resultS2(a) = S2Integer(best1D(a), best2D(a), ...
       bestGrRoundIndexS1(best1D(a), best2D(a), best3D(a), best4D(a)));
    resultRA(a) = RA(best1D(a), best2D(a));
    resultP1(a) = P1(best1D(a), best2D(a), ...
       bestGrRoundIndexS1(best1D(a), best2D(a), best3D(a), best4D(a)));
    resultP2(a) = P2(best1D(a), best2D(a), ...
       bestGrRoundIndexS1(best1D(a), best2D(a), best3D(a), best4D(a)));

    % Retrieve best coghwheel combinations for fixed step
    resultSF(a) = SF(best3D(a), best4D(a));
    resultPF(a) = PF(best3D(a), best4D(a));
    resultRF(a) = RF(best3D(a), best4D(a));

    % Retrieve fixed step gear ratios for best combined gear ratios
    resultGrF(a) = (-1) * resultRF(a) / resultSF(a);

    % Run through desired evenly distributed number of planets
    for b = 3: 1: 5

        % Find applicable number of planets for fixed step
        nPPossiblePF(a,b-2) = nPControlPF(best3D(a), best4D(a), b-2) ...
           + meshControlPF(best3D(a), best4D(a), b-2);
        % Find applicable number of planets for stage 1 of actuated step
        nPPossibleP1(a,b-2) = nPControlP1(best1D(a), best2D(a), ...
           bestGrRoundIndexS1(best1D(a), best2D(a), best3D(a), ...
           best4D(a)) ,b-2) + meshControlP1(best1D(a), best2D(a), ...
           bestGrRoundIndexS1(best1D(a), best2D(a), best3D(a), ...
           best4D(a)), b-2);
        % Find applicable number of planets for stage 2 of actuated step
        nPPossibleP2(a,b-2) = nPControlP2(best1D(a), best2D(a), ...
           bestGrRoundIndexS2(best1D(a), best2D(a), best3D(a), ...
```

```
            best4D(a)), b-2) + meshControlP2(best1D(a), best2D(a), ...
            bestGrRoundIndexS2(best1D(a), best2D(a), best3D(a), ...
            best4D(a)), b-2);

        % Result must allow for value of 2 (matching both dimension and
        % meshing).

    end

end

toc % Record used time for runthrough
```

Appendix B:
Gearbox & Actuator Calculations

Below is the Matlab script used to dimension the gearbox and the actuator system, which method are described in chapter 2.7, 2.8, 3, and 4.

```
tic
clc; clear all; close all;

%% Definitions

% nP  = Number of planets
% S   = Number of teeth sun
% R   = Number of teeth ring
% P   = Number of teeth planet
% w   = Rotational speed [rad/s]
% rpm = Rotational speed [rpm]
% v   = Linear/peripheral speed
% r   = Radius
% d   = Diameter2

% A = Actuated step
% F = Fixed step
% 1 = Actuated stage 1
% 2 = Actuated stage 2


%% Declare values

SF = 1.15;          % Safety factor
Tm = 625 * SF;      % Motor Torque
rpmMotor = 2300;    % Nominal speed motor
lambda = 15;        % Gear mounting factor
maxModule = 10;     % Max test module
phi = 20;           % Pressure angle

% Declare number of teeth and number of planets
% Actuated step
RA = 121;

S1 = 87;
P1 = (RA - S1)/2;
nP1 = 4;

S2 = 15;
P2 = (RA - S2)/2;
nP2 = 3;
```

```
% Fixed step
RF = 86;
SF = 16;
PF = (RF - SF)/2;
nPF = 3;

% Find local gear ratios
gr1 = RA / S1;
gr2 = RA / S2;
grF = RF / SF;

% Declare material properties
EModulus = 210e3;  % E-modulus
poissonsRatio = 0.3;    % Poison's ratio

%% Base Calculations

module = 1: 1: maxModule;               % Declare all modules

% Find radii of gears
rC1 = (S1 * module + RA * module) / 4;  % Carrier 1
rS1 = (S1 * module / 2);                % Sun 1
rP1 = (RA * module - S1 * module) / 4;  % Planet 1

rC2 = (S2 * module + RA * module) / 4;  % Carrier 2
rS2 = (S2 * module / 2);                % Sun 2
rP2 = (RA * module - S2 * module) / 4;  % Planet 2

rRA = (RA * module / 2);                % Ring A

rCF = (SF * module + RF * module) / 4;  % Radius Carrier fixed step
rSF = (SF * module / 2);                % Radius Sun gear fixed step
rPF = (RF * module - SF * module) / 4;  % Radius Planet gear fixed step
rRF = (RF * module / 2);                % Radius Ring gear fixed step


%% Velocities
% Actuated Step

% Declaration of constant velocities

% Input velocity in rad/s (equal for high and low)
wC1  = ones(1,maxModule)*(rpmMotor * 2 * pi / 60);

wRAL = 0;                       % Velocity of ring A, low gear
vRAL = 0;

wS1H = 0;                       % Velocity of sun 1, high gear
vS1H = 0;

wS2H = wS1H;                    % Velocity of sun 2, high gear
vS2H = 0;

wS1L = wC1 * (gr1 + 1);         % Velocity of sun 1, low gear
wRAH = (gr1 + 1) * wC1 / gr1;   % Velocity of ring A, high gear
```

```
wS2L = wS1L;                    % Velocity of sun 2, low gear

% Peripheral and rotational velocity for all modules.
for a = 1: 1: maxModule

    % Stage 1
    % Peripheral velocity
    vS1L(a) = S1 * a * wS1L(a) * 1e-3 / 2;      % S1, low gear
    vP1L(a) = vS1L(a);                          % P1, low gear

    vRAH(a) = RA * a * wRAH(a) * 1e-3 / 2;      % R, high gear
    vP1H(a) = vRAH(a);                          % P1, high gear

    % Rotational velocity
    wP1L(a) = vP1L(a) /( a * P1 * 1e-3);        % P1, low gear
    wP1H(a) = vP1H(a) /( a * P1 * 1e-3);        % P1, high gear

    % Stage 2
    % Peripheral velocity
    vS2L(a) = S2 * a / 2 * wS1L(a) * 1e-3;      % S2, low gear
    vP2L(a) = vS2L(a);                          % P2, low gear

    vP2H(a) = vRAH(a);                          % P2, high gear

    % Rotational velocity
    wP2L(a) = vP2L(a) /( a * P2 * 1e-3);        % P2, low gear
    wC2L = (gr2 * wRAL + wS1L(a)) / (gr2 + 1);  % C2, low gear

    wP2H(a) = vP2H(a) /( a * P2 * 1e-3);        % P2, high gear
    wC2H = (gr2 * wRAH + wS1H) / (gr2 + 1);     % C2, high gear

end

% Convert velocities to rpm
rpmS1H = wS1H(1) * 60 / (2 * pi);
rpmS1L = wS1L(1) * 60 / (2 * pi);

rpmP1H = wP1H(1) * 60 / (2 * pi);
rpmP1L = wP1L(1) * 60 / (2 * pi);

rpmC1H = wC1(1) * 60 / (2 * pi);
rpmC1L = wC1(1) * 60 / (2 * pi);

rpmP2H = wP2H(1) * 60 / (2 * pi);
rpmP2L = wP2L(1) * 60 / (2 * pi);

rpmS2H = wS2H(1) * 60 / (2 * pi);
rpmS2L = wS2L(1) * 60 / (2 * pi);

rpmRAH = wRAH(1) * 60 / (2 * pi);
rpmRAL = wRAL(1) * 60 / (2 * pi);

rpmC2H = wC2H(1) * 60 / (2 * pi);
rpmC2L = wC2L(1) * 60 / (2 * pi);
```

```
% Fixed step
% Carrier always locked

% Declaration of velocities

wSFL = wC2L;
wRFL = abs(- wSFL / grF);

wSFH = wC2H;
wRFH = abs(- wSFH / grF);

% Calculate peripheral and rotational velocity for all modules.
for a = 1: 1: maxModule

    vSFL(a) = SF * a / 2 * wSFL * 1e-3;       % SF, low gear
    vPFL(a) = vSFL(a);                        % PF, low gear
    vRFL(a) = vSFL(a);                        % RF, low gear

    vSFH(a) = SF * a / 2 * wSFH(a) * 1e-3;    % SF, high gear
    vPFH(a) = vSFH(a);                        % PF, high gear
    vRFH(a) = vSFL(a);                        % RF, high gear

    wPFH(a) = vPFH(a) /( a * PF * 1e-3);      % PF, high gear
    wPFL(a) = vPFL(a) /( a * PF * 1e-3);      % PF, low gear

end

% Convert velocities to rpm
rpmSFH = wSFH(1) * 60 / (2 * pi);
rpmSFL = wSFL(1) * 60 / (2 * pi);

rpmPFH = wPFH(1) * 60 / (2 * pi);
rpmPFL = wPFL(1) * 60 / (2 * pi);

rpmRFH = wRFH(1) * 60 / (2 * pi);
rpmRFL = wRFL(1) * 60 / (2 * pi);


%% Gear Ratios

gr = [wC1(1) / wRFL(1), wC1(1) / wRFH(1)];  % Total gear ratio
grA = [wC1(1) / wC2L(1), wC1(1) / wC2H(1)]; % Actuated step gear ratio


%% Gear Tooth Bending Stress

% Stage 1

TP1 = Tm / nP1;                 % Torque distributed to each planet

% Velocity factors for each gear
KvP1L = sqrt((5.56 + sqrt(vP1L)) / 5.56);
KvS1L = sqrt((5.56 + sqrt(vS1L)) / 5.56);
KvP2L = sqrt((5.56 + sqrt(vP2L)) / 5.56);
KvS2L = sqrt((5.56 + sqrt(vS2L)) / 5.56);
KvRAL = sqrt((5.56 + sqrt(vRAL)) / 5.56);
```

```
KvP1H = sqrt((5.56 + sqrt(vP1H)) / 5.56);
KvS1H = sqrt((5.56 + sqrt(vS1H)) / 5.56);
KvP2H = sqrt((5.56 + sqrt(vP2H)) / 5.56);
KvS2H = sqrt((5.56 + sqrt(vS2H)) / 5.56);
KvRAH = sqrt((5.56 + sqrt(vRAH)) / 5.56);

width = module * lambda;                % Width of gears

TShaftP1(1:1, 1:length(module)) = TP1;  % Organize torque on P1 into ...
    array

LewisFactor1 = 0.29;                    % Lewis form factor for P1
LewisFactor2 = 0.29;                    % Lewis form factor for S2

% Mid-shaft torque put into array
TMidShaftL(1:1, 1:length(module)) = Tm * grA(1);
TMidShaftH(1:1, 1:length(module)) = Tm * grA(2);

% Bendinng stresses and forces in actuated step for all modules
for a=1: 1: length(module)

    % Tangential force on S1, P1, R2
    FtA1L(a) = TShaftP1(a) / rC1(a) / 1e-3 / 2;
    FtA1H(a) = TShaftP1(a) / rC1(a) / 1e-3 / 2;

    % Tangential force on S2, P2, R2
    FtA2L(a) = TMidShaftL(a) / rC2(a) / 1e-3 / nP2 / 2;
    FtA2H(a) = TMidShaftH(a) / rC2(a) / 1e-3 / nP2 / 2;

    % Lewis bending stresses
    sigmaBendingA1L(a) = (FtA1L(a) * KvP1L(a)) / (module(a) * ...
        width(a) * LewisFactor1);
    sigmaBendingA1H(a) = (FtA1H(a) * KvP1H(a)) / (module(a) * ...
        width(a) * LewisFactor1);

    sigmaBendingA2L(a) = (FtA2L(a) * KvP2L(a)) / (module(a) * ...
        width(a) * LewisFactor2);
    sigmaBendingA2H(a) = (FtA2H(a) * KvP2H(a)) / (module(a) * ...
        width(a) * LewisFactor2);

end

% Fixed step

% Velocity factors for each gear
KvPFL = sqrt((5.56 + sqrt(vPFL)) / 5.56);
KvSFL = sqrt((5.56 + sqrt(vSFL)) / 5.56);
KvRFL = sqrt((5.56 + sqrt(vRFL)) / 5.56);

KvPFH = sqrt((5.56 + sqrt(vPFH)) / 5.56);
KvSFH = sqrt((5.56 + sqrt(vSFH)) / 5.56);
KvRFH = sqrt((5.56 + sqrt(vRFH)) / 5.56);

% Fixed sun torque put into array
TSFL(1:1,1:length(module)) = Tm * grA(1) / nPF;
```

```
TSFH(1:1,1:length(module)) = Tm * grA(2) / nPF;

LewisFactorF = 0.29;     % Lewis form factor for SF

% Bending stresses and forces in fixed step for all modules
for a=1: 1: length(module)

    % Tangential force on SF, PF, RF
    FtFL(a) = TSFL(a) / (rSF(a) * 1e-3) / 2;
    FtFH(a) = TSFH(a) / (rSF(a) * 1e-3) / 2;

    % Lewis bending stress
    sigmaBendingFL(a) = (FtFL(a) * KvPFL(a)) / (module(a) * width(a) ...
        * LewisFactorF);
    sigmaBendingFH(a) = (FtFH(a) * KvPFH(a)) / (module(a) * width(a) ...
        * LewisFactorF);

end


%% Gear Tooth Contact Stress

% Elasticity factor
Cp = 0.564 * sqrt(1 / (2 * (1 - poissonsRatio^2) / EModulus));

Ko = 1.25;  % Overload factor
Km = 1.4;   % Mounting factor

% Contact stresses for all modules
for a=1: 1: maxModule

    % Diametric pitches
    dpA1(a) = module(a) * S1;
    dpA2(a) = module(a) * S2;
    dpF(a) = module(a) * SF;

    % Geometry factors
    IA1 = sind(phi) * cosd(phi) / 2 * gr1/(gr1+1);
    IA2 = sind(phi) * cosd(phi) / 2 * gr2/(gr2+1);
    IF  = sind(phi) * cosd(phi) / 2 * grF/(grF+1);

    %Hertzian contact stresses
    sigmaContactA1L(a) = Cp * sqrt(FtA1L(a) / (width(a) * dpA1(a) * ...
        IA1) * KvP1L(a) * Ko * Km);
    sigmaContactA2L(a) = Cp * sqrt(FtA2L(a) / (width(a) * dpA2(a) * ...
        IA2) * KvP2L(a) * Ko * Km);
    sigmaContactFL(a)  = Cp * sqrt(FtFL(a)  / (width(a) * dpF(a)  * ...
        IF)  * KvPFL(a) * Ko * Km);

    sigmaContactA1H(a) = Cp * sqrt(FtA1H(a) / (width(a) * dpA1(a) * ...
        IA1) * KvP1H(a) * Ko * Km);
    sigmaContactA2H(a) = Cp * sqrt(FtA2H(a) / (width(a) * dpA2(a) * ...
        IA2) * KvP2H(a) * Ko * Km);
    sigmaContactFH(a)  = Cp * sqrt(FtFH(a)  / (width(a) * dpF(a)  * ...
        IF)  * KvPFH(a) * Ko * Km);
```

```
end


%% Contact Ratio and Interference

% Chosen modules
mA = 3;                         % Actuated step
mF = 5;                         % Fixed step

% Center distance between meshing gears
cSP1 = rP1(mA) + rS1(mA);       % SP1
cRP1 = rP1(mA) - rRA(mA);       % RP1
cSP2 = rP2(mA) + rS2(mA);       % SP2
cRP2 = rP2(mA) - rRA(mA);       % RP2
cSPF = rPF(mA) + rSF(mA);       % SPF
cRPF = rPF(mF) - rRF(mF);       % RPF

% Base/Dedendum radius of gears
rbS1 = rS1(mA) * cosd(phi);     % Sun 1
rbS2 = rS2(mA) * cosd(phi);     % Sun 2
rbP1 = rP1(mA) * cosd(phi);     % Planet 1
rbP2 = rP2(mA) * cosd(phi);     % Planet 2
rbRA = rRA(mA) * cosd(phi);     % Ring A
rbSF = rSF(mF) * cosd(phi);     % Sun fixed
rbPF = rPF(mF) * cosd(phi);     % Planet fixed
rbRF = rRF(mF) * cosd(phi);     % Planet fixed

% Base pitch of planets (equal for whole stage of meshing gears)
pb1 = pi * rbP1 * 2 / P1;       % Stage 1
pb2 = pi * rbP2 * 2 / P2;       % Stage 2
pbF = pi * rbPF * 2 / PF;       % Fixed step

% Addendum radius of gears
raS1 = rS1(mA) + mA;            % Sun 1
raS2 = rS2(mA) + mA;            % Sun 2
raP1 = rP1(mA) + mA;            % Planet 1
raP2 = rP2(mA) + mA;            % Planet 2
raRA = rRA(mA) + mA;            % Ring actuated
raSF = rSF(mF) + mF;            % Sun fixed
raPF = rPF(mF) + mF;            % Planet fixed
raRF = rRF(mF) + mF;            % Ring fixed

% Contact ratios of the meshing gears
crSP1 = ( sqrt( raP1^2 - rbP1^2 ) + sqrt( raS1^2 - rbS1^2 ) - cSP1 * ...
    sind(phi) ) / pb1;
crSP2 = ( sqrt( raS2^2 - rbS2^2 ) + sqrt( raP2^2 - rbP2^2 ) - cSP2 * ...
    sind(phi) ) / pb2;
crSPF = ( sqrt( raSF^2 - rbSF^2 ) + sqrt( raPF^2 - rbPF^2 ) - cSPF * ...
    sind(phi) ) / pbF;

crRP1 = ( sqrt( raP1^2 - rbP1^2 ) - sqrt( raRA^2 - rbRA^2 ) + cRP1 * ...
    sind(phi) ) / pb1;
crRP2 = ( sqrt( raP2^2 - rbP2^2 ) - sqrt( raRA^2 - rbRA^2 ) + cRP2 * ...
    sind(phi) ) / pb2;
crRPF = ( sqrt( raPF^2 - rbPF^2 ) - sqrt( raRF^2 - rbRF^2 ) + cRPF * ...
    sind(phi) ) / pbF;
```

```
% Gather results
cr = [crSP1, crRP1, crSP2, crRP2, crSPF, crRPF];

% Control for interference through addendum radius
raControlS1 = sqrt(rbS1^2 + (cSP1 * sind(phi))^2) - raS1;
raControlP1 = sqrt(rbP1^2 + (cSP1 * sind(phi))^2) - raP1;
raControlS2 = sqrt(rbS2^2 + (cSP2 * sind(phi))^2) - raS2;
raControlP2 = sqrt(rbP2^2 + (cSP2 * sind(phi))^2) - raP2;
raControlSF = sqrt(rbSF^2 + (cSPF * sind(phi))^2) - raSF;
raControlPF = sqrt(rbPF^2 + (cSPF * sind(phi))^2) - raPF;

% Gather resuls
raControl=[raControlS1, raControlP1, raControlS2, raControlP2, ...
    raControlSF, raControlPF];


%% Shafts

% Width of spacers on planet shafts
WidthPSpacer = 2e-3;


% Declare allowable stresses for shafts

% Yield strength
sigmaYieldShaft = 390;
% Allowable normal stress
sigmaNormalAllowableShaft = sigmaYieldShaft / 3;
% Allowable shear stress
sigmaShearAllowableShaft = sigmaYieldShaft / 3;

% Bending load on shafts
MbCommon = 0;

% Minimum diameter of input shaft
minDShaftC1 = (32 * sqrt((MbCommon * 1e3)^2 + 0.75 * (Tm*1e3)^2)/(pi ...
    * sigmaNormalAllowableShaft))^(1/3);

% Bending moment on P1 shaft, force from sun and ring
MbP1 = (FtA1L(mA) * 2 * ( WidthPSpacer + width(mA) / 2)) / 4;

kShear = 4/3;       % Shear factor for solid round

maxDelta = 0.001;   % Allowable deflection

% Minimum diameter of P1 shaft for 3 failure criteria
minDShaftP1(1) = (32 * sqrt(MbP1^2 + 0.75 * (0*1e3)^2)/(pi * ...
    sigmaShearAllowableShaft))^(1/3);
minDShaftP1(2) = sqrt(kShear * FtA1L(mA) * 2 * 4 / (pi * ...
    sigmaShearAllowableShaft));
minDShaftP1(3) = ( FtA1L(mA) * 2 * ( 2*10 + width(mA)) * 64 / ( 48 * ...
    EModulus * pi * maxDelta ) )^(1/4);

% Torque SA shaft
TShaftSA = FtA1L(mA) * S1 * module(mA) * 1e-3 / 2;
```

```
% Minimum diameter of SA shaft
minDShaftSA = (32 * sqrt((MbCommon * 1e3)^2 + 0.75 * (TShaftSA * ...
    1e3)^2)/(pi * sigmaNormalAllowableShaft))^(1/3);

% Maximum bending moment on P2 shaft, force from sun and ring
MbP2 = (FtA2L(3) * 2 * ( WidthPSpacer + width(mA) / 2)) / 4;

% Minimum diameter of P2 shaft for 3 failure criteria
minDShaftP2(1) = (32 * sqrt(MbP2^2 + 0.75 * (0*1e3)^2)/(pi * ...
    sigmaShearAllowableShaft))^(1/3);
minDShaftP2(2) = sqrt(kShear * FtA2L(mA) * 2 * 4 / (pi * ...
    sigmaShearAllowableShaft));
minDShaftP2(3) = ( FtA2L(mA) * 2 * ( 2*10 + width(mA)) * 64 / ( 48 * ...
    EModulus * pi * maxDelta ) )^(1/4);

% Intermediate shaft dimensions
doMidShaft = 55;    % Outer diameter
diMidShaft = 42;    % Inner diameter

% Control for stress in intermediate shaft
sigmaMidShaft = (32 * sqrt( MbCommon^2 + 0.75 * (TMidShaftL(mA))^2 )) ...
    / (pi * (doMidShaft - diMidShaft)^3);

% Bending moment on PF shaft, force from sun and ring
MbPF = (FtFL(mF) * 2 * ( WidthPSpacer + width(mF) / 2)) / 4;

% Minimum diameter of PF shaft for 3 failure criteria
minDShaftPF(1) = (32 * sqrt(MbPF^2 + 0.75 * (0*1e3)^2)/(pi * ...
    sigmaShearAllowableShaft))^(1/3);
minDShaftPF(2) = sqrt(kShear * FtFL(mF) * 2 * 4 / (pi * ...
    sigmaShearAllowableShaft));
minDShaftPF(3) = ( FtFL(mF) * 2 * ( 2*20 + width(mF)) * 64 / ( 48 * ...
    EModulus * pi * maxDelta ) )^(1/4);

%% Bearings

% Declare constants

% Basic dynamic load rating for tested bearings
C_NKX30 = 22.9e3;
C_NKX70 = 44.6e3;
C_NA4909 = 45.7e3;
C_30211 = 111e3;
C_30216 = 184e3;
C_33012 = 113e3;
C_K15x21x21 = 18.7e3;
C_K20x28x20 = 22.9e3;
C_K30x40x18 = 30.3e3;
C_K30x40x30 = 46.8e3;
C_K35x45x30 = 50.1e3;

% Link bearings to location
bearingRA_a = C_33012;
bearingRA_b = C_NKX70;
```

```
bearingSA_a = C_NKX30;
bearingSA_b = C_NKX30;

bearingC1_a = C_NKX70;
bearingC1_b = C_NKX30;

bearingC2_a = C_NKX30;
bearingC2_b = C_30216;

bearingAll_a = C_33012;
bearingAll_b = C_30216;

bearingP1 = C_K15x21x21;
bearingP2 = C_K30x40x18;
bearingP3 = C_K35x45x30;

% Bearing type factor
pRoller = 10/3;
pBall = 3;

% Actuated ring
% Lengths and weight
L1 = 50;
L3 = 75;
L2 = L1 + L3;
G = 62.9 * 9.81;

% Reaction forces
Rb = (G * L2) / L3;
Ra = Rb - G;

% Life expectancy for bearings
LifeHoursRAH_a = bearings(bearingRA_a, Ra, pRoller, rpmRAH);
LifeHoursRAH_b = bearings(bearingRA_b, Rb, pRoller, rpmRAH);

LifeHoursRAL_a = bearings(bearingRA_a, Ra, pRoller, rpmRAL);
LifeHoursRAL_b = bearings(bearingRA_b, Rb, pRoller, rpmRAL);

% Actuated sun haft
% Lengths and weight
L1 = 55;
L2 = 110;
G = 21.2 * 9.81;

% Reaction forces
Rb = (G * L1)/L2;
Ra = G - Rb;

% Life expectancy for bearings
LifeHoursSAH_a = bearings(bearingSA_a, Ra, pRoller, rpmS1H);
LifeHoursSAH_b = bearings(bearingSA_b, Rb, pRoller, rpmS1H);

LifeHoursSAL_a = bearings(bearingSA_a, Ra, pRoller, rpmS1L);
LifeHoursSAL_b = bearings(bearingSA_b, Rb, pRoller, rpmS1L);

% Carrier 1
```

```
% Lengths and weight
L1 = 40;
L2 = 30;
G = 19.2 * 9.81;

% Reaction forces
Rb = (G * (L1 + L2))/L1;
Ra = abs(G - Rb);

% Life expectancy for bearings
LifeHoursC1H_a = bearings(bearingC1_a, Ra, pRoller, rpmC1H);
LifeHoursC1H_b = bearings(bearingC1_b, Rb, pRoller, rpmC1H);

LifeHoursC1L_a = bearings(bearingC1_a, Ra, pRoller, rpmC1L);
LifeHoursC1L_b = bearings(bearingC1_b, Rb, pRoller, rpmC1L);

% Carrier 2
% Lengths and weight
L1 = 30;
L2 = 25;
G = 37.5 * 9.81;

% Reaction forces
Ra = (G * (L1 + L2))/L2;
Rb = abs(G - Ra);

% Life expectancy for bearings
LifeHoursC2H_a = bearings(bearingC2_a, Ra, pRoller, rpmC2H);
LifeHoursC2H_b = bearings(bearingC2_b, Rb, pRoller, rpmC2H);

LifeHoursC2L_a = bearings(bearingC2_a, Ra, pRoller, rpmC2L);
LifeHoursC2L_b = bearings(bearingC2_b, Rb, pRoller, rpmC2L);

% Planets auto 1
% Applied forces
FrP1H = FtA1H(mA) * 2 / 2;
FrP1L = FtA1L(mA) * 2 / 2;

% Life expectancy for bearings
LifeHoursP1H = bearings(bearingP1, FrP1H, pRoller, rpmP1H);
LifeHoursP1L = bearings(bearingP1, FrP1L, pRoller, rpmP1L);

% Plantes auto 2
% Applied forces
FrP2H = FtA2H(mA) * 2 / 2;
FrP2L = FtA2L(mA) * 2 / 2;

% Life expectancy for bearings
LifeHoursP2H = bearings(bearingP2, FrP2H, pRoller, rpmP2H);
LifeHoursP2L = bearings(bearingP2, FrP2L, pRoller, rpmP2L);

% Planets fixed
% Applied forces
FrPFH = FtFH(mF) * 2 / 2;
FrPFL = FtFL(mF) * 2 / 2;
% Life expectancy for bearings
```

```
LifeHoursPFH = bearings(bearingP3, FrPFH, pRoller, rpmPFH);
LifeHoursPFL = bearings(bearingP3, FrPFL, pRoller, rpmPFL);

% Internals
% Lengths
L1 = 235;
L2 = 85;
G = 151 * 9.81;

% Applied Forces
Rb = G * L1 / (L1 + L2);
Ra = G - Rb;

% Life expectancy for bearings
LifeHoursAllH_a = bearings(bearingAll_a, Ra, pRoller, rpmC1L);
LifeHoursAllH_b = bearings(bearingAll_b, Rb, pRoller, rpmC2L);

LifeHoursAllL_a = bearings(bearingAll_a, Ra, pRoller, rpmC1L);
LifeHoursAllL_b = bearings(bearingAll_b, Rb, pRoller, rpmC2L);


%% Brakes

SFBrake = 1.5; % Safety factor for brakes

% Torque required of clutches
TBrakeSunRequired  = SFBrake * Tm * (S1/(RA + S1));
TBrakeRingRequired = SFBrake * Tm * (RA/(RA + S1));

% Dynamic friction coefficients
frictionWet = 0.06;
frictionDry = 0.25;

% Ring
% Declaration of brake disk parameters
% Outer diameter
doBrakeRing = 370e-3;
% Inner diameter
diBrakeRing = 260e-3;
% Suface area of disk
ABrakeRing = pi * (doBrakeRing^2 - diBrakeRing^2) / 4;

pMaxBrakeRing = 1.03e6; % Maximum applied pressure to disks

% Sun
% Outer diameter
doBrakeSun = 250e-3;
% Inner diameter
diBrakeSun = 150e-3;
% Suface area of disk
ABrakeSun = pi * (doBrakeSun^2 -diBrakeSun^2) / 4;

pMaxBrakeSun = 1.03e6;  % Maximum applied pressure to disks

% Find required number of brake pads for ring
FMaxBrakeRingUPressure = 1/4 * pi * pMaxBrakeRing * ( doBrakeRing^2 - ...
```

```
    diBrakeRing^2 );
TMaxBrakeRingUPressurePerPlate = 1/12 * pi * frictionWet * ...
    pMaxBrakeRing * (doBrakeRing^3 - diBrakeRing^3);
nPlatesBrakeRingUPressure = ceil(TBrakeRingRequired / ...
    TMaxBrakeRingUPressurePerPlate / 2);
TMaxBrakeRingUPressure = TMaxBrakeRingUPressurePerPlate * ...
    nPlatesBrakeRingUPressure * 2;
FMinBrakeRingUPressure = FMaxBrakeRingUPressure * TBrakeRingRequired ...
    / TMaxBrakeRingUPressure;

FMaxBrakeRingUWear = 1/2 * pi * pMaxBrakeRing * diBrakeRing * ...
    (doBrakeRing - diBrakeRing);
TMaxBrakeRingUWearPerPlate = 1/8 * pi * pMaxBrakeRing * frictionWet * ...
    diBrakeRing * (doBrakeRing^2 - diBrakeRing^2);
nPlatesBrakeRingUWear = ceil(TBrakeRingRequired / ...
    TMaxBrakeRingUWearPerPlate / 2);
TMaxBrakeRingUWear = TMaxBrakeRingUWearPerPlate * ...
    nPlatesBrakeRingUWear * 2;
FMinBrakeRingUWear = FMaxBrakeRingUWear * TBrakeRingRequired / ...
    TMaxBrakeRingUWear;

% Find required number of brake pads for sun
FMaxBrakeSunUPressure = 1/4 * pi * pMaxBrakeSun * ( doBrakeSun^2 - ...
    diBrakeSun^2 );
TMaxBrakeSunUPressurePerPlate = 1/12 * pi * frictionDry * ...
    pMaxBrakeSun * (doBrakeSun^3 - diBrakeSun^3);
nPlatesBrakeSunUPressure = ceil(TBrakeSunRequired / ...
    TMaxBrakeSunUPressurePerPlate/2);
TMaxBrakeSunUPressure = TMaxBrakeSunUPressurePerPlate * ...
    nPlatesBrakeSunUPressure * 2;
FMinBrakeSunUPressure = FMaxBrakeSunUPressure * TBrakeSunRequired / ...
    TMaxBrakeSunUPressure;

FMaxBrakeSunUWear = 1/2 * pi * pMaxBrakeSun * diBrakeSun * ...
    (doBrakeSun - diBrakeSun);
TMaxBrakeSunUWearPerPlate = 1/8 * pi * pMaxBrakeSun * frictionDry * ...
    diBrakeSun * (doBrakeSun^2 - diBrakeSun^2);
nPlatesBrakeSunUWear = ceil(TBrakeSunRequired / ...
    TMaxBrakeSunUWearPerPlate / 2);
TMaxBrakeSunUWear = TMaxBrakeSunUWearPerPlate * nPlatesBrakeSunUWear ...
    * 2;
FMinBrakeSunUWear = FMaxBrakeSunUWear * TBrakeSunRequired / ...
    TMaxBrakeSunUWear;

%% Sun shaft for brake

% Minimum diameter of SA shaft
minDShaftSABrake = (32 * sqrt((MbCommon * 1e3)^2 + 0.75 * ...
    (TBrakeSunRequired*1e3/1.5)^2) / (pi * ...
    sigmaNormalAllowableShaft))^(1/3);


%% Electric Actuator

% Define general properties.
fluxDensity = 1.35;     % IEC 60404-8-1 - 360/90
```

```
resistivity = 1.724e-8; % Resistivity for annealed copper

% Declare length of brake stroke
strokeCylBrakeRing = 5e-3;
strokeCylBrakeSun = 5e-3;

% Declare dimensions for windings on stator
doWindingBrakeRing = 400e-3;
diWindingBrakeRing = 260e-3;
dmWindingBrakeRing = (doWindingBrakeRing + diWindingBrakeRing) / 2;

bWindingBrakeRing = 30e-3;
hWindingBrakeRing = (doWindingBrakeRing - diWindingBrakeRing) / 2;
ACrossWindingBrakeRing = bWindingBrakeRing * hWindingBrakeRing;

dWireBrakeRing = 1e-3;
AEffectiveWireBrakeRing = dWireBrakeRing^2;
AWireBrakeRing = pi * dWireBrakeRing^2 / 4 ;

doWindingBrakeSun = 270e-3;
diWindingBrakeSun = 150e-3;
dmWindingBrakeSun = (doWindingBrakeSun + diWindingBrakeSun) / 2;

bWindingBrakeSun = 25e-3;
hWindingBrakeSun = (doWindingBrakeSun - diWindingBrakeSun) / 2;
ACrossWindingBrakeSun = bWindingBrakeSun * hWindingBrakeSun;

dWireBrakeSun = 1e-3;
AEffectiveWireBrakeSun = dWireBrakeSun^2;
AWireBrakeSun = pi * dWireBrakeSun^2 / 4;

% Number of windings in cross section
nWiresCrossBrakeRing = ACrossWindingBrakeRing / AEffectiveWireBrakeRing;
nWiresCrossBrakeSun = ACrossWindingBrakeSun / AEffectiveWireBrakeSun;

% Total length of wires
lengthWireBrakeRing = nWiresCrossBrakeRing * dmWindingBrakeRing * pi;
lengthWireBrakeSun = nWiresCrossBrakeSun * dmWindingBrakeSun * pi;

% Resistance in wires
RWireBrakeRing = resistivity * lengthWireBrakeRing / AWireBrakeRing ;
RWireBrakeSun = resistivity * lengthWireBrakeSun / AWireBrakeSun ;

% Current for required forces
iBrakeRing = FMinBrakeRingUWear / (fluxDensity * lengthWireBrakeRing);
iBrakeSun = FMinBrakeSunUWear / (fluxDensity * lengthWireBrakeSun);

% Current for maximum forces
iMaxBrakeRing = iBrakeRing * FMaxBrakeRingUWear / FMinBrakeRingUWear;
iMaxBrakeSun = iBrakeSun * FMaxBrakeSunUWear / FMinBrakeSunUWear;

% Produced effect in wires
PWireBrakeRing = RWireBrakeRing * iBrakeRing^2;
PWireBrakeSun = RWireBrakeSun * iBrakeSun^2;

% Maximum produced effect in wires
```

```
PMaxWireBrakeRing = RWireBrakeRing * iMaxBrakeRing^2;
PMaxWireBrakeSun = RWireBrakeSun * iMaxBrakeSun^2;

% Required voltage
uBrakeRing = RWireBrakeRing * iBrakeRing;
uBrakeSun = RWireBrakeSun * iBrakeSun;

% Maximum voltage
uMaxBrakeRing = RWireBrakeRing * iMaxBrakeRing;
uMaxBrakeSun = RWireBrakeSun * iMaxBrakeSun;

% Mass of coils
massDensityCopper = 8930;

mCoilRing = massDensityCopper * lengthWireBrakeRing * AWireBrakeRing;
mCoilSun = massDensityCopper * lengthWireBrakeSun * AWireBrakeSun;

% Temperatur increase
heatCapacity = 385;
heatIncrease = 100;

timeToOverheatBrakeRing = mCoilRing * heatCapacity * heatIncrease / ...
    PWireBrakeRing;
timeToOverheatBrakeSun = mCoilSun * heatCapacity * heatIncrease / ...
    PWireBrakeSun;

timeToOverheatBrakeRingMax = mCoilRing * heatCapacity * heatIncrease ...
    / PMaxWireBrakeRing;
timeToOverheatBrakeSunMax = mCoilSun * heatCapacity * heatIncrease / ...
    PMaxWireBrakeSun;

toc


%% Bearing life expectancy calculation

function [out] = bearings(C,P,p,rpm)

L10 = ( C / P )^(p);                % Life million cycles

L10h = (L10 * 1e6) / ( rpm * 60);   % Life expectancy hours

out = L10h;                         % Return value

end
```

Appendix C:
Free Body Diagrams for Bearings

In this appendix are the free body diagrams (FBD) for the dimensioning of the bearings described in chapter 4.4.

Table C.1 shows the forces and the moment arms that work on the bearings in the gearbox. The figures following the table show how the lengths, forces, and center of mass for the corresponding bearings. Where there are multiple bearings on the same system, the different bearings are called A or B, which is replicated and corresponding in the Matlab script in appendix B, which performed the calculations.

Table C.1: Loads and dimensions on bearings.

Part	**m**	**F**	**L1**	**L2**	**Figure**
Actuated Ring	53.50	NA	50.00	75	C.7
Sun Shaft	10.70	NA	55.00	110	C.8
Actuated Carrier 1	19.20	NA	40.00	30	C.5
Actuated Carrier 2	37.50	NA	30.00	25	C.6
Actuated Planet 1	NA	600.00	22.50	22.5	C.2
Actuated Planet 2	NA	4632.00	22.50	22.5	C.3
Fixed Planet	NA	11812.00	37.50	37.5	C.4
Main Bearings	151.00	NA	235.00	85	C.1
Fixed Sun	4.70	NA	107.75	NA	C.9

The parameters in the table are the following:

$\boldsymbol{F}$	Force	$[N]$
$\boldsymbol{m}$	Mass	$[kg]$
$\boldsymbol{L1}$	Length 1	$[mm]$
$\boldsymbol{L2}$	Length 2	$[mm]$

The last column, "Figure", references to the corresponding FBD figure, who are shown below. In the following FBD, note that main bearing B, and carrier 2 bearing B is the same bearing. This is also true for carrier 1 B and sun shaft A, and carrier 2 A and sun shaft B.

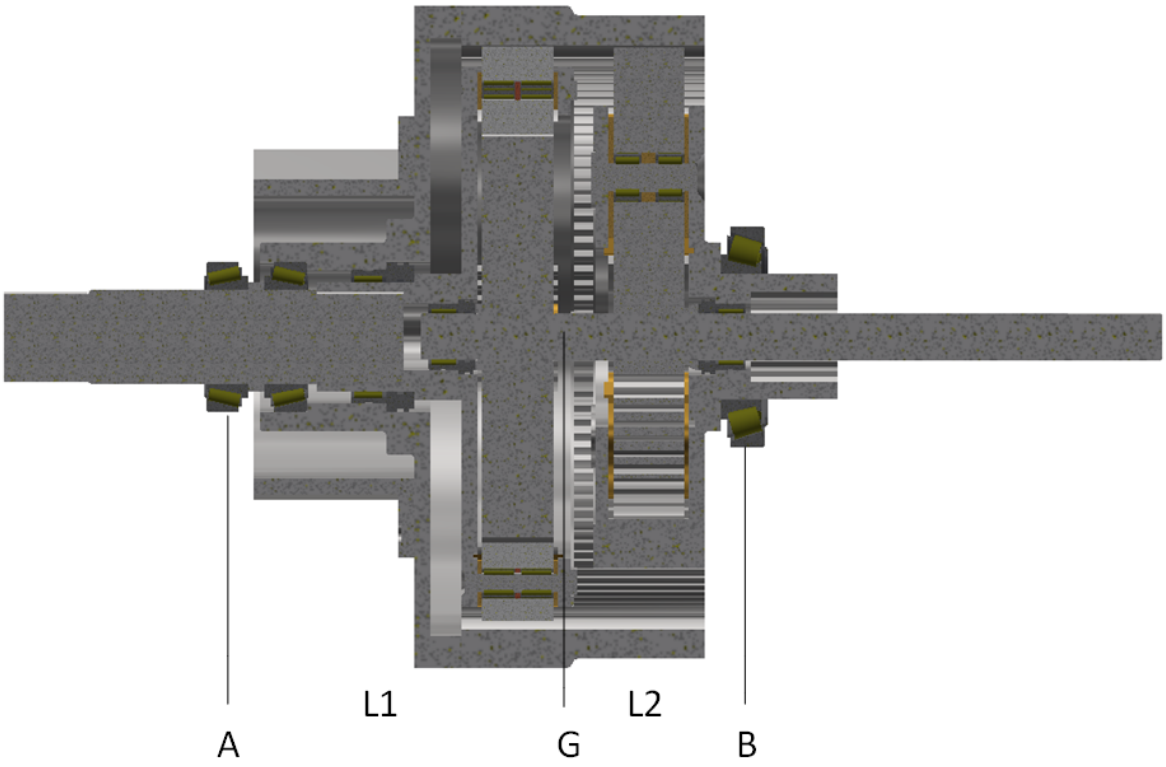

Figure C.1: FBD for main bearings for actuated step.

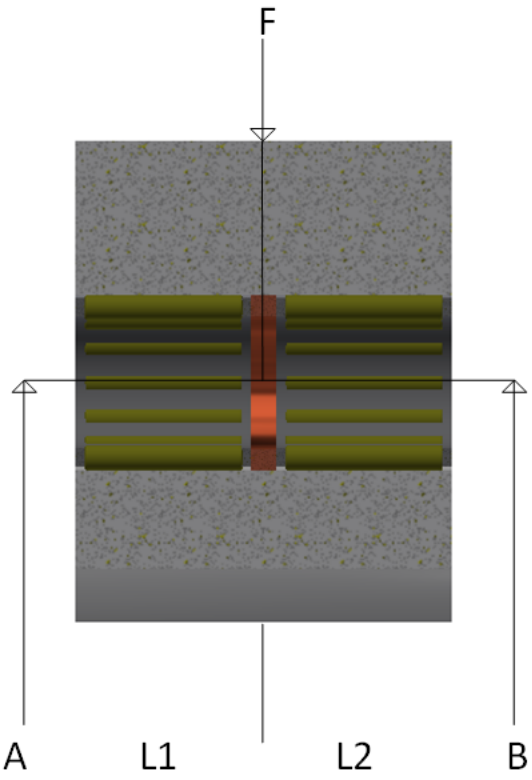

Figure C.2: FBD for planet 1 bearing.

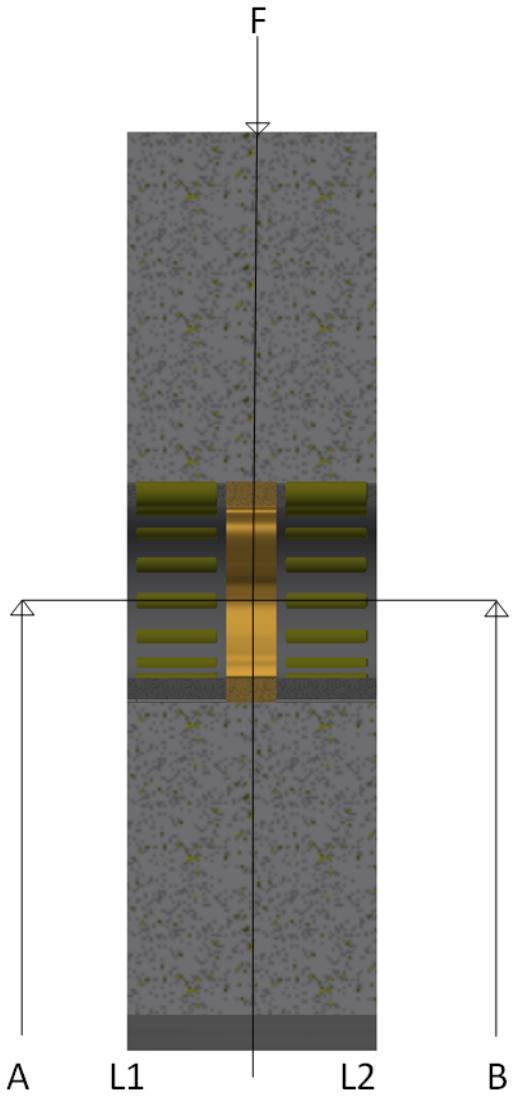

Figure C.3: FBD for planet 2 bearing.

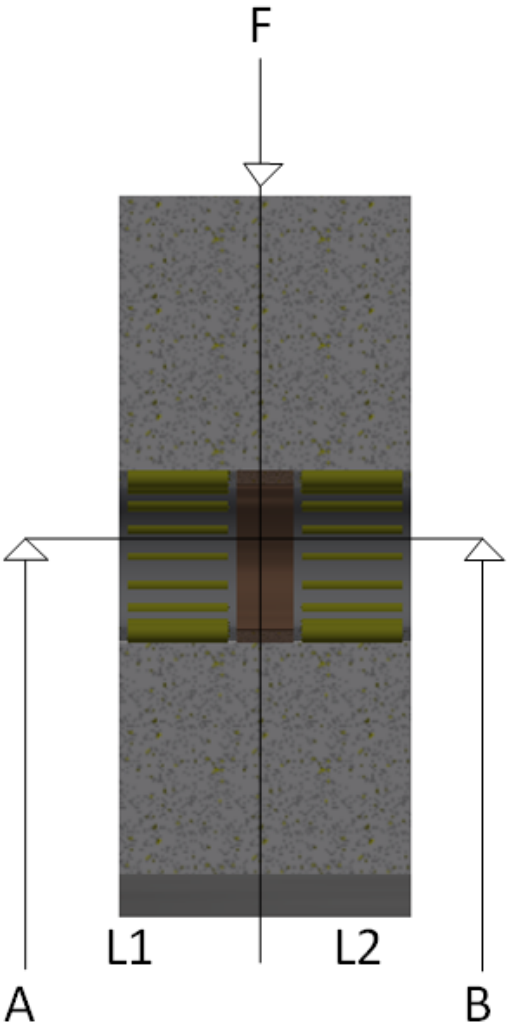

Figure C.4: FBD for fixed step planet bearing.

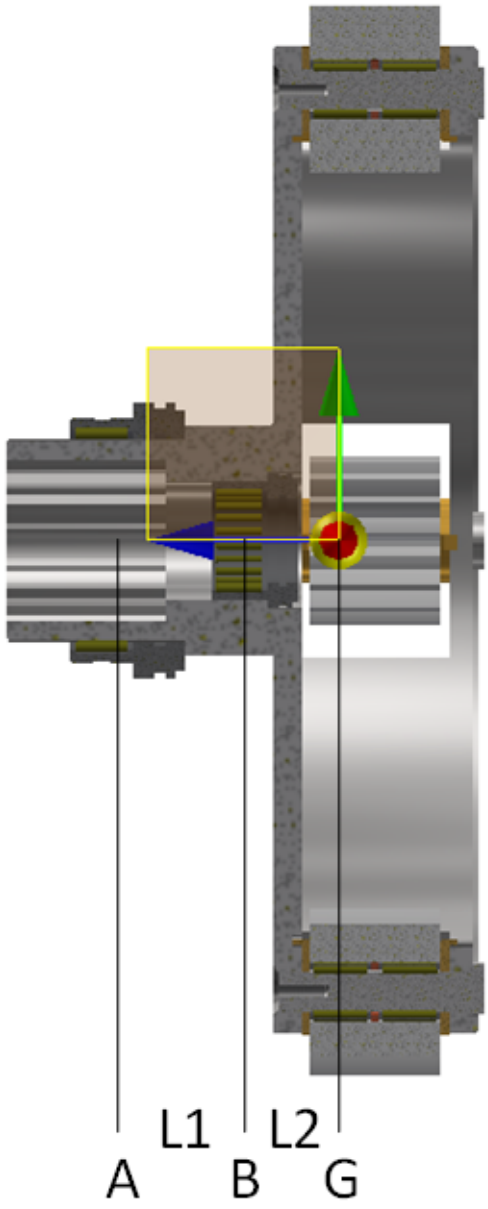

Figure C.5: FBD for carrier 1 bearing.

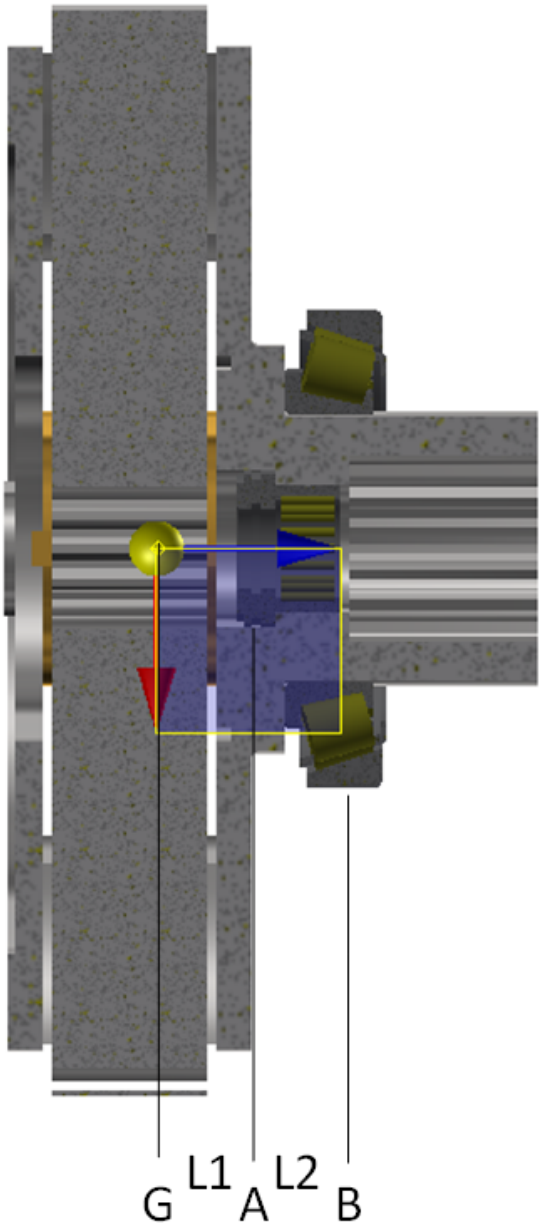

Figure C.6: FBD for carrier 2 bearing.

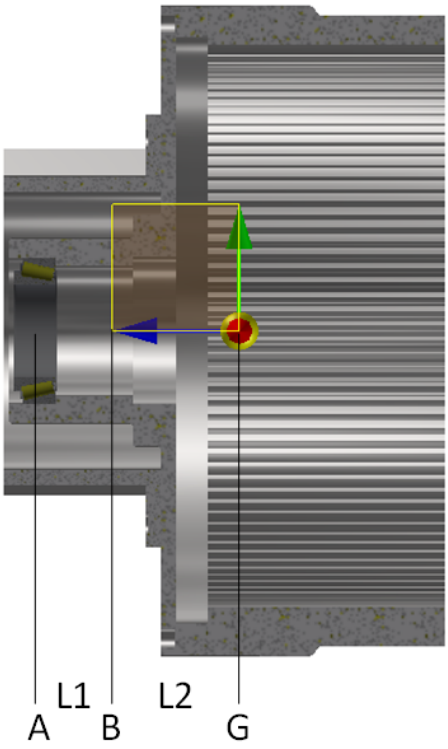

Figure C.7: FBD for actuated ring bearing.

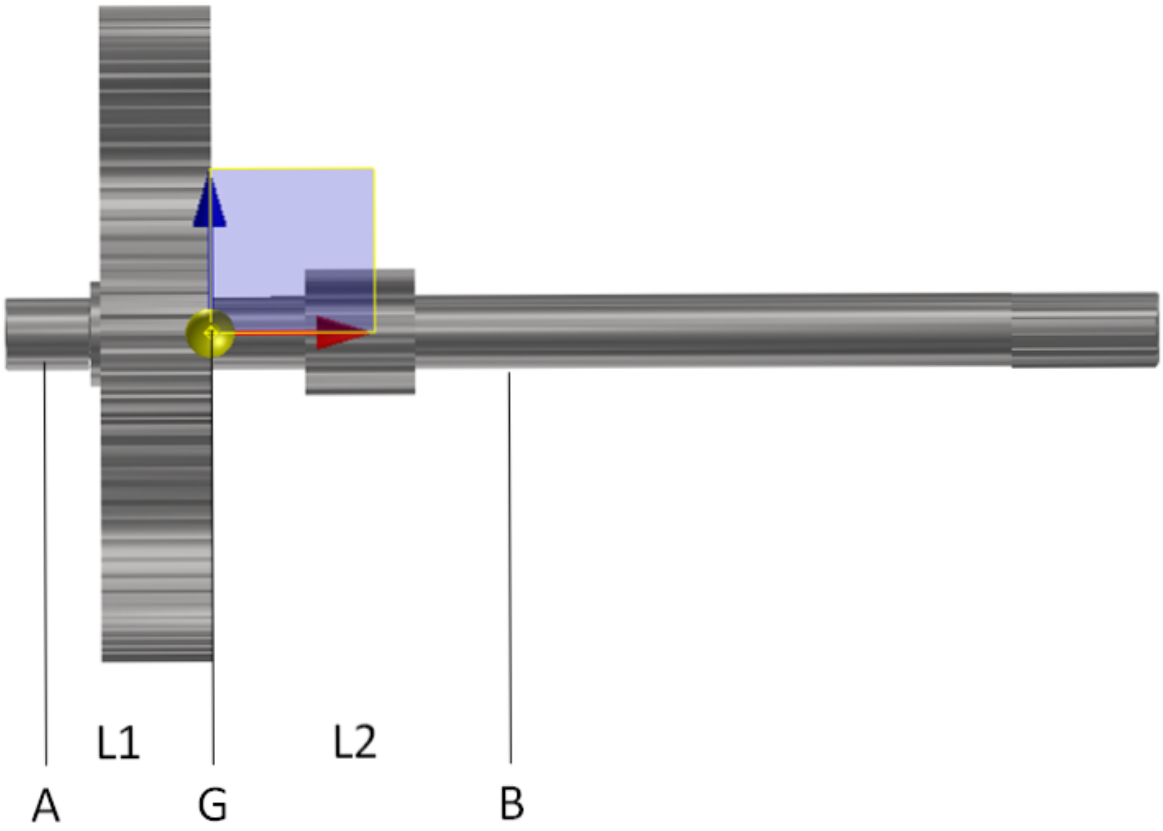

Figure C.8: FBD for sun shaft bearing.

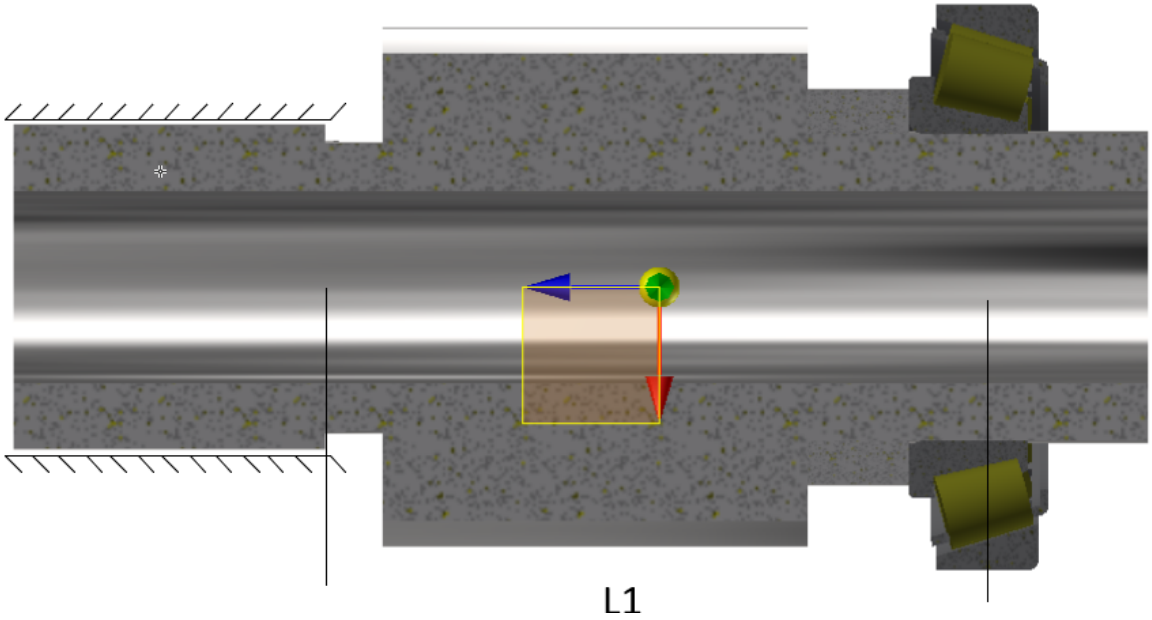

Figure C.9: FBD for fixed sun bearing.

Appendix D:
Equivalent Inertia & Transfer Functions

Below is the Matlab script used to find the local gear ratios in the gearbox, through them the equivalent inertias as seen by the motor, and lastly the transfer functions of the system. The method for the script is explained in chapter 5.4, 5.5, and 5.6.

```
tic
clc; clear all; close all;


%% Declaration of gears

% Declare number of teeth and number of planets
% Actuated step
RA = 121;

S1 = 87;
P1 = (RA - S1)/2;
nP1 = 4;

S2 = 15;
P2 = (RA - S2)/2;
nP2 = 3;

% Fixed step
RF = 86;
SF = 16;
PF = (RF - SF)/2;
nPF = 3;


%% Declaration of inertias [kgm^2]

IM  = 0.285;    % Motor
IC1 = 0.38679;  % Carrier 1
IP1 = 0.00026;  % Planets 1
IRA = 1.52261;  % Actuated ring
ISA = 0.08378;  % Actuated sun shaft
IP2 = 0.02221;  % Planets 2
IC2 = 0.45600;  % Carrier 2
ISF = 0.00436;  % Fixed sun
IPF = 0.05521;  % Fixed planets
IRF = 0;        % Fixed ring
IL  = 25.149;   % Drum


%% Gear Ratios
```

```
% Fixed step
GrF  = - RF / SF;

% Actuated step low and high
GrAL = (S1 * (RA + S2)) / (S2 * (RA + S1));
GrAH = (RA + S2) / (RA + S1);

% Total low and high
GrL  = GrF * GrAL;
GrH  = GrF * GrAH;

% Planets 1
GrP1 = 2 * P1 / (RA + S1);

% Actuated ring (high gear)
GrRA = RA / ( RA + S1);

% Actuated sun shaft (low gear)
GrSA = S1 / ( RA + S1);

% Planets 2 low and high
GrP2L = (2 * P2 / (RA + S2)) * GrAL;
GrP2H = 2 * P2 / (RA + S2) * GrAH;

% Fixed planets low and high
GrPFL = - PF / SF * GrAL;
GrPFH = - PF / SF * GrAH;


%% Equivalent inertia
% Low gear equivalent inertia (ring gear at standstill)
IEqL = IM + IC1 + nP1 * IP1 / GrP1^2 + ISA / GrSA^2 + nP2 * IP2 / ...
    GrP2L^2 + (IC2 + ISF) / GrAL^2 + nPF * IPF / GrPFL^2 + IRF / GrL^2 ...
    + IL / GrL^2;

% High gear equivalent inertia (sun shaft at standstill)
IEqH = IM + IC1 + nP1 * IP1 / GrP1^2 + IRA / GrRA^2 + nP2 * IP2 / ...
    GrP2H^2 + (IC2 + ISF) / GrAH^2 + nPF * IPF / GrPFH^2 + IRF / GrH^2 ...
    + IL / GrH^2;


%% Transfer functions

TFL = minreal(tf(1, [GrL * IEqL, 0]));  % Transfer function low gear
TFH = minreal(tf(1, [GrH * IEqH, 0]));  % Transfer function high gear

% Transfer function of ideal torque source & sensor
TFS = tf(1000,[1, 1000]);

%TFLC = TFL * TFS;    % Combined open loop transfer function low gear.
%TFHC = TFH * TFS;    % Combined open loop transfer function high gear.

% Simulink transfer function low gear.
TFLSim = minreal(tf(-37.952,[1, 1000, 0]) / TFS);
% Simulink transfer function high gear.
TFHSim = minreal(tf(-32.853,[1, 1000, 0]) / TFS);
```

```
% Plot bode plot of theoretical and simulink systems.
figure
bode(TFL,TFH)
legend('Low gear','High gear');
grid on;
grid minor;
title('');
print('-depsc2', '-loose', 'TF_System.eps');

toc
```

Appendix E:
Results for Brake Force Profile Tuning

The data in this appendix show the parameters and results for the tuning of the brake profiles described in chapter 5.11 and 5.12.

E.1 No-Load Test Values

The table below show the results of the no-load tuning, and are related to chapter 5.12.2. The empty cells for the up-shit error indicate that the values were not tested.

Table E.1: Results and parameters for brake profile tests for no-load scenario.

Shift time $[s]$	Slope-factor $[1/s]$	Crossover $[-]$	Max error $[rpm]$	
			Up-Shift	Down-Shift
0.20	0.50	0.487503	500.1477	494.9085
0.20	1.00	0.475021	500.1039	494.8284
0.20	10.00	0.268941	293.0108	470.1331
0.20	20.00	0.119203	107.9947	377.2553
0.20	30.00	0.047426	57.0337	326.7046
0.20	40.00	0.017986	62.1245	323.0133
0.20	50.00	0.006693	67.0793	326.8483
0.20	60.00	0.002473	71.8185	333.7941
0.40	20.00	0.017986	34.6594	261.2179
0.40	30.00	0.002473	49.2699	285.5699
0.40	40.00	0.000335	57.8848	308.6265
0.60	10.00	0.047426	19.2529	240.6864
0.60	15.00	0.010987	21.7491	218.4211
0.60	20.00	0.002473	32.7119	240.7227
0.60	5.00	0.182426	327.9803	475.1621
0.80	10.00	0.017986	17.1692	178.1173
0.80	15.00	0.002473	20.6439	202.5151
0.80	12.50	0.006693	14.5913	186.0940

Continued on next page

Shift time [s]	Slope-factor [$^1/_s$]	Crossover [$-$]	Max error [rpm]	
			Up-Shift	Down-Shift
0.80	11.25	0.010987	11.6333	178.3397
0.80	10.50	0.014774	19.5615	176.9286
1.00	10.00	0.006693	9.0984	151.9972
1.00	12.50	0.001927	13.8947	173.7495
1.00	7.50	0.022977	4.8044	149.1075
1.00	7.00	0.029312	4.7875	157.1908
1.00	8.00	0.017986	5.0050	146.0097
1.00	6.00	0.047426	6.1487	191.0467
1.20	8.00	0.008163	8.9173	121.1401
1.20	9.00	0.004496	11.8455	130.5688
1.20	7.00	0.014774	3.9978	118.1930
1.20	6.00	0.026597	9.8718	128.6207
1.40	7.00	0.007392	3.8189	98.7435
1.40	8.00	0.003684	11.3472	109.9750
1.40	6.00	0.014774	5.1191	95.9299
1.40	6.50	0.010457	6.7892	96.0250
1.40	5.50	0.020836	9.6258	100.4327
1.60	6.00	0.008163	3.8189	77.6793
1.60	5.00	0.017986		78.3345
1.60	7.00	0.003684		87.8415
1.60	4.00	0.039166		117.1857
1.80	6.25	0.003594		69.7804
1.80	6.75	0.002294		77.5846
1.80	5.75	0.005624		63.7980
1.80	5.25	0.008793		59.2322
2.00	5.00	0.006693		47.1066
2.00	6.00	0.002473		60.3106
2.00	4.00	0.017986		48.6544
2.50	4.50	0.003594		25.4751
2.50	3.50	0.012432		20.0315
2.50	5.50	0.001032		40.9223
2.50	4.25	0.004905		22.5794
3.00	3.00	0.010987		6.7532

Continued on next page

Shift time $[s]$	Slope-factor $[1/s]$	Crossover $[-]$	Max error $[rpm]$	
			Up-Shift	Down-Shift
3.00	2.50	0.022977		14.2683
3.00	3.50	0.005220		7.3893
3.00	2.75	0.015906		8.4311
3.00	3.25	0.007577		6.6062
3.50	3.25	0.003377		4.1255
3.50	3.00	0.005220		4.0027
3.50	3.50	0.002183		4.4949
3.50	2.50	0.012432		4.0337
3.50	4.00	0.000911		7.6459
4.00	2.75	0.004070		3.5090
4.00	3.00	0.002473		3.6454
4.00	3.25	0.001501		3.8314
4.00	3.50	0.000911		4.0560
4.00	2.50	0.006693		3.4544
4.00	2.25	0.010987		3.5387
4.00	2.00	0.017986		3.8239

E.2 Positive/Opposing Load Test Results

The figures below show the speeds of the motor and gearbox when shifting gears for different positive loads using the brake force profiles tuned for the no-load case, the results are related to chapter 5.12.3.

In the captions, f is the shift-time, and a is the slope-factor of the brake force profiles described in chapter 5.9.

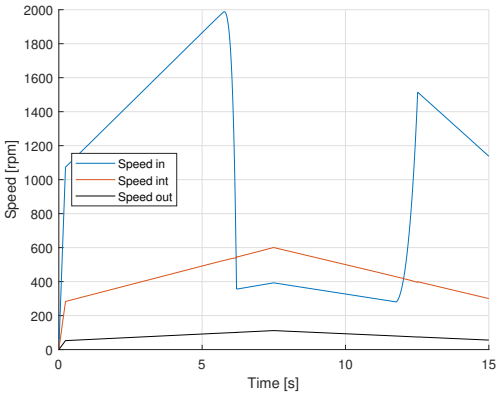

Figure E.1: Speeds of gearbox.
Load = $250[Nm]$.
Up-shift:$f = 1.40[s]$, $a = 7.00\,[1/s]$.
Down-shift:$f = 3.50[s]$, $a = 2.50\,[1/s]$.
Up-shift at $5[s]$. Down-shift at $10[s]$.

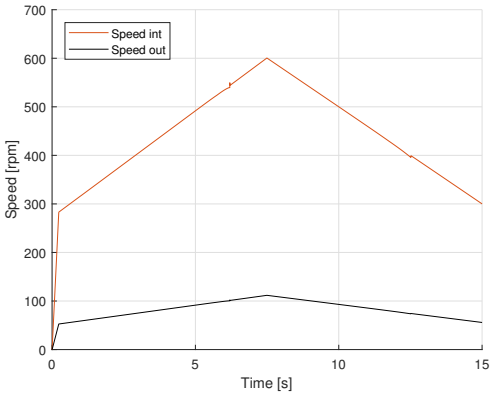

Figure E.2: Speeds of gearbox.
Load = $250[Nm]$.
Up-shift:$f = 1.40[s]$, $a = 7.00\,[1/s]$.
Down-shift:$f = 3.50[s]$, $a = 2.50\,[1/s]$.
Up-shift at $5[s]$. Down-shift at $10[s]$.

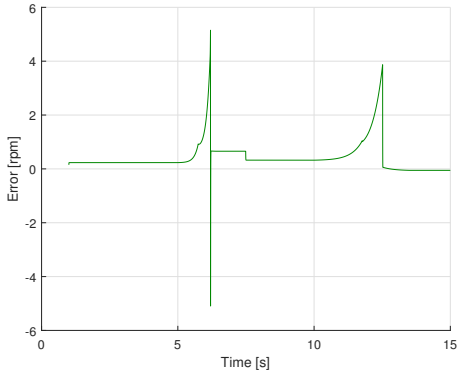

Figure E.3: Error of intermediate shaft velocity in relation to setpoint.
Load = $250[Nm]$.
Up-shift:$f = 1.40[s]$, $a = 7.00\,[1/s]$.
Down-shift:$f = 3.50[s]$, $a = 2.50\,[1/s]$.
Up-shift at $5[s]$. Down-shift at $10[s]$.

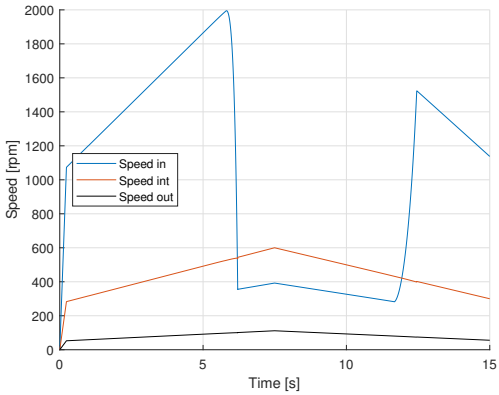

Figure E.4: Speeds of gearbox.
Load = 500[Nm].
Up-shift:$f = 1.40[s]$, $a = 7.00\,[1/s]$.
Down-shift:$f = 3.50[s]$, $a = 2.50\,[1/s]$.
Up-shift at 5[s]. Down-shift at 10[s].

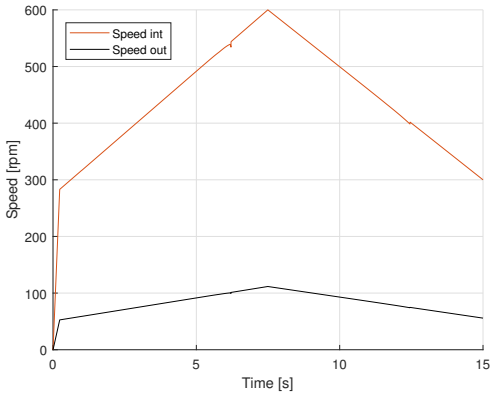

Figure E.5: Speeds of gearbox.
Load = 500[Nm].
Up-shift:$f = 1.40[s]$, $a = 7.00\,[1/s]$.
Down-shift:$f = 3.50[s]$, $a = 2.50\,[1/s]$.
Up-shift at 5[s]. Down-shift at 10[s].

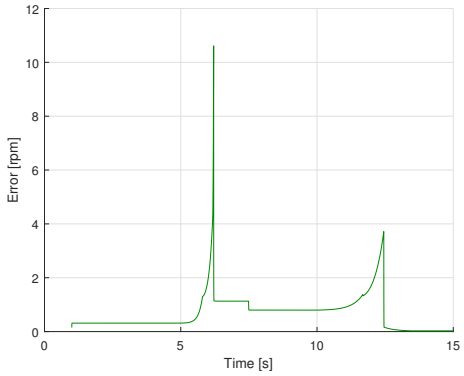

Figure E.6: Error of intermediate shaft velocity in relation to setpoint.
Load = 500[Nm].
Up-shift:$f = 1.40[s]$, $a = 7.00\,[1/s]$.
Down-shift:$f = 3.50[s]$, $a = 2.50\,[1/s]$.
Up-shift at 5[s]. Down-shift at 10[s].

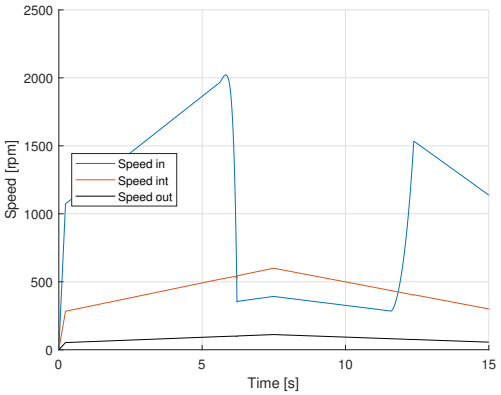

Figure E.7: Speeds of gearbox.
Load = 750[Nm].
Up-shift:$f = 1.40[s]$, $a = 7.00\,[1/s]$.
Down-shift:$f = 3.50[s]$, $a = 2.50\,[1/s]$.
Up-shift at 5[s]. Down-shift at 10[s].

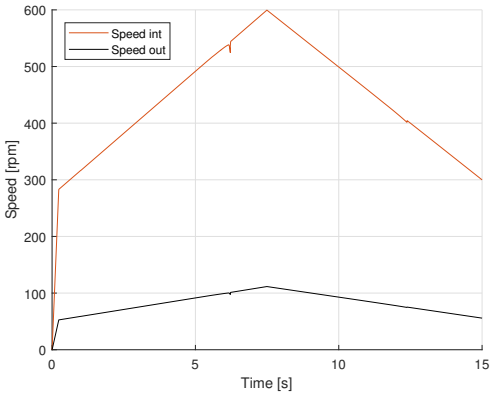

Figure E.8: Speeds of gearbox.
Load = 750[Nm].
Up-shift:$f = 1.40[s]$, $a = 7.00\,[1/s]$.
Down-shift:$f = 3.50[s]$, $a = 2.50\,[1/s]$.
Up-shift at 5[s]. Down-shift at 10[s].

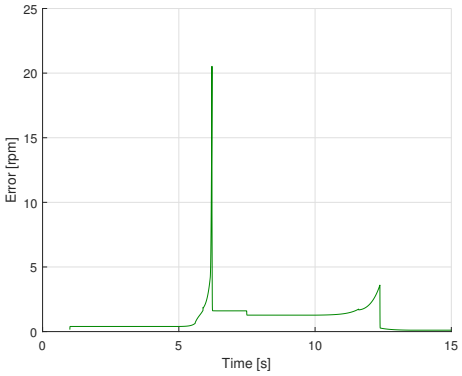

Figure E.9: Error of intermediate shaft velocity in relation to setpoint.
Load = 750[Nm].
Up-shift:$f = 1.40[s]$, $a = 7.00\,[1/s]$.
Down-shift:$f = 3.50[s]$, $a = 2.50\,[1/s]$.
Up-shift at 5[s]. Down-shift at 10[s].

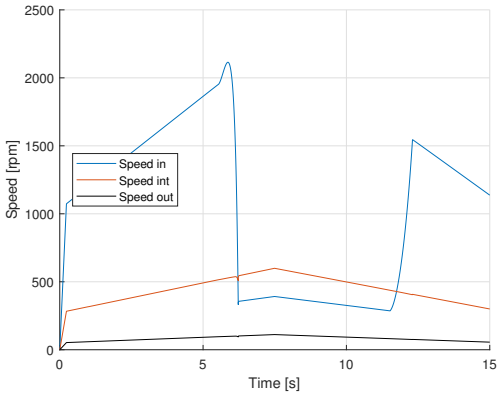

Figure E.10: Speeds of gearbox.
Load = 1000[Nm].
Up-shift:$f = 1.40[s]$, $a = 7.00\,[1/s]$.
Down-shift:$f = 3.50[s]$, $a = 2.50\,[1/s]$.
Up-shift at 5[s]. Down-shift at 10[s].

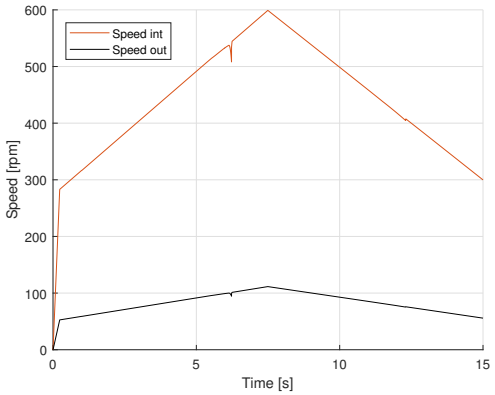

Figure E.11: Speeds of gearbox.
Load = 1000[Nm].
Up-shift:$f = 1.40[s]$, $a = 7.00\,[1/s]$.
Down-shift:$f = 3.50[s]$, $a = 2.50\,[1/s]$.
Up-shift at 5[s]. Down-shift at 10[s].

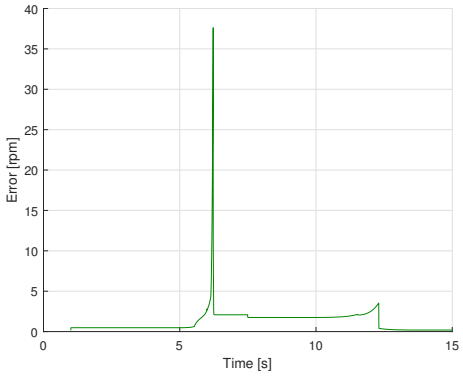

Figure E.12: Error of intermediate shaft velocity in relation to setpoint.
Load = 1000[Nm].
Up-shift:$f = 1.40[s]$, $a = 7.00\,[1/s]$.
Down-shift:$f = 3.50[s]$, $a = 2.50\,[1/s]$.
Up-shift at 5[s]. Down-shift at 10[s].

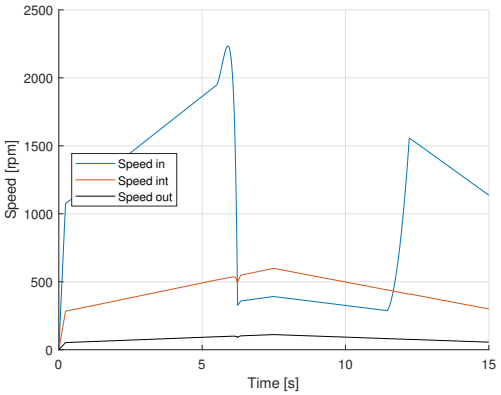

Figure E.13: Speeds of gearbox.
Load = 1250$[Nm]$.
Up-shift:$f = 1.40[s]$, $a = 7.00\,[1/s]$.
Down-shift:$f = 3.50[s]$, $a = 2.50\,[1/s]$.
Up-shift at 5$[s]$. Down-shift at 10$[s]$.

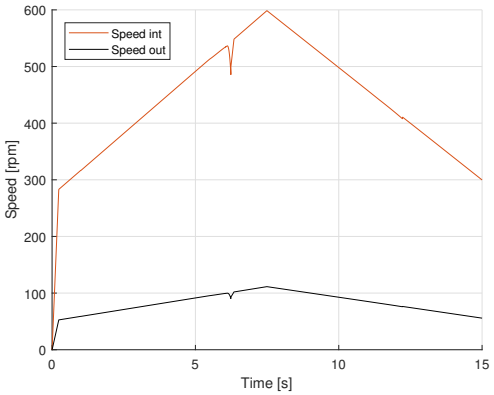

Figure E.14: Speeds of gearbox.
Load = 1250$[Nm]$.
Up-shift:$f = 1.40[s]$, $a = 7.00\,[1/s]$.
Down-shift:$f = 3.50[s]$, $a = 2.50\,[1/s]$.
Up-shift at 5$[s]$. Down-shift at 10$[s]$.

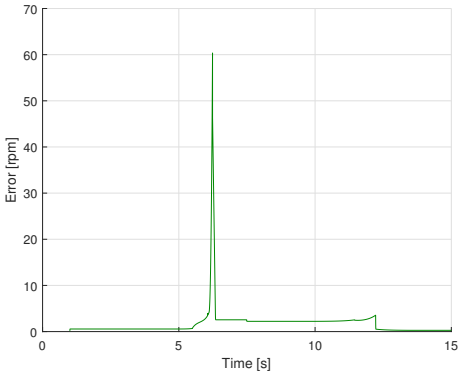

Figure E.15: Error of intermediate shaft velocity in relation to setpoint.
Load = 1250$[Nm]$.
Up-shift:$f = 1.40[s]$, $a = 7.00\,[1/s]$.
Down-shift:$f = 3.50[s]$, $a = 2.50\,[1/s]$.
Up-shift at 5$[s]$. Down-shift at 10$[s]$.

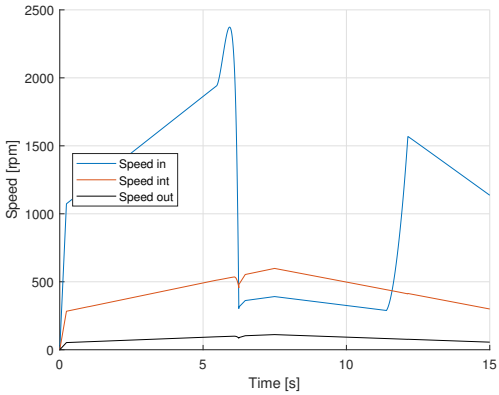

Figure E.16: Speeds of gearbox.
Load = 1500$[Nm]$.
Up-shift:$f = 1.40[s]$, $a = 7.00\,[1/s]$.
Down-shift:$f = 3.50[s]$, $a = 2.50\,[1/s]$.
Up-shift at 5$[s]$. Down-shift at 10$[s]$.

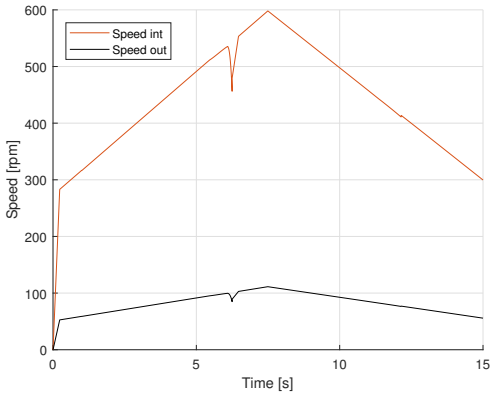

Figure E.17: Speeds of gearbox.
Load = 1500$[Nm]$.
Up-shift:$f = 1.40[s]$, $a = 7.00\,[1/s]$.
Down-shift:$f = 3.50[s]$, $a = 2.50\,[1/s]$.
Up-shift at 5$[s]$. Down-shift at 10$[s]$.

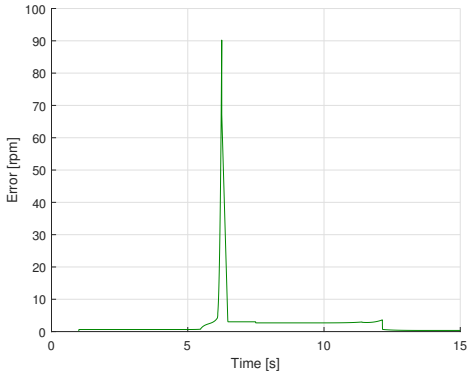

Figure E.18: Error of intermediate shaft velocity in relation to setpoint.
Load = 1500$[Nm]$.
Up-shift:$f = 1.40[s]$, $a = 7.00\,[1/s]$.
Down-shift:$f = 3.50[s]$, $a = 2.50\,[1/s]$.
Up-shift at 5$[s]$. Down-shift at 10$[s]$.

E.3 Negative/Contributing Load Test Results

The figures below show the speeds of the motor and gearbox when shifting gears for different negative loads using the brake force profiles tuned for the no-load case, the results are related to chapter 5.12.4.

In the captions, f is the shift-time, and a is the slope-factor of the brake force profiles described in chapter 5.9.

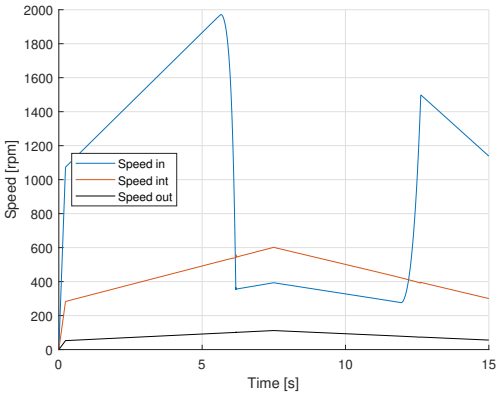

Figure E.19: Speeds of gearbox.
Load $= -250[Nm]$.
Up-shift:$f = 1.40[s]$, $a = 7.00\,[1/s]$.
Down-shift:$f = 3.50[s]$, $a = 2.50\,[1/s]$.
Up-shift at $5[s]$. Down-shift at $10[s]$.

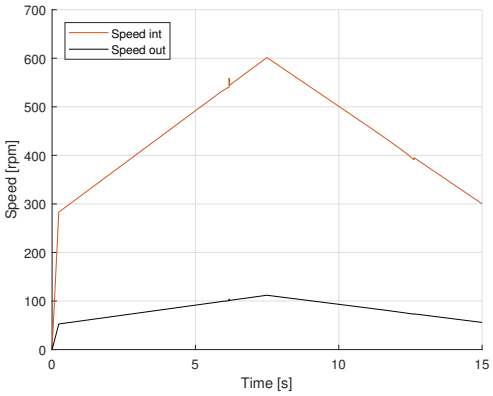

Figure E.20: Speeds of gearbox.
Load $= -250[Nm]$.
Up-shift:$f = 1.40[s]$, $a = 7.00\,[1/s]$.
Down-shift:$f = 3.50[s]$, $a = 2.50\,[1/s]$.
Up-shift at $5[s]$. Down-shift at $10[s]$.

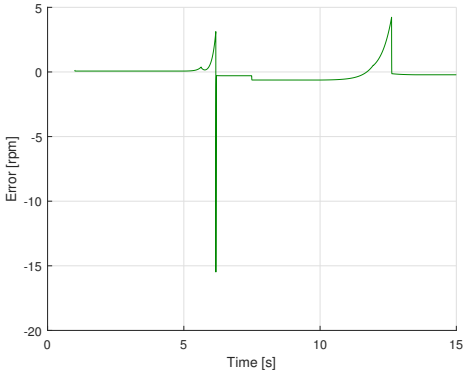

Figure E.21: Error of intermediate shaft velocity in relation to setpoint.
Load $= -250[Nm]$.
Up-shift:$f = 1.40[s]$, $a = 7.00\,[1/s]$.
Down-shift:$f = 3.50[s]$, $a = 2.50\,[1/s]$.
Up-shift at $5[s]$. Down-shift at $10[s]$.

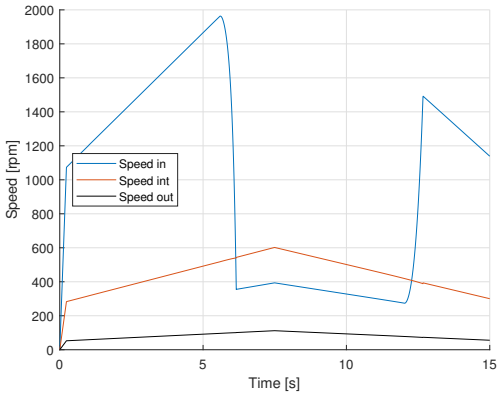

Figure E.22: Speeds of gearbox.
Load $= -500[Nm]$.
Up-shift:$f = 1.40[s]$, $a = 7.00\,[1/s]$.
Down-shift:$f = 3.50[s]$, $a = 2.50\,[1/s]$.
Up-shift at $5[s]$. Down-shift at $10[s]$.

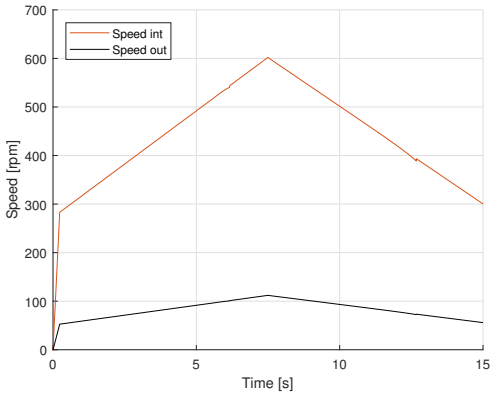

Figure E.23: Speeds of gearbox.
Load $= -500[Nm]$.
Up-shift:$f = 1.40[s]$, $a = 7.00\,[1/s]$.
Down-shift:$f = 3.50[s]$, $a = 2.50\,[1/s]$.
Up-shift at $5[s]$. Down-shift at $10[s]$.

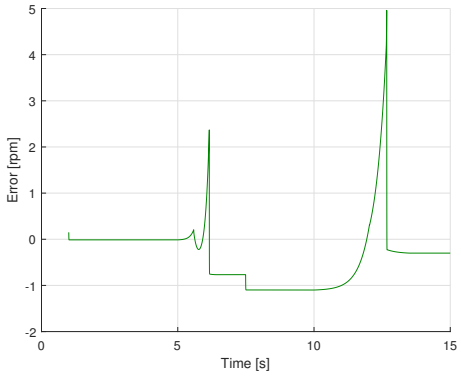

Figure E.24: Error of intermediate shaft velocity in relation to setpoint.
Load $= -500[Nm]$.
Up-shift:$f = 1.40[s]$, $a = 7.00\,[1/s]$.
Down-shift:$f = 3.50[s]$, $a = 2.50\,[1/s]$.
Up-shift at $5[s]$. Down-shift at $10[s]$.

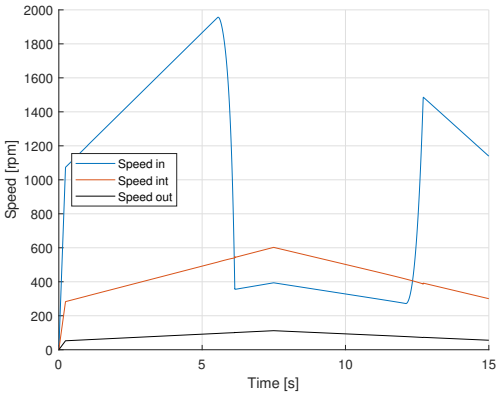

Figure E.25: Speeds of gearbox.
Load $= -750[Nm]$.
Up-shift: $f = 1.40[s]$, $a = 7.00\,[1/s]$.
Down-shift: $f = 3.50[s]$, $a = 2.50\,[1/s]$.
Up-shift at $5[s]$. Down-shift at $10[s]$.

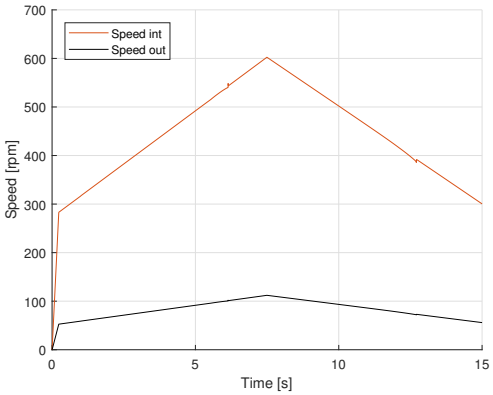

Figure E.26: Speeds of gearbox.
Load $= -750[Nm]$.
Up-shift: $f = 1.40[s]$, $a = 7.00\,[1/s]$.
Down-shift: $f = 3.50[s]$, $a = 2.50\,[1/s]$.
Up-shift at $5[s]$. Down-shift at $10[s]$.

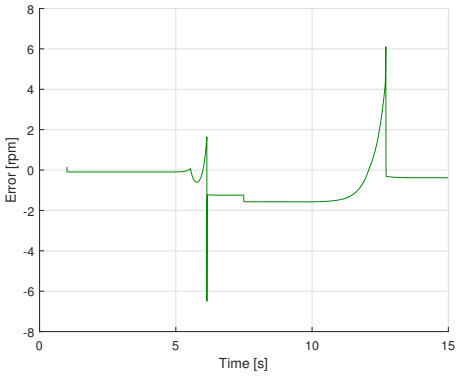

Figure E.27: Error of intermediate shaft velocity in relation to setpoint.
Load $= -750[Nm]$.
Up-shift: $f = 1.40[s]$, $a = 7.00\,[1/s]$.
Down-shift: $f = 3.50[s]$, $a = 2.50\,[1/s]$.
Up-shift at $5[s]$. Down-shift at $10[s]$.

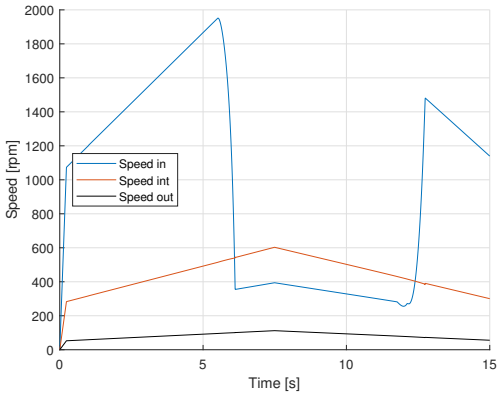

Figure E.28: Speeds of gearbox.
Load $= -1000[Nm]$.
Up-shift:$f = 1.40[s]$, $a = 7.00\,[1/s]$.
Down-shift:$f = 3.50[s]$, $a = 2.50\,[1/s]$.
Up-shift at $5[s]$. Down-shift at $10[s]$.

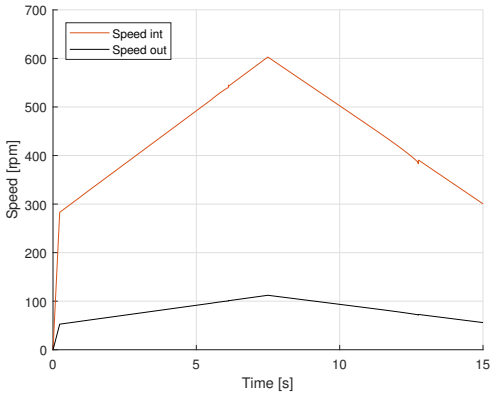

Figure E.29: Speeds of gearbox.
Load $= -1000[Nm]$.
Up-shift:$f = 1.40[s]$, $a = 7.00\,[1/s]$.
Down-shift:$f = 3.50[s]$, $a = 2.50\,[1/s]$.
Up-shift at $5[s]$. Down-shift at $10[s]$.

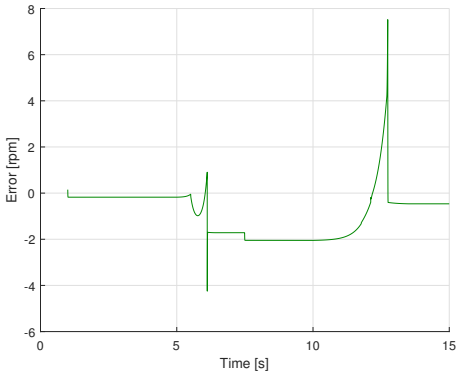

Figure E.30: Error of intermediate shaft velocity in relation to setpoint.
Load $= -1000[Nm]$.
Up-shift:$f = 1.40[s]$, $a = 7.00\,[1/s]$.
Down-shift:$f = 3.50[s]$, $a = 2.50\,[1/s]$.
Up-shift at $5[s]$. Down-shift at $10[s]$.

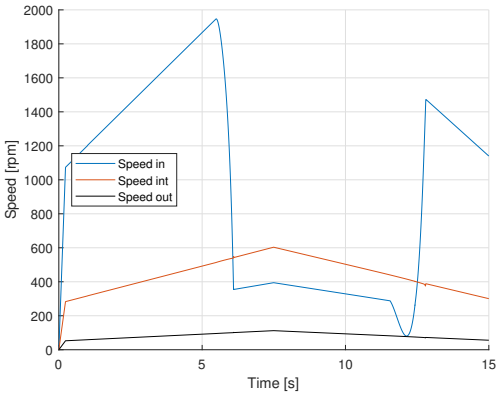

Figure E.31: Speeds of gearbox.
Load $= -1250[Nm]$.
Up-shift: $f = 1.40[s]$, $a = 7.00\,[1/s]$.
Down-shift: $f = 3.50[s]$, $a = 2.50\,[1/s]$.
Up-shift at $5[s]$. Down-shift at $10[s]$.

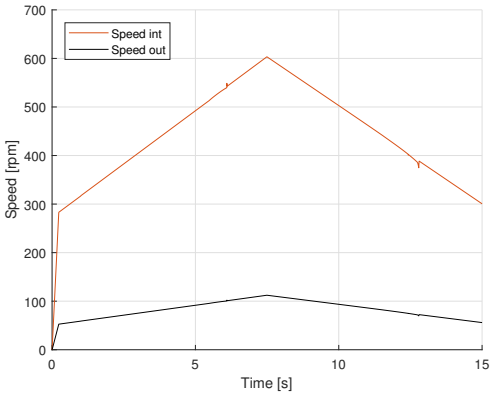

Figure E.32: Speeds of gearbox.
Load $= -1250[Nm]$.
Up-shift: $f = 1.40[s]$, $a = 7.00\,[1/s]$.
Down-shift: $f = 3.50[s]$, $a = 2.50\,[1/s]$.
Up-shift at $5[s]$. Down-shift at $10[s]$.

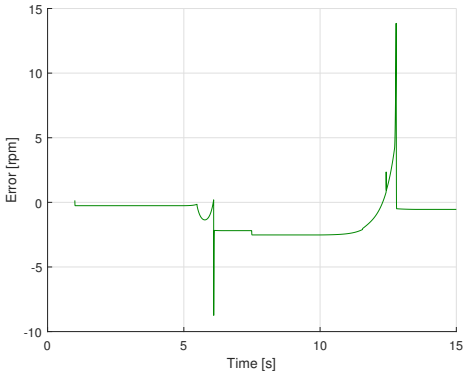

Figure E.33: Error of intermediate shaft velocity in relation to setpoint.
Load $= -1250[Nm]$.
Up-shift: $f = 1.40[s]$, $a = 7.00\,[1/s]$.
Down-shift: $f = 3.50[s]$, $a = 2.50\,[1/s]$.
Up-shift at $5[s]$. Down-shift at $10[s]$.

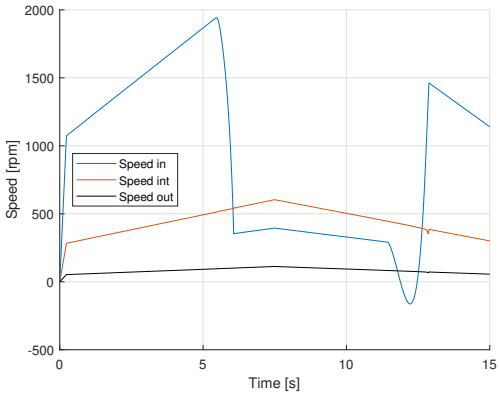

Figure E.34: Speeds of gearbox.
Load $= -1500[Nm]$.
Up-shift:$f = 1.40[s]$, $a = 7.00\,[1/s]$.
Down-shift:$f = 3.50[s]$, $a = 2.50\,[1/s]$.
Up-shift at $5[s]$. Down-shift at $10[s]$.

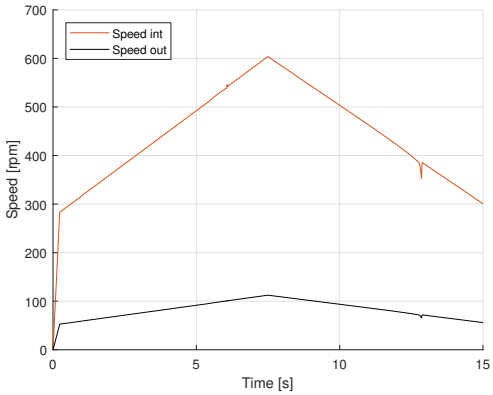

Figure E.35: Speeds of gearbox.
Load $= -1500[Nm]$.
Up-shift:$f = 1.40[s]$, $a = 7.00\,[1/s]$.
Down-shift:$f = 3.50[s]$, $a = 2.50\,[1/s]$.
Up-shift at $5[s]$. Down-shift at $10[s]$.

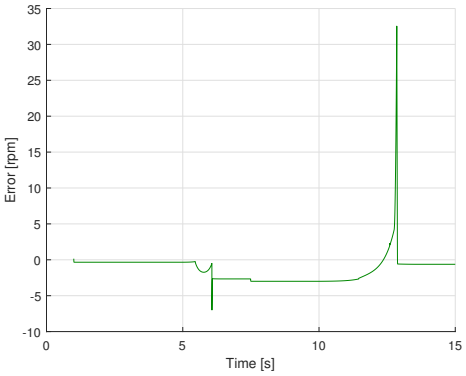

Figure E.36: Error of intermediate shaft velocity in relation to setpoint.
Load $= -1500[Nm]$.
Up-shift:$f = 1.40[s]$, $a = 7.00\,[1/s]$.
Down-shift:$f = 3.50[s]$, $a = 2.50\,[1/s]$.
Up-shift at $5[s]$. Down-shift at $10[s]$.

E.4 Results for Negative Load Tuning

The figures below show the results from the tuning of the down-shift for negative loads, the results are related to chapter 5.12.5.

In the captions, f is the shift-time, and a is the slope-factor of the brake force profiles described in chapter 5.9.

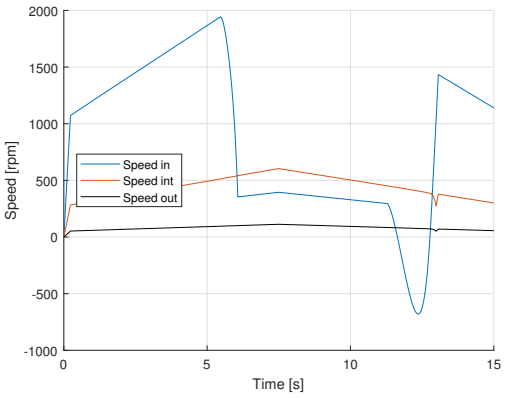

Figure E.37: Speeds of gearbox.
Load $= -1500[Nm]$.
Up-shift:$f = 1.40[s]$, $a = 7.00\,[1/s]$.
Down-shift:$f = 3.50[s]$, $a = 2.75\,[1/s]$.
Up-shift at $5[s]$. Down-shift at $10[s]$.

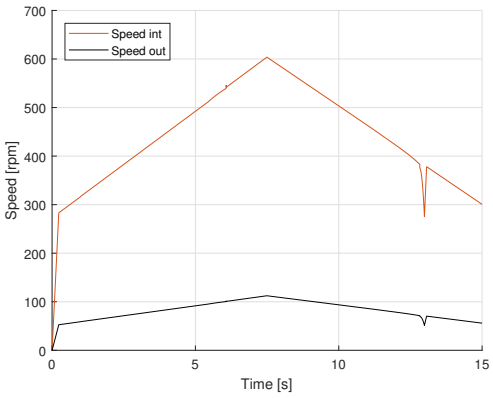

Figure E.38: Speeds of gearbox.
Load $= -1500[Nm]$.
Up-shift:$f = 1.40[s]$, $a = 7.00\,[1/s]$.
Down-shift:$f = 3.50[s]$, $a = 2.75\,[1/s]$.
Up-shift at $5[s]$. Down-shift at $10[s]$.

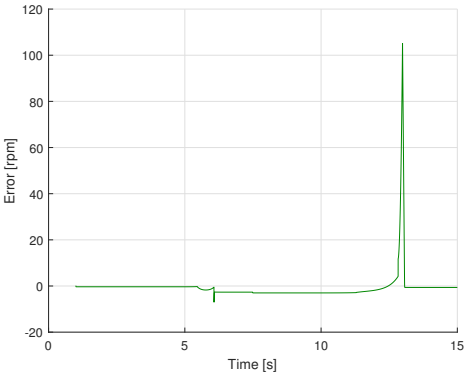

Figure E.39: Error of intermediate shaft velocity in relation to setpoint.
Load $= -1500[Nm]$.
Up-shift:$f = 1.40[s]$, $a = 7.00\,[1/s]$.
Down-shift:$f = 3.50[s]$, $a = 2.75\,[1/s]$.
Up-shift at $5[s]$. Down-shift at $10[s]$.

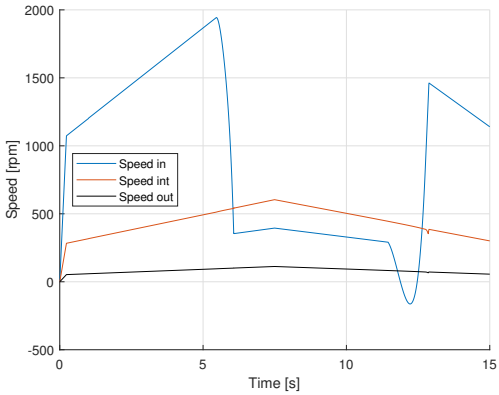

Figure E.40: Speeds of gearbox.
Load $= -1500[Nm]$.
Up-shift:$f = 1.40[s]$, $a = 7.00\,[1/s]$.
Down-shift:$f = 3.50[s]$, $a = 2.50\,[1/s]$.
Up-shift at $5[s]$. Down-shift at $10[s]$.

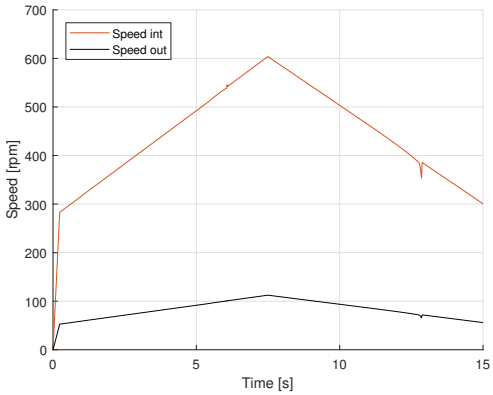

Figure E.41: Speeds of gearbox.
Load $= -1500[Nm]$.
Up-shift:$f = 1.40[s]$, $a = 7.00\,[1/s]$.
Down-shift:$f = 3.50[s]$, $a = 2.50\,[1/s]$.
Up-shift at $5[s]$. Down-shift at $10[s]$.

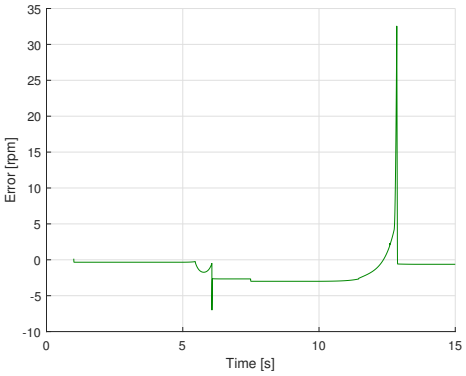

Figure E.42: Error of intermediate shaft velocity in relation to setpoint.
Load $= -1500[Nm]$.
Up-shift:$f = 1.40[s]$, $a = 7.00\,[1/s]$.
Down-shift:$f = 3.50[s]$, $a = 2.50\,[1/s]$.
Up-shift at $5[s]$. Down-shift at $10[s]$.

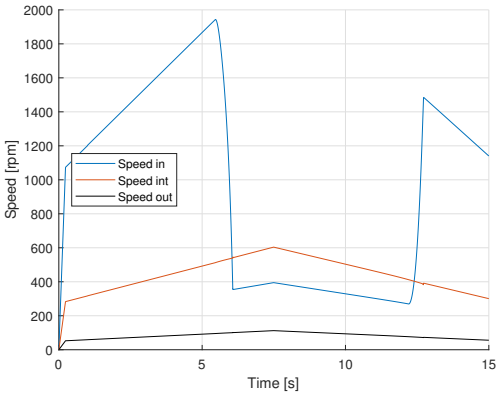

Figure E.43: Speeds of gearbox.
Load $= -1500[Nm]$.
Up-shift: $f = 1.40[s]$, $a = 7.00\,[1/s]$.
Down-shift: $f = 3.50[s]$, $a = 2.25\,[1/s]$.
Up-shift at $5[s]$. Down-shift at $10[s]$.

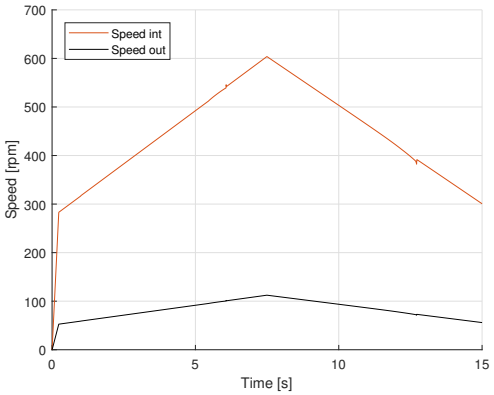

Figure E.44: Speeds of gearbox.
Load $= -1500[Nm]$.
Up-shift: $f = 1.40[s]$, $a = 7.00\,[1/s]$.
Down-shift: $f = 3.50[s]$, $a = 2.25\,[1/s]$.
Up-shift at $5[s]$. Down-shift at $10[s]$.

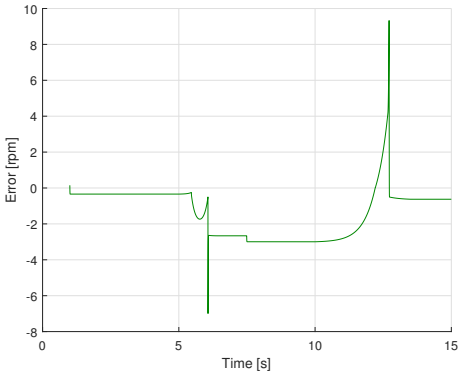

Figure E.45: Error of intermediate shaft velocity in relation to setpoint.
Load $= -1500[Nm]$.
Up-shift: $f = 1.40[s]$, $a = 7.00\,[1/s]$.
Down-shift: $f = 3.50[s]$, $a = 2.25\,[1/s]$.
Up-shift at $5[s]$. Down-shift at $10[s]$.

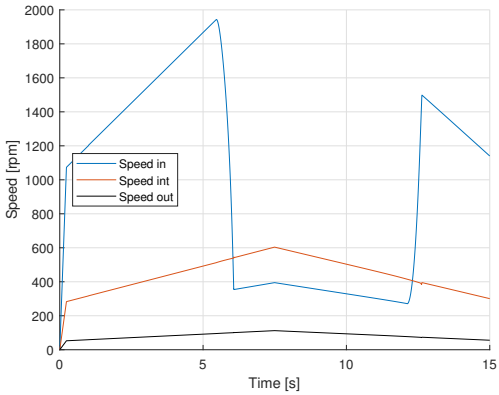

Figure E.46: Speeds of gearbox.
Load $= -1500[Nm]$.
Up-shift:$f = 1.40[s]$, $a = 7.00\,[1/s]$.
Down-shift:$f = 3.50[s]$, $a = 2.00\,[1/s]$.
Up-shift at $5[s]$. Down-shift at $10[s]$.

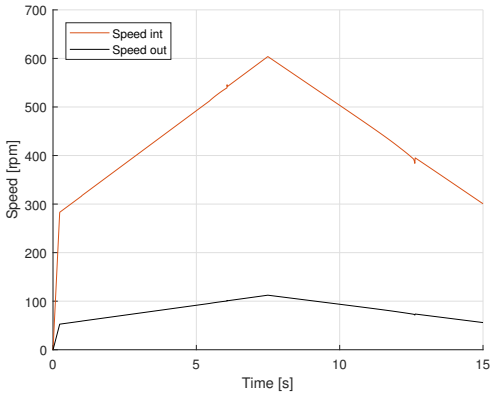

Figure E.47: Speeds of gearbox.
Load $= -1500[Nm]$.
Up-shift:$f = 1.40[s]$, $a = 7.00\,[1/s]$.
Down-shift:$f = 3.50[s]$, $a = 2.00\,[1/s]$.
Up-shift at $5[s]$. Down-shift at $10[s]$.

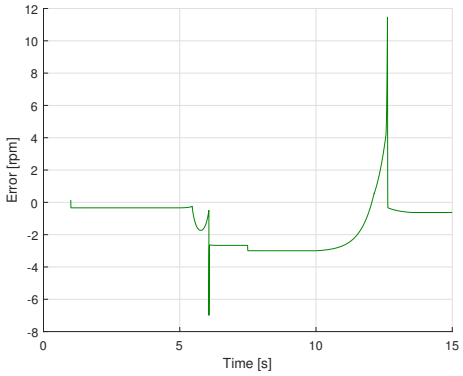

Figure E.48: Error of intermediate shaft velocity in relation to setpoint.
Load $= -1500[Nm]$.
Up-shift:$f = 1.40[s]$, $a = 7.00\,[1/s]$.
Down-shift:$f = 3.50[s]$, $a = 2.00\,[1/s]$.
Up-shift at $5[s]$. Down-shift at $10[s]$.

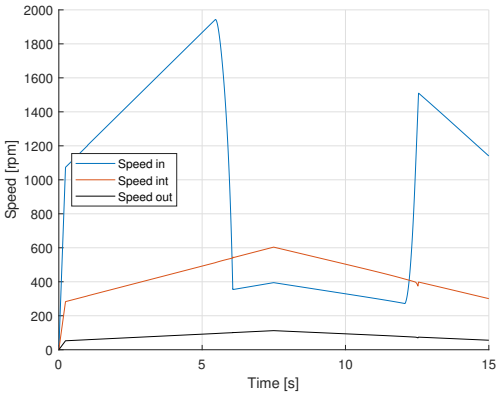

Figure E.49: Speeds of gearbox.
Load $= -1500[Nm]$.
Up-shift:$f = 1.40[s]$, $a = 7.00\,[1/s]$.
Down-shift:$f = 3.50[s]$, $a = 1.75\,[1/s]$.
Up-shift at $5[s]$. Down-shift at $10[s]$.

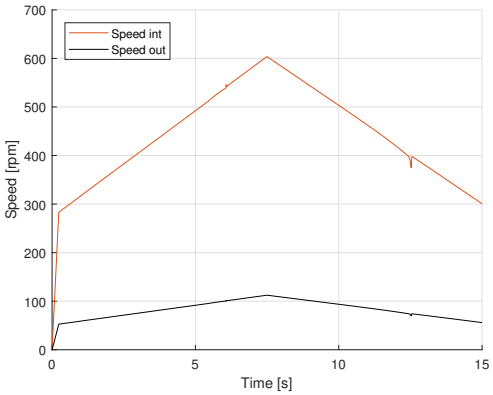

Figure E.50: Speeds of gearbox.
Load $= -1500[Nm]$.
Up-shift:$f = 1.40[s]$, $a = 7.00\,[1/s]$.
Down-shift:$f = 3.50[s]$, $a = 1.75\,[1/s]$.
Up-shift at $5[s]$. Down-shift at $10[s]$.

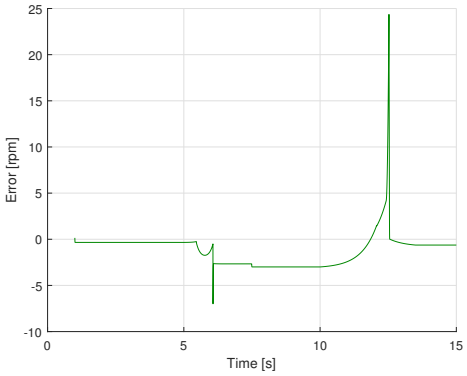

Figure E.51: Error of intermediate shaft velocity in relation to setpoint.
Load $= -1500[Nm]$.
Up-shift:$f = 1.40[s]$, $a = 7.00\,[1/s]$.
Down-shift:$f = 3.50[s]$, $a = 1.75\,[1/s]$.
Up-shift at $5[s]$. Down-shift at $10[s]$.

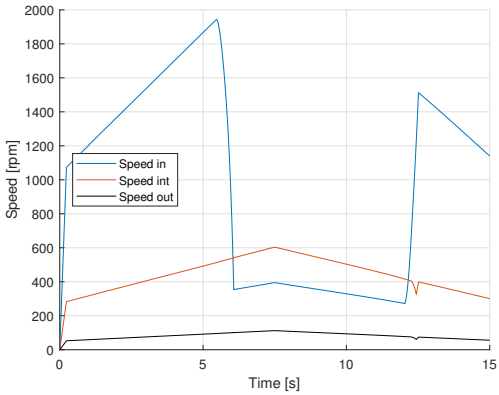

Figure E.52: Speeds of gearbox.
Load $= -1500[Nm]$.
Up-shift:$f = 1.40[s]$, $a = 7.00\,[1/s]$.
Down-shift:$f = 3.50[s]$, $a = 1.50\,[1/s]$.
Up-shift at $5[s]$. Down-shift at $10[s]$.

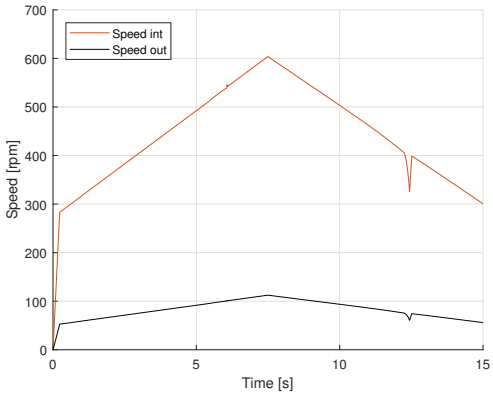

Figure E.53: Speeds of gearbox.
Load $= -1500[Nm]$.
Up-shift:$f = 1.40[s]$, $a = 7.00\,[1/s]$.
Down-shift:$f = 3.50[s]$, $a = 1.50\,[1/s]$.
Up-shift at $5[s]$. Down-shift at $10[s]$.

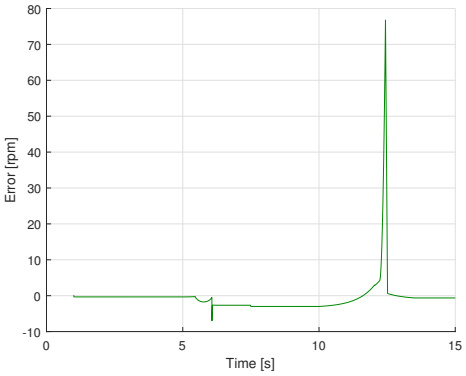

Figure E.54: Error of intermediate shaft velocity in relation to setpoint.
Load $= -1500[Nm]$.
Up-shift:$f = 1.40[s]$, $a = 7.00\,[1/s]$.
Down-shift:$f = 3.50[s]$, $a = 1.50\,[1/s]$.
Up-shift at $5[s]$. Down-shift at $10[s]$.

E.5 Results for Positive Load Tuning

The figures below show the results from the tuning of the up-shift with a load of *1250*$[Nm]$, the results are related to chapter 5.12.6.

In the captions, f is the shift-time, and a is the slope-factor of the brake force profiles described in chapter 5.9.

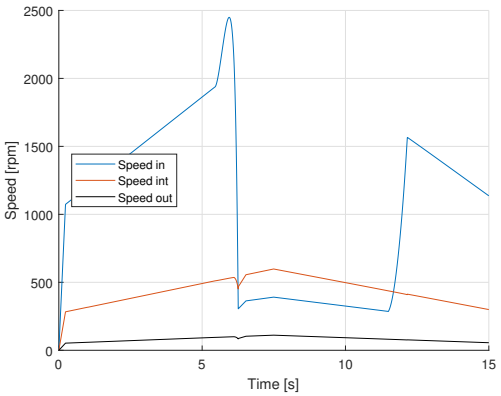

Figure E.55: Speeds of gearbox.
Load = 1500$[Nm]$.
Up-shift:$f = 1.40[s]$, $a = 7.25\,[1/s]$.
Down-shift:$f = 3.50[s]$, $a = 2.25\,[1/s]$.
Up-shift at 5$[s]$. Down-shift at 10$[s]$.

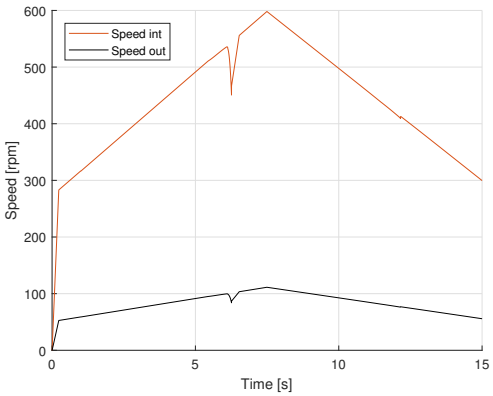

Figure E.56: Speeds of gearbox.
Load = 1500$[Nm]$.
Up-shift:$f = 1.40[s]$, $a = 7.25\,[1/s]$.
Down-shift:$f = 3.50[s]$, $a = 2.25\,[1/s]$.
Up-shift at 5$[s]$. Down-shift at 10$[s]$.

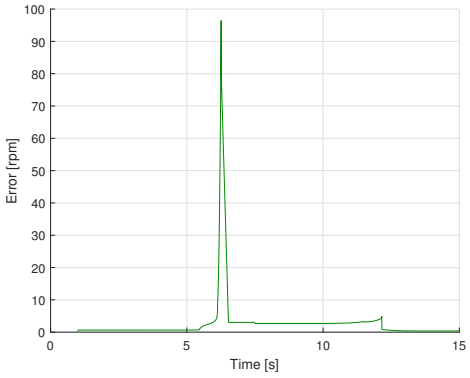

Figure E.57: Error of intermediate shaft velocity in relation to setpoint.
Load = 1500$[Nm]$.
Up-shift:$f = 1.40[s]$, $a = 7.25\,[1/s]$.
Down-shift:$f = 3.50[s]$, $a = 2.25\,[1/s]$.
Up-shift at 5$[s]$. Down-shift at 10$[s]$.

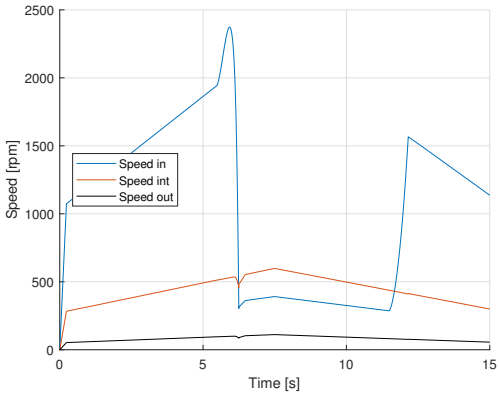

Figure E.58: Speeds of gearbox.
Load = 1500[Nm].
Up-shift:$f = 1.40[s]$, $a = 7.00\,[1/s]$.
Down-shift:$f = 3.50[s]$, $a = 2.25\,[1/s]$.
Up-shift at 5[s]. Down-shift at 10[s].

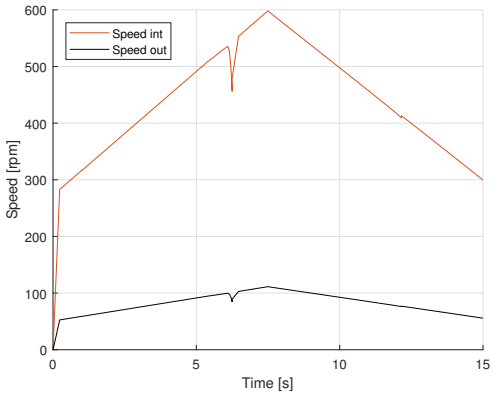

Figure E.59: Speeds of gearbox.
Load = 1500[Nm].
Up-shift:$f = 1.40[s]$, $a = 7.00\,[1/s]$.
Down-shift:$f = 3.50[s]$, $a = 2.25\,[1/s]$.
Up-shift at 5[s]. Down-shift at 10[s].

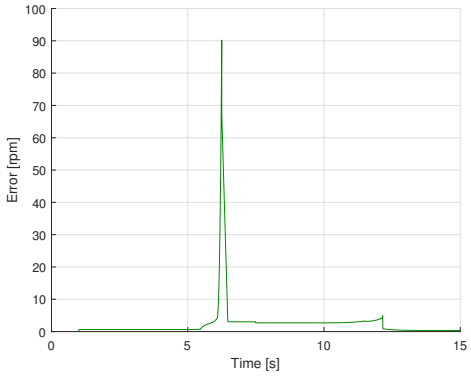

Figure E.60: Error of intermediate shaft velocity in relation to setpoint.
Load = 1500[Nm].
Up-shift:$f = 1.40[s]$, $a = 7.00\,[1/s]$.
Down-shift:$f = 3.50[s]$, $a = 2.25\,[1/s]$.
Up-shift at 5[s]. Down-shift at 10[s].

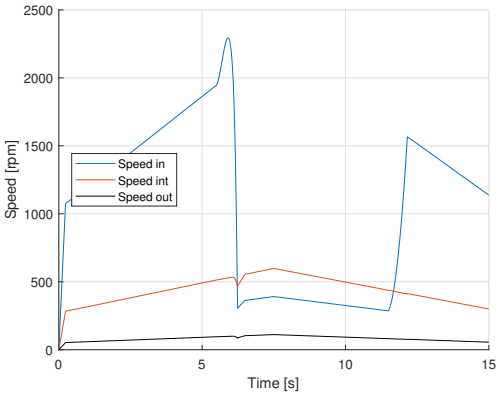

Figure E.61: Speeds of gearbox.
Load = 1500$[Nm]$.
Up-shift:$f = 1.40[s]$, $a = 6.75\,[1/s]$.
Down-shift:$f = 3.50[s]$, $a = 2.25\,[1/s]$.
Up-shift at 5$[s]$. Down-shift at 10$[s]$.

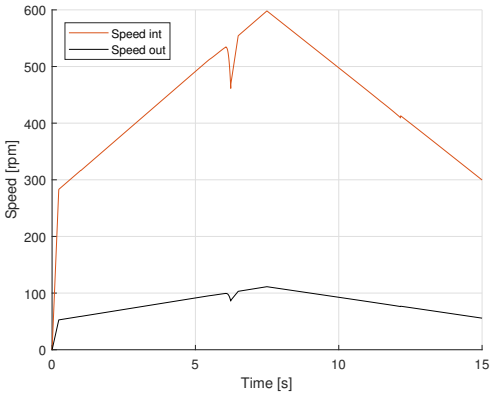

Figure E.62: Speeds of gearbox.
Load = 1500$[Nm]$.
Up-shift:$f = 1.40[s]$, $a = 6.75\,[1/s]$.
Down-shift:$f = 3.50[s]$, $a = 2.25\,[1/s]$.
Up-shift at 5$[s]$. Down-shift at 10$[s]$.

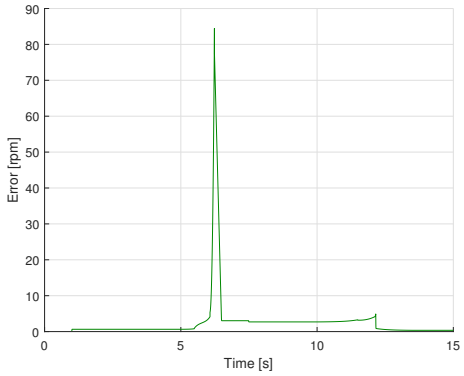

Figure E.63: Error of intermediate shaft velocity in relation to setpoint.
Load = 1500$[Nm]$.
Up-shift:$f = 1.40[s]$, $a = 6.75\,[1/s]$.
Down-shift:$f = 3.50[s]$, $a = 2.25\,[1/s]$.
Up-shift at 5$[s]$. Down-shift at 10$[s]$.

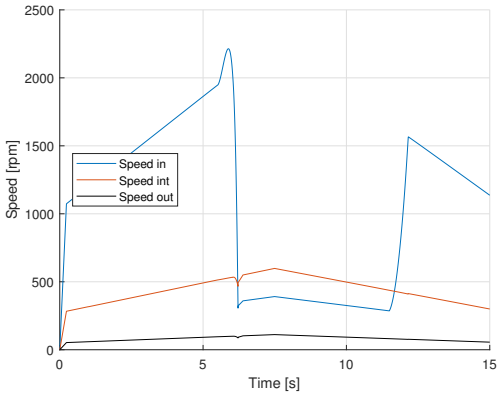

Figure E.64: Speeds of gearbox.
Load = 1500[Nm].
Up-shift:$f = 1.40[s]$, $a = 6.50\,[1/s]$.
Down-shift:$f = 3.50[s]$, $a = 2.25\,[1/s]$.
Up-shift at 5[s]. Down-shift at 10[s].

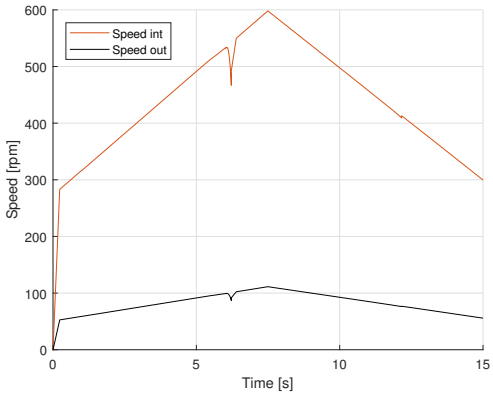

Figure E.65: Speeds of gearbox.
Load = 1500[Nm].
Up-shift:$f = 1.40[s]$, $a = 6.50\,[1/s]$.
Down-shift:$f = 3.50[s]$, $a = 2.25\,[1/s]$.
Up-shift at 5[s]. Down-shift at 10[s].

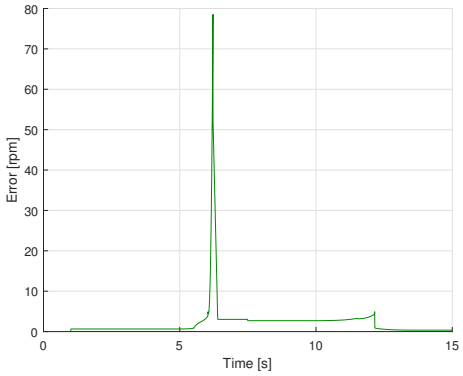

Figure E.66: Error of intermediate shaft velocity in relation to setpoint.
Load = 1500[Nm].
Up-shift:$f = 1.40[s]$, $a = 6.50\,[1/s]$.
Down-shift:$f = 3.50[s]$, $a = 2.25\,[1/s]$.
Up-shift at 5[s]. Down-shift at 10[s].

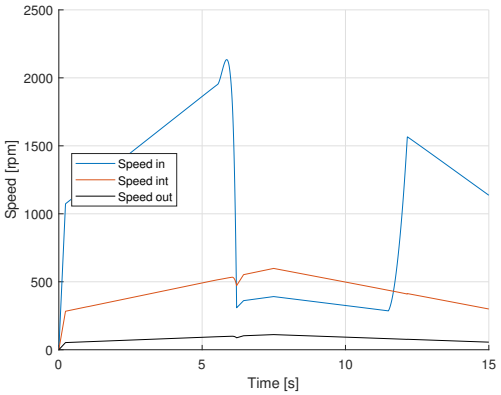

Figure E.67: Speeds of gearbox.
Load = 1500$[Nm]$.
Up-shift:$f = 1.40[s]$, $a = 6.25\,[1/s]$.
Down-shift:$f = 3.50[s]$, $a = 2.25\,[1/s]$.
Up-shift at 5$[s]$. Down-shift at 10$[s]$.

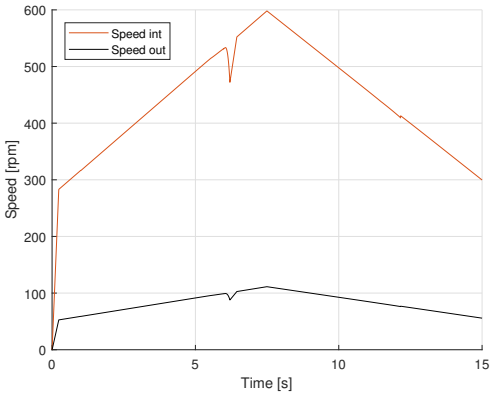

Figure E.68: Speeds of gearbox.
Load = 1500$[Nm]$.
Up-shift:$f = 1.40[s]$, $a = 6.25\,[1/s]$.
Down-shift:$f = 3.50[s]$, $a = 2.25\,[1/s]$.
Up-shift at 5$[s]$. Down-shift at 10$[s]$.

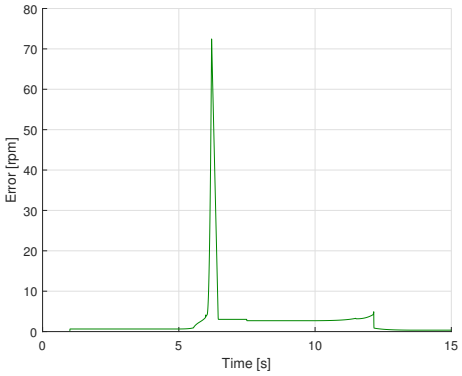

Figure E.69: Error of intermediate shaft velocity in relation to setpoint.
Load = 1500$[Nm]$.
Up-shift:$f = 1.40[s]$, $a = 6.25\,[1/s]$.
Down-shift:$f = 3.50[s]$, $a = 2.25\,[1/s]$.
Up-shift at 5$[s]$. Down-shift at 10$[s]$.

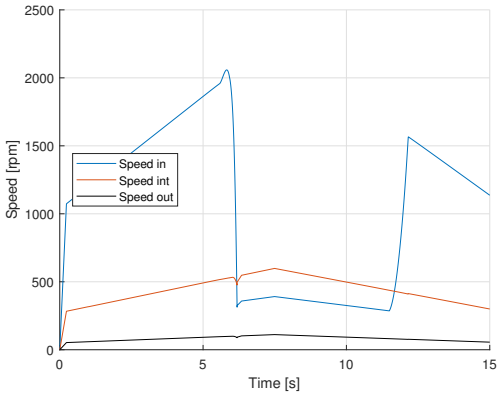

Figure E.70: Speeds of gearbox.
Load = 1500[Nm].
Up-shift:$f = 1.40[s]$, $a = 6.00\,[1/s]$.
Down-shift:$f = 3.50[s]$, $a = 2.25\,[1/s]$.
Up-shift at 5[s]. Down-shift at 10[s].

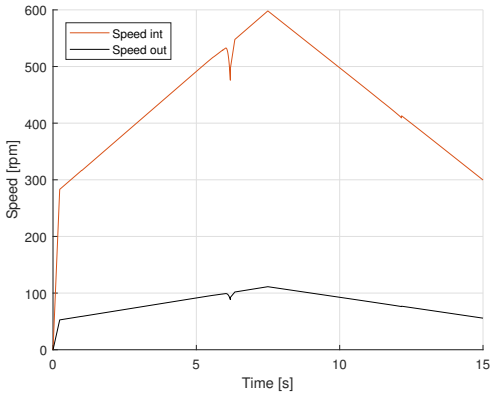

Figure E.71: Speeds of gearbox.
Load = 1500[Nm].
Up-shift:$f = 1.40[s]$, $a = 6.00\,[1/s]$.
Down-shift:$f = 3.50[s]$, $a = 2.25\,[1/s]$.
Up-shift at 5[s]. Down-shift at 10[s].

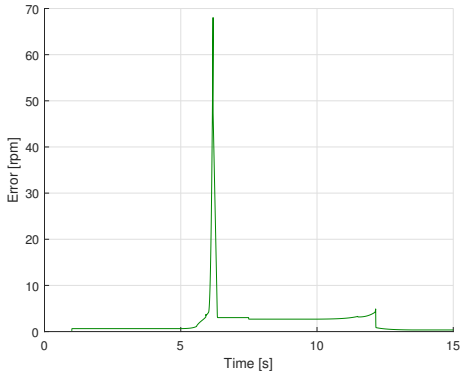

Figure E.72: Error of intermediate shaft velocity in relation to setpoint.
Load = 1500[Nm].
Up-shift:$f = 1.40[s]$, $a = 6.00\,[1/s]$.
Down-shift:$f = 3.50[s]$, $a = 2.25\,[1/s]$.
Up-shift at 5[s]. Down-shift at 10[s].

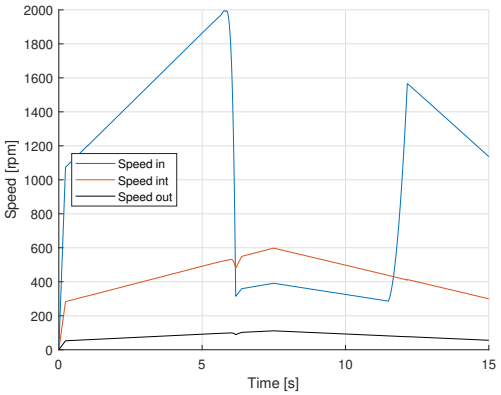

Figure E.73: Speeds of gearbox.
Load = 1500$[Nm]$.
Up-shift:$f = 1.40[s]$, $a = 5.75\,[1/s]$.
Down-shift:$f = 3.50[s]$, $a = 2.25\,[1/s]$.
Up-shift at 5$[s]$. Down-shift at 10$[s]$.

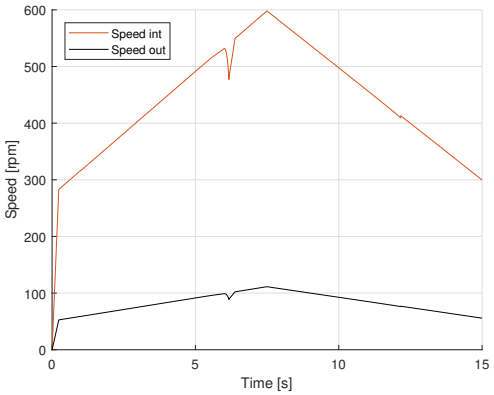

Figure E.74: Speeds of gearbox.
Load = 1500$[Nm]$.
Up-shift:$f = 1.40[s]$, $a = 5.75\,[1/s]$.
Down-shift:$f = 3.50[s]$, $a = 2.25\,[1/s]$.
Up-shift at 5$[s]$. Down-shift at 10$[s]$.

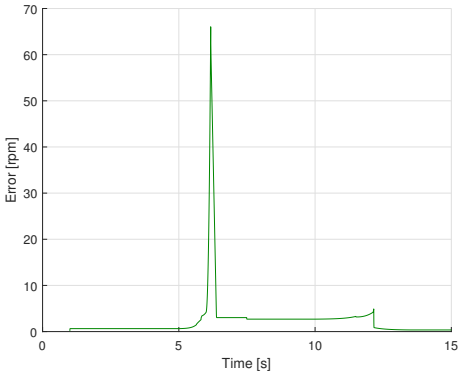

Figure E.75: Error of intermediate shaft velocity in relation to setpoint.
Load = 1500$[Nm]$.
Up-shift:$f = 1.40[s]$, $a = 5.75\,[1/s]$.
Down-shift:$f = 3.50[s]$, $a = 2.25\,[1/s]$.
Up-shift at 5$[s]$. Down-shift at 10$[s]$.

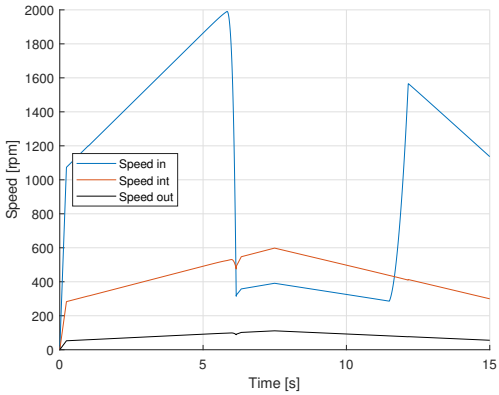

Figure E.76: Speeds of gearbox.
Load = 1500$[Nm]$.
Up-shift:$f = 1.40[s]$, $a = 5.50\,[1/s]$.
Down-shift:$f = 3.50[s]$, $a = 2.25\,[1/s]$.
Up-shift at 5$[s]$. Down-shift at 10$[s]$.

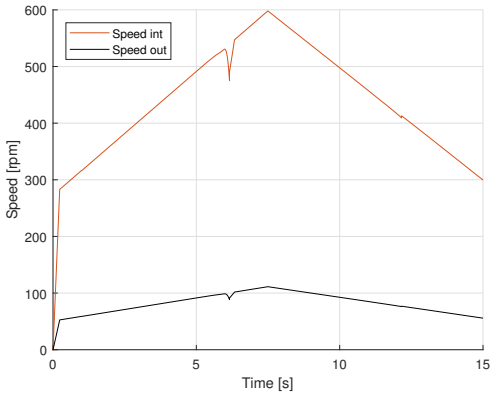

Figure E.77: Speeds of gearbox.
Load = 1500$[Nm]$.
Up-shift:$f = 1.40[s]$, $a = 5.50\,[1/s]$.
Down-shift:$f = 3.50[s]$, $a = 2.25\,[1/s]$.
Up-shift at 5$[s]$. Down-shift at 10$[s]$.

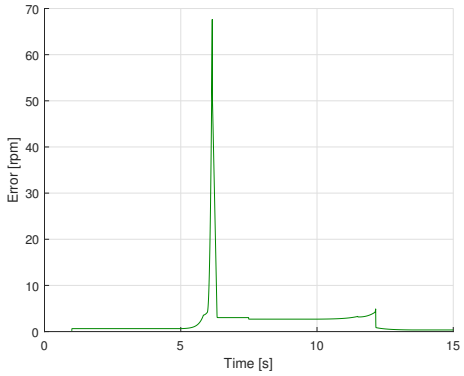

Figure E.78: Error of intermediate shaft velocity in relation to setpoint.
Load = 1500$[Nm]$.
Up-shift:$f = 1.40[s]$, $a = 5.50\,[1/s]$.
Down-shift:$f = 3.50[s]$, $a = 2.25\,[1/s]$.
Up-shift at 5$[s]$. Down-shift at 10$[s]$.

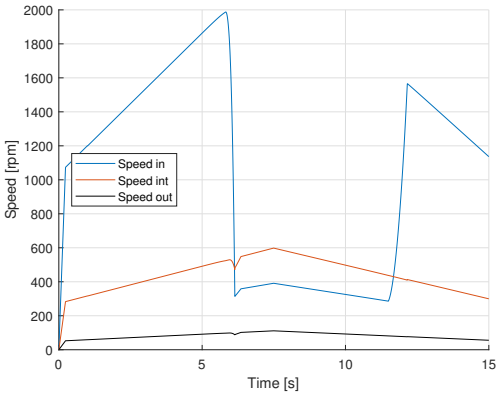

Figure E.79: Speeds of gearbox.
Load = 1500$[Nm]$.
Up-shift:$f = 1.40[s]$, $a = 5.25\,[1/s]$.
Down-shift:$f = 3.50[s]$, $a = 2.25\,[1/s]$.
Up-shift at 5$[s]$. Down-shift at 10$[s]$.

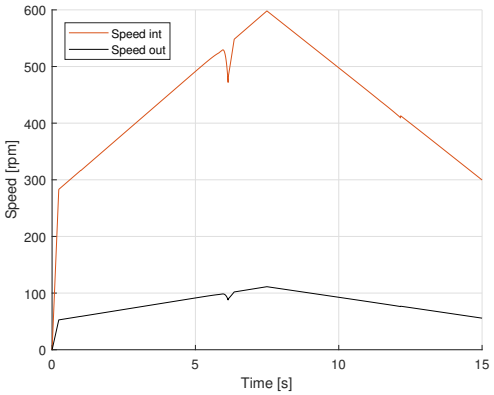

Figure E.80: Speeds of gearbox.
Load = 1500$[Nm]$.
Up-shift:$f = 1.40[s]$, $a = 5.25\,[1/s]$.
Down-shift:$f = 3.50[s]$, $a = 2.25\,[1/s]$.
Up-shift at 5$[s]$. Down-shift at 10$[s]$.

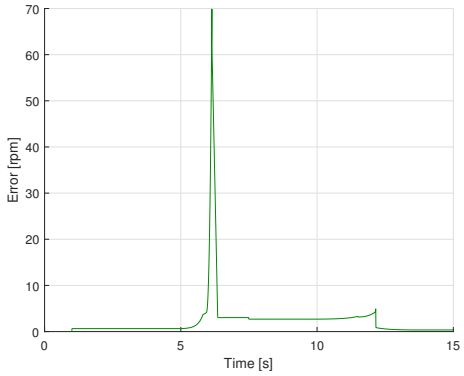

Figure E.81: Error of intermediate shaft velocity in relation to setpoint.
Load = 1500$[Nm]$.
Up-shift:$f = 1.40[s]$, $a = 5.25\,[1/s]$.
Down-shift:$f = 3.50[s]$, $a = 2.25\,[1/s]$.
Up-shift at 5$[s]$. Down-shift at 10$[s]$.

E.6 Results for Final Tuning

The figures below show the behavior of the motor and gearbox when shifting gears using the final result of the brake force profile tuning. The figures show the behavior for loads between *-1500*$[Nm]$ and *1500*$[Nm]$, with steps of *250*$[Nm]$. The results are related to chapter 5.12.7.

In the captions, f is the shift-time, and a is the slope-factor of the brake force profiles described in chapter 5.9.

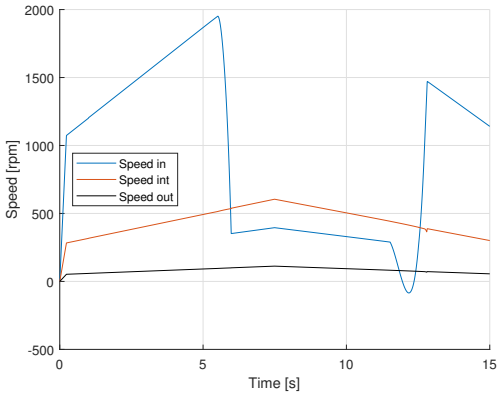

Figure E.82: Speeds of gearbox.
Load $= -2000[Nm]$.
Up-shift:$f = 1.40[s]$, $a = 5.50\,[1/s]$.
Down-shift:$f = 3.50[s]$, $a = 2.25\,[1/s]$.
Up-shift at $5[s]$. Down-shift at $10[s]$.

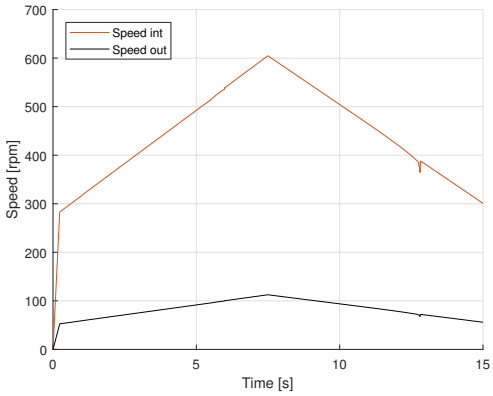

Figure E.83: Speeds of gearbox.
Load $= -2000[Nm]$.
Up-shift:$f = 1.40[s]$, $a = 5.50\,[1/s]$.
Down-shift:$f = 3.50[s]$, $a = 2.25\,[1/s]$.
Up-shift at $5[s]$. Down-shift at $10[s]$.

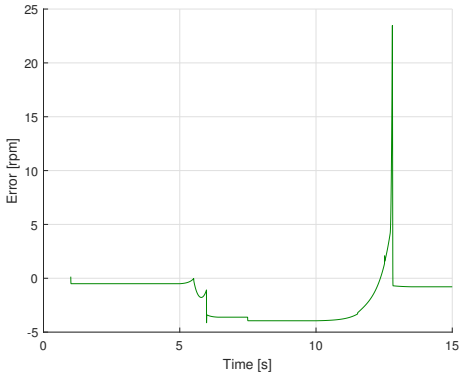

Figure E.84: Error of intermediate shaft velocity in relation to setpoint.
Load $= -2000[Nm]$.
Up-shift:$f = 1.40[s]$, $a = 5.50\,[1/s]$.
Down-shift:$f = 3.50[s]$, $a = 2.25\,[1/s]$.
Up-shift at $5[s]$. Down-shift at $10[s]$.

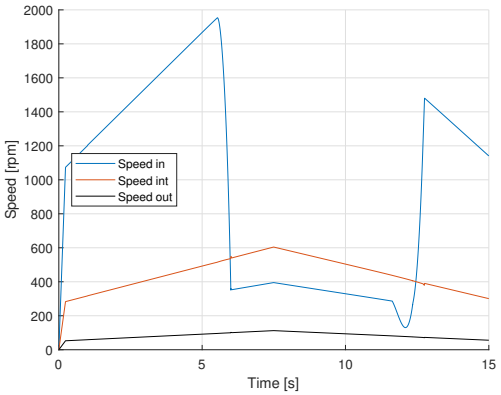

Figure E.85: Speeds of gearbox.
Load $= -1750[Nm]$.
Up-shift:$f = 1.40[s]$, $a = 5.50\,[1/s]$.
Down-shift:$f = 3.50[s]$, $a = 2.25\,[1/s]$.
Up-shift at $5[s]$. Down-shift at $10[s]$.

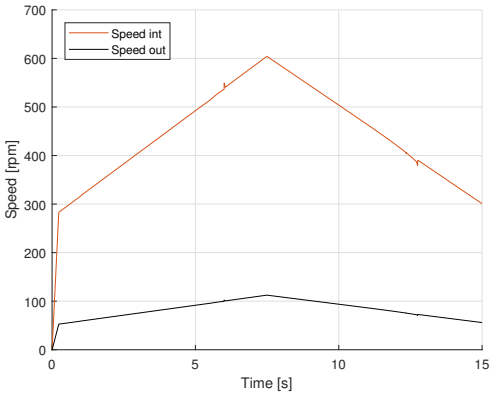

Figure E.86: Speeds of gearbox.
Load $= -1750[Nm]$.
Up-shift:$f = 1.40[s]$, $a = 5.50\,[1/s]$.
Down-shift:$f = 3.50[s]$, $a = 2.25\,[1/s]$.
Up-shift at $5[s]$. Down-shift at $10[s]$.

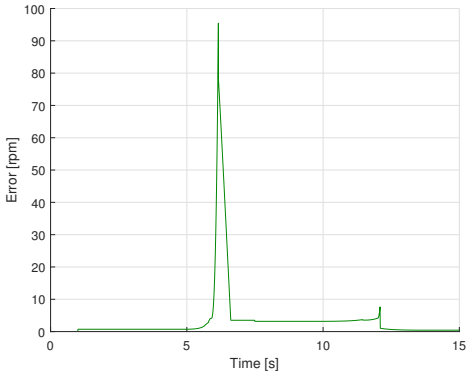

Figure E.87: Error of intermediate shaft velocity in relation to setpoint.
Load $= -1750[Nm]$.
Up-shift:$f = 1.40[s]$, $a = 5.50\,[1/s]$.
Down-shift:$f = 3.50[s]$, $a = 2.25\,[1/s]$.
Up-shift at $5[s]$. Down-shift at $10[s]$.

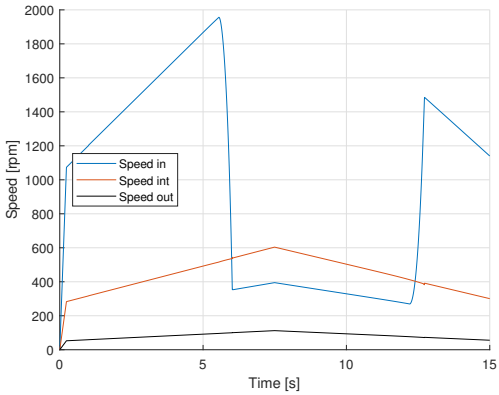

Figure E.88: Speeds of gearbox.
Load $= -1500[Nm]$.
Up-shift:$f = 1.40[s]$, $a = 5.50\,[1/s]$.
Down-shift:$f = 3.50[s]$, $a = 2.25\,[1/s]$.
Up-shift at $5[s]$. Down-shift at $10[s]$.

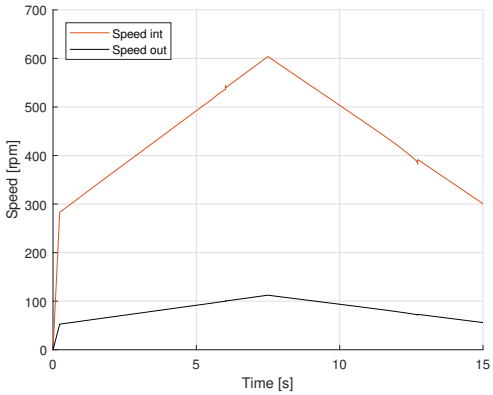

Figure E.89: Speeds of gearbox.
Load $= -1500[Nm]$.
Up-shift:$f = 1.40[s]$, $a = 5.50\,[1/s]$.
Down-shift:$f = 3.50[s]$, $a = 2.25\,[1/s]$.
Up-shift at $5[s]$. Down-shift at $10[s]$.

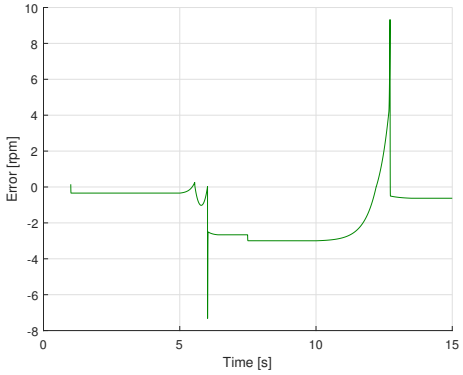

Figure E.90: Error of intermediate shaft velocity in relation to setpoint.
Load $= -1500[Nm]$.
Up-shift:$f = 1.40[s]$, $a = 5.50\,[1/s]$.
Down-shift:$f = 3.50[s]$, $a = 2.25\,[1/s]$.
Up-shift at $5[s]$. Down-shift at $10[s]$.

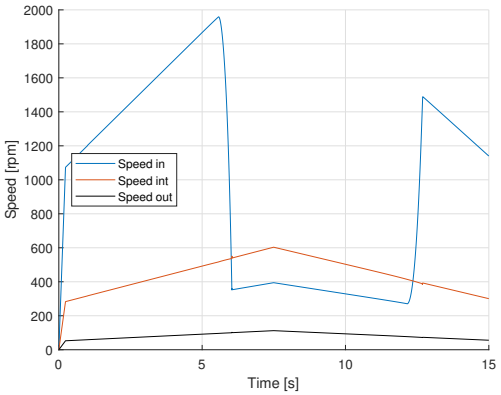

Figure E.91: Speeds of gearbox.
Load $= -1250[Nm]$.
Up-shift: $f = 1.40[s]$, $a = 5.50\,[1/s]$.
Down-shift: $f = 3.50[s]$, $a = 2.25\,[1/s]$.
Up-shift at $5[s]$. Down-shift at $10[s]$.

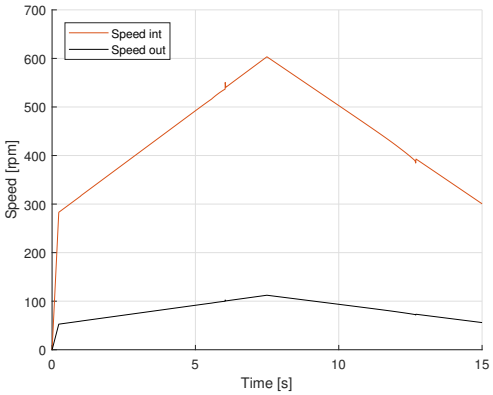

Figure E.92: Speeds of gearbox.
Load $= -1250[Nm]$.
Up-shift: $f = 1.40[s]$, $a = 5.50\,[1/s]$.
Down-shift: $f = 3.50[s]$, $a = 2.25\,[1/s]$.
Up-shift at $5[s]$. Down-shift at $10[s]$.

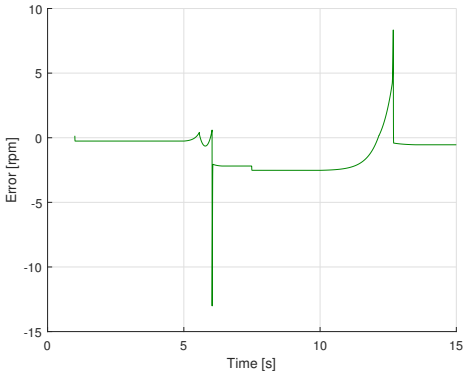

Figure E.93: Error of intermediate shaft velocity in relation to setpoint.
Load $= -1250[Nm]$.
Up-shift: $f = 1.40[s]$, $a = 5.50\,[1/s]$.
Down-shift: $f = 3.50[s]$, $a = 2.25\,[1/s]$.
Up-shift at $5[s]$. Down-shift at $10[s]$.

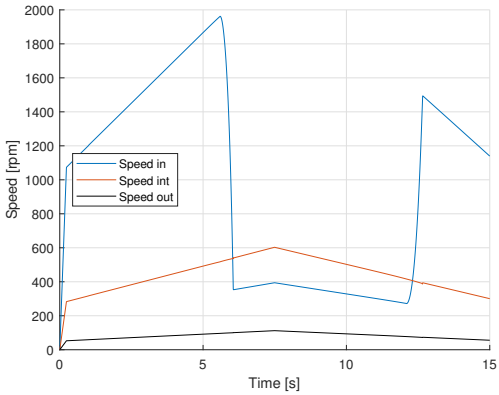

Figure E.94: Speeds of gearbox.
Load $= -1000[Nm]$.
Up-shift:$f = 1.40[s]$, $a = 5.50\,[1/s]$.
Down-shift:$f = 3.50[s]$, $a = 2.25\,[1/s]$.
Up-shift at $5[s]$. Down-shift at $10[s]$.

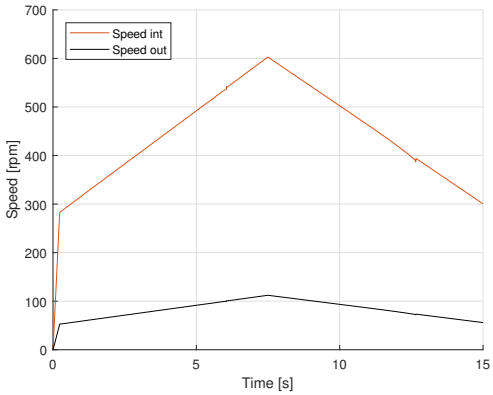

Figure E.95: Speeds of gearbox.
Load $= -1000[Nm]$.
Up-shift:$f = 1.40[s]$, $a = 5.50\,[1/s]$.
Down-shift:$f = 3.50[s]$, $a = 2.25\,[1/s]$.
Up-shift at $5[s]$. Down-shift at $10[s]$.

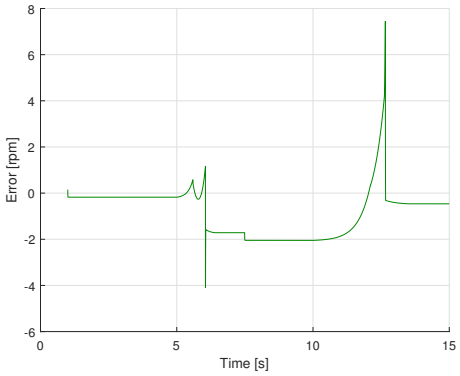

Figure E.96: Error of intermediate shaft velocity in relation to setpoint.
Load $= -1000[Nm]$.
Up-shift:$f = 1.40[s]$, $a = 5.50\,[1/s]$.
Down-shift:$f = 3.50[s]$, $a = 2.25\,[1/s]$.
Up-shift at $5[s]$. Down-shift at $10[s]$.

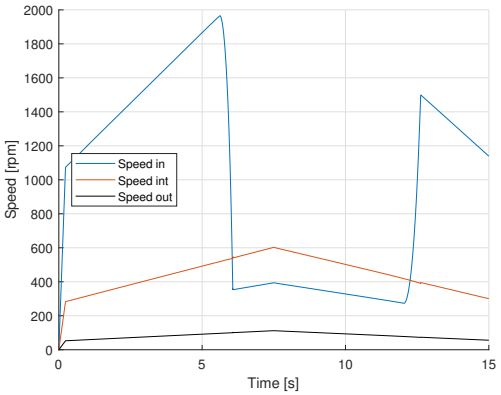

Figure E.97: Speeds of gearbox.
Load $= -750[Nm]$.
Up-shift:$f = 1.40[s]$, $a = 5.50\,[1/s]$.
Down-shift:$f = 3.50[s]$, $a = 2.25\,[1/s]$.
Up-shift at $5[s]$. Down-shift at $10[s]$.

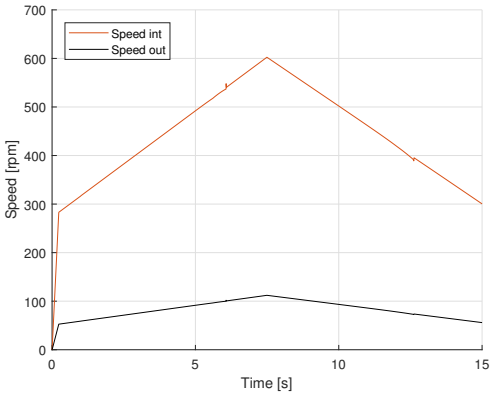

Figure E.98: Speeds of gearbox.
Load $= -750[Nm]$.
Up-shift:$f = 1.40[s]$, $a = 5.50\,[1/s]$.
Down-shift:$f = 3.50[s]$, $a = 2.25\,[1/s]$.
Up-shift at $5[s]$. Down-shift at $10[s]$.

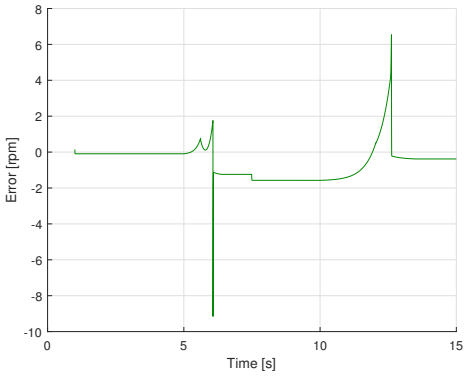

Figure E.99: Error of intermediate shaft velocity in relation to setpoint.
Load $= -750[Nm]$.
Up-shift:$f = 1.40[s]$, $a = 5.50\,[1/s]$.
Down-shift:$f = 3.50[s]$, $a = 2.25\,[1/s]$.
Up-shift at $5[s]$. Down-shift at $10[s]$.

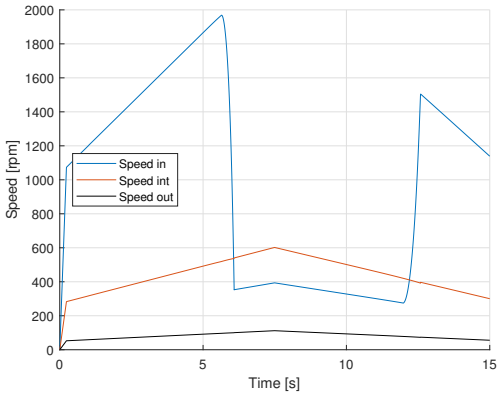

Figure E.100: Speeds of gearbox.
Load $= -500[Nm]$.
Up-shift:$f = 1.40[s]$, $a = 5.50\,[1/s]$.
Down-shift:$f = 3.50[s]$, $a = 2.25\,[1/s]$.
Up-shift at $5[s]$. Down-shift at $10[s]$.

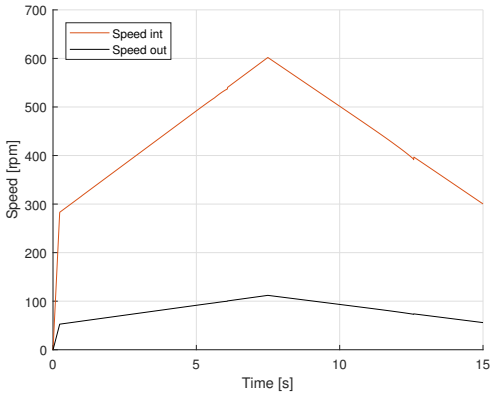

Figure E.101: Speeds of gearbox.
Load $= -500[Nm]$.
Up-shift:$f = 1.40[s]$, $a = 5.50\,[1/s]$.
Down-shift:$f = 3.50[s]$, $a = 2.25\,[1/s]$.
Up-shift at $5[s]$. Down-shift at $10[s]$.

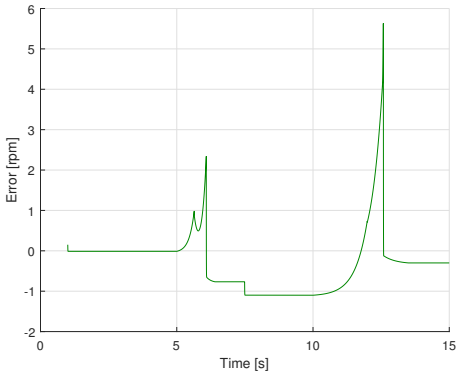

Figure E.102: Error of intermediate shaft velocity in relation to setpoint.
Load $= -500[Nm]$.
Up-shift:$f = 1.40[s]$, $a = 5.50\,[1/s]$.
Down-shift:$f = 3.50[s]$, $a = 2.25\,[1/s]$.
Up-shift at $5[s]$. Down-shift at $10[s]$.

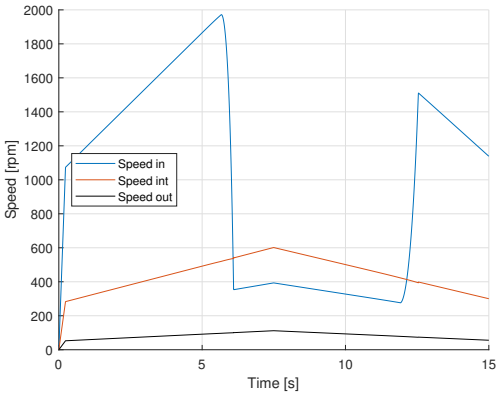

Figure E.103: Speeds of gearbox.
Load $= -250[Nm]$.
Up-shift: $f = 1.40[s]$, $a = 5.50\,[1/s]$.
Down-shift: $f = 3.50[s]$, $a = 2.25\,[1/s]$.
Up-shift at $5[s]$. Down-shift at $10[s]$.

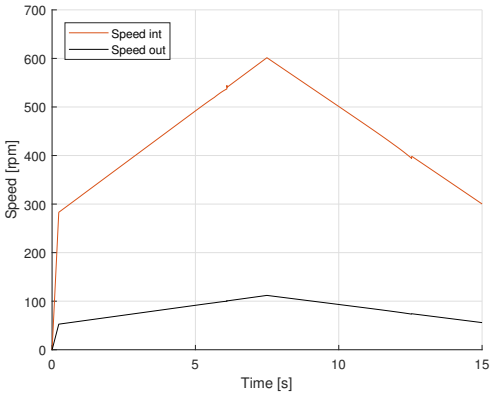

Figure E.104: Speeds of gearbox.
Load $= -250[Nm]$.
Up-shift: $f = 1.40[s]$, $a = 5.50\,[1/s]$.
Down-shift: $f = 3.50[s]$, $a = 2.25\,[1/s]$.
Up-shift at $5[s]$. Down-shift at $10[s]$.

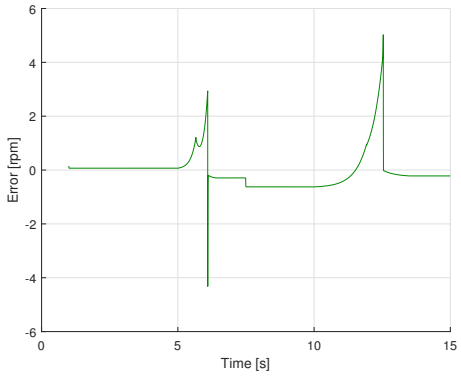

Figure E.105: Error of intermediate shaft velocity in relation to setpoint.
Load $= -250[Nm]$.
Up-shift: $f = 1.40[s]$, $a = 5.50\,[1/s]$.
Down-shift: $f = 3.50[s]$, $a = 2.25\,[1/s]$.
Up-shift at $5[s]$. Down-shift at $10[s]$.

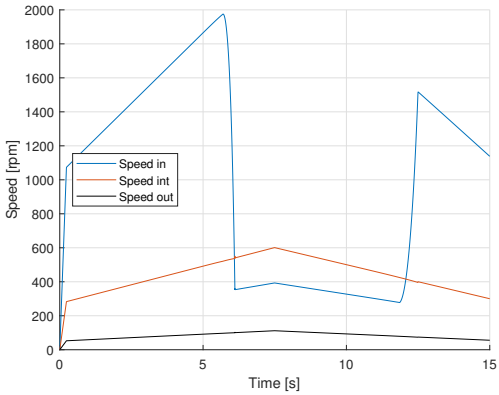

Figure E.106: Speeds of gearbox.
Load = $0[Nm]$.
Up-shift:$f = 1.40[s]$, $a = 5.50\,[1/s]$.
Down-shift:$f = 3.50[s]$, $a = 2.25\,[1/s]$.
Up-shift at $5[s]$. Down-shift at $10[s]$.

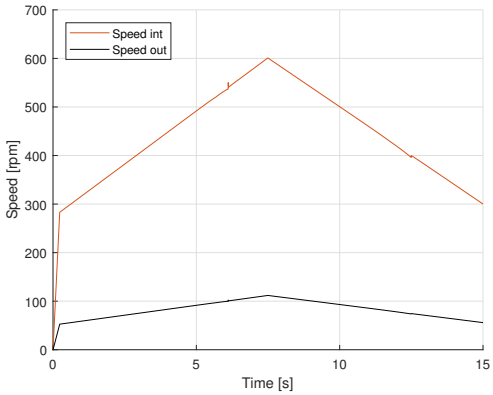

Figure E.107: Speeds of gearbox.
Load = $0[Nm]$.
Up-shift:$f = 1.40[s]$, $a = 5.50\,[1/s]$.
Down-shift:$f = 3.50[s]$, $a = 2.25\,[1/s]$.
Up-shift at $5[s]$. Down-shift at $10[s]$.

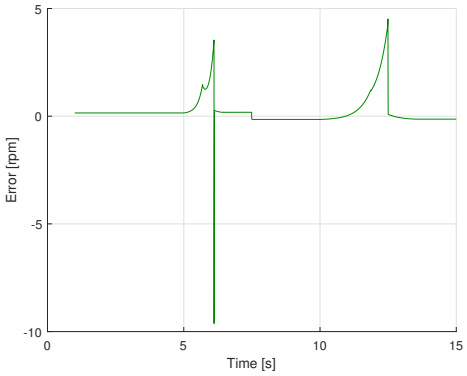

Figure E.108: Error of intermediate shaft velocity in relation to setpoint.
Load = $0[Nm]$.
Up-shift:$f = 1.40[s]$, $a = 5.50\,[1/s]$.
Down-shift:$f = 3.50[s]$, $a = 2.25\,[1/s]$.
Up-shift at $5[s]$. Down-shift at $10[s]$.

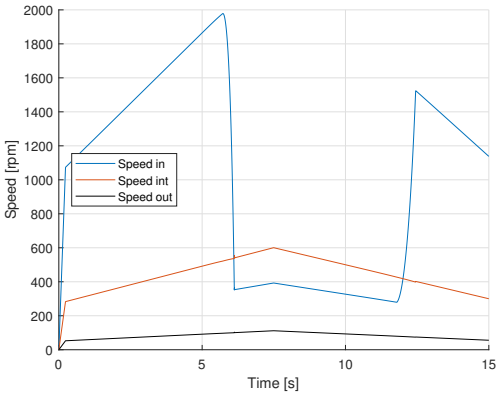

Figure E.109: Speeds of gearbox.
Load = 250[Nm].
Up-shift:$f = 1.40[s]$, $a = 5.50\,[1/s]$.
Down-shift:$f = 3.50[s]$, $a = 2.25\,[1/s]$.
Up-shift at 5[s]. Down-shift at 10[s].

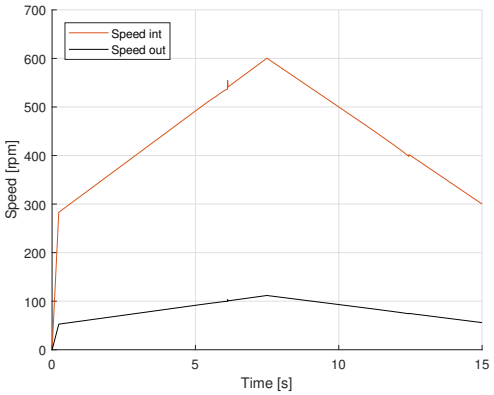

Figure E.110: Speeds of gearbox.
Load = 250[Nm].
Up-shift:$f = 1.40[s]$, $a = 5.50\,[1/s]$.
Down-shift:$f = 3.50[s]$, $a = 2.25\,[1/s]$.
Up-shift at 5[s]. Down-shift at 10[s].

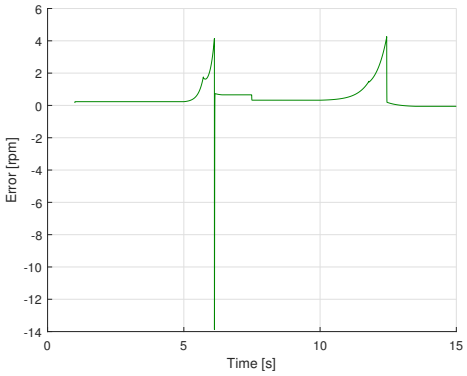

Figure E.111: Error of intermediate shaft velocity in relation to setpoint.
Load = 250[Nm].
Up-shift:$f = 1.40[s]$, $a = 5.50\,[1/s]$.
Down-shift:$f = 3.50[s]$, $a = 2.25\,[1/s]$.
Up-shift at 5[s]. Down-shift at 10[s].

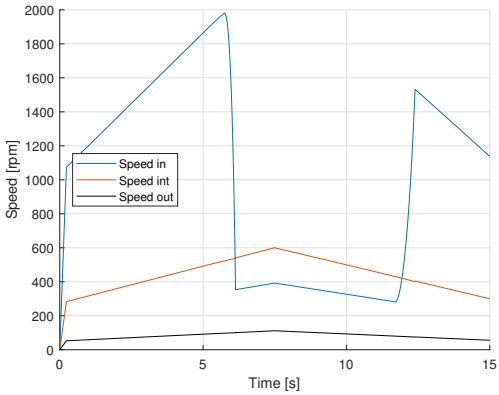

Figure E.112: Speeds of gearbox.
Load $= 500[Nm]$.
Up-shift:$f = 1.40[s]$, $a = 5.50\,[1/s]$.
Down-shift:$f = 3.50[s]$, $a = 2.25\,[1/s]$.
Up-shift at $5[s]$. Down-shift at $10[s]$.

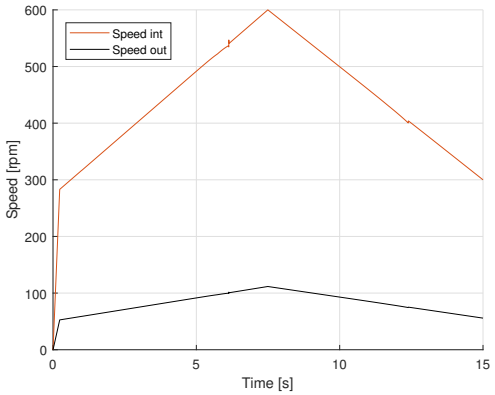

Figure E.113: Speeds of gearbox.
Load $= 500[Nm]$.
Up-shift:$f = 1.40[s]$, $a = 5.50\,[1/s]$.
Down-shift:$f = 3.50[s]$, $a = 2.25\,[1/s]$.
Up-shift at $5[s]$. Down-shift at $10[s]$.

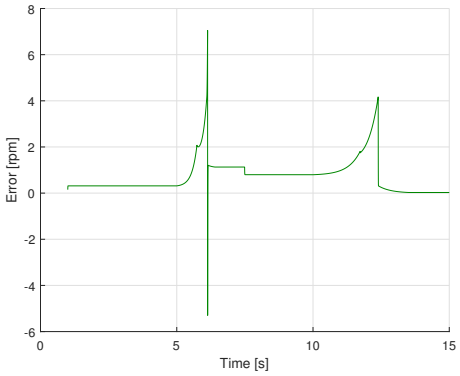

Figure E.114: Error of intermediate shaft velocity in relation to setpoint.
Load $= 500[Nm]$.
Up-shift:$f = 1.40[s]$, $a = 5.50\,[1/s]$.
Down-shift:$f = 3.50[s]$, $a = 2.25\,[1/s]$.
Up-shift at $5[s]$. Down-shift at $10[s]$.

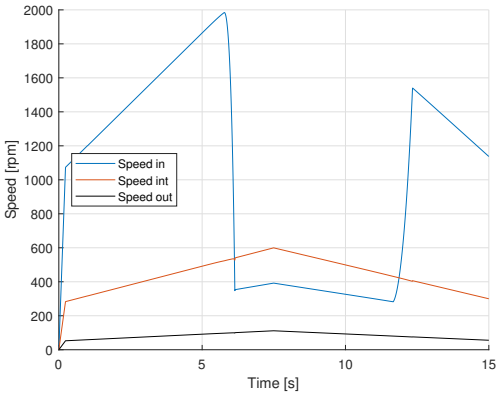

Figure E.115: Speeds of gearbox.
Load = 750[Nm].
Up-shift:$f = 1.40[s]$, $a = 5.50\,[1/s]$.
Down-shift:$f = 3.50[s]$, $a = 2.25\,[1/s]$.
Up-shift at 5[s]. Down-shift at 10[s].

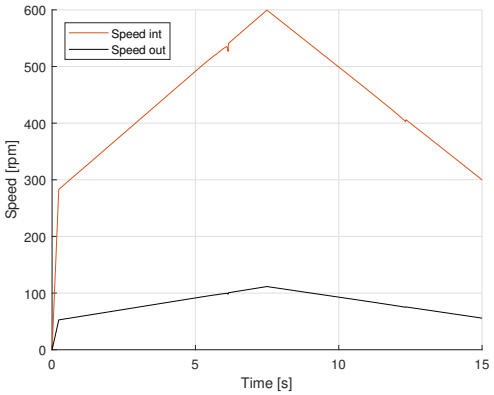

Figure E.116: Speeds of gearbox.
Load = 750[Nm].
Up-shift:$f = 1.40[s]$, $a = 5.50\,[1/s]$.
Down-shift:$f = 3.50[s]$, $a = 2.25\,[1/s]$.
Up-shift at 5[s]. Down-shift at 10[s].

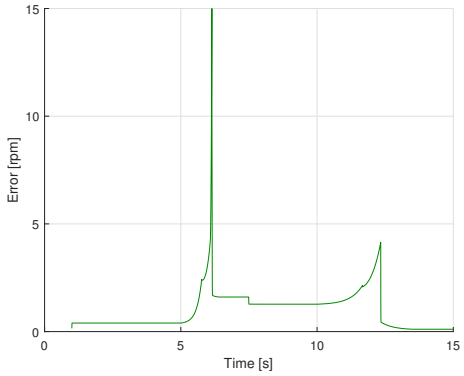

Figure E.117: Error of intermediate shaft velocity in relation to setpoint.
Load = 750[Nm].
Up-shift:$f = 1.40[s]$, $a = 5.50\,[1/s]$.
Down-shift:$f = 3.50[s]$, $a = 2.25\,[1/s]$.
Up-shift at 5[s]. Down-shift at 10[s].

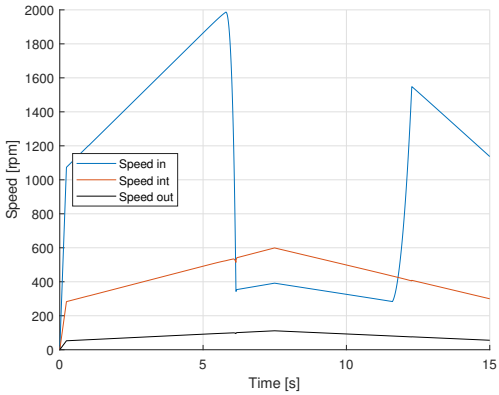

Figure E.118: Speeds of gearbox.
Load = 1000$[Nm]$.
Up-shift:$f = 1.40[s]$, $a = 5.50\,[1/s]$.
Down-shift:$f = 3.50[s]$, $a = 2.25\,[1/s]$.
Up-shift at 5$[s]$. Down-shift at 10$[s]$.

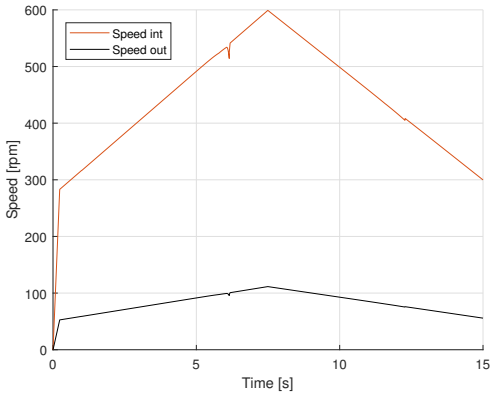

Figure E.119: Speeds of gearbox.
Load = 1000$[Nm]$.
Up-shift:$f = 1.40[s]$, $a = 5.50\,[1/s]$.
Down-shift:$f = 3.50[s]$, $a = 2.25\,[1/s]$.
Up-shift at 5$[s]$. Down-shift at 10$[s]$.

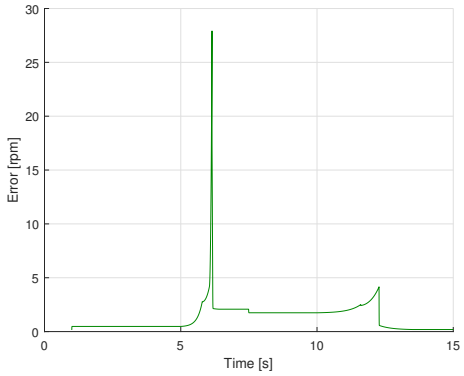

Figure E.120: Error of intermediate shaft velocity in relation to setpoint.
Load = 1000$[Nm]$.
Up-shift:$f = 1.40[s]$, $a = 5.50\,[1/s]$.
Down-shift:$f = 3.50[s]$, $a = 2.25\,[1/s]$.
Up-shift at 5$[s]$. Down-shift at 10$[s]$.

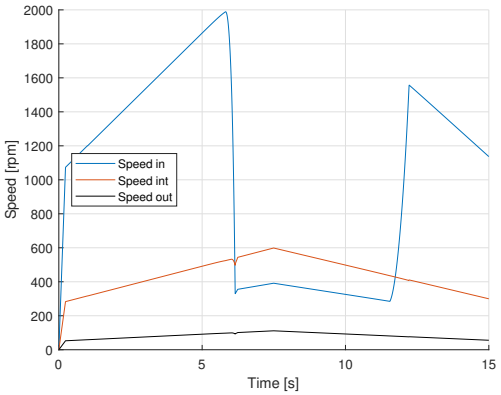

Figure E.121: Speeds of gearbox.
Load $= 1250[Nm]$.
Up-shift:$f = 1.40[s]$, $a = 5.50\,[1/s]$.
Down-shift:$f = 3.50[s]$, $a = 2.25\,[1/s]$.
Up-shift at $5[s]$. Down-shift at $10[s]$.

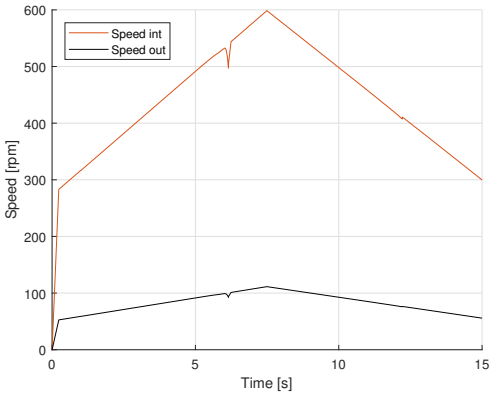

Figure E.122: Speeds of gearbox.
Load $= 1250[Nm]$.
Up-shift:$f = 1.40[s]$, $a = 5.50\,[1/s]$.
Down-shift:$f = 3.50[s]$, $a = 2.25\,[1/s]$.
Up-shift at $5[s]$. Down-shift at $10[s]$.

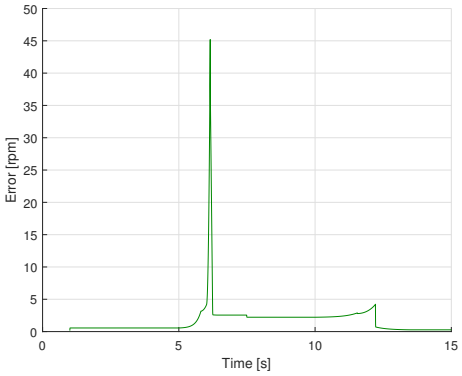

Figure E.123: Error of intermediate shaft velocity in relation to setpoint.
Load $= 1250[Nm]$.
Up-shift:$f = 1.40[s]$, $a = 5.50\,[1/s]$.
Down-shift:$f = 3.50[s]$, $a = 2.25\,[1/s]$.
Up-shift at $5[s]$. Down-shift at $10[s]$.

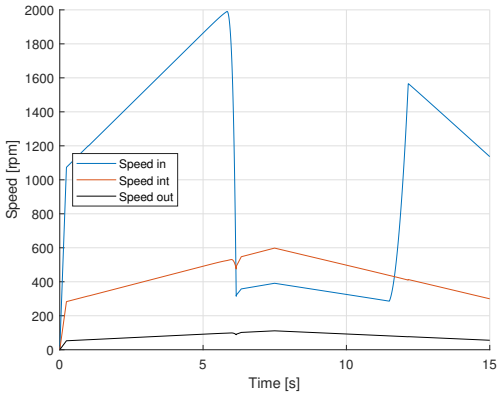

Figure E.124: Speeds of gearbox.
Load = 1500$[Nm]$.
Up-shift:$f = 1.40[s]$, $a = 5.50\,[1/s]$.
Down-shift:$f = 3.50[s]$, $a = 2.25\,[1/s]$.
Up-shift at 5$[s]$. Down-shift at 10$[s]$.

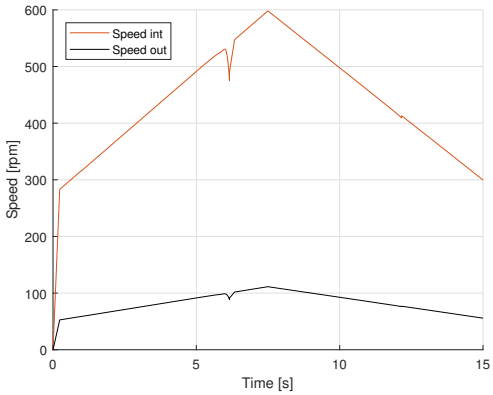

Figure E.125: Speeds of gearbox.
Load = 1500$[Nm]$.
Up-shift:$f = 1.40[s]$, $a = 5.50\,[1/s]$.
Down-shift:$f = 3.50[s]$, $a = 2.25\,[1/s]$.
Up-shift at 5$[s]$. Down-shift at 10$[s]$.

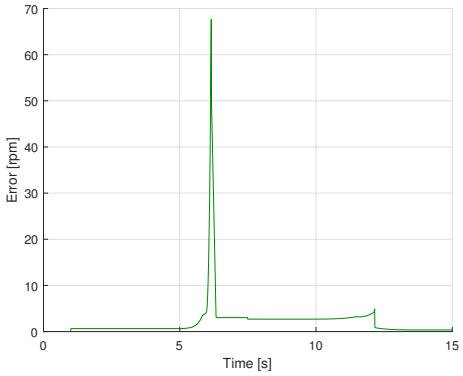

Figure E.126: Error of intermediate shaft velocity in relation to setpoint.
Load = 1500$[Nm]$.
Up-shift:$f = 1.40[s]$, $a = 5.50\,[1/s]$.
Down-shift:$f = 3.50[s]$, $a = 2.25\,[1/s]$.
Up-shift at 5$[s]$. Down-shift at 10$[s]$.

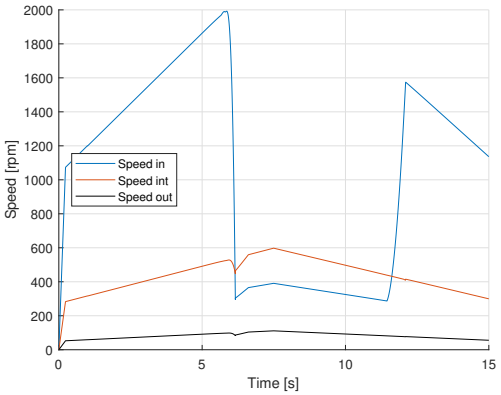

Figure E.127: Speeds of gearbox.
Load = 1750$[Nm]$.
Up-shift:$f = 1.40[s]$, $a = 5.50\,[1/s]$.
Down-shift:$f = 3.50[s]$, $a = 2.25\,[1/s]$.
Up-shift at 5$[s]$. Down-shift at 10$[s]$.

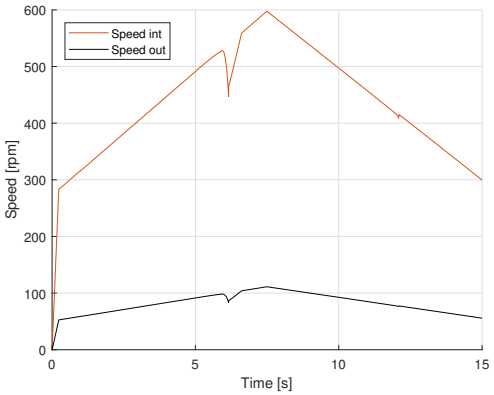

Figure E.128: Speeds of gearbox.
Load = 1750$[Nm]$.
Up-shift:$f = 1.40[s]$, $a = 5.50\,[1/s]$.
Down-shift:$f = 3.50[s]$, $a = 2.25\,[1/s]$.
Up-shift at 5$[s]$. Down-shift at 10$[s]$.

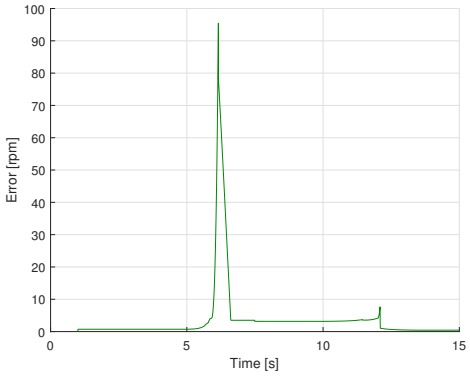

Figure E.129: Error of intermediate shaft velocity in relation to setpoint.
Load = 1750$[Nm]$.
Up-shift:$f = 1.40[s]$, $a = 5.50\,[1/s]$.
Down-shift:$f = 3.50[s]$, $a = 2.25\,[1/s]$.
Up-shift at 5$[s]$. Down-shift at 10$[s]$.

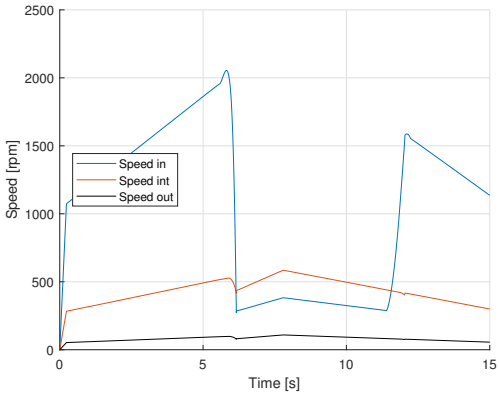

Figure E.130: Speeds of gearbox.
Load = 2000$[Nm]$.
Up-shift:$f = 1.40[s]$, $a = 5.50\,[1/s]$.
Down-shift:$f = 3.50[s]$, $a = 2.25\,[1/s]$.
Up-shift at $5[s]$. Down-shift at $10[s]$.

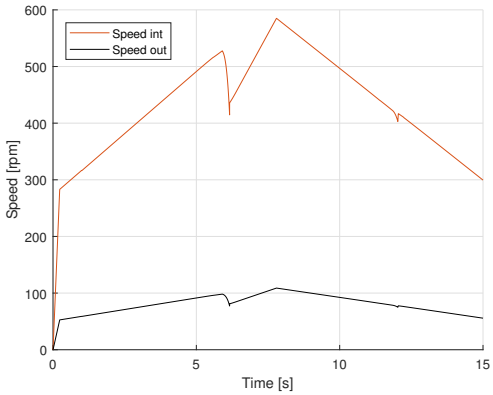

Figure E.131: Speeds of gearbox.
Load = 2000$[Nm]$.
Up-shift:$f = 1.40[s]$, $a = 5.50\,[1/s]$.
Down-shift:$f = 3.50[s]$, $a = 2.25\,[1/s]$.
Up-shift at $5[s]$. Down-shift at $10[s]$.

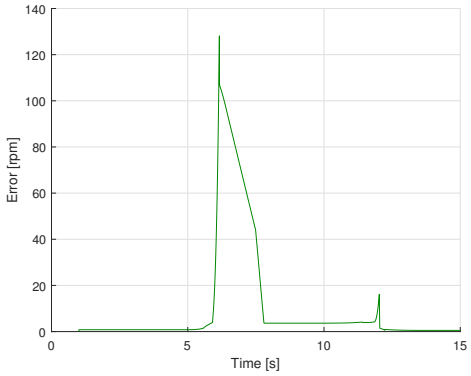

Figure E.132: Error of intermediate shaft velocity in relation to setpoint.
Load = 2000$[Nm]$.
Up-shift:$f = 1.40[s]$, $a = 5.50\,[1/s]$.
Down-shift:$f = 3.50[s]$, $a = 2.25\,[1/s]$.
Up-shift at $5[s]$. Down-shift at $10[s]$.

Appendix F:
Gearbox Assembly Guide

The gearbox is designed in such a way that it can be assembled by lowering all the parts into it from one side, while providing the ability to access the brakes from ether side without having to disassemble the whole gearbox. Given the size and complexity of the gearbox, some parts have to be assembled separately before they are put into the gearbox.

Following is the assembly guide for the gearbox, where the text is organized to the order of assembly.

F.1 Actuated Carrier 1

Figure F.1 shows the carrier 1 assembly.

Carrier 1 (1) is the input to the actuated step of the gearbox. *Carrier 1* (1) has four *planets* (6) attached to it, where only two are shown in the figure, for readability.

The *planets* (6) are supported by two *roller-bearings* [SKF K 15x21x21] (8). The *bearings* (8) are placed inside the *planet* (6) with a *spacer* (7) between them, so that the *bearings* (8) are located at either end of the *planet* (6).

Trust-washers (3) are installed between the *planet gear* (6) and the carrier (1) giving a sacrificial part to take any axial forces. The *planet* (6), with *bearings* (8) inside, is mounted to the *carrier* (1) with a *shaft* (2) that is secured in place with a *bolt* (not shown) that goes into a threaded hole on the *shaft* (2).

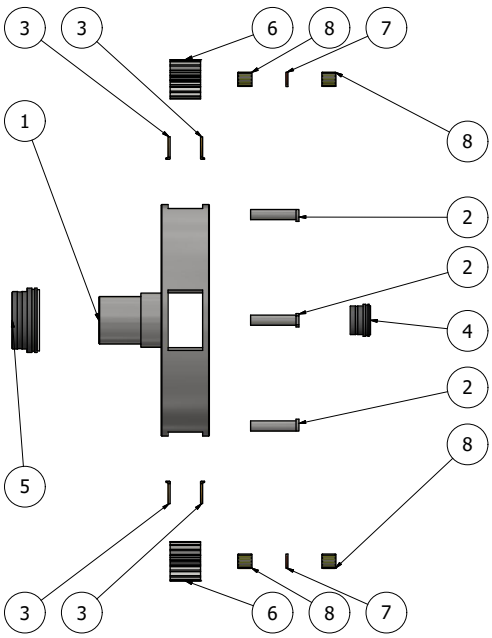

Figure F.1: Carrier 1 assembly.

The *carrier* (1) is supported by two roller/trust-bearings. The external *bearing* [SKF NKX 70] (5) is mounted against a machined edge on the *carrier's* (1) outer surface of the input shaft on the left-hand side of the figure. The internal *bearing* [SKF NKX 30] (4) is pressed into place against a machined edge on the *carrier's* (1) inner surface on the right-hand side in the figure.

F.2 Actuated Carrier 2

Figure F.2 shows the carrier 2 assembly.

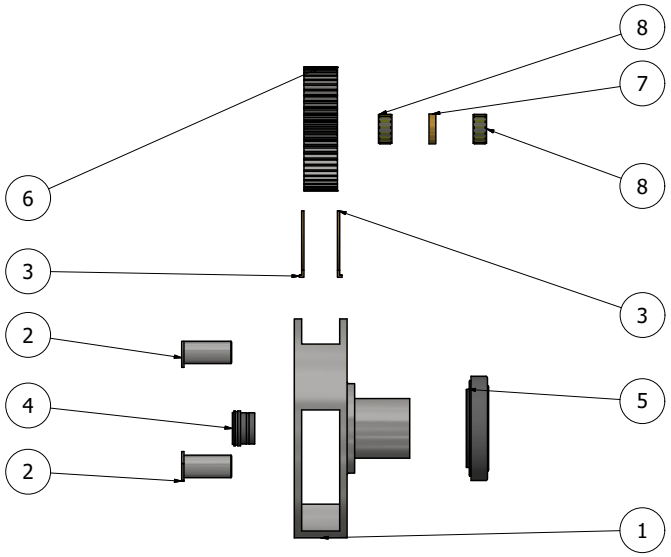

Figure F.2: Carrier 2 assembly.

Carrier 2 (1) is the output of the actuated part of the gearbox. The carrier has three *planets* (6) attached to it, where one *planet* (6) is shown in the figure due to readability.

The *planets* (6) are supported by two *roller-bearings* [SKF K 30x40x18] (8). The *bearings* (8) are placed inside the *planet* (6) with a *spacer* (7) between them, so that the *bearings* (8) are located at either end of the *planet* (6).

Trust-washers (3) are installed between the *planet* (6) and the carrier (1) giving a sacrificial part to take any axial forces. The *planet* (6), with *bearings* (8) inside, is mounted to the *carrier* (1) with a *shaft* (2) that is secured in place with a *bolt* (not shown) that goes into a threaded hole on the *shaft* (2).

The *carrier* (1) is supported by two roller/trust-bearings. The external *bearing* [SKF 30216] (5) is mounted against a machined edge on the *carrier's* (1) outer surface of the output shaft on the right-hand side of the figure. While the internal *bearing* [SKF NKX 30] (4) is pressed into place against a machined edge on the *carrier's* (1) inner surface on the left-hand side in the figure.

F.3 Actuated Ring

Figure F.3 shows the assembly of the actuated ring.

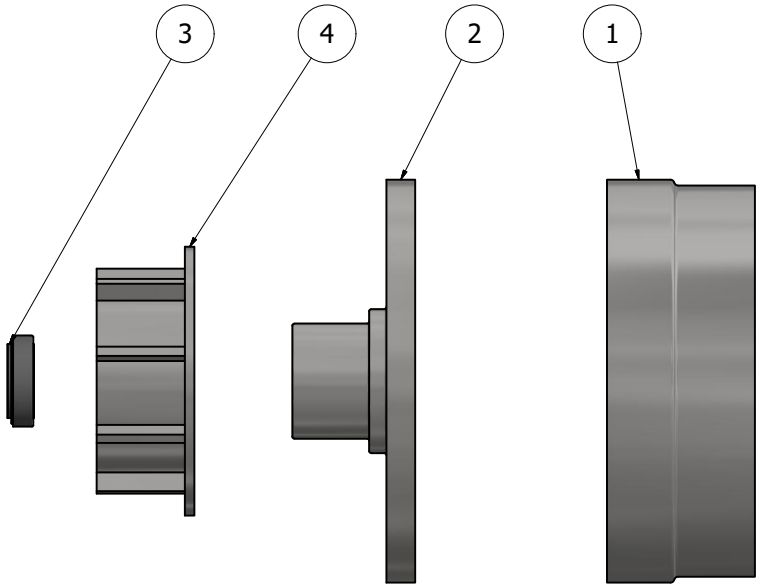

Figure F.3: Actuated ring gear assembly.

The ring-gear assembly for the actuated part consist of four parts. The *ring-gear* (1) is bolted to the *mounting plate* (2) with *bolts* (not shown). The *hub* (4) for the brake discs are bolted to the *mounting plate* (2) with *bolts* (not shown) and a tapered *roller-bearing* [SKF 33012] (3) is pressed into a hole on the *mounting plate* (2).

F.4 Fixed Step Carrier

Figure F.4 shows the fixed step carrier assembly.

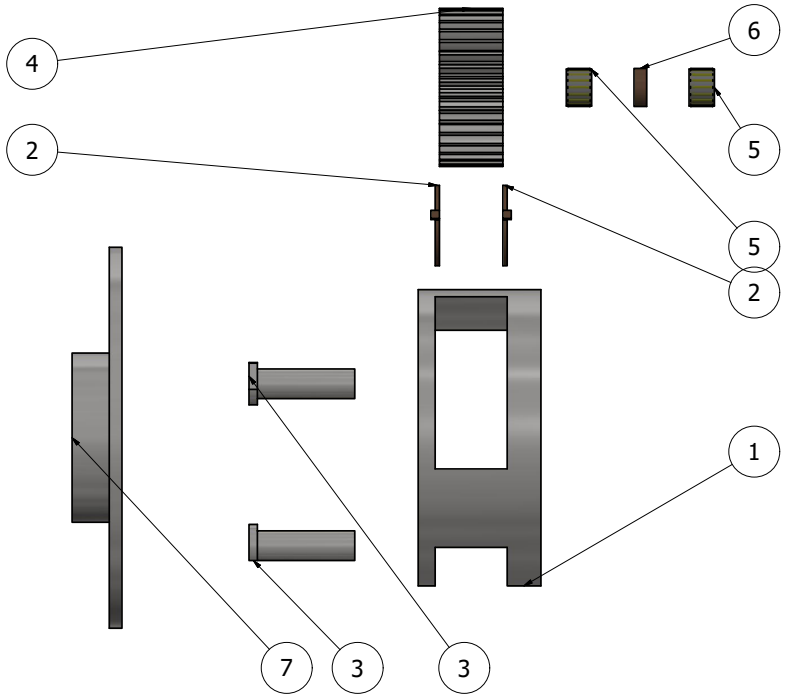

Figure F.4: Fixed step carrier assembly.

There are three *planets* (4) in the fixed step carrier assembly, where only one is shown in the figure due to readability.

The *planets* (4) are supported by two *roller-bearings* [SKF K 35x45x30] (5). The *bearings* (5) are placed inside the *gear* (4) with a *spacer* (6) between them, so that the bearings are located at either end of the gear.

Trust-washers (2) are installed between the *planet* (4) and the carrier (1) giving a sacrificial part to take any axial forces. The *planet* (4), with *bearings* (5) inside, is mounted to the *carrier* (1) with a *shaft* (3) that is secured in place with a *bolt* (not shown) that goes into a threaded hole on the *shaft* (2).

After the carrier is assembled, it is fixed to the *end-cover* (7) with bolts (not shown).

F.5 Complete Gearbox

Figure F.5 shows the final assembly of the gearbox.

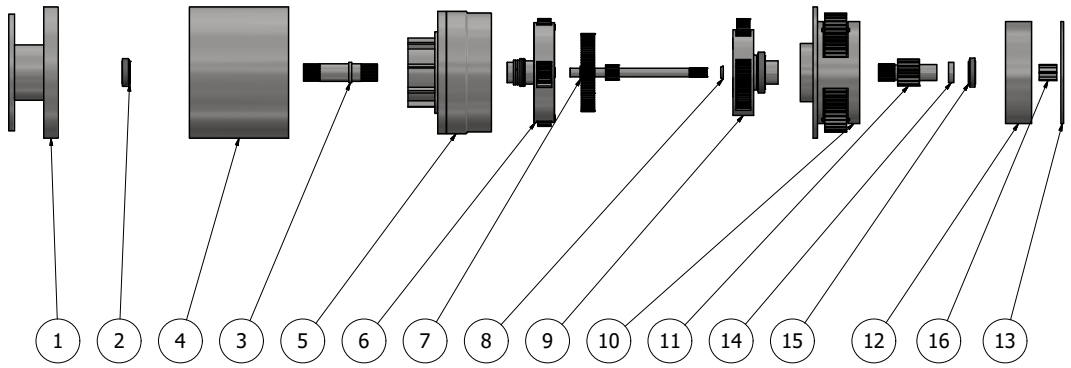

Figure F.5: Final gearbox assembly.

The gearbox is assembled from left to right. A *bearing* [SKF 33012] (2) is pressed into the *housing end cover* (1). The *housing for the actuated part* (4) is then bolted to the *end cover* (1). The *input shaft* (3) is placed in the*bearing* (2).

The *actuated ring assembly* (5) is lowered onto the *input-shaft* (3), and *carrier 1* (6) is lowered into the *ring assembly* (5). The *sun-shaft* (7) with gears are placed in the *bearing* [SKF NXK 30] inside *carrier 1* (6) and the *spacer* (8) that sets the distance between the second sun-gear and *carrier 2* (8) is placed on the *sun-shaft* (7), then *carrier 2* (9) is lowered onto the *sun-shaft* (8). The actuated part of the gearbox is sealed when the *fixed-step carrier assembly* (10) is bolted onto the *housing*. In order to pre-tension the bearings in the gearbox, a *specialized spring* (not shown) must be placed between the bearing on *carrier 2* and the *fixed-step carrier assembly* (10).

The hollow *fixed sun-gear* (11) is connected by a spline to *carrier 2* and a *spacer* (14), is placed on the *fixed sun-gear's* shaft (11). A *bearing* [SKF 30211] (15) is then placed on the *fixed sun-gear's* shaft. To pre-tension the *bearing* (15), a *specialized spring* (not shown) is placed between the *bearing* (15) and the *sun-brake housing* (12). The *hub* (16) for the brakes on the *sun-shaft* (7) is connected by a spline on to the *sun-shaft* (7) and secured in place with a *bolt* (not shown). The *sun-brake cover* (13) is bolted on to complete the gearbox.

F.5.1 Brakes

The brakes, and actuators for the ring-brake can be installed to the *end-cover* (1) prior to installation. Otherwise, the *end-cover* (1) may be removed at any time to mount the brake and actuator system.

The sun-brake with its actuators is mounted to the *sun-brake cover* (13). The installation of the sun-brake may be performed prior, during, or after the full assembly, as with the ring-brake.

Appendix G:
Mechanical Drawings

PARTS LIST			
ITEM	QTY	PART NUMBER	DESCRIPTION
1	1	Housing Endcover	
2	1	33012	BT1_001_101-Tapered roller bearings, single row. Internal
3	1	Input shaft	Internal.
4	1	Housing Actuated	Internal.
5	1	Ring Actuated Assembly	Internal.
6	1	Carrier1 Actuated Assembly	Internal.
7	1	Sun Shaft	Internal.
8	1	Spacer Sun Shaft	Internal.
9	1	Carrier2 Actuated Assembly	Internal.
10	1	Fixed Step Assembly	
11	1	Sun Fixed	Internal.
12	1	Sunbrake Housing	
13	1	Sunbrake Cover	
14	1	Fixed Sun Spacer	Internal.
15	1	30211	BT1_001_101-Tapered roller bearings, single row. Internal.
16	1	Sunbrake Hub	Internal

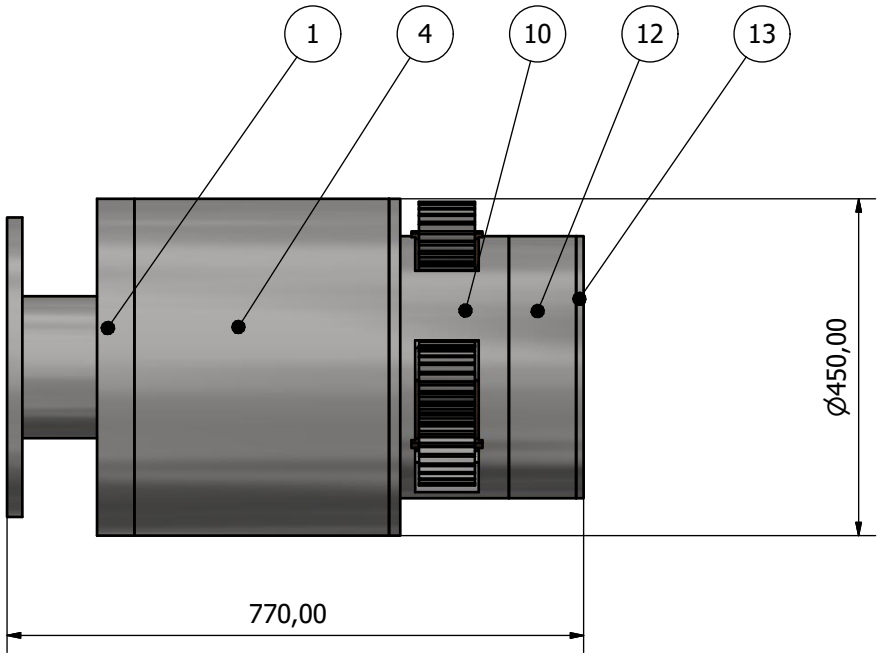

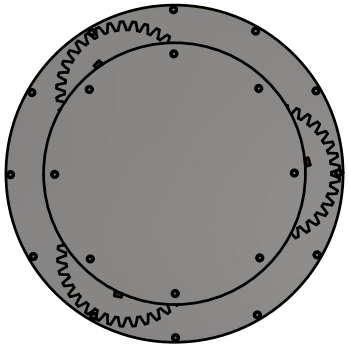

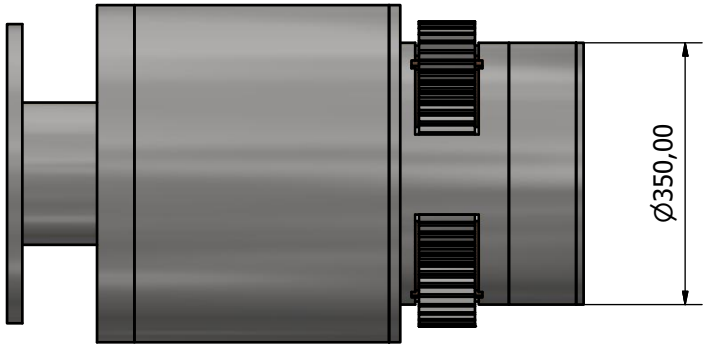

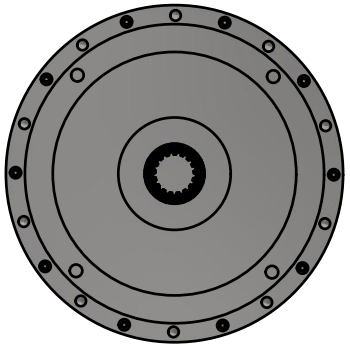

A3-Scale (0.14 : 1)

Designed by: Strandene and Tørnby	Approved by	Date		Date: 21.03.2018	
University of Agder	Gearbox				
	Gearbox		Edition: 1	Sheet: 1 / 1	

PARTS LIST		
ITEM	QTY	PART NUMBER
1	1	Planet Carrier Fixed
2	6	Bushing Planet Fixed
3	3	Planet Shaft Fixed
4	3	Planet Fixed w/Bearings
5	1	Housing Endcover Actuated

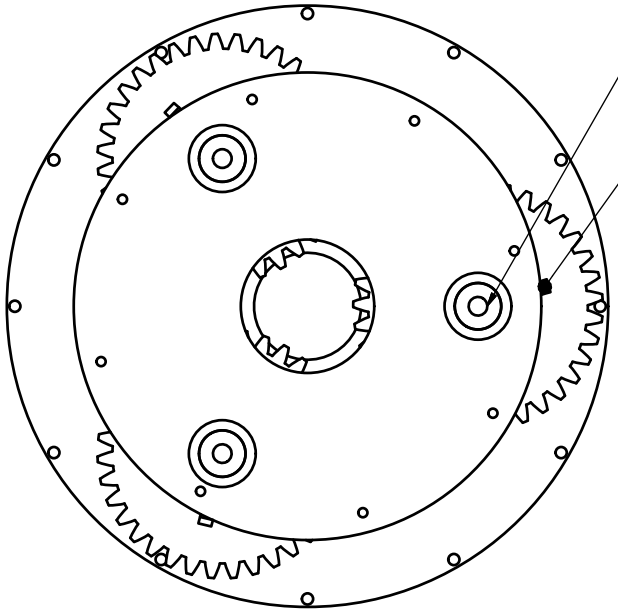

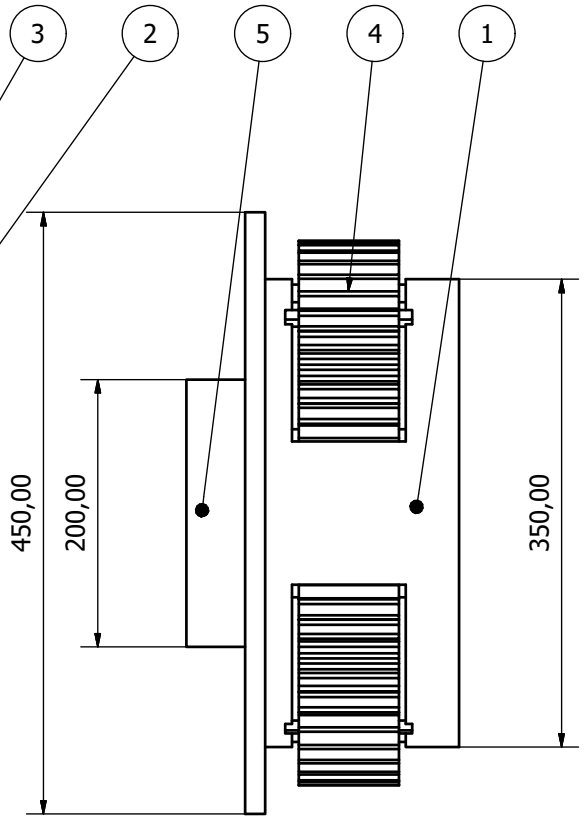

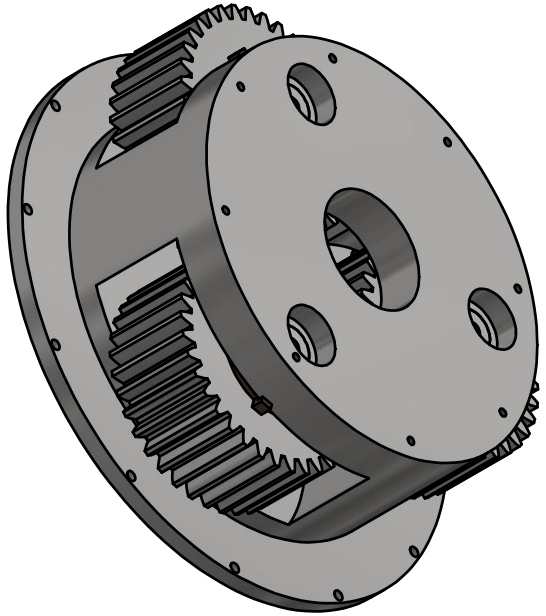

A3-Scale (1 : 4)

Designed by: Strandene and Tørby	Approved by	Date		Date: 21.03.2018	
University of Agder	Gearbox				
	Fixed Step		Edition	Sheet: 1 / 1	

PARTS LIST			
ITEM	QTY	PART NUMBER	DESCRIPTION
1	1	Ring Gear	
2	1	Ring Drum	
3	1	33012	BT1_001_101-Tapered roller bearings, single row. Internal
4	1	Ringbrake Inner	

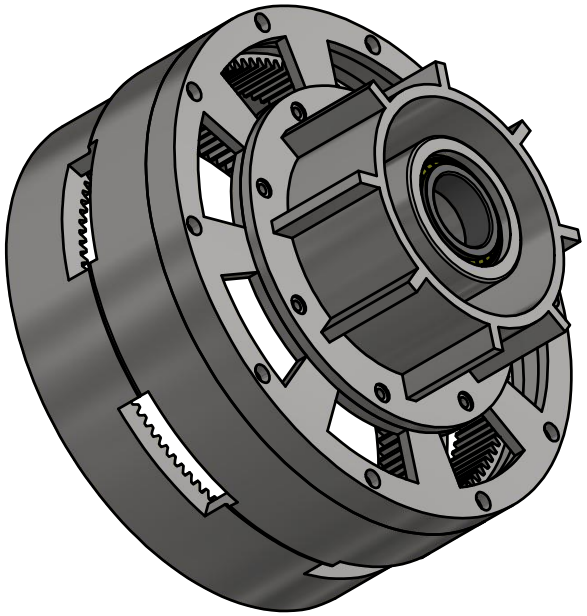

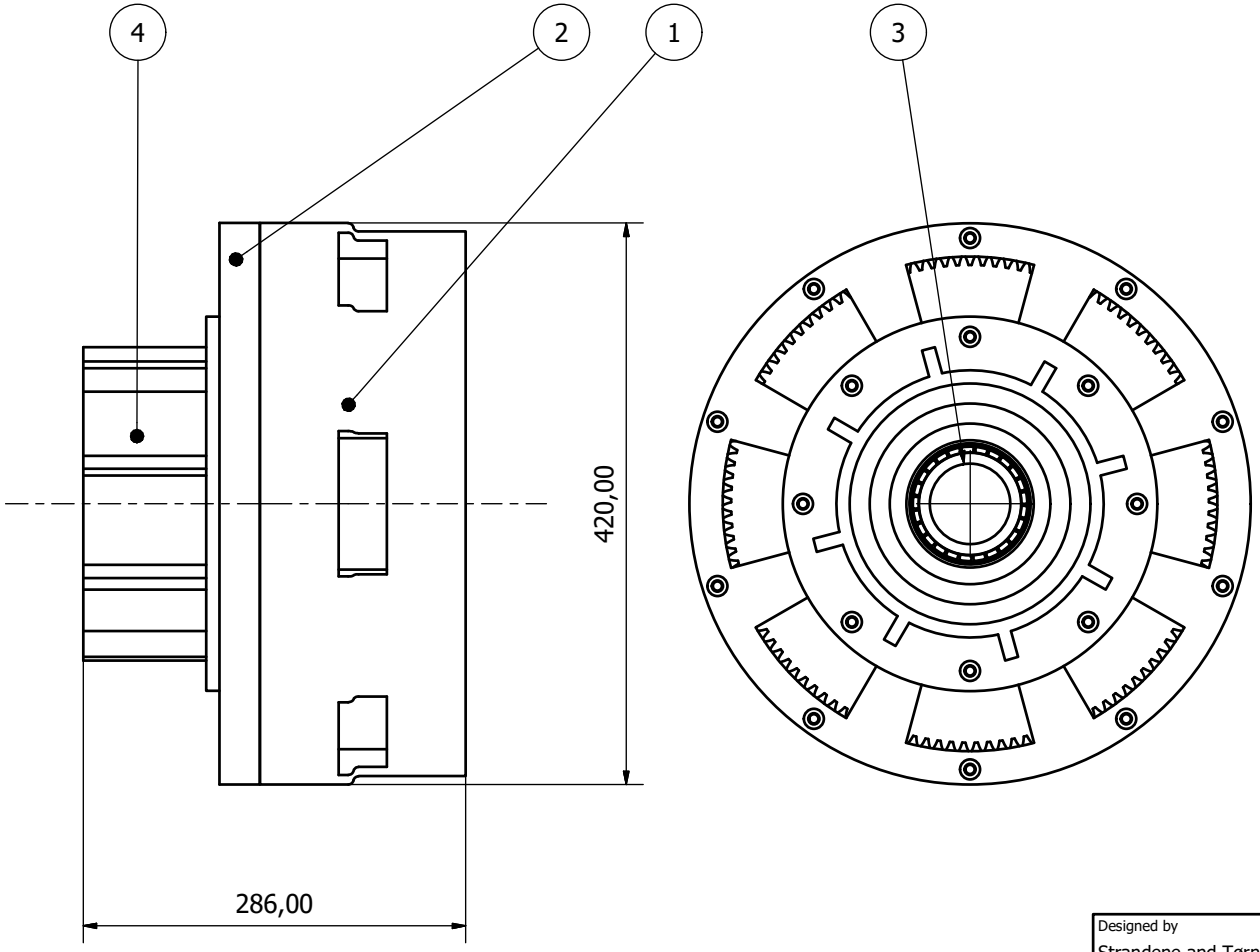

A3-Scale (1 : 4)

Designed by: Strandene and Tørnby	Approved by	Date		Date: 21.03.2018	
University of Agder	Gearbox				
	Ring Actuated Assembly		Edition	Sheet: 1 / 1	

PARTS LIST			
ITEM	QTY	PART NUMBER	DESCRIPTION
1	1	Gear Planet1 Actuated	
2	1	Bushing Planet1	
3	2	K 15x21x21	BN1_001-Needle roller and cage assemblies

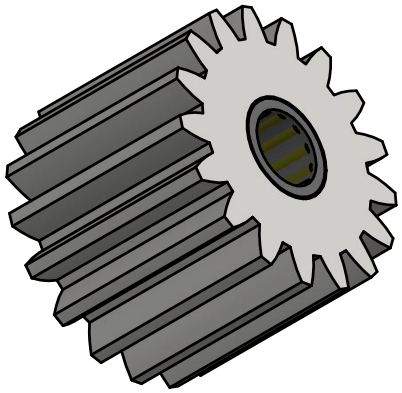

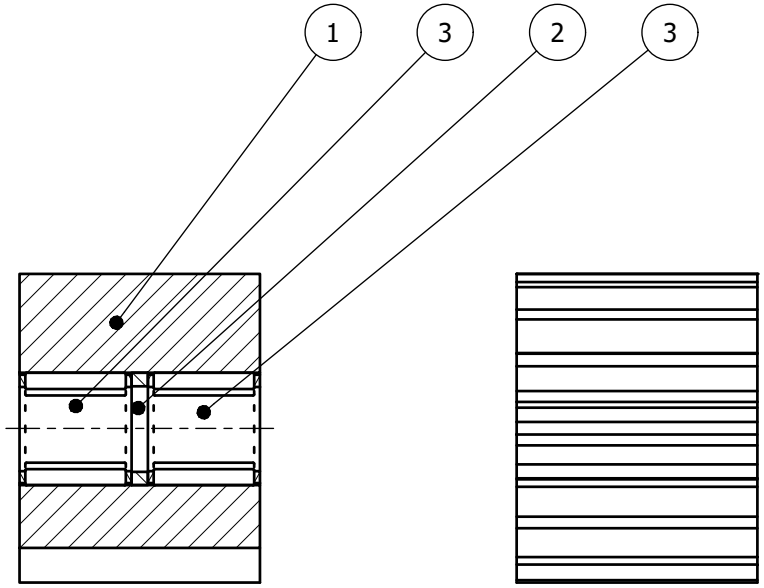

A-A (1 : 1)

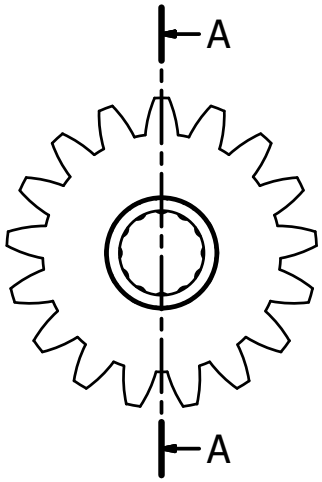

A3-Scale (1 : 1)

Designed by: Strandene and Tørnby	Approved by	Date		Date: 21.03.2018	
University of Agder	Gearbox				
	Planet1 Actuated w/Bearings		Edition	Sheet: 1 / 1	

PARTS LIST			
ITEM	QTY	PART NUMBER	DESCRIPTION
1	1	Planet2 Gear Actuated	
2	1	Bushing Planet 2	
3	2	K 30x40x18	BN1_001-Needle roller and cage assemblies

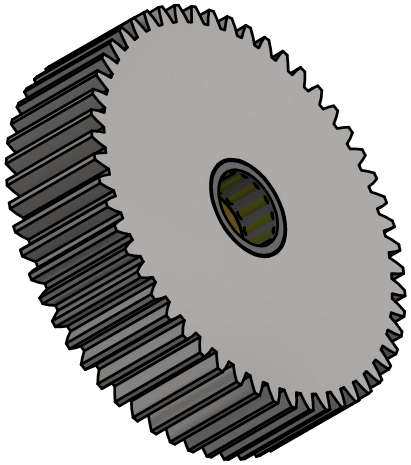

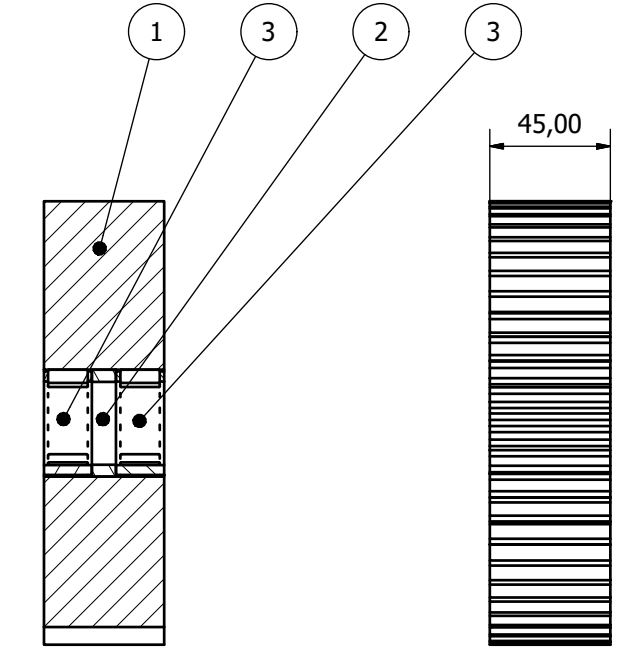

A-A (1 : 2)

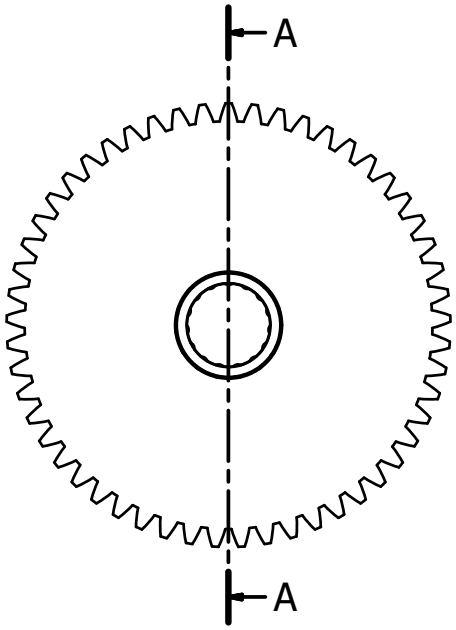

A3-Scale (1 : 2)

Designed by	Approved by	Date		Date	
Strandene and Tørnby				21.03.2018	

University of Agder	Gearbox		
	Planet2 Actuated Assembly	Edition	Sheet 1 / 1

PARTS LIST			
ITEM	QTY	PART NUMBER	DESCRIPTION
1	1	Planet Fixed Step	
2	2	K 35x45x30	BN1_001-Needle roller and cage assemblies
3	1	Bushing_planet_fixed_45	

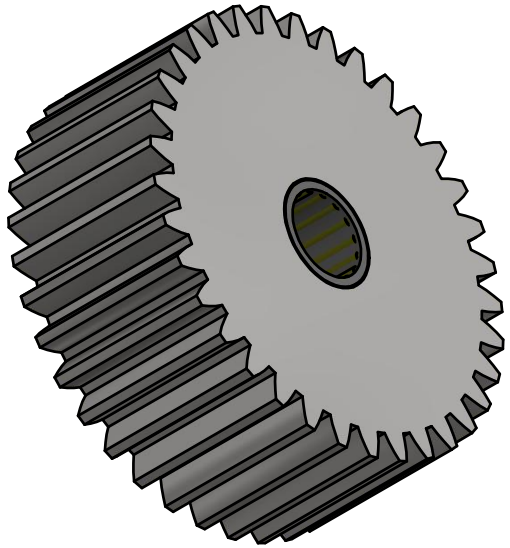

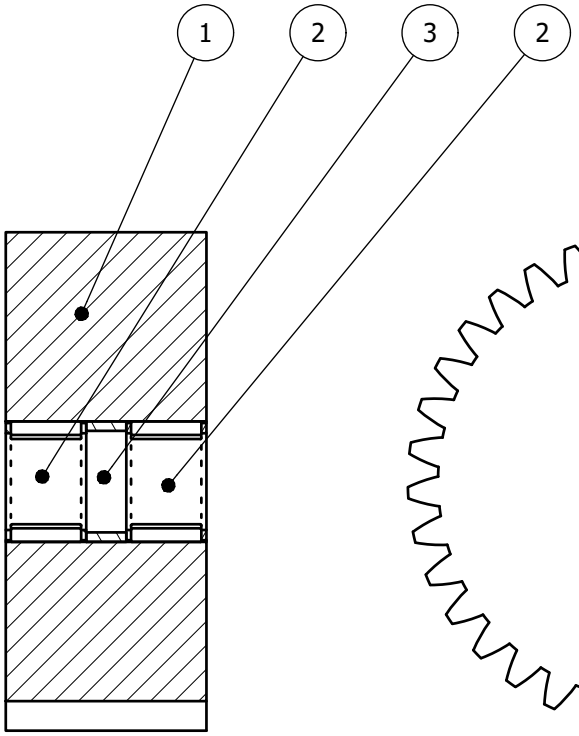

A-A (1 : 2)

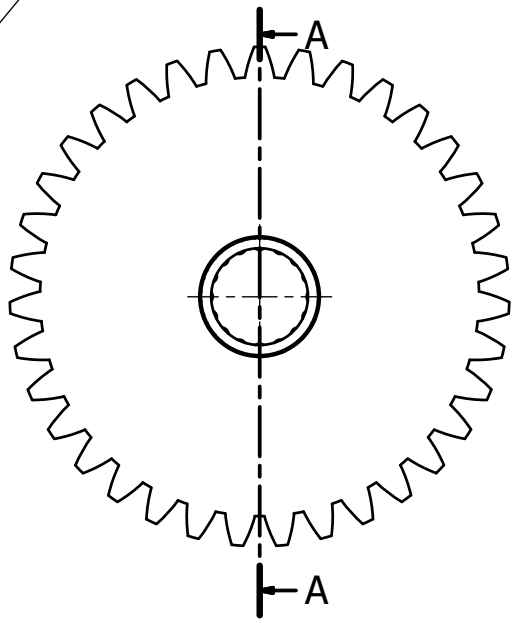

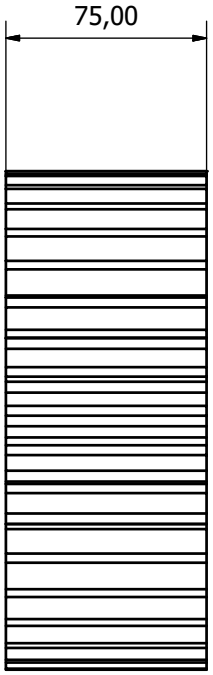

A3-Scale (1 : 2)

Designed by	Approved by	Date		Date	
Strandene and Tørnby				21.03.2018	

University of Agder	Gearbox		
	Planet Fixed w/bearings	Edition	Sheet 1 / 1

PARTS LIST			
ITEM	QTY	PART NUMBER	DESCRIPTION
1	1	Carrier1 Actuated	
2	4	Planet Gearbolt Actuated	
3	8	Bushing Planet1 End	
4	1	NKX 30	BVN_002_003-thrust rolling bearings
5	1	NKX 70	BVN_002_003-thrust rolling bearings
6	4	Planet1 Actuated w/Bearings	

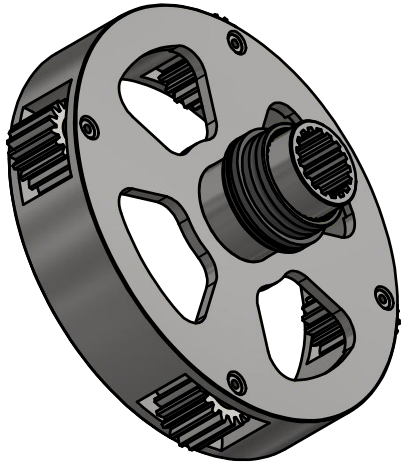

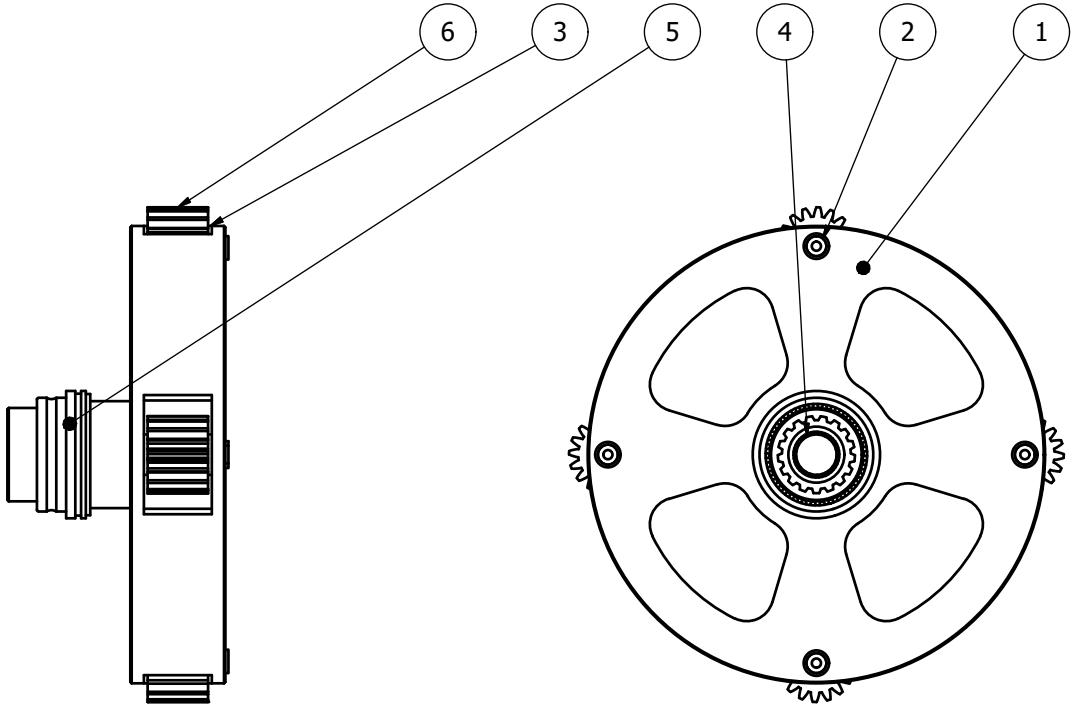

A3-Scale (1 : 4)

Designed by	Approved by	Date		Date	
Strandene and Tørnby				22.03.2018	

University of Agder	Gearbox		
	Carrier1 Actuated Assembly	Edition	Sheet 1 / 1

PARTS LIST			
ITEM	QTY	PART NUMBER	DESCRIPTION
1	1	Carrier2 Actuated	
2	3	Planet Actuated 2 gearbolt	
3	6	Bushing Planet2 End	
4	1	NKX 30	BVN_002_003-thrust rolling bearings
5	1	30216	BT1_001_101-Tapered roller bearings, single row
6	3	Planet2 Actuated w/bearing	

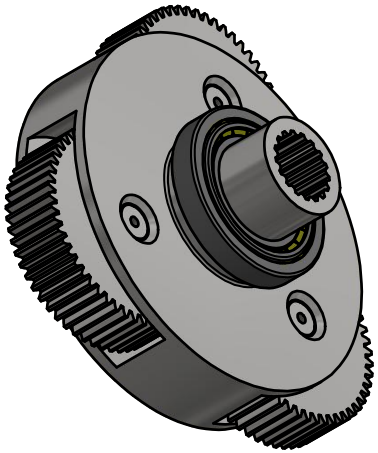

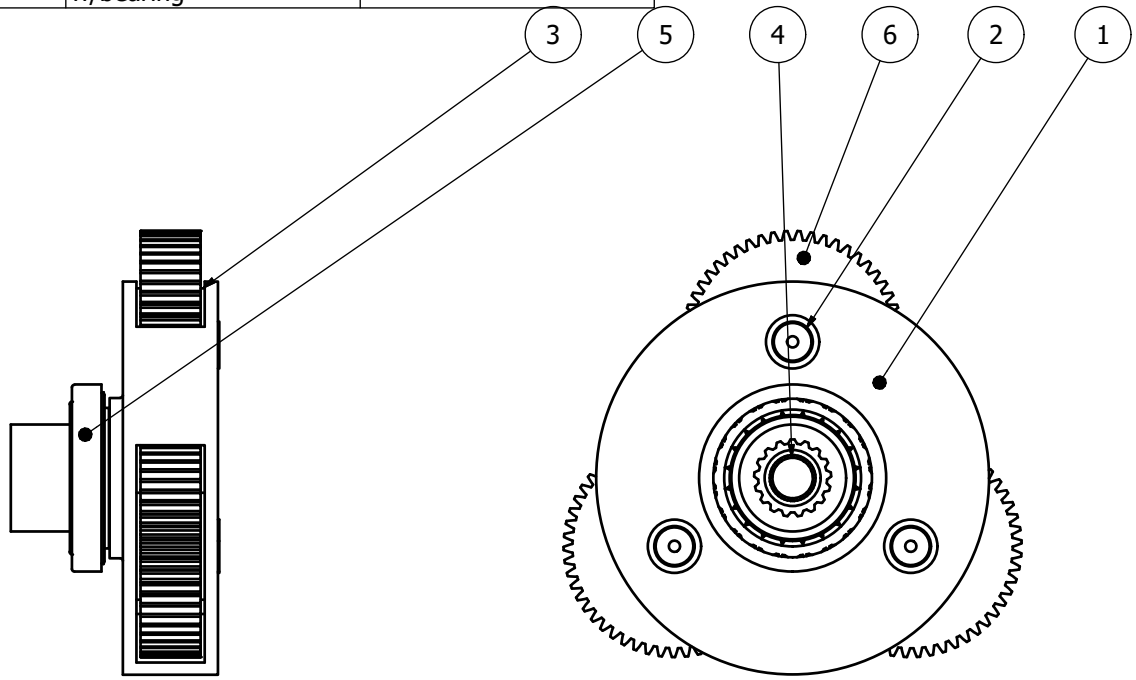

A3-Scale (1 : 4)

Designed by: Strandene and Tørnby	Approved by	Date		Date: 22.03.2018	
University of Agder	Gearbox				
	Carrier2 Actuated Assembly		Edition	Sheet: 1 / 1	

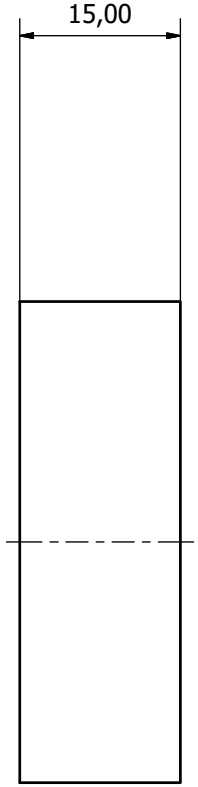

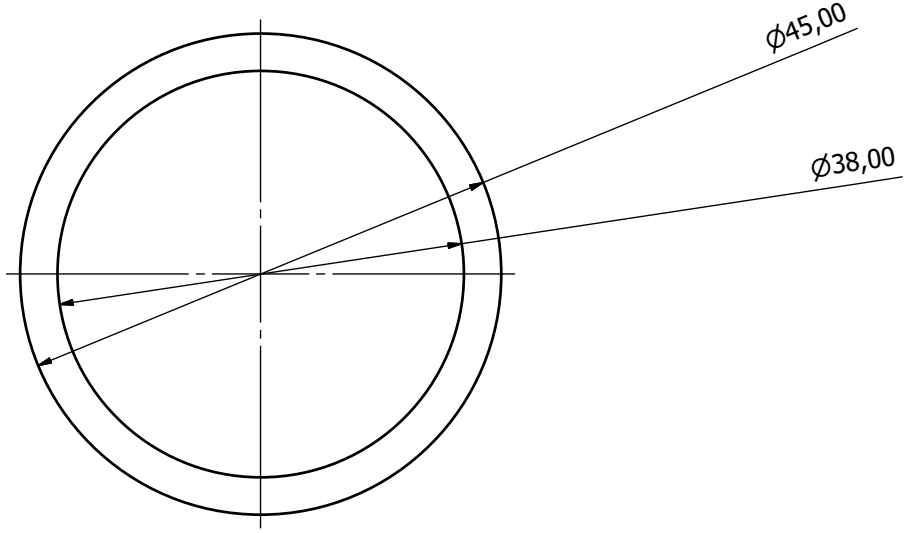

A3-Scale (2 : 1)

Designed by Strandene and Tørnby	Approved by	Date		Date 26.03.2018	
University of Agder	Gearbox				
	Bushing Planet Fixed		Edition	Sheet 1 / 1	

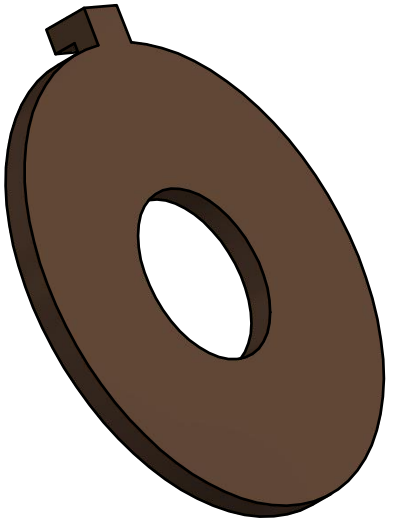

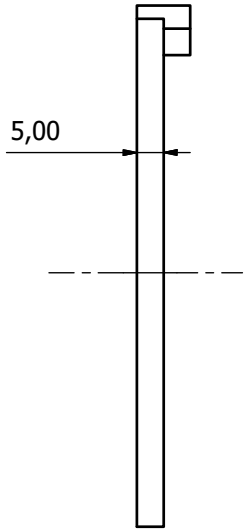

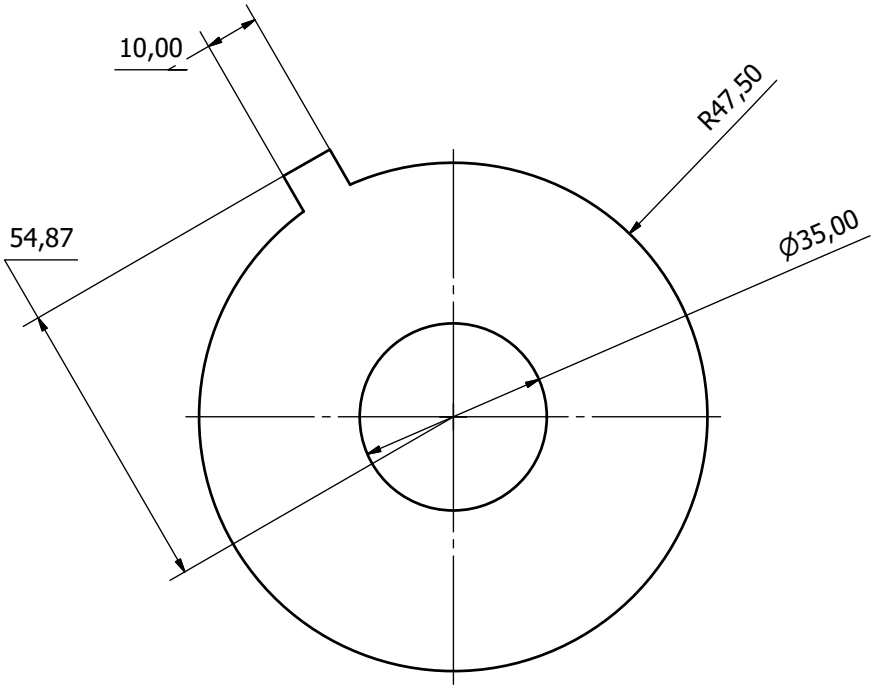

A3-Scale (1 : 1)

Designed by: Strandene and Tørnby	Approved by	Date		Date: 26.03.2018	
University of Agder	Gearbox				
	Bushing Planet Fixed End		Edition	Sheet: 1 / 1	

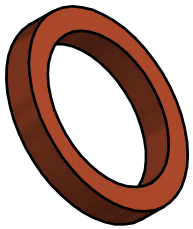

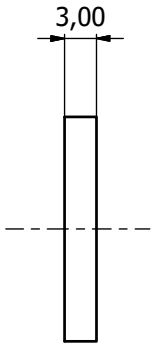

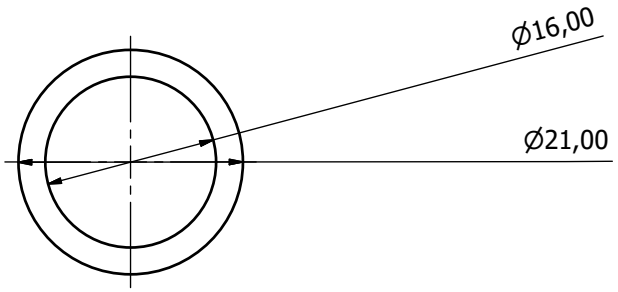

A3-Scale (2 : 1)

Designed by Strandene and Tørnby	Approved by	Date		Date 26.03.2018	
University of Agder			Gearbox		
			Bushing Planet 1	Edition	Sheet 1 / 1

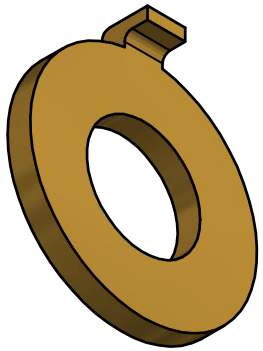

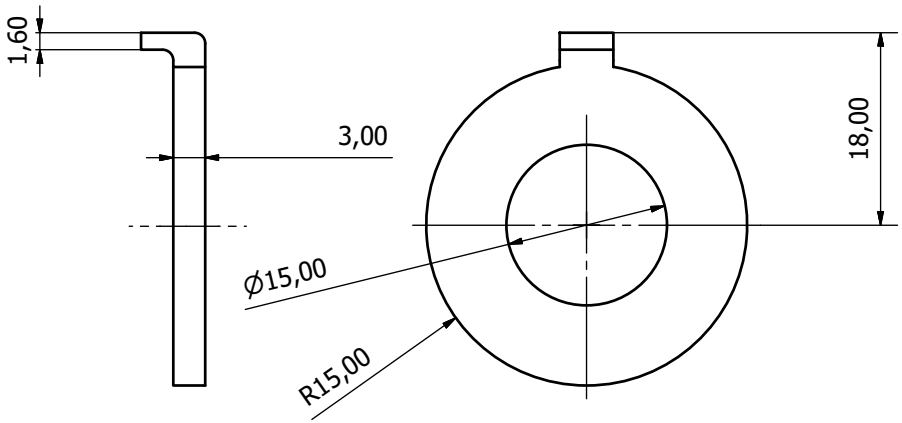

Designed by: Strandene and Tørnby	Approved by	Date		Date: 26.03.2018	
University of Agder	Gearbox				
	Bushing Planet 1 End		Edition	Sheet: 1 / 1	

A3-Scale (2 : 1)

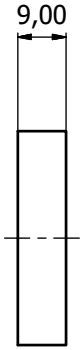

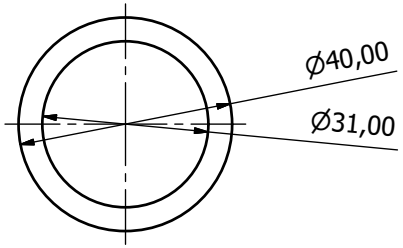

A3-Scale (1 : 1)

Designed by Strandene and Tørnby	Approved by	Date		Date 26.03.2018	
University of Agder	Gearbox				
	Bushing Planet 2		Edition	Sheet 1 / 1	

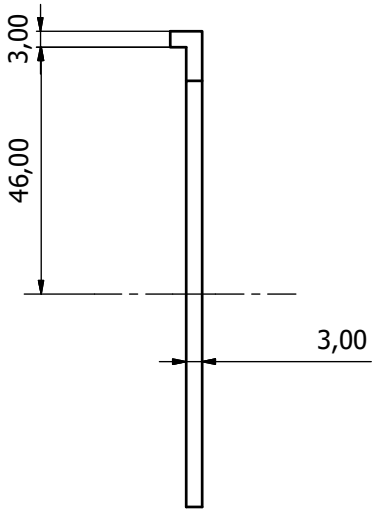

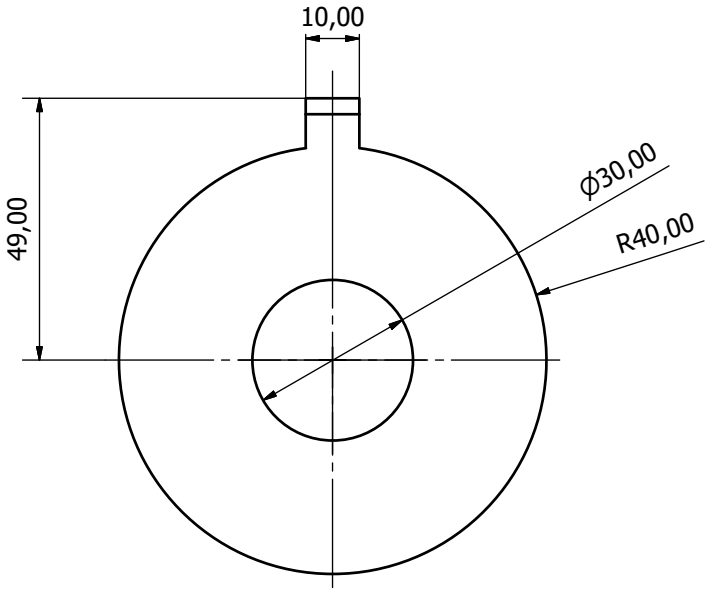

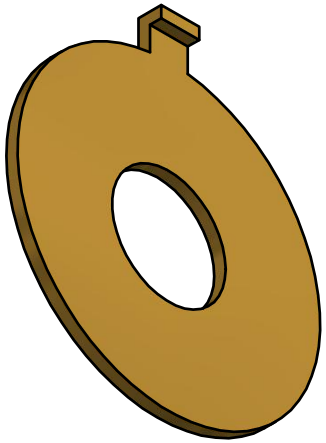

A3-Scale (1 : 1)

Designed by: Strandene and Tørnby	Approved by	Date		Date: 26.03.2018	
University of Agder	Gearbox				
	Bushing Planet2 End		Edition	Sheet: 1 / 1	

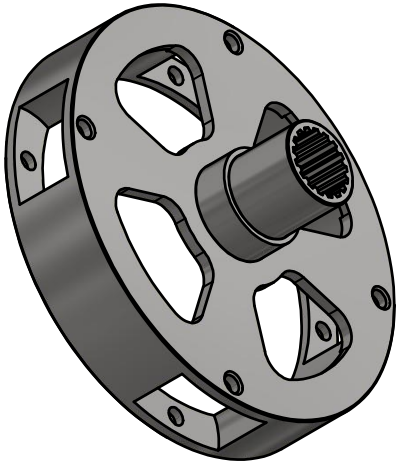

A-A (1 : 4)

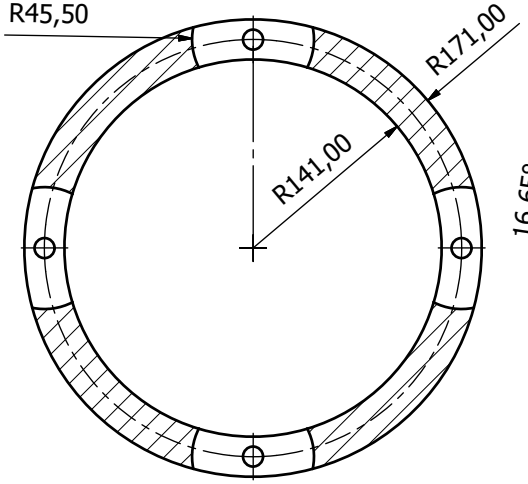

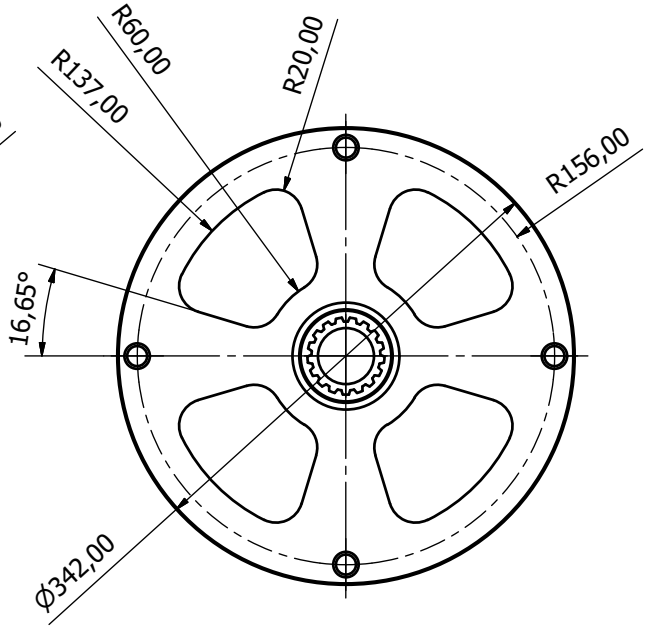

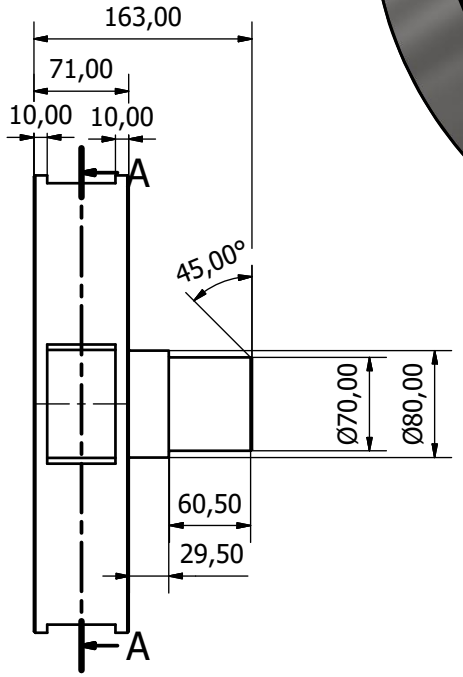

B-B (1 : 4)

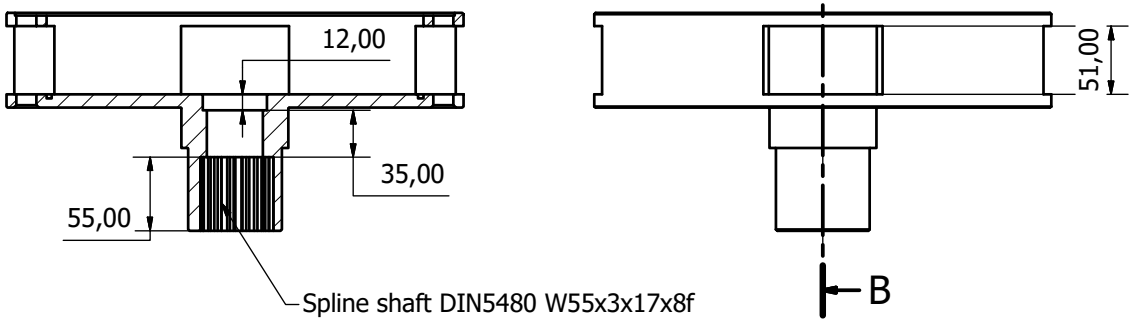

A3-Scale (1 : 4)

Designed by: Strandene and Tørnby	Approved by	Date		Date: 22.03.2018	
Universitetet i Agder	Gearbox				
	Carrier 1 Actuated		Edition	Sheet: 1 / 1	

A-A (1 : 4)

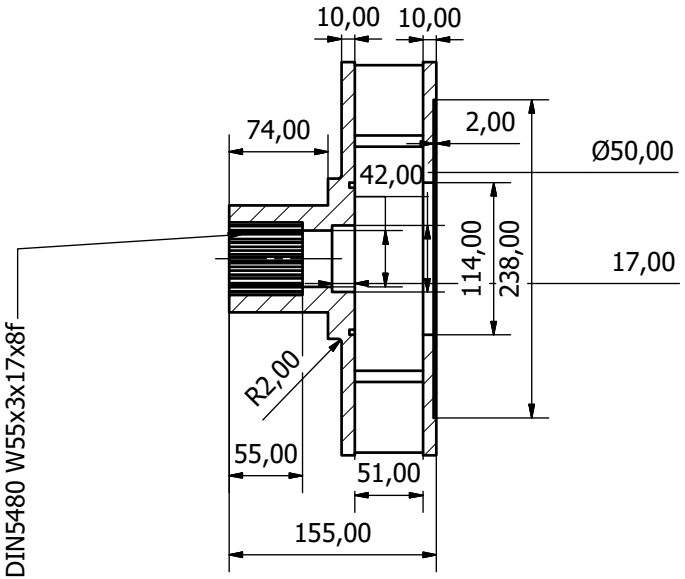

C-C (1 : 4)

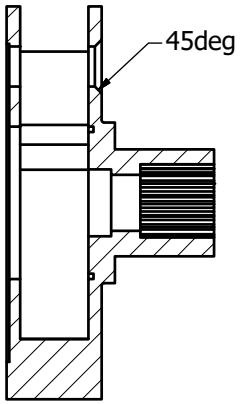

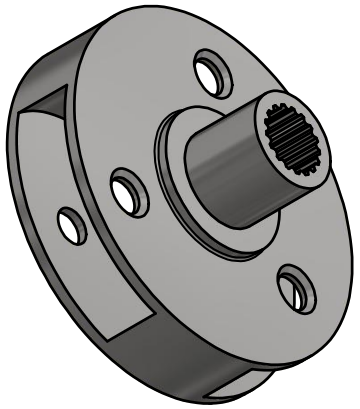

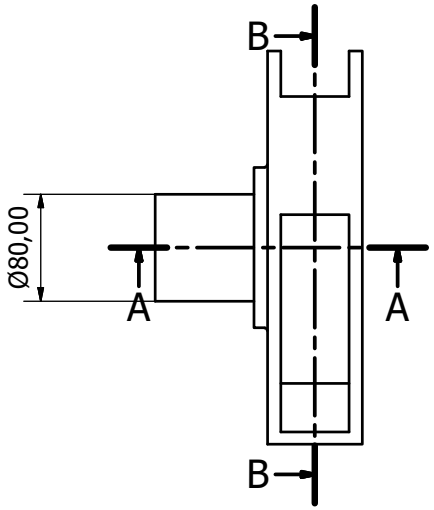

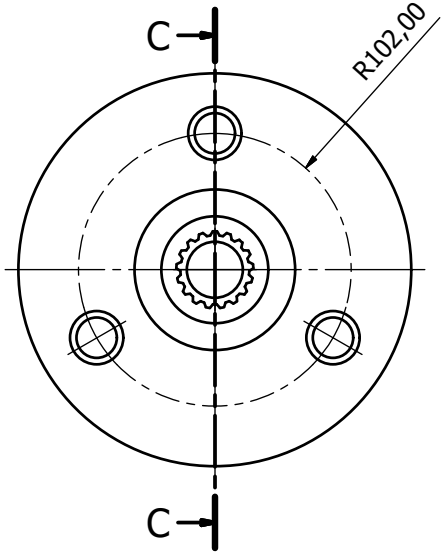

B-B (1 : 4)

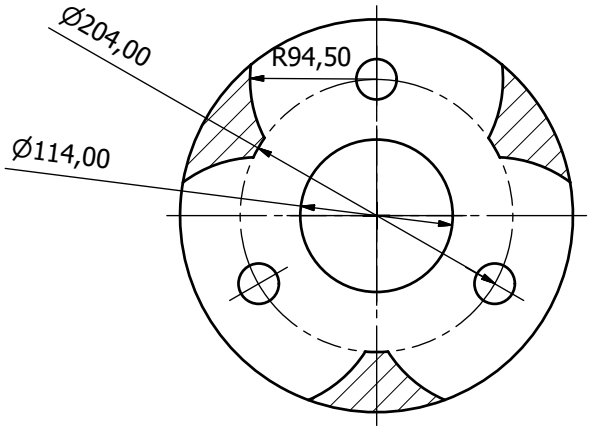

A3-Scale (1 : 4)

Designed by Strandene and Tørnby	Approved by	Date		Date 22.03.2018	
University of Agder	Gearbox				
	Carrier2 Actuated		Edition	Sheet 1 / 1	

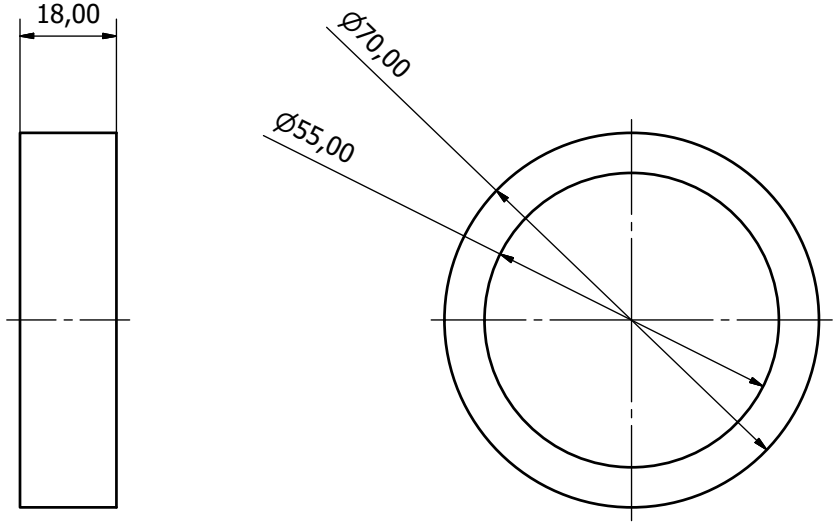

A3-Scale (1 : 1)

Designed by: Strandene and Tørnby	Approved by	Date		Date: 22.03.2018	
University of Agder	Gearbox				
	Fixed Sun Spacer		Edition	Sheet: 1 / 1	

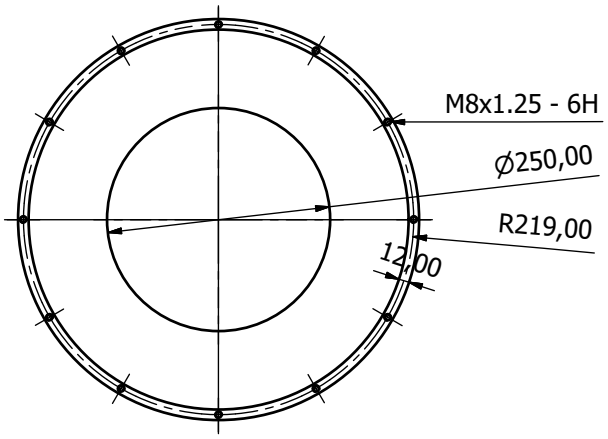

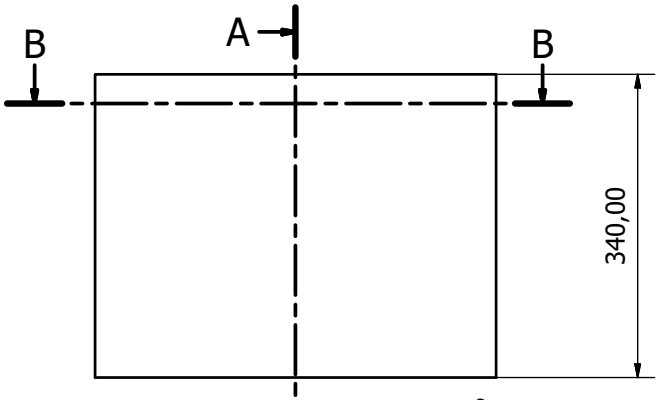

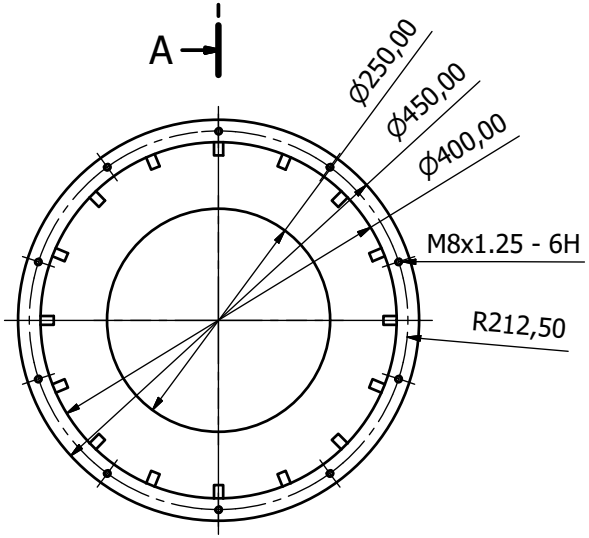

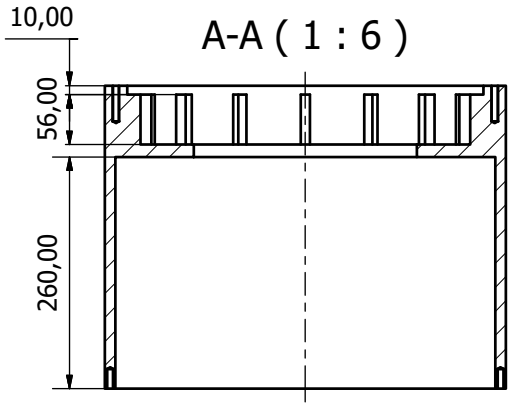

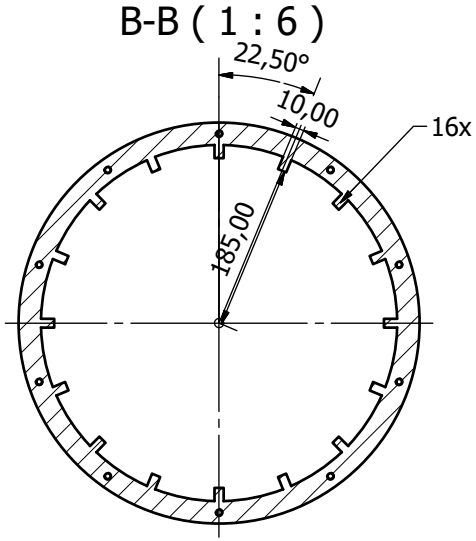

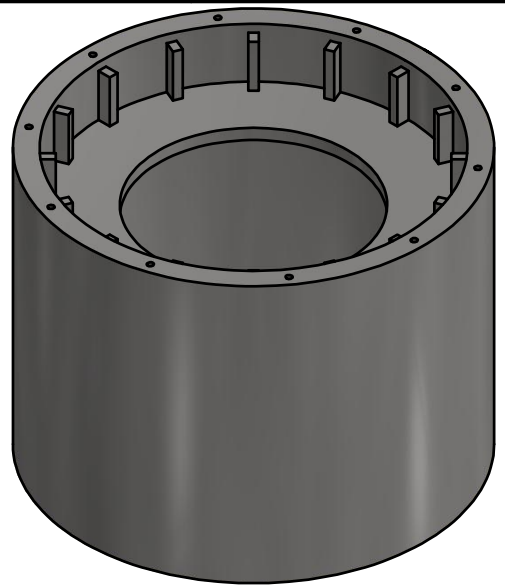

A3-Scale (1 : 6)

Designed by: Strandene and Tørnby	Approved by	Date		Date: 22.03.2018	
University of Agder	Gearbox				
	Housing Actuated		Edition	Sheet: 1 / 1	

A-A (1 : 5)

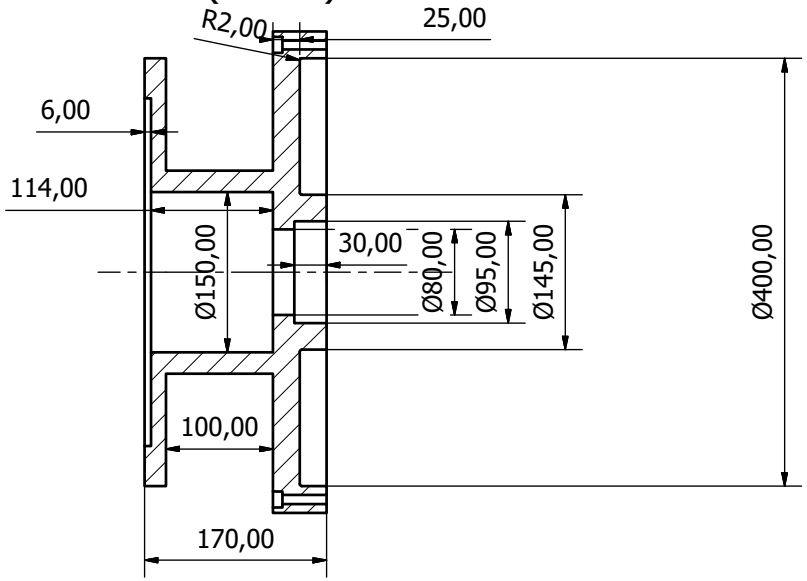

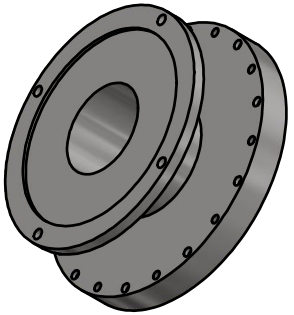

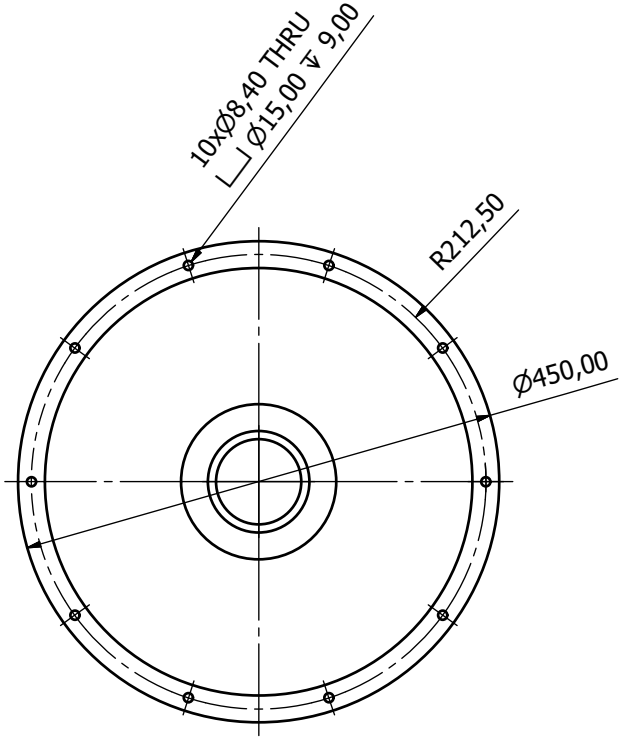

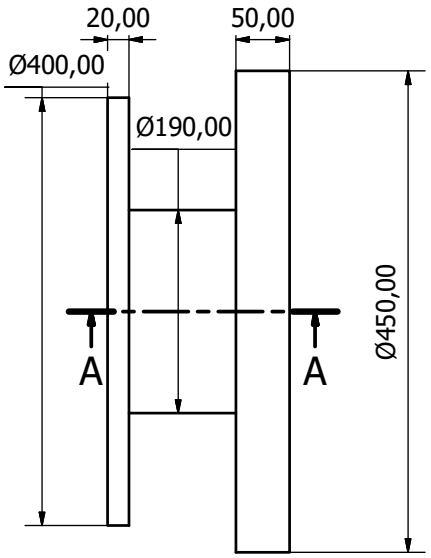

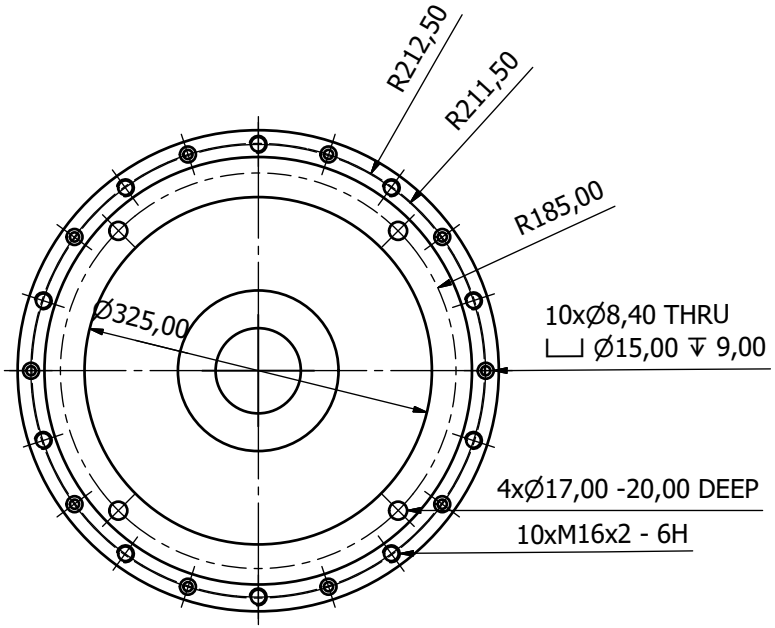

A3-Scale (1 : 5)

Designed by	Approved by	Date		Date	
Strandene and Tørnby				22.03.2018	

University of Agder	Gearbox		
	Housing Endcover Motorside	Edition	Sheet 1 / 1

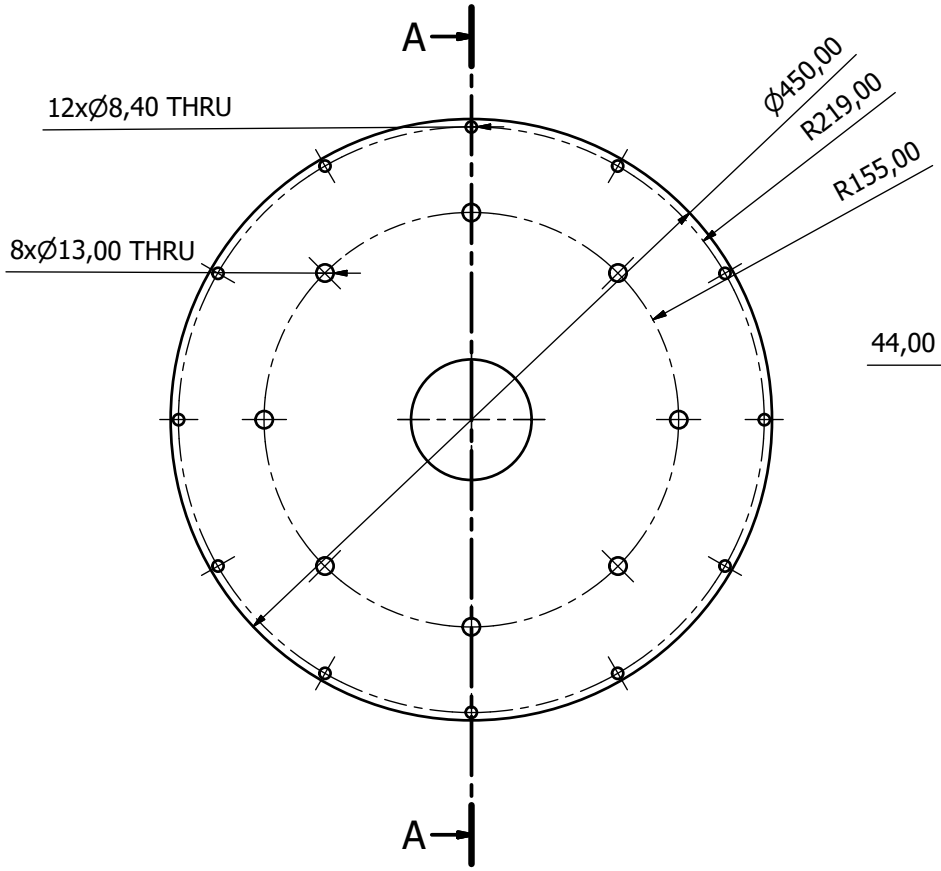

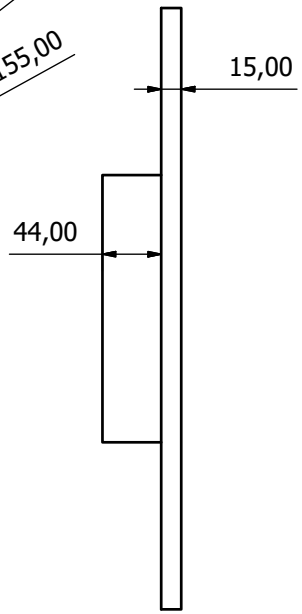

A-A (1 : 4)

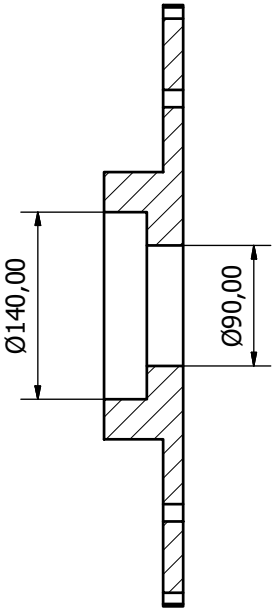

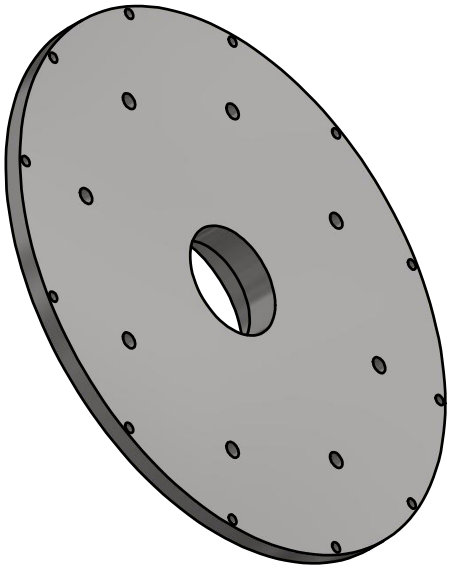

A3-Scale (1 : 4)

Designed by: Strandene and Tørnby	Approved by	Date		Date: 22.03.2018	
University of Agder	Gearbox				
	Housing Endcover Actuated		Edition	Sheet: 1 / 1	

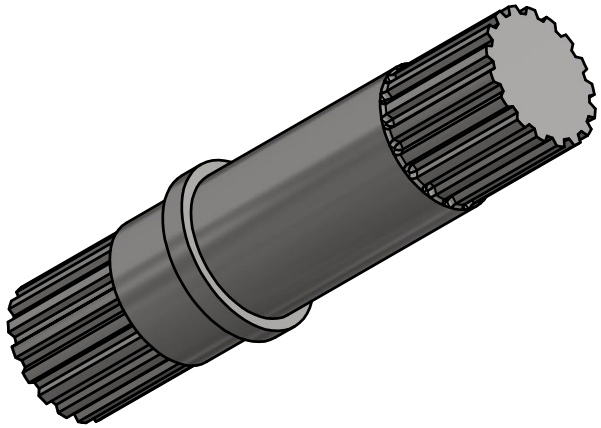

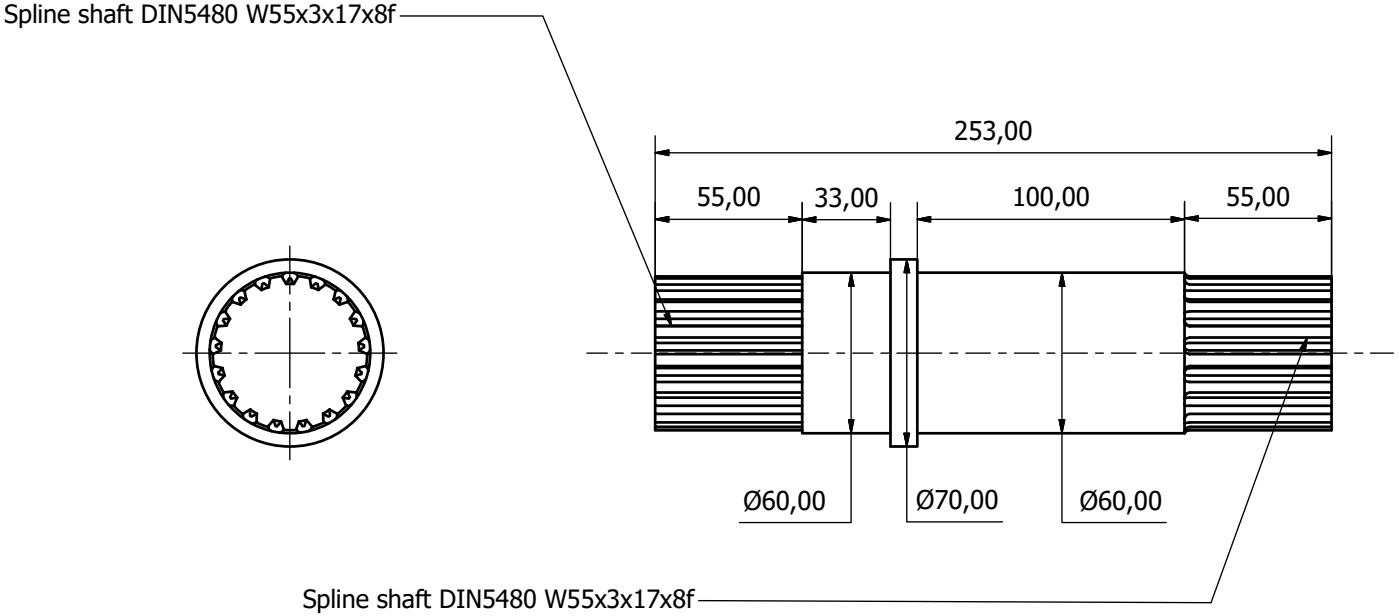

Designed by: Strandene and Tørnby	Approved by	Date		Date: 22.03.2018	
University of Agder	Gearbox				
	Input Shaft		Edition	Sheet: 1 / 1	

A3-Scale (1 : 2)

A-A (1 : 4)

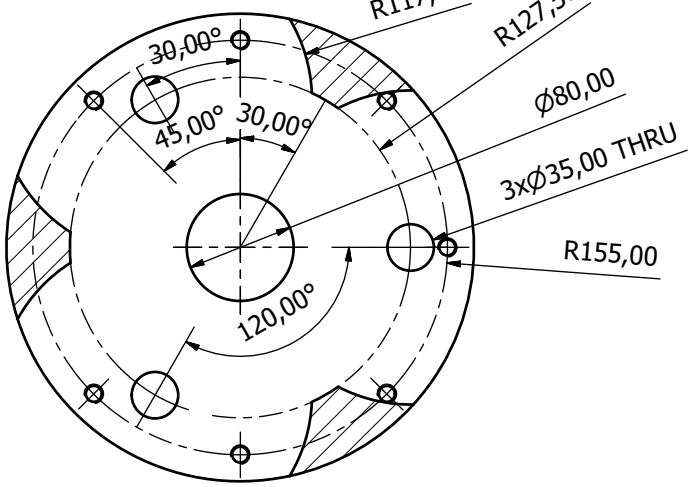

B-B (1 : 4)

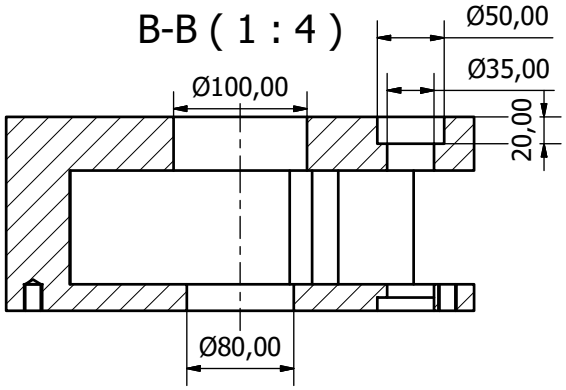

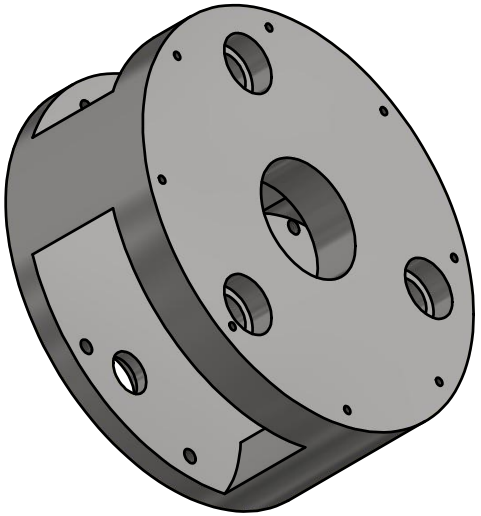

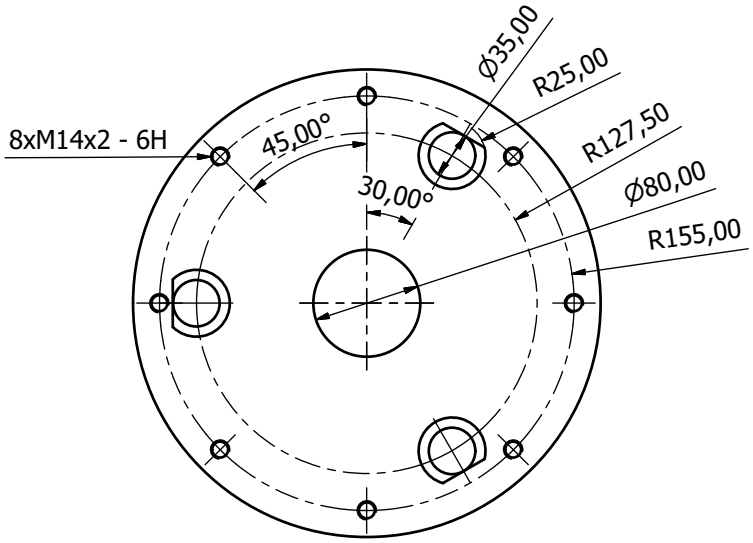

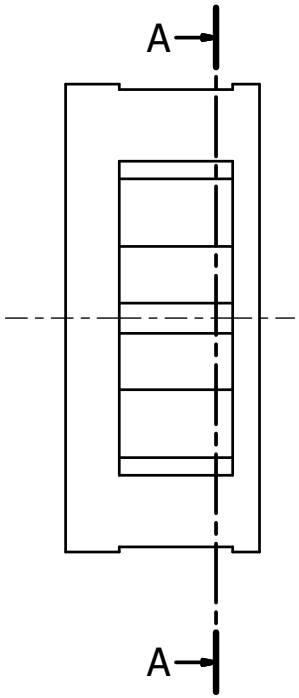

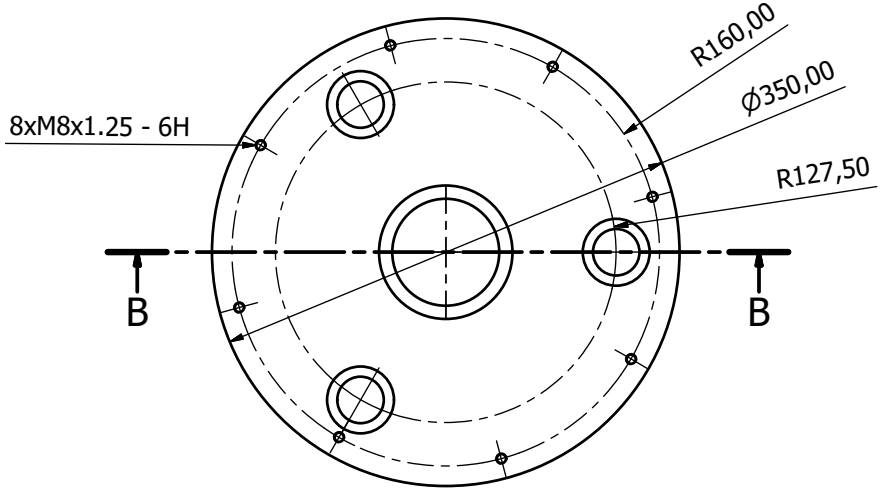

A3-Scale (1 : 4)

Designed by	Approved by	Date		Date	
Strandene and Tørnby				21.03.2018	

University of Agder	Gearbox		
	Planet Carrier Fixed Step	Edition	Sheet 1 / 1

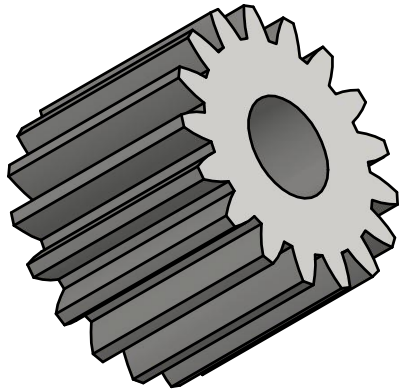

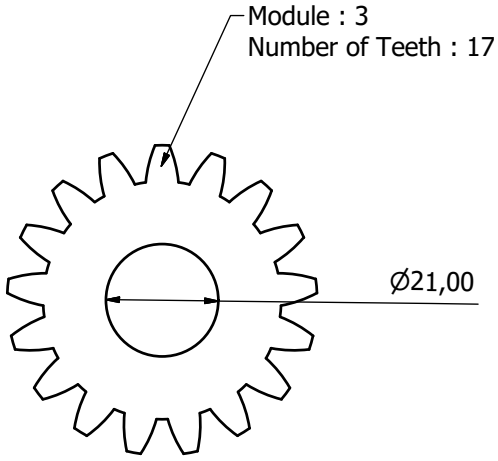

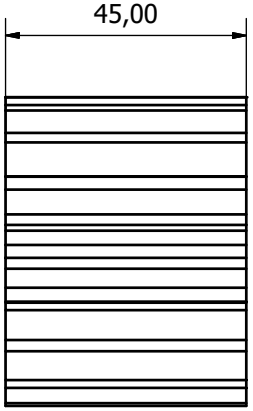

A3-Scale (1 : 1)

Designed by: Strandene and Tørby	Approved by	Date		Date: 22.03.2018	
University of Agder	Gearbox				
	Planet1 Actuated		Edition	Sheet: 1 / 1	

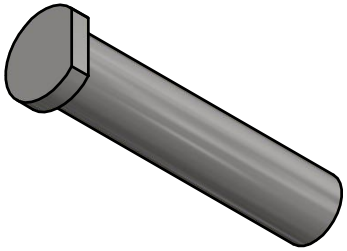

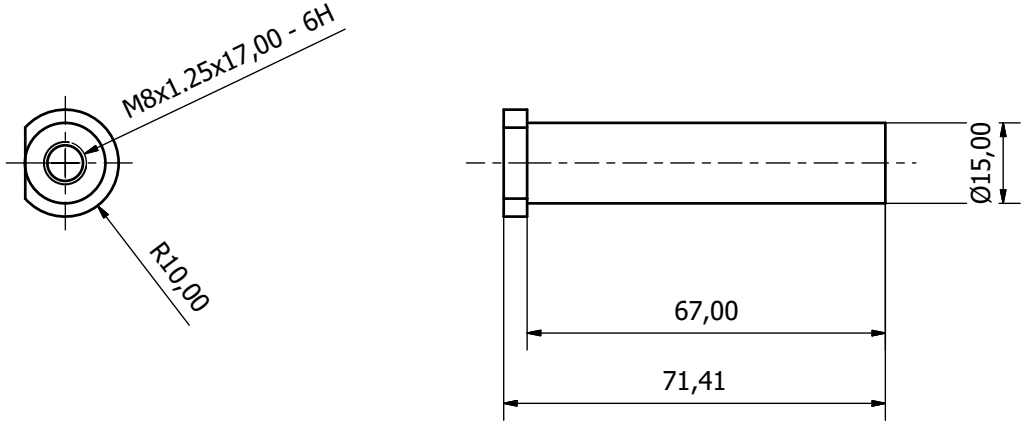

A3-Scale (1 : 1)

Designed by: Strandene and Tørnby	Approved by	Date		Date: 21.03.2018	
University of Agder	Gearbox				
	Bolt Planet1 Actuated		Edition	Sheet: 1 / 1	

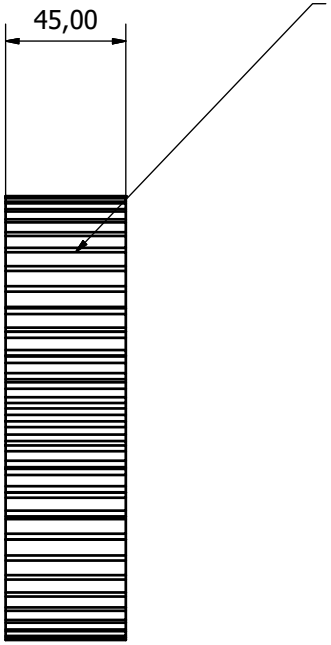

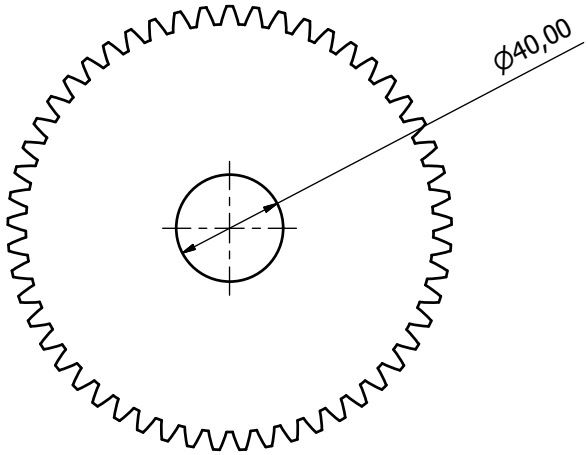

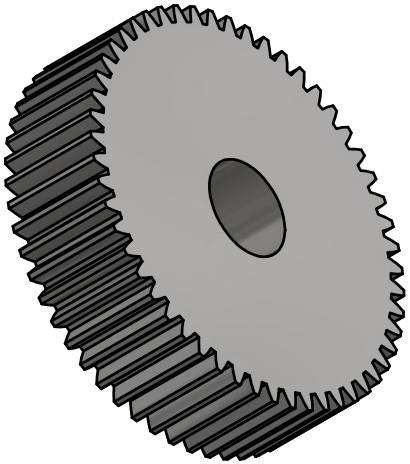

A3-Scale (1 : 2)

Designed by: Strandene and Tørnby	Approved by	Date		Date: 21.03.2018	
University of Agder	Gearbox				
	Planet2 Actuated		Edition	Sheet: 1 / 1	

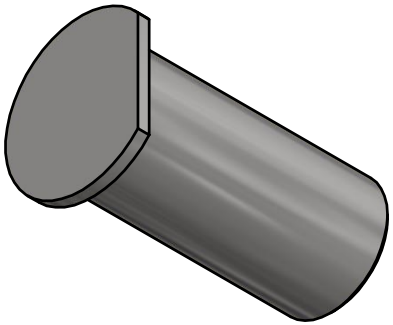

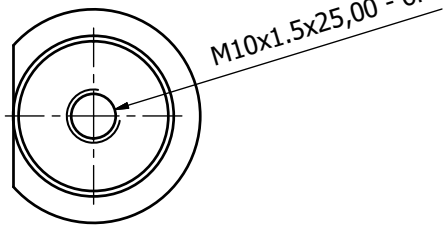

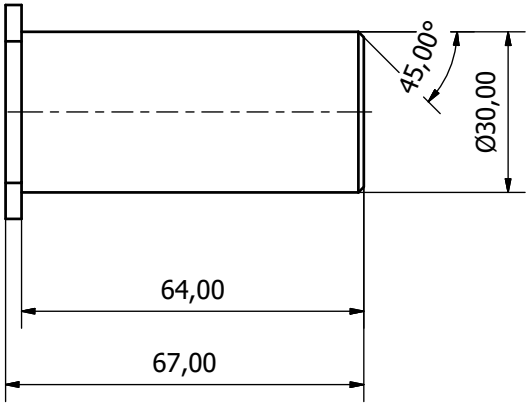

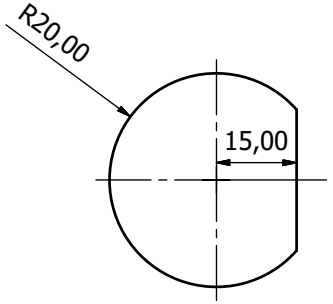

Designed by	Checked by	Approved by	Date		Date	
Strandene and Tørnby					21.03.2018	

A3-Scale (1 : 1)

University of Agder	Gearbox		
	Bolt Planet2 Actuated	Edition	Sheet 1 / 1

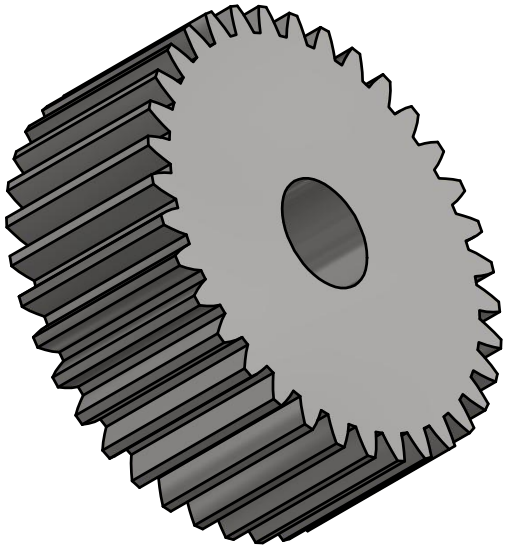

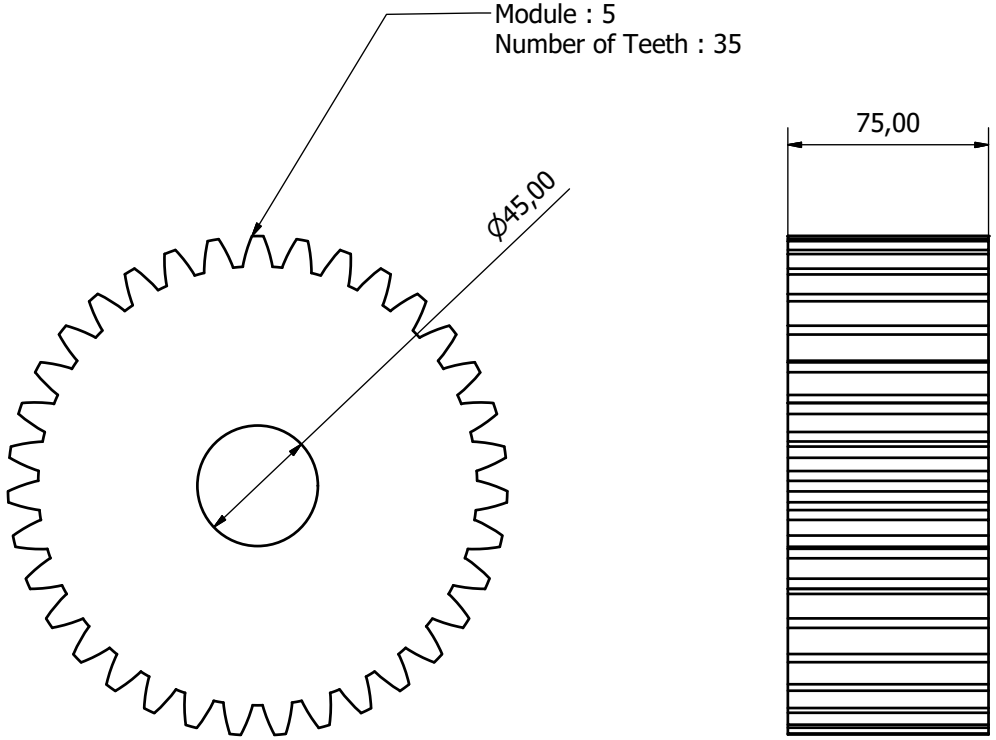

Designed by Strandene and Tørnby	Approved by	Date		Date 21.03.2018	
University of Agder	Gearbox				
	Planet Fixed Step		Edition	Sheet 1 / 1	

A3-Scale (1 : 2)

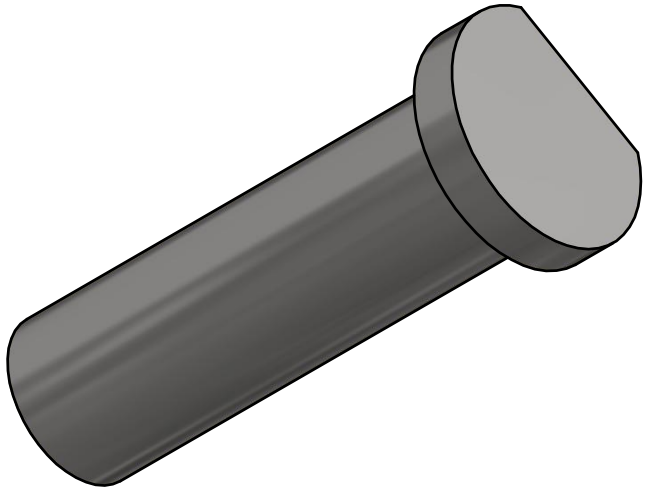

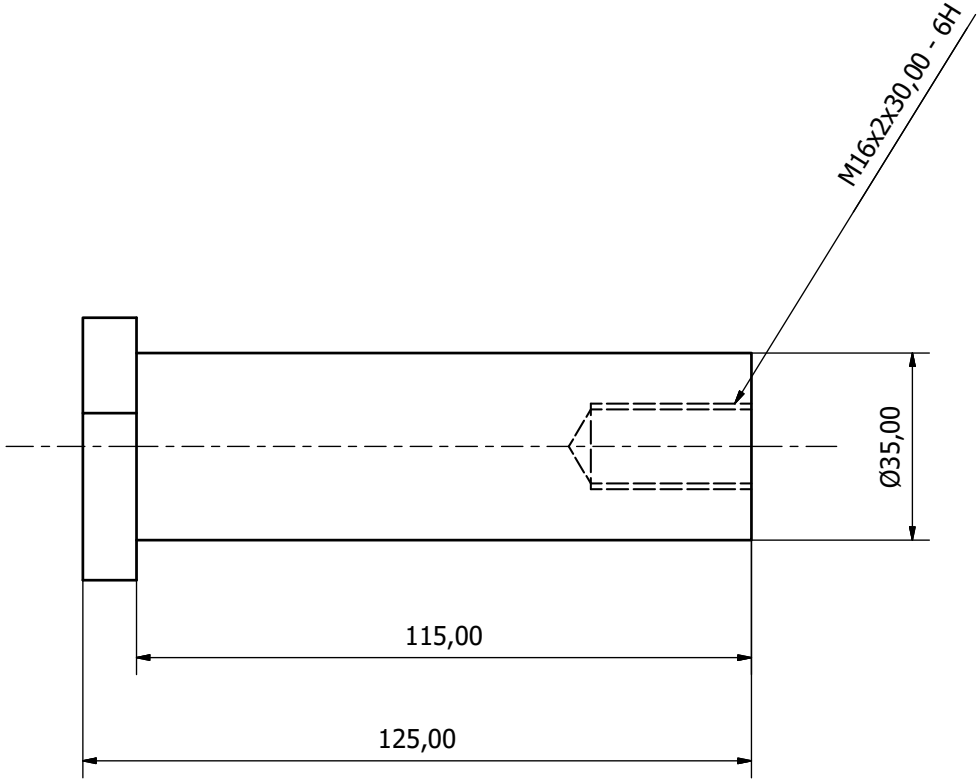

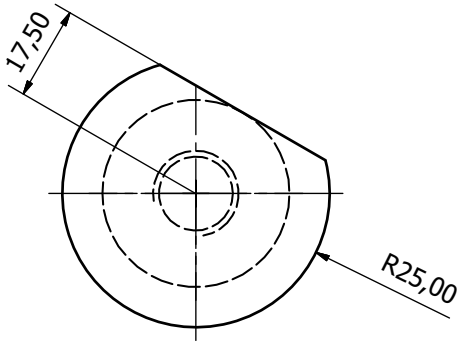

A3-Scale (1 : 1)

Designed by: Strandene and Tørnby	Approved by	Date		Date: 21.03.2018	
University of Agder	Gearbox				
	Planet Shaft Fixed Step		Edition	Sheet: 1 / 1	

A-A (1 : 4)

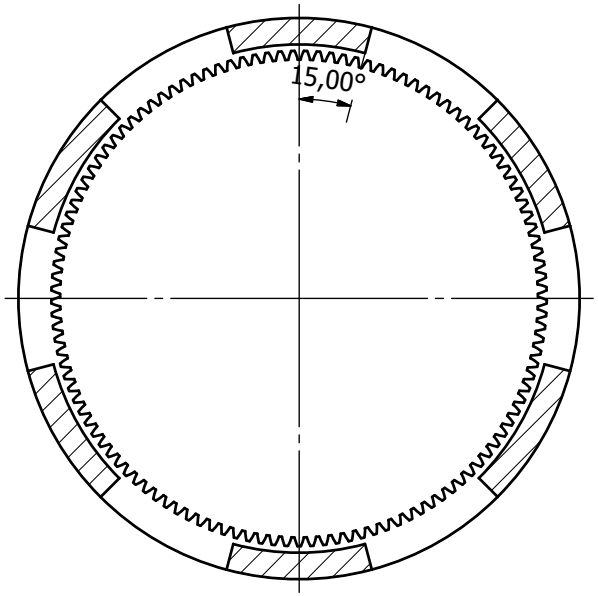

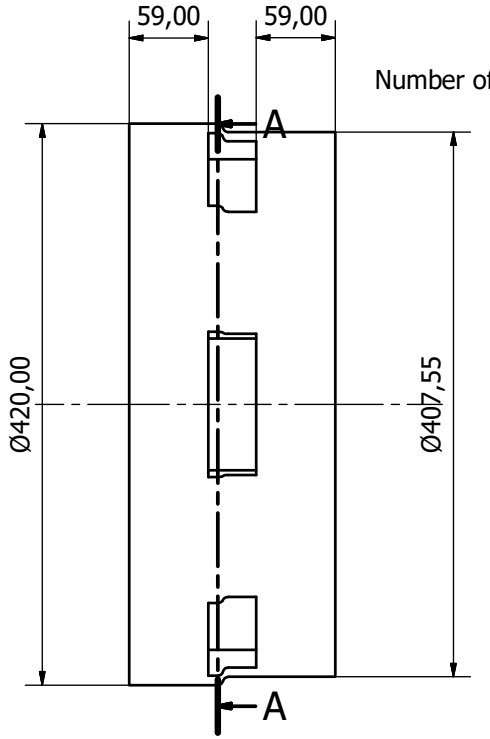

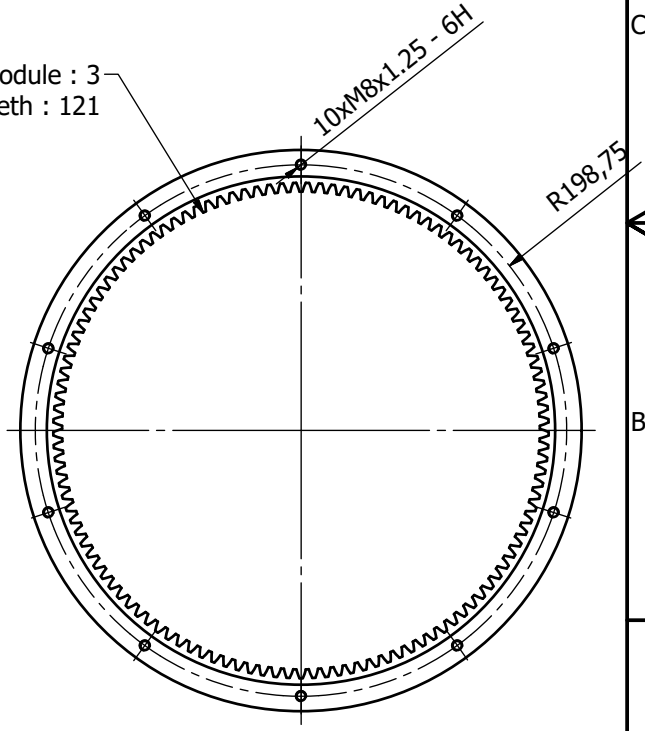

A3-Scale (1 : 4)

Designed by: Strandene and Tørnby	Approved by	Date		Date: 21.03.2018	
University of Agder	Gearbox				
	Ring Auto		Edition	Sheet: 1 / 1	

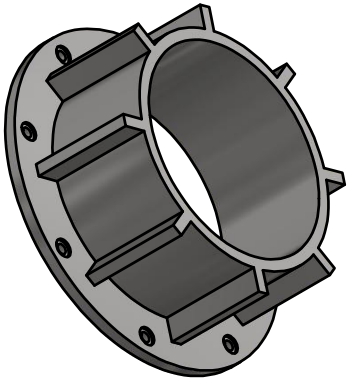

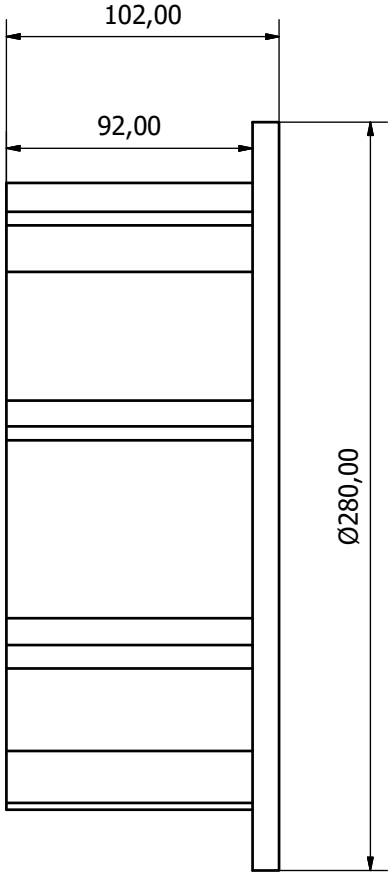

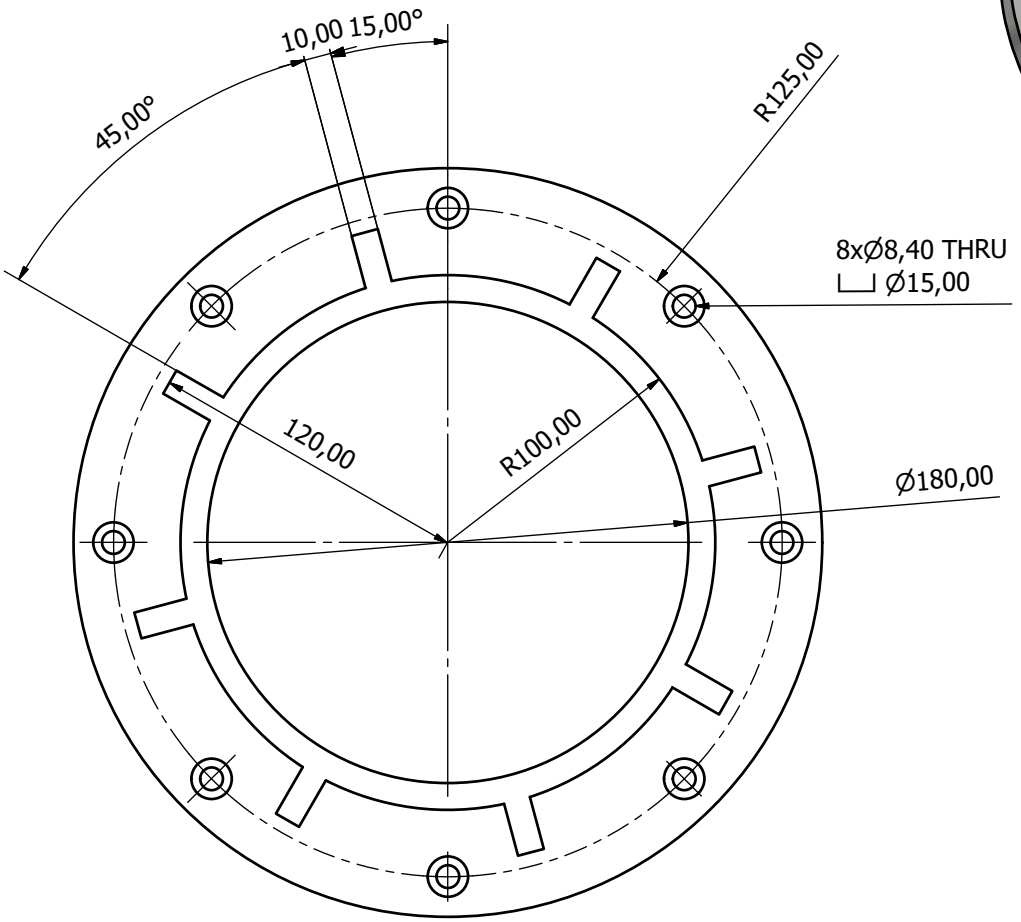

A3-Scale (1 : 2)

Designed by: Strandene and Tørnby	Approved by	Date		Date: 21.03.2018	
University of Agder	Gearbox				
	Ring Brake Inner Ring		Edition	Sheet: 1 / 1	

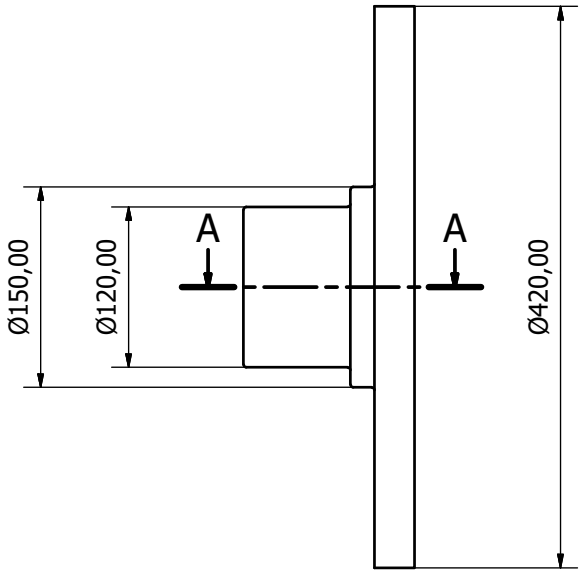

A-A (1 : 4)

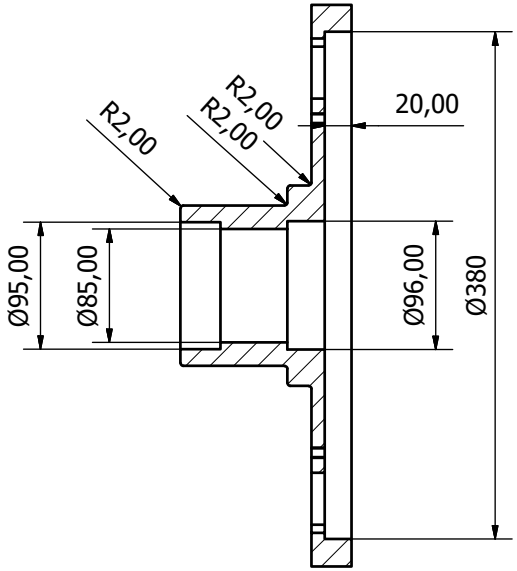

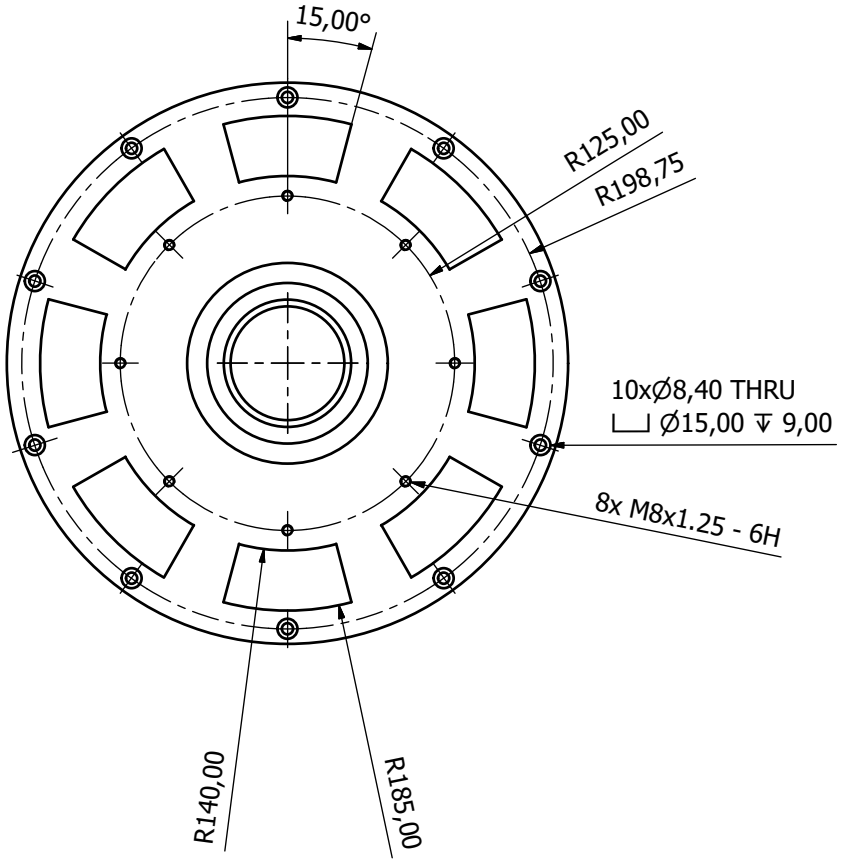

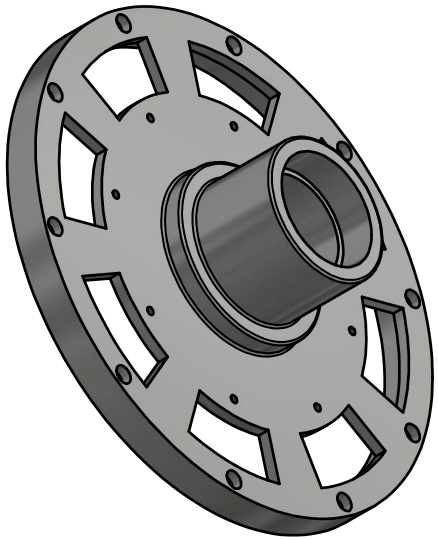

A3-Scale (1 : 4)

Designed by: Strandene and Tørnby	Approved by	Date		Date: 21.03.2018	
University of Agder	Gearbox				
	Ring Drum		Edition	Sheet: 1 / 1	

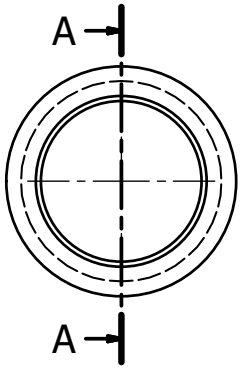

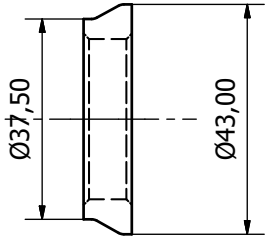

A-A (1 : 1)

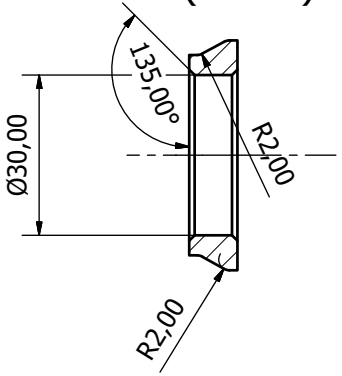

A3-Scale (1 : 1)

Designed by Strandene and Tørnby	Approved by	Date		Date 21.03.2018	
University of Agder	Gearbox				
	Spacer Sun Shaft		Edition	Sheet 1 / 1	

B-B (1 : 1)

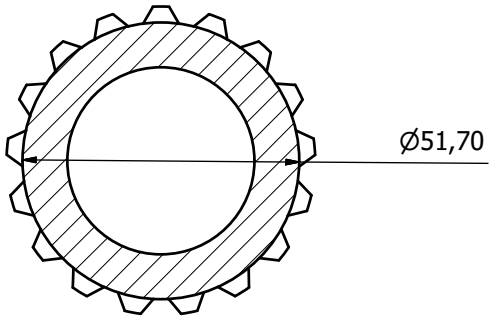

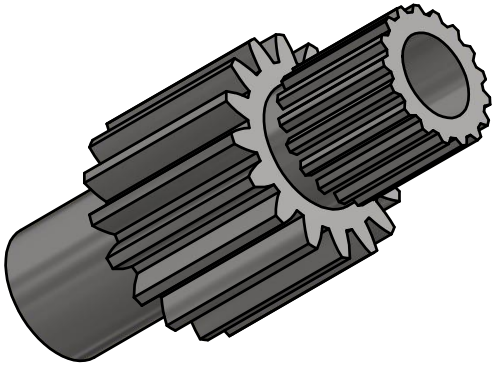

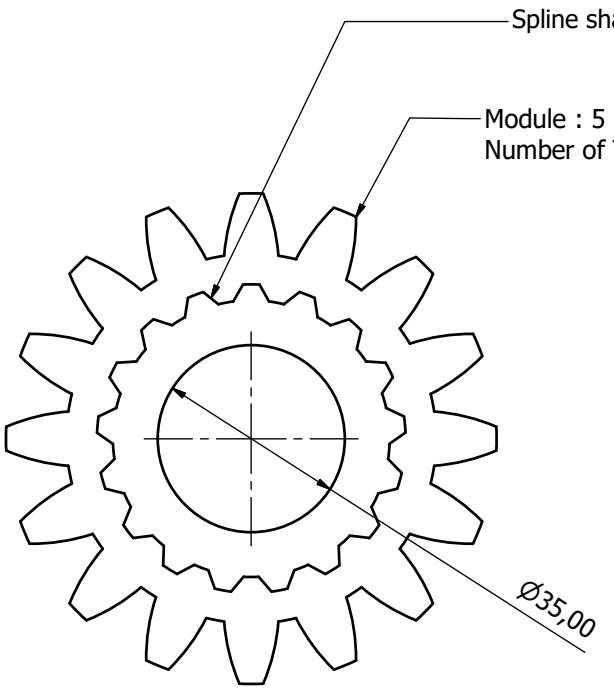

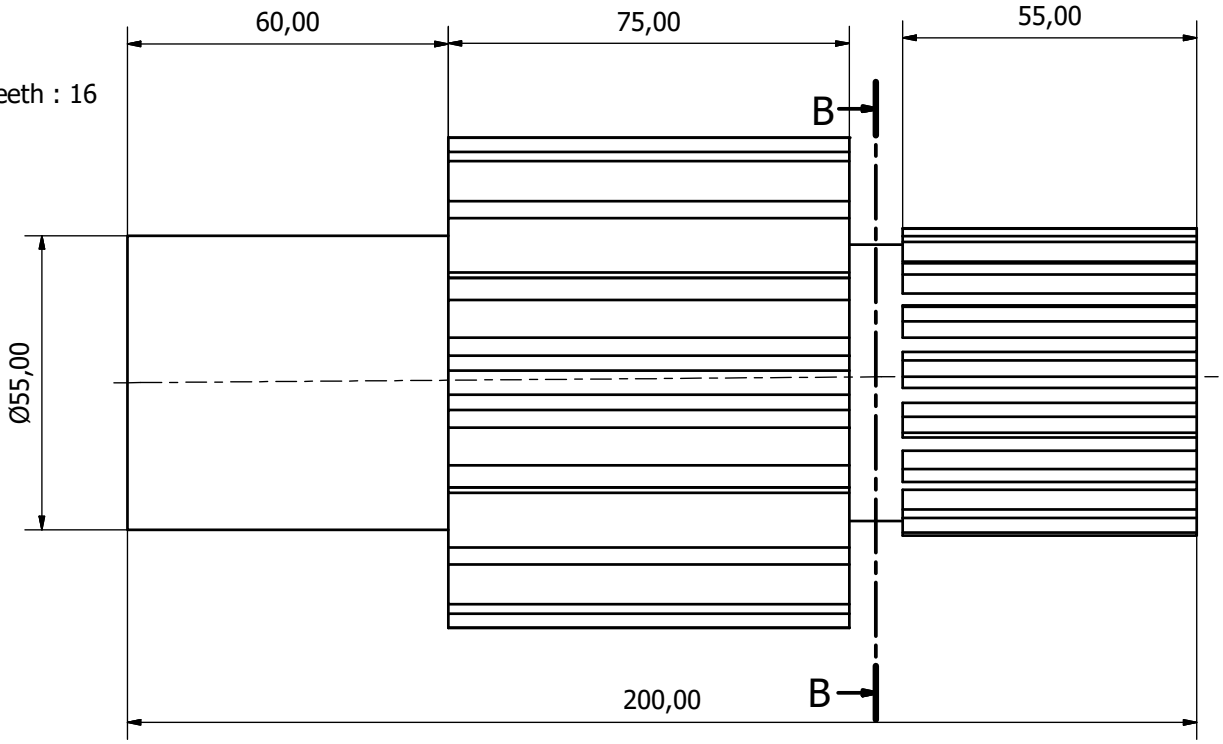

Designed by	Approved by	Date		Date	
Strandene and Tørnby				21.03.2018	

University of Agder	Gearbox		
	Sun Fixed	Edition	Sheet 1 / 1

A3-Scale (1 : 1)

A-A (1 : 4)

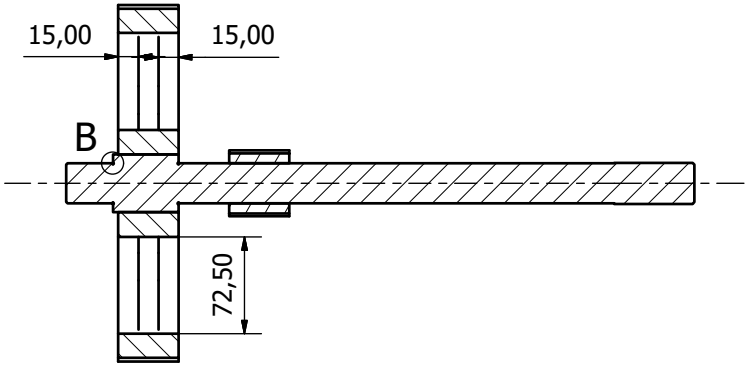

B (2 : 1)

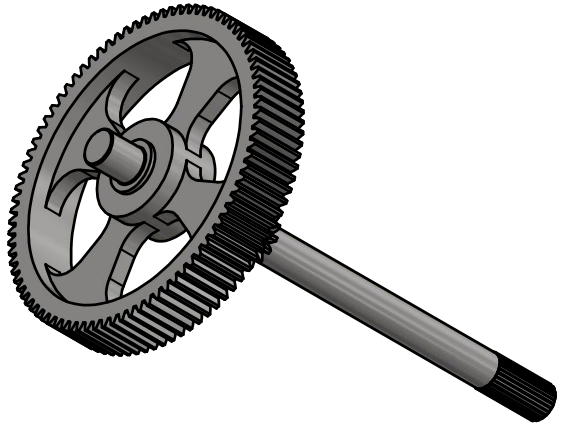

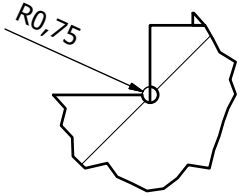

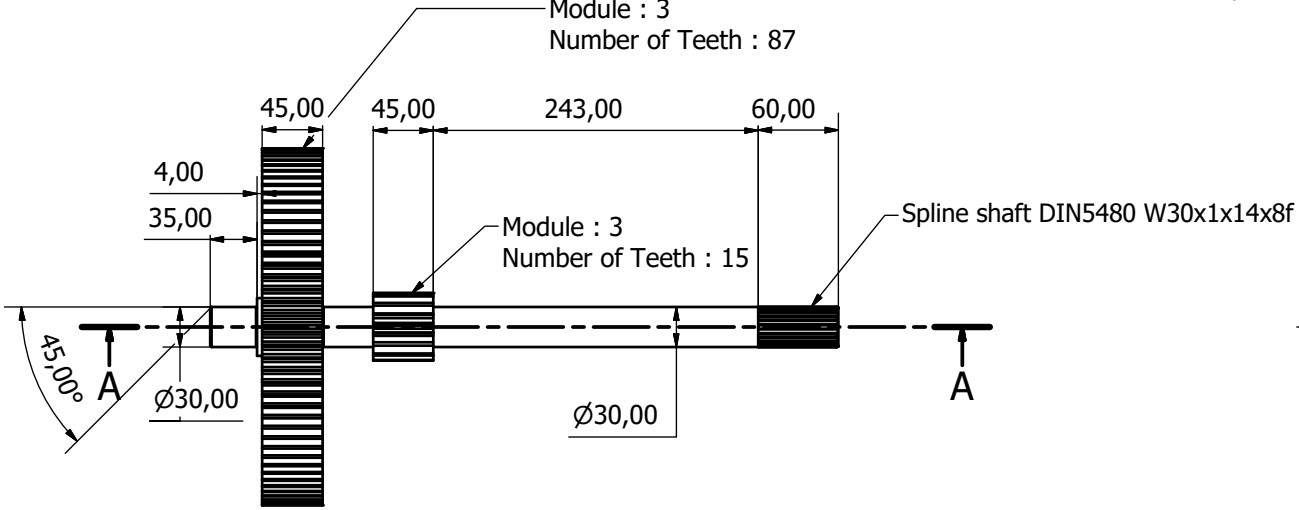

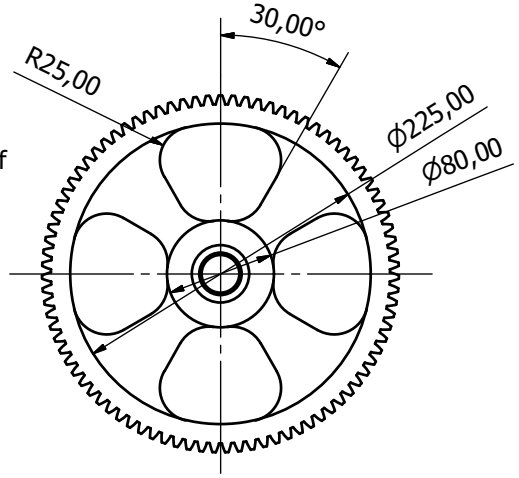

A3-Scale (1 : 4)

Designed by Strandene and Tørnby	Approved by	Date		Date 03.05.2018	
University of Agder	Gearbox				
	Sun shaft		Edition	Sheet 1 / 1	

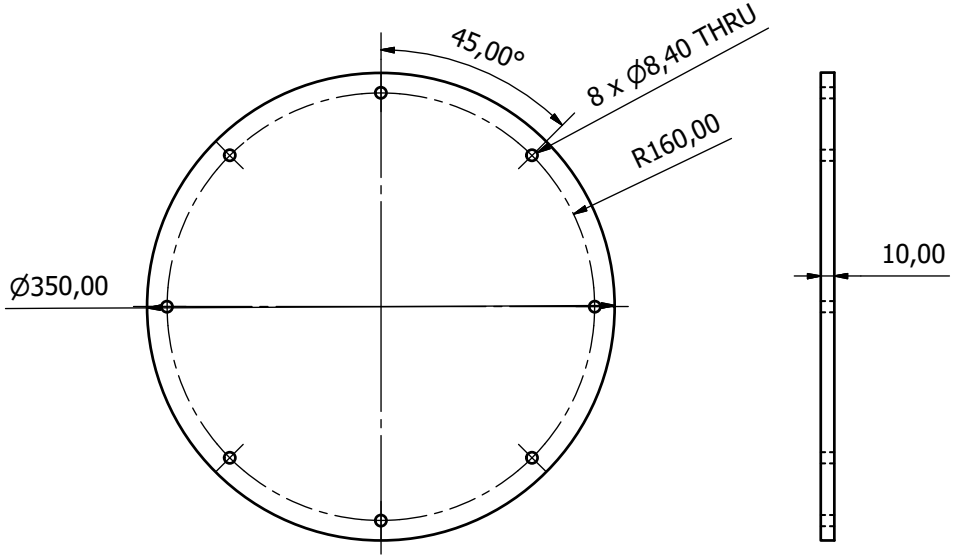

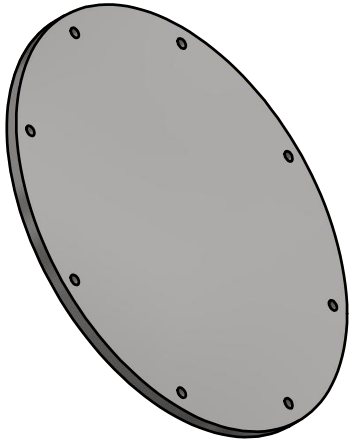

A3-Scale (1 : 4)

Designed by: Strandene and Tørnby	Approved by	Date		Date: 21.03.2018	
University of Agder	Gearbox				
	Sunbrake Cover		Edition	Sheet: 1 / 1	

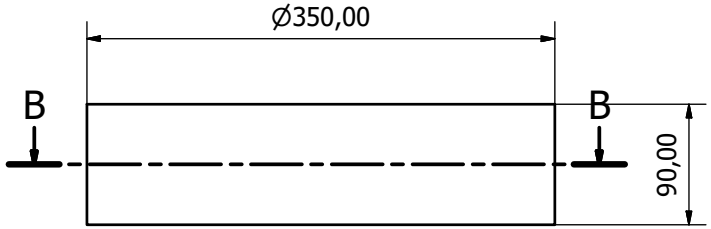

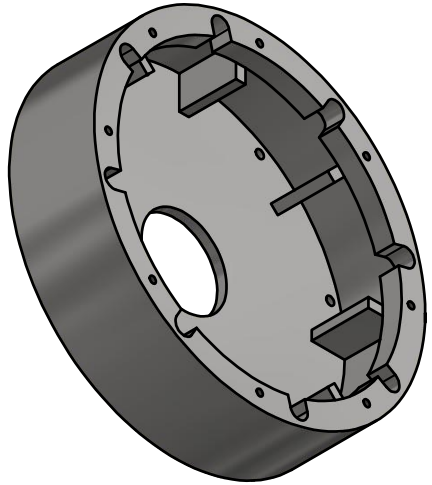

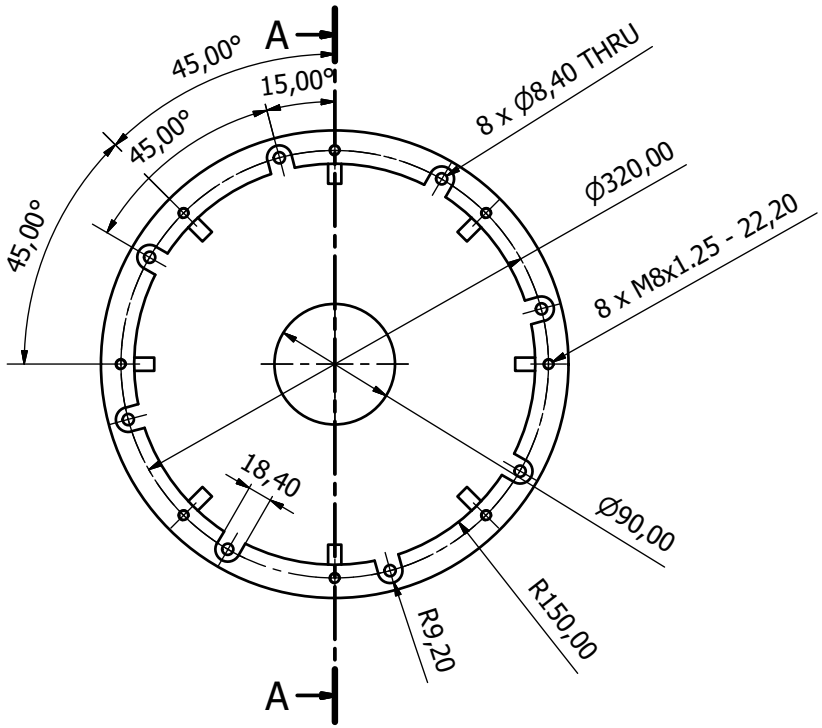

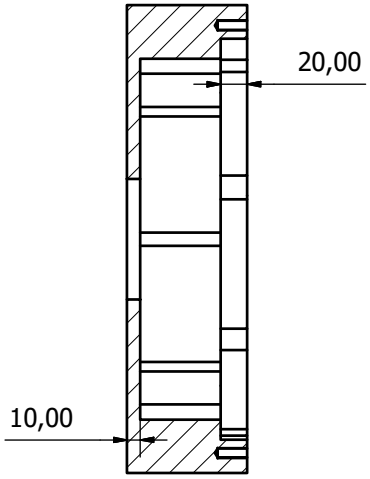

A-A (1 : 4)

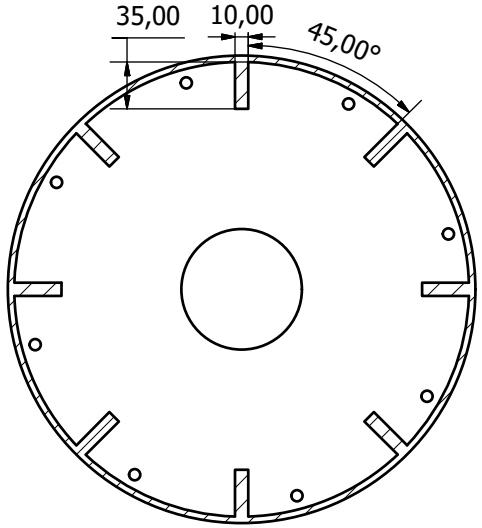

B-B (1 : 4)

A3-Scale (1 : 4)

Designed by Strandene and Tørnby	Approved by	Date		Date 21.03.2018	
University of Agder	Gearbox				
	Sunbrake Housing		Edition	Sheet 1 / 1	

A-A (1 : 1)

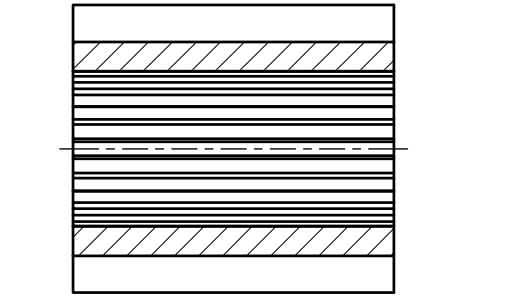

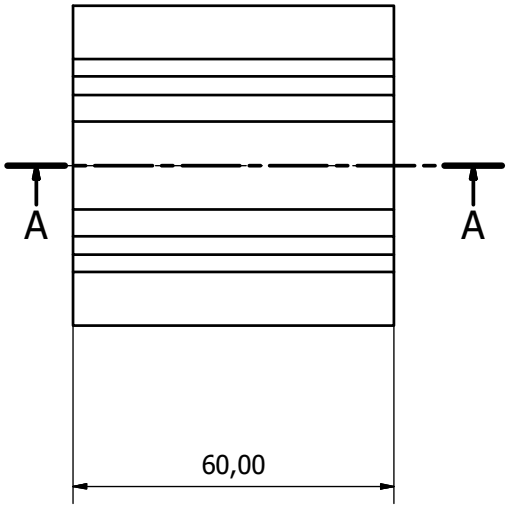

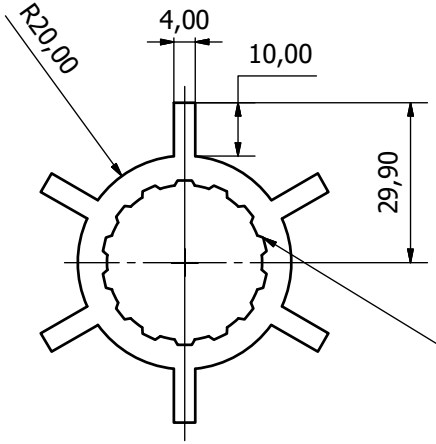

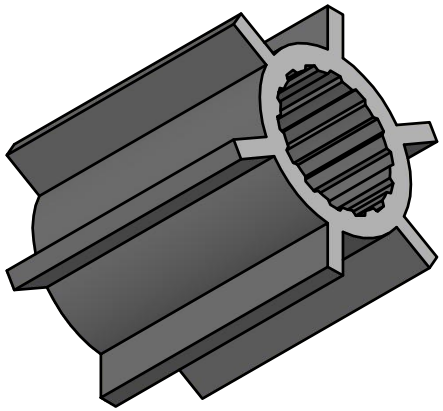

A3-Scale (1 : 1)

Designed by: Strandene and Trønby	Approved by	Date		Date: 26.03.2018	
University of Agder	Gearbox				
	Sunbrake Hub		Edition	Sheet: 1 / 1	

Appendix H:
Datasheet for SKF Bearings

K 15x21x21

Dimensions

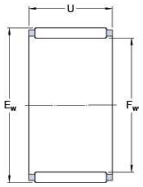

F_w	15	mm
E_w	21	mm
U	21	mm

Calculation data

Basic dynamic load rating	C	18.7	kN
Basic static load rating	C_0	24.5	kN
Fatigue load limit	P_u	3	kN
Reference speed		24000	r/min
Limiting speed		26000	r/min

Mass

Mass needle roller and cage assembly	0.017	kg

Associated products

Designation associated G design radial shaft seal with a low cross-sectional height	G 15x21x3
Designation associated SD design radial shaft seal with a low cross-sectional height	SD 15x21x3

K 30x40x18

Dimensions

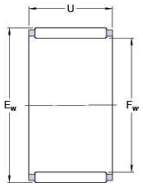

F_w	30	mm
E_w	40	mm
U	18	mm

Calculation data

Basic dynamic load rating	C	30.3	kN
Basic static load rating	C_0	40	kN
Fatigue load limit	P_u	4.9	kN
Reference speed		12000	r/min
Limiting speed		14000	r/min

Mass

Mass needle roller and cage assembly	0.048	kg

Associated products

Designation associated G design radial shaft seal with a low cross-sectional height	G 30x40x4
Designation associated SD design radial shaft seal with a low cross-sectional height	SD 30x40x4

K 35x45x30

Dimensions

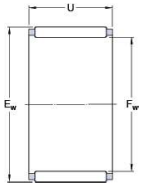

F_w	35	mm
E_w	45	mm
U	30	mm

Calculation data

Basic dynamic load rating	C	50.1	kN
Basic static load rating	C_0	80	kN
Fatigue load limit	P_u	10	kN
Reference speed		11000	r/min
Limiting speed		12000	r/min

Mass

Mass needle roller and cage assembly	0.08	kg

Associated products

Designation associated G design radial shaft seal with a low cross-sectional height	G 35x45x4
Designation associated SD design radial shaft seal with a low cross-sectional height	SD 35x45x4

NKX 30

Dimensions

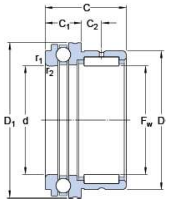

F_w		30	mm
D		42	mm
C		30	mm
C_1		11	mm
C_2		9.5	mm
d		30	mm
D_1		47.1	mm
$r_{1,2}$	min.	0.6	mm

Abutment dimensions

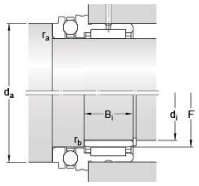

d_a	min.	42.7	mm
r_a	max.	0.6	mm
r_b	max.	0.3	mm
d_i		25	mm
F		30	mm
B_i		20	mm

Calculation data

Basic dynamic load rating, radial direction	C	22.9	kN
Basic static load rating, radial direction	C_0	38	kN
Basic dynamic load rating, axial direction	C	20.3	kN
Basic static load rating, axial direction	C_0	45.5	kN
Fatigue load limit, radial direction	P_u	4.8	kN
Fatigue load limit, axial direction	P_u	1.7	kN
Minimum axial load factor	A	0.01	
Reference speed		6000	r/min
Limiting speed		8500	r/min

Mass

Mass bearing	0.14	kg

Associated products

Inner ring	IR 25x30x20

NKX 70

Dimensions

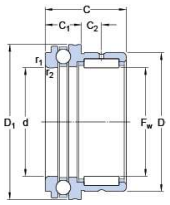

F_w		70	mm
D		85	mm
C		40	mm
C_1		18	mm
C_2		11	mm
d		70	mm
D_1		95.2	mm
$r_{1,2}$	min.	1	mm

Abutment dimensions

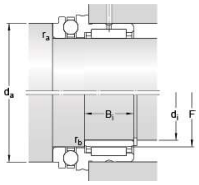

d_a	min.	90.5	mm
r_a	max.	1	mm
r_b	max.	1	mm
d_i		60	mm
F		70	mm
B_i		25	mm

Calculation data

Basic dynamic load rating, radial direction	C	44.6	kN
Basic static load rating, radial direction	C_0	98	kN
Basic dynamic load rating, axial direction	C	43.6	kN
Basic static load rating, axial direction	C_0	137	kN
Fatigue load limit, radial direction	P_u	12.2	kN
Fatigue load limit, axial direction	P_u	5.1	kN
Minimum axial load factor	A	0.097	
Reference speed		3400	r/min
Limiting speed		4500	r/min

Mass

Mass bearing	0.5	kg

Associated products

Inner ring	IR 60x70x25

30211

SKF Explorer

Dimension series	3DB

Dimensions

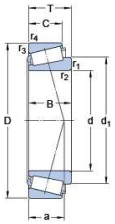

d		55	mm
D		100	mm
T		22.75	mm
d_1		74.7	mm
B		21	mm
C		18	mm
$r_{1,2}$	min.	2	mm
$r_{3,4}$	min.	1.5	mm
a		20.251	mm

Abutment dimensions

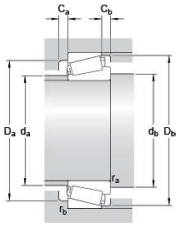

d_a	max.	64	mm
d_b	min.	65	mm
D_a	min.	88	mm
D_a	max.	92	mm
D_b	min.	94	mm
C_a	min.	4	mm
C_b	min.	4.5	mm

Calculation data

Basic dynamic load rating	C	111	kN
Basic static load rating	C_0	106	kN
Fatigue load limit	P_u	12	kN
Reference speed		5300	r/min
Limiting speed		6700	r/min
Calculation factor	e	0.4	
Calculation factor	Y	1.5	
Calculation factor	Y_0	0.8	

Mass

Mass bearing	0.7	kg

30216

SKF Explorer

Dimension series	3EB

Dimensions

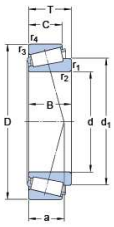

d		80	mm
D		140	mm
T		28.25	mm
d_1		105	mm
B		26	mm
C		22	mm
$r_{1,2}$	min.	2.5	mm
$r_{3,4}$	min.	2	mm
a		27.531	mm

Abutment dimensions

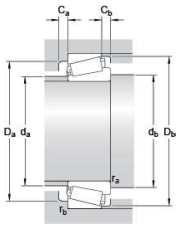

d_a	max.	92	mm
d_b	min.	92	mm
D_a	min.	124	mm
D_a	max.	130	mm
D_b	min.	132	mm
C_a	min.	4	mm
C_b	min.	6	mm
r_a	max.	2.5	mm
r_b	max.	2	mm

Calculation data

Basic dynamic load rating	C	184	kN
Basic static load rating	C_0	183	kN
Fatigue load limit	P_u	21.2	kN
Reference speed		3800	r/min
Limiting speed		4800	r/min
Calculation factor	e	0.43	
Calculation factor	Y	1.4	
Calculation factor	Y_0	0.8	

33012

SKF Explorer

Dimension series	2CE

Dimensions

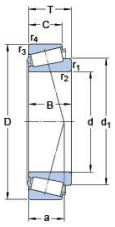

d		60	mm
D		95	mm
T		27	mm
d_1		77.2	mm
B		27	mm
C		21	mm
$r_{1,2}$	min.	1.5	mm
$r_{3,4}$	min.	1.5	mm
a		19.91	mm

Abutment dimensions

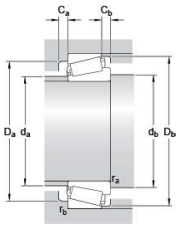

d_a	max.	67	mm
d_b	min.	69	mm
D_a	min.	85	mm
D_a	max.	87	mm
D_b	min.	90	mm
C_a	min.	5	mm
C_b	min.	6	mm
r_a	max.	1.5	mm
r_b	max.	1.5	mm

Calculation data

Basic dynamic load rating	C	113	kN
Basic static load rating	C_0	143	kN
Fatigue load limit	P_u	16	kN
Reference speed		5300	r/min
Limiting speed		6700	r/min
Calculation factor	e	0.33	
Calculation factor	Y	1.8	
Calculation factor	Y_0	1	

Appendix I:
Datasheet for LWW DAMIDBOND 200

DAMIDBOND 200

Round enamelled winding wire of copper, bondable, class 200

Product name:
Damidbond 200 - Gr 1B
Damidbond 200 - Gr 2B

Specifications:
IEC 60317-38

UL approval:
Approved: Damidbond 200
UL-file no: E101843

Class: 200
Temperature index ≥ 200°C
Heat shock: ≥ 220°C

Conductor material:
EN 1977 - ETP1 CW003 A
EN 1977 - ETP CW004A
ASTM B49 - ETP C11000/C11040

Insulation:
Basecoat: THEIC-modified polyester or polyesterimide
Overcoat: Polyamide-imide
Bondingcoat: Modified aromatic polyamide

Properties:
- High heat resistance
- Suitable for winding in high speed machines
- Very good resistance to transformer oils
- Very good resistance to typical solvent
- Freon resistant
- Excellent resistance to mechanical stress
- Bondable at 180°C-220°C
- High re-softening temperature (190°C)

Field of application:
- Electric motors
- Hermetic compressors
- Solenoid coils
- Relay coils

Dimension range:

Damidbond 200 Gr 1B	0,200 ≤ Ø ≤ 1,500 mm
Damidbond 200 Gr 2B	0,200 ≤ Ø ≤ 1,500 mm

Standard packaging:

0,200 ≤ Ø ≤ 1,500 mm	A250/400, A315/500, A400/630

Shelf life:
2 years, under normal ambient conditions

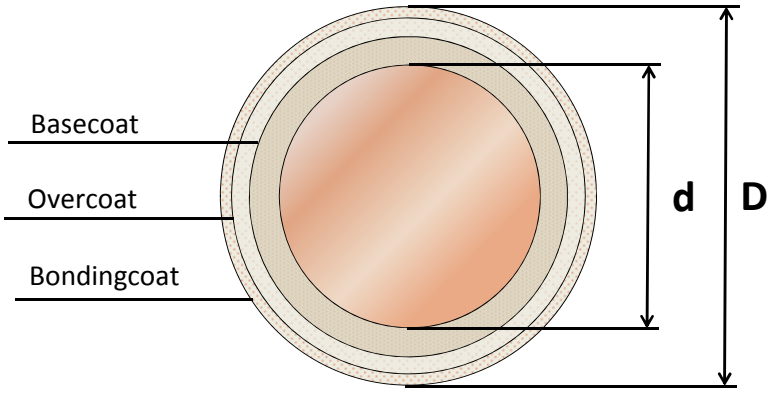

D - d = Increase

DAMIDBOND 200

Round enamelled winding wire of copper, bondable, class 200

Properties for DAMIDBOND 200

Main characteristics	Test method	Acceptance criteria	Test values for a Damidbond 200 sample (0,56 mm, Gr1B)
Thermal properties			
Heat shock	IEC 60851 - 6.3	≥ 220°C	≥ 220°C
Cut-through	IEC 60851 - 6.4	≥ 320°C	OK at 330°C
Temperature index	IEC 60172	≥ 200°C[1)]	≥ 200°C[1)]
Electrical properties			
Conductor resistance	IEC 60851 - 5.3	0,01724 Ωmm²/m	0,01724 Ωmm²/m
Conductivity	1/R	> 58 m/(Ωmm²)	> 58 m/(Ωmm²)
Breakdown voltage	IEC 60851 - 5.4	IEC 60317-0-1[2)]	6,0 kV
Mechanical properties			
Elongation	IEC 60851-3.3	IEC 60317-0-1[2)]	40%
Springiness	IEC 60851-3.4	IEC 60317-0-1[2)]	39°
Flexibility	IEC 60851-3.5 Mandrel wind.	1xØ	10 % elongation + 1xØ
Adherence	IEC 60851-3.5 Jerktest[3)]	No loss of adhesion	OK
	Peeltest[4)]	min. 110[5)]	-
Bonding	IEC 60851-3.7	IEC 60317-38.18	2,5 N at 190°C

1. According to supplier certificate
2. Values depend on dimension and grade
3. Up to an including 1,00 mm
4. Over 1,00 mm
5. Revolutions x nominal dimension

Values above are for information only. All values noted are typical and can vary between lots and dimensions.

Bonding strenght

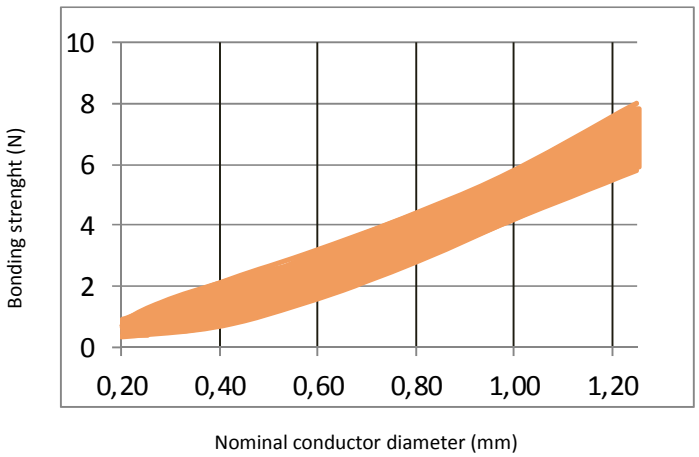

The technical data included is up to date at the time of printing.

LWW reserves the right to make any amendments deemed necessary

Ed.A(4)

LWW group

dahréntråd Part of LWW Group | isodraht Part of LWW Group | śląska Part of LWW Group | 利里达尔线材 liljedahl wire Part of LWW Group

Certified according to ISO 9001:2000, ISO-TS 16949, ISO 14001